Coral Reef Functioning Along a Cross-shelf Environmental Gradient:

Abiotic and Biotic Drivers of Coral Reef Growth in the Red Sea

Dissertation by

Anna Roik

In Partial Fulfillment of the Requirements

For the Degree of

Doctor of Philosophy

King Abdullah University of Science and Technology,

Thuwal, Kingdom of Saudi Arabia

June 2016

EXAMINATION COMMITTEE APPROVALS FORM

The dissertation of Anna Roik is approved by the examination committee.

Committee Chairperson:

Prof. Christian R. Voolstra

Committee Members:

Prof. Burt Jones, Prof. Timothy Ravasi, Prof. Malcolm McCulloch

ABSTRACT

Coral Reef Functioning Along a Cross-shelf Environmental Gradient:

Abiotic and Biotic Drivers of Coral Reef Growth in the Red Sea

Anna Roik

Despite high temperature and salinity conditions that challenge reef growth in other oceans, the Red Sea maintains amongst the most biodiverse and productive coral reefs worldwide. It is therefore an important region for the exploration of coral reef functioning, and expected to contribute valuable insights towards the understanding of coral reefs in challenging environments.

This dissertation assessed the baseline variability of *in situ* abiotic conditions (temperature, dissolved oxygen, pH, and total alkalinity, among others) in the central Red Sea and highlights these environmental regimes in a global context. Further, focus was directed on biotic factors (biofilm community dynamics, calcification and bioerosion), which underlie reef growth processes and are crucial for maintaining coral reef functioning and ecosystem services. Using full-year data from an environmental cross-shelf gradient, the dynamic interplay of abiotic and biotic factors was investigated.

In situ observations demonstrate that central Red Sea coral reefs were highly variable on spatial, seasonal, and diel scales, and exhibited comparably high temperature, high salinity, and low dissolved oxygen levels, which on the one hand reflect future ocean predictions. Under these conditions epilithic bacterial and algal assemblages were mainly driven by variables (i.e., temperature, salinity, dissolved oxygen) which are

predicted to change strongly in the progression of global climate change, implying an influential bottom up effect on reef-building communities. On the other hand, measured alkalinity and other carbonate chemistry value were close to the estimates of preindustrial global ocean surface water and thus in favor of reef growth processes. Despite this beneficial carbonate chemistry, calcification and carbonate budgets in the reefs were not higher than in other coral reef regions. In this regard, seasonal calcification patterns suggest that summer temperatures may be exceeding the optima of calcifiers.

As a possible interpretation of the here observed environmental regimes, it can be concluded that the central Red Sea may be less sensitive to ocean acidification, but is already impacted by ocean warming. Importantly, this dissertation provides valuable present-day baseline data of the natural variability of relevant abiotic drivers together with benthic community and reef growth dynamics. These data will be important for future comparative studies and efforts to quantify the impact of future environmental change in the region.

ACKNOWLEDGEMENTS

I would like to thank my advisor C. R. Voolstra for giving me this great opportunity of working in his lab, providing support, advice, and resources to conduct research for my dissertation and beyond. I am grateful to the committee members, B. Jones, T. Ravasi, and M. McCulloch for their valuable comments on this disseration. My research would not have been possible to accomplish without the help, collaboration, and company of my "field & research buddies" T. Röthig and M. Ziegler, who stood by my side on the boat, in the reef, in the lab, and also when hiking volcanos, or chasing camels, whales, and sharks. I would like to thank C. Roder for setting ground for my first research projects and for preparing the monitoring stations together with C. Walcher, F. Mallon, and P. Müller. Thanks to L. Smith, M. Pantalita, S. Mahmoud, D. Pallett, H. and R. Al-Jahdali for the support with oceanographic instruments, dive safety supervision, and logistics. A great "shukran" to the boat captains E., A., W., and G. Al- Jahdali for taking me out to the reefs on regular basis. Thanks to C. Michell and the KAUST BioScience Core Laboratory team for the sequencing of biofilm samples. Also, I am very grateful for many scientific discussions and advices, diving support, and lunch and coffee breaks with collegues from the Voolstra Lab and the Red Sea Research Center. I would like to thank T. Bayer for sharing good times with me during the years of my dissertation and for his endless patience in times when I needed to focus on work more than on everything else. Lastly, I would like to thank my family and friends back at home for staying in touch with me over these years. I am especially grateful for the love, and encouragement from my mom and dad - and for their growing enthusiasm about my work and marine life.

TABLE OF CONTENTS

LIST OF TABLES

LIST OF FIGURES

LIST OF EQUATIONS

1. INTRODUCTION

1.1. Coral Reefs

Coral reefs maintain unique species diversity, comparable to tropical rainforests, and provide important ecosystem services: food, income and coastal protection, among others (Reaka-Kudla 1997; Moberg and Folke 1999). The ecological and economic importance of coral reefs is bound to the coral reef framework which is essential for ecosystem functioning. Reef framework formation, i.e. reef growth, strongly depends on the abundance and performance of reef-building coral holobionts, which rely on the obligate symbiosis with intra-cellular dinoflagellate protists, and encrusting coralline algae (Goreau 1963). These communities of calcifiers facilitate rapid accretion of calcium carbonate ($CaCO_3$), building three-dimensional structures that create essential habitat for coral reef species and thereby a fundament for ecosystem productivity (Graham 2014). Reef-building communities prefer warm, sun lit, oligotrophic and aragonite saturated waters predominantly found in the tropical oceans (Achituv and Dubinsky 1990; Buddemeier 1997; Hoegh-Guldberg 2014). Since coral reefs have essentially evolved under relatively stable abiotic environments of equatorial oceans (Achituv and Dubinsky 1990; Wood 1999), coral reef communities are mostly adapted to a relatively narrow environmental range and live close to their e.g. thermal limits. Consequently, coral reefs are amongst the ecosystems most threatened by rapid environmental change today (Hughes et al. 2003). Besides global drivers such as ocean warming and acidification which contribute to increasing temperatures and decreasing pH and aragonite saturation

state, local environmental stressors, such as eutrophication and pollution of coastal waters, also challenge coral reefs worldwide (Wilkinson 1999; Bellwood et al. 2004).

1.2. Importance of reef communities in coral reef functioning

Benthic reef-building communities are fundamental for coral reef functioning and have been a major focus of the earliest coral reef studies (Benayahu and Loya 1977; Luckhurst and Luckhurst 1978; Done 1982). Community dynamics have functional implications for the ecosystem. A transition from coral-dominated to coral-depleted states implies a decrease in reef growth (Glynn 1997), as well as changes of the ecosystem productivity state (Done 1992; Hoytema et al. 2016). Community composition and their dynamics have been studied as indicator for "reef health" (Downs et al. 2005), and are frequently used to quantify the recovery potential of coral reefs after disturbance events, such as coral bleaching (Graham et al. 2015). Dynamics of benthic assemblages are addressed by many contemporary studies (Bauman et al. 2013; Furby et al. 2013; Jouffray et al. 2015), but more recently the importance of epilithic assemblages of bacteria and algae in coral reef biofilms has been increasingly emphasized (Wilson et al. 2003; Sawall et al. 2012; Witt et al. 2012a; Jessen et al. 2013a). These microscopic communities play pivotal roles in coral reef functioning, which encompasses significance in ecosystem productivity and crucial contribution to biogeochemical cycles (Battin et al. 2003; Wilson et al. 2003) to the facilitation of the larval recruitment of reef-building corals (Heyward and Negri 1999; Webster et al. 2004). For instance, coralline algae dominated assemblages fulfill central functions, on the one hand through their contribution to carbonate accretion (Perry and Hepburn 2008), on the other hand they sustain bacterial biofilm

communities that induce higher settlement rates of coral larvae than bacterial communities associated with other epilithic substrate (Sneed et al. 2015). As a result coralline algal dominance is associated with sustainable reef growth, but under unfavorable conditions (e.g., high nutrient levels or overfishing) this state can rapidly shift towards a community dominated by green and brown turf algae, which then may be likely to further advance to algal-dominated states and lead to the degradation of the coral reef habitat (Hughes et al. 2007). Since microscopic components of benthic communities have the potential to alter reef-building communities, a better understanding of their environmental drivers and dynamics is of great importance.

1.3. Importance of calcification in coral reef functioning

Reef-building corals and coralline algae assemblages are imperative for the formation and persistence of coral reef habitats, which is attributable to their ability to accrete $CaCO_3$ skeletons and form calcareous crusts (Borowitzka and Larkum 1987; Allemand et al. 2011). Biogenic calcification (e.g., $Ca^{2+} + CO_3^{2-} \Rightarrow CaCO_3$, Allemand et al. 2011) is a fundamental process that maintains reef framework and coral reef functioning. It strongly responds to abiotic drivers, among which temperature and the state of carbonate chemistry are the most influential factors, implying the susceptibility of calcifiers to ocean warming and acidification (Clausen and Roth 1975a; Schneider and Erez 2006; Anthony et al. 2008; McCoy and Kamenos 2015). Increasing temperatures, that remain below a certain threshold, can enhance calcification rates in reef-building corals, which can be observed along latitudinal gradients (Lough and Barnes 2000; Carricart-Ganivet 2004). However, as soon as a critical thermal limit is exceeded calcification rates decline as a result of thermal stress (Marshall and Clode 2004).

Specifically in reef-building corals, thermal stress disturbs efficiency of the coral-dinoflagellate symbiosis by cutting off an important energy supply (Weis 2008). Thereby, on the long term elevated temperatures outside the tolerated range cause coral bleaching, which is regarded one of the greatest threats to coral reefs (Hoegh-Guldberg 1999). Additionally, calcification strongly depends the state of carbonate chemistry of seawater. Aragonite is the most abundant form of $CaCO_3$ precipitated in the present-day tropical oceans and the abundance of carbonate and bicarbonate ions in seawater can be indirectly measured by determination of e.g. total alkalinity and pH. The decrease of pH alongside with decreases in aragonite saturation state and total alkalinity can lead to sub-optimal calcification performance in both coral and algal calcifiers, which is why ocean acidification is expected to cause a decline in the reef-building capacities of reef calcifiers (Schneider and Erez 2006; Martin and Gattuso 2009). Often performance of calcifiers is altered as a consequence of different environmental regimes that naturally occur along spatial gradients (Castillo and Helmuth 2005; Manzello et al. 2015) or alongside with seasonal environmental change (Silverman et al. 2007a; Bates et al. 2010). Typically, calcification is higher when local seawater temperatures meet the thermal optimum of the local calcifiers during the local summer season (Crossland 1984; Hibino and van Woesik 2000; Kuffner et al. 2013). An increased aragonite saturation state has been observed to have a positive effect on calcification during summer as well (Bates et al. 2010). On top of that, a moderate seasonal nutrient enrichment and moderately enhanced water column productivity can benefit reef-building corals, boosting heterotrophic feeding

that is often coupled with an increase in calcification rates (Houlbrèque and Ferrier-Pagès 2009).

1.4. Carbonate production states as a measure of coral reef persistence or degradation

Not only calcification contributes to reef growth, but processes of $CaCO_3$ removal, i.e. erosion and dissolution, simultaneously define the net-production of $CaCO_3$ in a reef (Glynn 1997; Perry et al. 2008). A holistic view of reef growth requires consideration of the delicate balance of calcification and erosion. Hence, examining the activity and abundances of calcifying benthic communities and bioeroders, such as parrotfish, sea urchins, and endolithic biota is essential (Glynn and Manzello 2015). The estimation of carbonate net-production states (= carbonate budgets) has proven valuable to identify and quantify reefs under significant degradation (Alvarez-Filip et al. 2009; Kennedy et al. 2013; Perry et al. 2013). Carbonate budget studies have revealed net-erosive states in many coral reefs worldwide, that often were related to an increased frequency of extreme climate events (Eakin 2001; Schuhmacher et al. 2005) or local human impacts, such as pollution and eutrophication (Edinger et al. 2000; Chazottes et al. 2002). The effect of environmental drivers on erosion differs from their effects on calcification. Erosion is usually higher in turbid and nutrient rich habitats, where it is driven by a higher abundance of endolithic bioeroders (e.g., worms and sponges) (Pari et al. 1998; Chazottes et al. 2002). Importantly, a lower pH can increase erosion rates (Wisshak et al. 2012; Fang et al. 2013), while it reduces calcification capacity, implying an additive negative effect of ocean acidification on overall reef growth.

1.5. Importance of the Red Sea for coral reef studies

The Red Sea is located in one of the warmest climate zones globally and is one of the most saline seas (Edwards and Head 1987; Sheppard et al. 1992; Riegl 2003). While the neighboring region of the Arabian/Persian Gulf host mostly marginal coral reef communities that hardly support reef growth as a consequence of harsh environmental conditions (Purkis and Riegl 2005), the Red Sea maintains a remarkable reef-building potential along the entire coastline (Price et al. 1998; Riegl et al. 2012).

In the Red Sea, challenging conditions such as high salinity and high temperatures are paired with mostly high total alkalinity and aragonite saturation state levels that, on the other hand, are beneficial for calcification and reef growth (Kleypas et al. 1999b; Allemand et al. 2011). Also, little terrestrial run-off and high light penetration favor coral reef growth (Schlichter et al. 1986; Rasul et al. 2015). Strong longitudinal gradients of temperature, salinity, and nutrients (Raitsos et al. 2013) give rise to a variaty of habitats which can in part be considered challenging for coral reefs, especially in the southern and central Red Sea, where average temperatures are highest. Moreover, the Red Sea is one of the northernmost tropical seas and exposed to significant seasonality over the annual cycle (Rasul et al. 2015). This unique combination of challenging and beneficial abiotic factors, as well as the environmental gradients and seasonality, make the Red Sea a valuable region for the study of coral reef dynamics under variable environmental conditions that partly reach beyond the global averages of coral reefs.

Furthermore, the Red Sea is subject to a warming rate which is three-fold higher per decade compared to the global average (Belkin 2009). Recent studies indicate that coral reef functioning in the Red Sea is jeopardized by this ongoing environmental change. Under a historical perspective, calcification rates in the massive coral *Diploastrea heliopora* from the central Red Sea declined most recently in correlation to the onset of an abrupt warming in the 1990ies, which was demonstrated for the entire basin based on remote sensing derived sea surface temperatures (Cantin et al. 2010; Raitsos et al. 2011). Also, community scale changes are measureable in Red Sea coral reefs. Over the past 20 years coral sizes have decreased and coral reef communities underwent shifts in species distribution, becoming more homogenous along the latitudinal gradient (Riegl et al. 2012), which may as well be a consequence of increasing local stressors. Ongoing and future changes in the Red Sea coral reefs can be only accurately quantified if abiotic and biotic variables are investigated *in situ*, considering the variability of habitats on spatial and temporal scales (Boyd and Hutchins 2012; Ban et al. 2014; Helmuth et al. 2014). Today, many data on the environmental conditions in the Red Sea are based on remote sensing or on only occasional sampling events. Especially in the central and southern Red Sea *in situ* data hardly exist for coral reefs.

Comprehensive studies are urgently needed for the coral reef region of the Red Sea that is increasingly impacted by environmental change, while its functioning is not yet fully understood. Its unique physicochemical setting including environmental gradients and seasonality also offers the opportunity to better understand coral reefs in challenging environments and predict responses to environmental change.

1.6. References

Achituv Y, Dubinsky Z (1990) Evolution and zoogeography of coral reefs. Ecosystems of the world. Elsevier, Amsterdam, pp 1–9

Allemand D, Tambutté É, Zoccola D, Tambutté S (2011) Coral calcification, cells to reefs. Coral Reefs Ecosyst Transit 119–150

Alvarez-Filip L, Dulvy NK, Gill JA, Côté IM, Watkinson AR (2009) Flattening of Caribbean coral reefs: region-wide declines in architectural complexity. Proc R Soc Lond B Biol Sci 276:3019–3025

Anthony KRN, Kline DI, Diaz-Pulido G, Dove S, Hoegh-Guldberg O (2008) Ocean acidification causes bleaching and productivity loss in coral reef builders. Proc Natl Acad Sci 105:17442–17446

Ban SS, Graham NAJ, Connolly SR (2014) Evidence for multiple stressor interactions and effects on coral reefs. Glob Change Biol 20:681–697

Bates NR, Amat A, Andersson AJ (2010) Feedbacks and responses of coral calcification on the Bermuda reef system to seasonal changes in biological processes and ocean acidification. Biogeosciences 7:2509–2530

Battin TJ, Kaplan LA, Denis Newbold J, Hansen CME (2003) Contributions of microbial biofilms to ecosystem processes in stream mesocosms. Nature 426:439–442

Bauman AG, Feary DA, Heron SF, Pratchett MS, Burt JA (2013) Multiple environmental factors influence the spatial distribution and structure of reef communities in the northeastern Arabian Peninsula. Mar Pollut Bull 72:302–312

Belkin IM (2009) Rapid warming of Large Marine Ecosystems. Prog Oceanogr 81:207–213

Bellwood DR, Hughes TP, Folke C, Nyström M (2004) Confronting the coral reef crisis. Nature 429:827–833

Benayahu Y, Loya Y (1977) Space partitioning by stony corals soft corals and benthic algae on the coral reefs of the northern Gulf of Eilat (Red Sea). Helgoländer Wiss Meeresunters 30:362–382

Borowitzka MA, Larkum AWD (1987) Calcification in algae: Mechanisms and the role of metabolism. Crit Rev Plant Sci 6:1–45

Boyd P, Hutchins D (2012) Understanding the responses of ocean biota to a complex matrix of cumulative anthropogenic change. Mar Ecol Prog Ser 470:125–135

Buddemeier RW (1997) Symbiosis: Making light work of adaptation. Nature 388:229–230

Cantin NE, Cohen AL, Karnauskas KB, Tarrant AM, McCorkle DC (2010) Ocean Warming Slows Coral Growth in the Central Red Sea. Science 329:322–325

Carricart-Ganivet JP (2004) Sea surface temperature and the growth of the West Atlantic reef-building coral *Montastraea annularis*. J Exp Mar Biol Ecol 302:249–260

Castillo KD, Helmuth BST (2005) Influence of thermal history on the response of *Montastraea annularis* to short-term temperature exposure. Mar Biol 148:261–270

Chazottes V, Le Campion-Alsumard T, Peyrot-Clausade M, Cuet P (2002) The effects of eutrophication-related alterations to coral reef communities on agents and rates of bioerosion (Reunion Island, Indian Ocean). Coral Reefs 21:375–390

Clausen CD, Roth AA (1975) Estimation of coral growth-rates from laboratory 45Ca-incorporation rates. Mar Biol 33:85–91

Crossland CJ (1984) Seasonal variations in the rates of calcification and productivity in the coral *Acropora formosa* on a high-latitude reef. Mar Ecol Prog Ser 15:135–140

Done TJ (1982) Patterns in the distribution of coral communities across the central Great Barrier Reef. Coral Reefs 1:95–107

Done TJ (1992) Phase shifts in coral reef communities and their ecological significance. In: Jaccarini V., Martens E. (eds) The Ecology of Mangrove and Related Ecosystems. Springer Netherlands, pp 121–132

Downs CA, Woodley CM, Richmond RH, Lanning LL, Owen R (2005) Shifting the paradigm of coral-reef "health" assessment. Mar Pollut Bull 51:486–494

Eakin CM (2001) A tale of two Enso Events: carbonate budgets and the influence of two warming disturbances and intervening variability, Uva Island, Panama. Bull Mar Sci 69:171–186

Edinger EN, Limmon GV, Jompa J, Widjatmoko W, Heikoop JM, Risk MJ (2000) Normal coral growth rates on dying reefs: Are coral growth rates good indicators of reef health? Mar Pollut Bull 40:404–425

Edwards AJ, Head SM (1987) Red Sea, Key Environments Series. Pergamon Press, Oxford, UK

Fang JKH, Mello-Athayde MA, Schönberg CHL, Kline DI, Hoegh-Guldberg O, Dove S (2013) Sponge biomass and bioerosion rates increase under ocean warming and acidification. Glob Change Biol 19:3581–3591

Furby KA, Bouwmeester J, Berumen ML (2013) Susceptibility of central Red Sea corals during a major bleaching event. Coral Reefs 32:505–513

Glynn PW (1997) Bioerosion and coral-reef growth: a dynamic balance. Chapman and Hall, USA,

Glynn PW, Manzello DP (2015) Bioerosion and Coral Reef Growth: A Dynamic Balance. In: Birkeland C. (eds) Coral Reefs in the Anthropocene. Springer Netherlands, pp 67–97

Goreau TF (1963) Calcium Carbonate Deposition by Coralline Algae and Corals in Relation to Their Roles as Reef-Builders. Ann N Y Acad Sci 109:127–167

Graham NAJ (2014) Habitat Complexity: Coral Structural Loss Leads to Fisheries Declines. Curr Biol 24:R359–R361

Graham NAJ, Jennings S, MacNeil MA, Mouillot D, Wilson SK (2015) Predicting climate-driven regime shifts versus rebound potential in coral reefs. Nature advance online publication:

Helmuth B, Russell BD, Connell SD, Dong Y, Harley CD, Lima FP, Sará G, Williams GA, Mieszkowska N (2014) Beyond long-term averages: making biological sense of a rapidly changing world. Clim Change Responses 1:

Heyward AJ, Negri AP (1999) Natural inducers for coral larval metamorphosis. Coral Reefs 18:273–279

Hibino K, van Woesik R (2000) Spatial differences and seasonal changes of net carbonate accumulation on some coral reefs of the Ryukyu Islands, Japan. J Exp Mar Biol Ecol 252:1–14

Hoegh-Guldberg O (1999) Climate change, coral bleaching and the future of the world's coral reefs. Mar Freshw Res 50:839

Hoegh-Guldberg O (2014) Coral reefs in the Anthropocene: persistence or the end of the line? Geol Soc Lond Spec Publ 395:167–183

Houlbrèque F, Ferrier-Pagès C (2009) Heterotrophy in Tropical Scleractinian Corals. Biol Rev 84:1–17

Hoytema N van, Bednarz VN, Cardini U, Naumann MS, Al-Horani FA, Wild C (2016) The influence of seasonality on benthic primary production in a Red Sea coral reef. Mar Biol 163:1–14

Hughes TP, Baird AH, Bellwood DR, Card M, Connolly SR, Folke C, Grosberg R, Hoegh-Guldberg O, Jackson JBC, Kleypas J, Lough JM, Marshall P, Nyström M, Palumbi SR, Pandolfi JM, Rosen B, Roughgarden J (2003) Climate Change, Human Impacts, and the Resilience of Coral Reefs. Science 301:929–933

Hughes TP, Rodrigues MJ, Bellwood DR, Ceccarelli D, Hoegh-Guldberg O, McCook L, Moltschaniwskyj N, Pratchett MS, Steneck RS, Willis B (2007) Phase Shifts, Herbivory, and the Resilience of Coral Reefs to Climate Change. Curr Biol 17:360–365

Jessen C, Roder C, Villa Lizcano JF, Voolstra CR, Wild C (2013) In-Situ Effects of Simulated Overfishing and Eutrophication on Benthic Coral Reef Algae Growth, Succession, and Composition in the Central Red Sea. PLoS ONE 8:e66992

Jouffray J-B, Nyström M, Norström AV, Williams ID, Wedding LM, Kittinger JN, Williams GJ (2015) Identifying multiple coral reef regimes and their drivers across the Hawaiian archipelago. Philos Trans R Soc B Biol Sci 370:20130268

Kennedy EV, Perry CT, Halloran PR, Iglesias-Prieto R, Schönberg CHL, Wisshak M, Form AU, Carricart-Ganivet JP, Fine M, Eakin CM, Mumby PJ (2013) Avoiding Coral Reef Functional Collapse Requires Local and Global Action. Curr Biol 23:912–918

Kleypas JA, McManus JW, Menez LAB (1999) Environmental Limits to Coral Reef Development: Where Do We Draw the Line? Am Zool 39:146–159

Kuffner IB, Hickey TD, Morrison JM (2013) Calcification rates of the massive coral *Siderastrea sidere*a and crustose coralline algae along the Florida Keys (USA) outer-reef tract. Coral Reefs 32:987–997

Lough JM, Barnes DJ (2000) Environmental controls on growth of the massive coral Porites. J Exp Mar Biol Ecol 245:225–243

Luckhurst BE, Luckhurst K (1978) Analysis of the influence of substrate variables on coral reef fish communities. Mar Biol 49:317–323

Manzello DP, Enochs IC, Kolodziej *G, Carlton R (2015) Coral growth patterns of Montastraea cavernosa and Porites astreoides* in the Florida Keys: The importance of thermal stress and inimical waters. J Exp Mar Biol Ecol 471:198–207

Marshall AT, Clode P (2004) Calcification rate and the effect of temperature in a zooxanthellate and an azooxanthellate scleractinian reef coral. Coral Reefs 23:218–224

Martin S, Gattuso J-P (2009) Response of Mediterranean coralline algae to ocean acidification and elevated temperature. Glob Change Biol 15:2089–2100

McCoy SJ, Kamenos NA (2015) Coralline algae (Rhodophyta) in a changing world: integrating ecological, physiological, and geochemical responses to global change. J Phycol 51:6–24

Moberg F, Folke C (1999) Ecological goods and services of coral reef ecosystems. Ecol Econ 29:215–233

Pari N, Peyrot-Clausade M, Le Champion-Alsumard T, Hutchings P, Chazottes V, Gobulic S, Le Champion J, Fontaine MF (1998) Bioerosion of experimental substrates on high islands and on atoll lagoons (French Polynesia) after two years of exposure. Mar Ecol Prog Ser 166:119–130

Perry CT, Hepburn LJ (2008) Syn-depositional alteration of coral reef framework through bioerosion, encrustation and cementation: Taphonomic signatures of reef accretion and reef depositional events. Earth-Sci Rev 86:106–144

Perry CT, Murphy GN, Kench PS, Smithers SG, Edinger EN, Steneck RS, Mumby PJ (2013) Caribbean-wide decline in carbonate production threatens coral reef growth. Nat Commun 4:1402

Perry CT, Spencer T, Kench PS (2008) Carbonate budgets and reef production states: a geomorphic perspective on the ecological phase-shift concept. Coral Reefs 27:853–866

Price AR g., Jobbins G, Shepherd ARD, Ormond RF g. (1998) An integrated environmental assessment of the Red Sea coast of Saudi Arabia. Environ Conserv 25:65–76

Purkis S, Riegl B (2005) Spatial and temporal dynamics of Arabian Gulf coral assemblages quantified from remote-sensing and in situ monitoring data. Mar Ecol Prog Ser 287:99–113

Raitsos DE, Hoteit I, Prihartato PK, Chronis T, Triantafyllou G, Abualnaja Y (2011) Abrupt warming of the Red Sea. Geophys Res Lett 38:L14601

Raitsos DE, Pradhan Y, Brewin RJW, Stenchikov G, Hoteit I (2013) Remote Sensing the Phytoplankton Seasonal Succession of the Red Sea. PLoS ONE 8:e64909

Rasul NMA, Stewart ICF, Nawab ZA (2015) Introduction to the Red Sea: Its Origin, Structure, and Environment. In: Rasul N.M.A., Stewart I.C.F. (eds) The Red Sea. Springer Berlin Heidelberg, pp 1–28

Reaka-Kudla ML (1997) The Global Biodiversity of Coral Reefs: A Comparison with Rainforests. In: Reaka-Kudla M.L., Wilson D.E., Wilson E.O. (eds) Biodiversity

II: Understanding and Protecting Our Biological Resources. The Joseph Henry Press, USA, pp 83–106

Riegl B (2003) Climate change and coral reefs: different effects in two high-latitude areas (Arabian Gulf, South Africa). Coral Reefs 22:433–446

Riegl BM, Bruckner AW, Rowlands GP, Purkis SJ, Renaud P (2012) Red Sea Coral Reef Trajectories over 2 Decades Suggest Increasing Community Homogenization and Decline in Coral Size. PLoS ONE 7:e38396

Sawall Y, Richter C, Ramette A (2012) Effects of Eutrophication, Seasonality and Macrofouling on the Diversity of Bacterial Biofilms in Equatorial Coral Reefs. PLoS ONE 7:e39951

Schlichter D, Fricke HW, Weber W (1986) Light harvesting by wavelength transformation in a symbiotic coral of the Red Sea twilight zone. Mar Biol 91:403–407

Schneider K, Erez J (2006) The effect of carbonate chemistry on calcification and photosynthesis in the hermatypic coral *Acropora eurystoma*. Limnol Oceanogr 51:1284–1293

Schuhmacher H, Loch K, Loch W, See WR (2005) The aftermath of coral bleaching on a Maldivian reef—a quantitative study. Facies 51:80–92

Sheppard C, Price A, Roberts C (1992) Reefs and coral communities. Marine ecology of the arabian region: Patterns and processes in extreme tropical environments. Academic Press London, London, pp 65–67

Silverman J, Lazar B, Erez J (2007) Community metabolism of a coral reef exposed to naturally varying dissolved inorganic nutrient loads. Biogeochemistry 84:67–82

Sneed JM, Ritson-Williams R, Paul VJ (2015) Crustose coralline algal species host distinct bacterial assemblages on their surfaces. ISME J 9:2527–2536

Webster NS, Smith LD, Heyward AJ, Watts JEM, Webb RI, Blackall LL, Negri AP (2004) Metamorphosis of a Scleractinian Coral in Response to Microbial Biofilms. Appl Environ Microbiol 70:1213–1221

Weis VM (2008) Cellular mechanisms of Cnidarian bleaching: stress causes the collapse of symbiosis. J Exp Biol 211:3059

Wilkinson CR (1999) Global and local threats to coral reef functioning and existence: review and predictions. Mar Freshw Res 50:867–878

Wilson SS, Bellwood DD, Choat HJ, Furnas MM (2003) Detritus in the epilithic algal matrix and its use by coral reef fishes. Oceanogr Mar Biol Annu Rev-Pages 41 279-309

Wisshak M, Schönberg CHL, Form A, Freiwald A (2012) Ocean Acidification Accelerates Reef Bioerosion. PLoS ONE 7:e45124

Witt V, Wild C, Uthicke S (2012) Terrestrial Runoff Controls the Bacterial Community Composition of Biofilms along a Water Quality Gradient in the Great Barrier Reef. Appl Environ Microbiol 78:7786–7791

Wood R (1999) Reef evolution. Oxford University Press on Demand, Oxford, UK

2. OBJECTIVES

This dissertation aimed to generate and contribute new *in situ* abiotic and biotic data that provide insights into coral reef functioning in the Red Sea. The lack of such data, especially for the central Red Sea region, was a major motivation for the herein presented studies. Three chapters explore the dynamics and interactions of various abiotic and biotic variables that are crucial for reef functioning. The here-presented studies made use of the natural environmental variability along a cross-shelf gradient during the four seasons of the year, including fore- and backreef sites in nearshore, midshore, and offshore reefs in the central Red Sea (

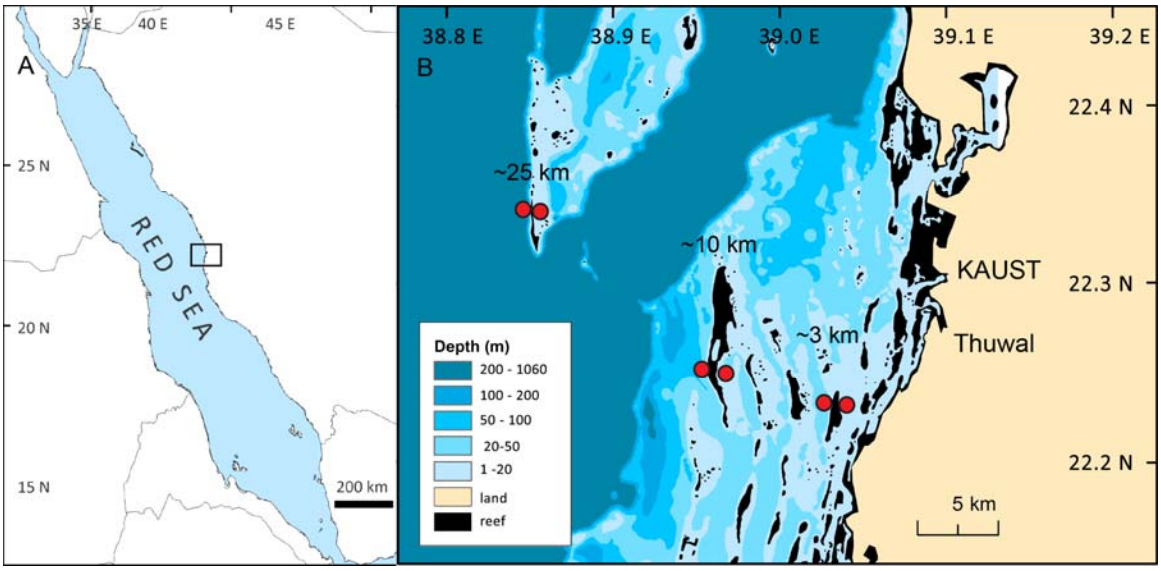

Figure 1). Continuous and seasonal measurements over more than one year were the basis for the evaluation of three important aspects in reef functioning: (A) community dynamics, (B) calcification dynamics, and (C) the overall reef growth as the result of calcification and bioerosion processes (Figure 2).

In brief, the first chapter (Figure 2 A) aimed at providing a baseline for coral reef studies in the region, by measuring crucial abiotic parameters (i.e., currents, temperature, salinity, dissolved oxygen, chlorophyll-a, turbidity, inorganic nutrients, sedimentation), and by monitoring the dynamics of microscopic assemblages of bacteria and algae in coral reef biofilms over a full year. This chapter intended to define the variability of environmental regimes in the region, and compares them against other coral reef locations, global coral reef averages, and future ocean predictions. Further, it aimed to assess the extent of spatio-temporal transition in biofilm communities and pinpoint abiotic drivers.

In the second chapter (Figure 2 B) calcification was measured in a full-year multi-species and multi-habitat approach. The goal was to quantify *in situ* calcification rates in reef-building corals and calcareous crusts and their abundances across the environmental gradient. This data was used to test the relationship of calcifiers' performance against their abundances in the habitats, and to explore the relationship of calcification dynamics with the seasonal change in temperature. This chapter also examined whether the Red Sea unique environmental setting maintains higher reef calcification rates compared to other coral reef regions.

The third chapter (Figure 2 C) aimed to determine the present-day seawater chemistry of coral reef habitats (with a focus on pH and total alkalinity) and to evaluate the reef growth potential in the central Red Sea. The synopsis of calcification and bioerosion data allowed to determine the census-based carbonate budgets for coral reef habitats along an environmental gradient. In contrast to other studies, which typically take into account either abiotic or biotic divers, this study took both variable types into consideration to identify potential drivers of reef growth for the region.

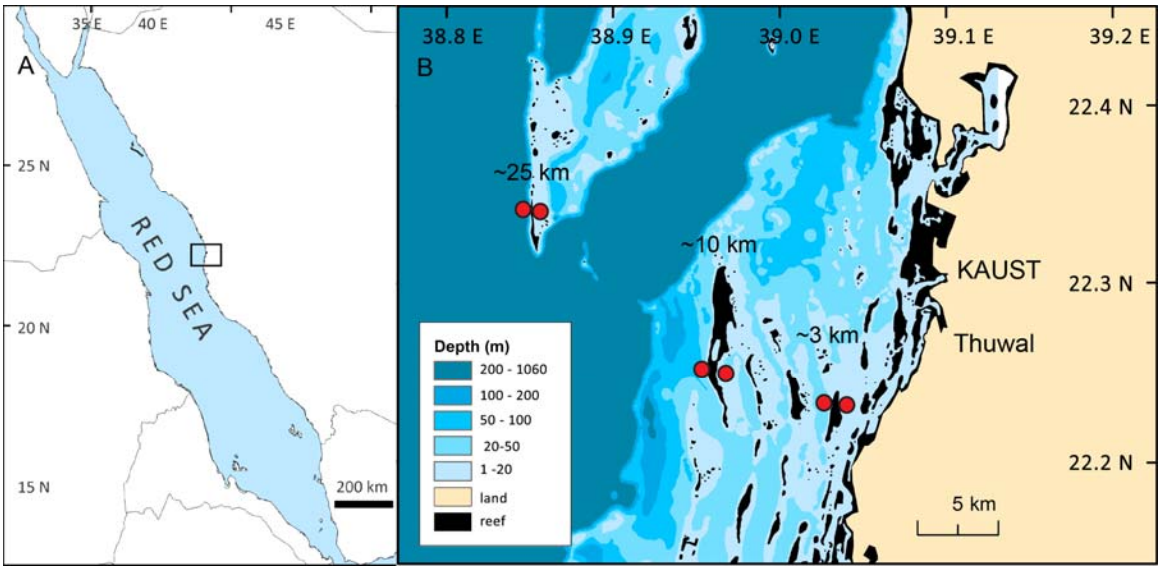

Figure 1 Study sites in the central Red Sea. A. The map shows the location of the study area in the Red Sea. B. Data collection for this dissertation was conducted in six reef sites along a cross-shelf environmental gradient, at distances of 3 km, 10 km and 25 km from the coastline (marked with red circles). KAUST = King Abdullah University of Science and Technology. Figure adapted from chapter two of this dissertation.

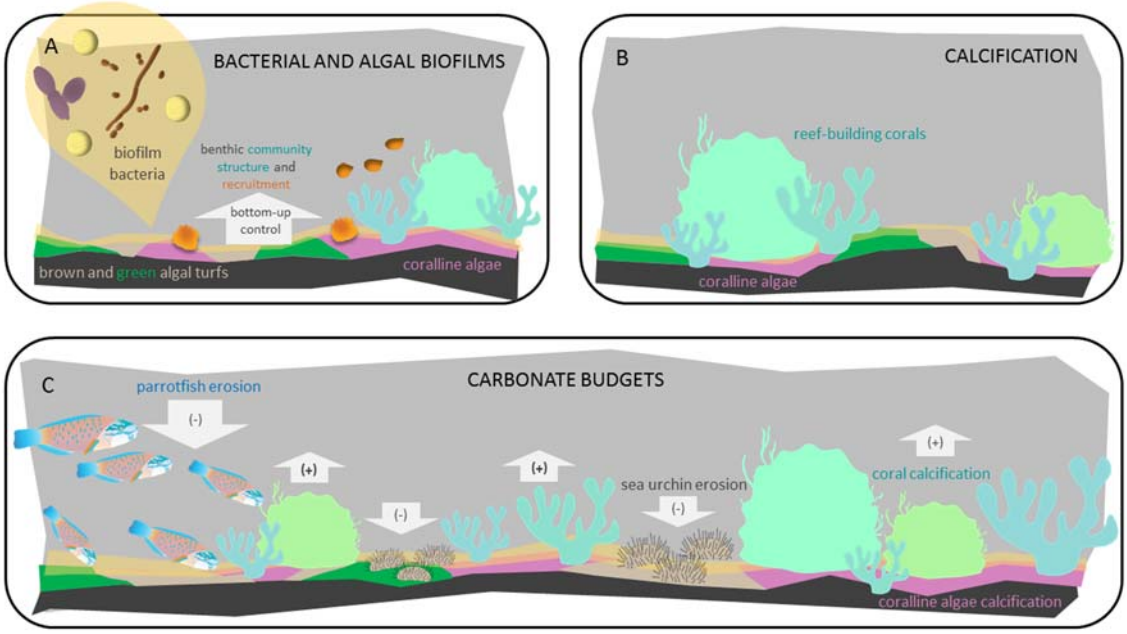

Figure 2 Schematic representation of the three aspects of coral reef functioning, which are topics of the three chapters in this dissertation. A. Community composition and dynamics, B. calcification, and C. reef growth dynamics. Image components adapted from http://ian.umces.edu/ (accessed in April 2016).

CHAPTER I

3. Year-long monitoring of physico-chemical and biological variables provide a comparative baseline of coral reef functioning in the central Red Sea

Anna Roik[1], Till Röthig[1], Cornelia Roder[1], Maren Ziegler[1], Stephan G. Kremb[1], Christian R Voolstra[1]

[1]Red Sea Research Center, Division of Biological and Environmental Science and Engineering, King Abdullah University of Science and Technology, Thuwal, Saudi Arabia

This manuscript has been submitted for publication with *PLoS ONE*

(In Revision, 6th June 2016)

Roik A, Röthig T, Roder C, Ziegler M, Kremb SG, Voolstra CR (In Revision) Year-long monitoring of physico-chemical and biological variables provide a comparative baseline of coral reef functioning in the central Red Sea. PLOS ONE PONE–S–15–69229

3.1. Abstract

Coral reefs in the central Red Sea are sparsely studied and *in situ* data on physico-chemical and key biotic variables are missing that provide an important comparative baseline. To address this gap, we simultaneously monitored three reefs along a cross-shelf gradient for an entire year (i.e., four seasons) collecting data on currents, temperature, salinity, dissolved oxygen (DO), chlorophyll-a, turbidity, inorganic nutrients, sedimentation, bacterial communities of reef water, and bacterial and algal composition of epilithic biofilms. Summer temperatures (29 - 33 °C) and salinity levels (39 PSU) exceeded average maxima for coral reefs globally, while DO levels were comparably low (2 - 4 mg L^{-1}). Reef environments were highly variable over time and between reefs. Temperature and salinity differences were most pronounced between seasons. Conversely, DO, chlorophyll-a, turbidity, and sedimentation varied strongest between reefs. Similarly, biotic communities were highly dynamic between reefs and seasons. Differences in bacterial biofilms were driven by differentially abundant families: Rhodobacteraceae, Flavobacteriaceae, Flammeovirgaceae, and Pseudanabaenaceae. In algal biofilms, green crusts, brown crusts, and crustose coralline algae were most abundant and accounted for most of the variability of the communities. Higher bacterial diversity of biofilms coincided with increased algal cover during spring and summer. By employing multivariate matching, we identified temperature, salinity, DO, and chlorophyll-a as the main contributing physico-chemical drivers of biotic community structures. These parameters are forecasted to change most with the progression of ocean warming and increased nutrient input, which also suggests an immediate bottom-up effect on Red Sea benthic communities

as a result of climate change and anthropogenic influence. In conclusion, our study presents foundation data that provide a comparative baseline to support coral reef studies in the region and to gain insight into coral reef functioning in the Red Sea.

3.2. Introduction

Coral reefs are marine ecosystems of high biodiversity and high economic value (Hoegh-Guldberg and et al. 2015). They depend on symbiotic reef-building corals that critically rely on sunlight, and are limited to the warm and oligotrophic conditions of equatorial oceans. Coral reefs were considered to exist in predominantly stable physico-chemical environments (Achituv and Dubinsky 1990), but more recently coral reefs have been described to thrive over a wide range of environmental gradients (Kleypas et al. 1999; Hume et al. 2013). Coral reefs exist in regions where seasonality, upwelling, or internal waves drive the variability of critical physico-chemical variables such as temperature, salinity, dissolved oxygen, and nutrient supply (Falter et al. 2012; Eidens et al. 2014; Wall et al. 2015). Distances of reefs to the shore are often associated with differences in certain physico-chemical properties; e.g., gradients of nutrient levels, sedimentation, and turbidity are common across spatial scales (Edinger et al. 2000; Fabricius 2005; Cooper et al. 2007). Physical forces such as hydrodynamics can alter physico-chemical variables by driving fluxes, the residence time of sea water in reef systems, and the exchange of coastal reef water with the open sea (Monismith 2007; Lowe and Falter 2015). As a consequence, physico-chemical variables of coral reef ecosystems can fluctuate from favorable to less-favorable conditions on spatial scales of kilometers and on temporal scales of months (Schaffelke et al. 2012; Guadayol et al. 2014).

Coral reefs are considered to be among the most sensitive ecosystems in regard to changing environmental conditions (Hughes et al. 2003). Many studies have focused on how anomalies and changes of physico-chemical variables (such as above-average summer temperatures or increased coastal nutrient input) can drive shifts in the ecology and composition of coral reef benthic invertebrate assemblages and associated reef fish communities (van Woesik et al. 1999; Fabricius et al. 2005; Bauman et al. 2013; Furby et al. 2013; Jouffray et al. 2015). The fundamental role of bacterial communities in coral reefs is well recognized (Ainsworth et al. 2010; Dinsdale and Rohwer 2011; Bourne and Webster 2013). Many studies focus on the role of bacterial consortia associated with coral or sponge host organisms in symbiosis or disease (Rosenberg and Ben-Haim 2002; Rosenberg et al. 2007; Sunagawa et al. 2010; Hentschel et al. 2012; Bayer et al. 2013; Webster et al. 2013). However, less is known about the drivers and dynamics in microscopic assemblages of epilithic biofilms, such as epilithic bacterial communities (hereafter 'bacterial biofilms'). These bacterial biofilms are ubiquitous on surfaces in coral reefs, significantly contribute to productivity, biogeochemical cycles (Battin et al. 2003), and facilitate larval recruitment of key reef-organisms, such as reef-building corals (Webster et al. 2004; Hadfield 2011; Sneed et al. 2015). Consequently, intact bacterial biofilms are important to maintain coral reef functioning, but local anthropogenic stressors, such as terrestrial runoff (Witt et al. 2012a) and eutrophication (Sawall et al. 2012), and global climate change related factors (i.e., rising temperature and pH) can induce changes in coral reef biofilm communities (Webster et al. 2011; Witt et al. 2011a, 2012b).

The algal component of biofilms (hereafter 'algal biofilms') is another crucial part of the coral reef benthos. Epilithic algal turfs and crusts comprise a great part of reef primary production and constitute an essential food source for grazing reef fish (Wilson et al. 2003; Bonaldo and Bellwood 2010). Epilithic algae provide substrate for bacterial growth with different algal exudates selecting for specific bacterial communities (Barott et al. 2011a; Haas et al. 2013), which also impact coral recruitment. While algal turfs reduce the settlement of marine invertebrates and inhibit the survival of coral recruits (Kuffner et al. 2006; Arnold et al. 2010; Webster et al. 2015), crusts of coralline algae promote and induce the settlement of coral larvae (Heyward and Negri 1999). At a later succession stage certain algal taxa typically compete with corals for space (McCook et al. 2014). Under unfavorable conditions (e.g., high nutrient levels or overfishing) this can result in a so-called phase-shift from a coral-dominated towards an algal-dominated reef community, entailing the degradation of reef habitat (Hughes et al. 2007). Similar to bacterial biofilms, algal biofilm communities are highly responsive to changes in the environment, e.g. to temperature variation or pollution (Hatcher and Larkum 1983; Diez et al. 1999; Ferrari et al. 2012).

Coral reefs in the central Red Sea are exposed to physico-chemical changes driven by a seasonal cycle (Rasul et al. 2015), as exemplified by the prominent variability of sea water temperatures (Davis et al. 2011). These coral reefs commonly stretch over coastal platforms and form offshore reef structures and lagoonal inshore areas that give rise to spatial environmental gradients (Pineda et al. 2013; Klaus 2015a; Roik et al. 2015a). This setting offers the opportunity to explore spatio-temporal coral reef

dynamics. As in other regions, coral reef studies in the Red Sea have typically targeted benthic assemblages, such as reef-building coral and fish communities (Afeworki et al. 2013; Furby et al. 2013; Khalil et al. 2013; Riegl et al. 2013; Sawall et al. 2014). Conversely, comparatively little is known about the composition and dynamics of microscopic biota such as bacterial and algal biofilms. However, first insights on coral-associated bacteria show variable microbiomes in response to natural environmental gradients (Roder et al. 2015) and anthropogenic stressors (Röthig et al.; Jessen et al. 2013b; Ansari et al. 2015; Ziegler et al. 2016), indicating variability on the microscopic biotic level of Red Sea reefs.

In recent years, consequences of global climate change have been reported to affect coral reefs in the Red Sea. For instance, the Red Sea is already experiencing measurable ocean warming (Raitsos et al. 2011), it is susceptible to coral bleaching (Furby et al. 2013), and there are indications for a temperature related decrease of coral growth (Cantin et al. 2010; Roik et al. 2015a). However, most data on the physico-chemical conditions are still based on remote sensing or occasional sampling events (Cantin et al. 2010; Ngugi et al. 2012; Kürten et al. 2014; Sawall and Al-Sofyani 2015), rather than on continuous and more accurate *in situ* measurements. With many ecosystems increasingly affected by local and global anthropogenic stressors, comprehensive studies are needed that simultaneously record multiple physical, chemical, and biotic variables *in situ* to disentangle spatio-temporal dynamics and to provide a baseline against which impacts can be measured (Boyd and Hutchins 2012; Ban et al. 2014; Helmuth et al. 2014).

The lack of *in situ* baseline data was an important motivation for monitoring and collecting continuous physico-chemical and biotic data in this study. We use these data to characterize the natural baselines of central Red Sea reef environments. We then link physico-chemical and biotic parameters to extract putative physico-chemical drivers that contribute insights into coral reef functioning. As such we address the natural environmental variability of coral reefs in the central Red Sea to serve as a foundation for coral reef studies estimating the impact of global and local environmental pressures in this region.

3.3. Material and Methods

3.3.1. Study sites and design

This study was conducted in the Saudi Arabian central Red Sea encompassing three reefs along a cross-shelf gradient. Monitoring stations were set up at 7.5 - 9 m depth on the fore-reef slope of three geographically and visually distinct reef sites facing the open sea, 3 km (nearshore), 10 km (midshore), and 25 km (offshore) from the coast (Figure 3 A and B). The nearshore site is surrounded by comparably turbid inshore waters and by other nearshore reefs in close proximity. The mid- and offshore sites represent well-mixed habitats that are fully exposed to the open sea. NW-winds are characteristic for the study area throughout the year (Bower and Farrar 2015). Benthic cover differs between the three reefs with 24 % live benthos in the nearshore site and ~70 % in the midshore and offshore site. Calcifiers (corals and coralline algal crusts) are increasing in abundance from near- to offshore, while macro and turf algae are decreasing. Further details of reef habitat descriptions are available in a recent study detailing reef calcification by Roik et al. (2015a).

Each reef monitoring setup was comprised of one aluminum tripod for mooring of oceanographic instrumentation and one aluminum frame for deployment of sediment traps and terracotta tiles (Figure 3 C and D). Four seasons were consecutively measured over 3-month intervals from September 2012 to September 2013. Seasons were based on annual water temperature profiles from the region (Davis et al. 2011) as follows: fall starting on 15 September 2012, winter on 15 December 2012, spring on 15 March 2013, and summer on 15 June 2013 (for ease of reference seasons are arranged from spring to winter hereafter). Discrete seasonal samples such as sediment traps and settlement tiles were recovered at the end of each season (± 5 d) (Table 1, Supplementary Table 1). The Saudi Coastguard Authority under the auspices of KAUST issued sailing permits to the sites that included sample collection.

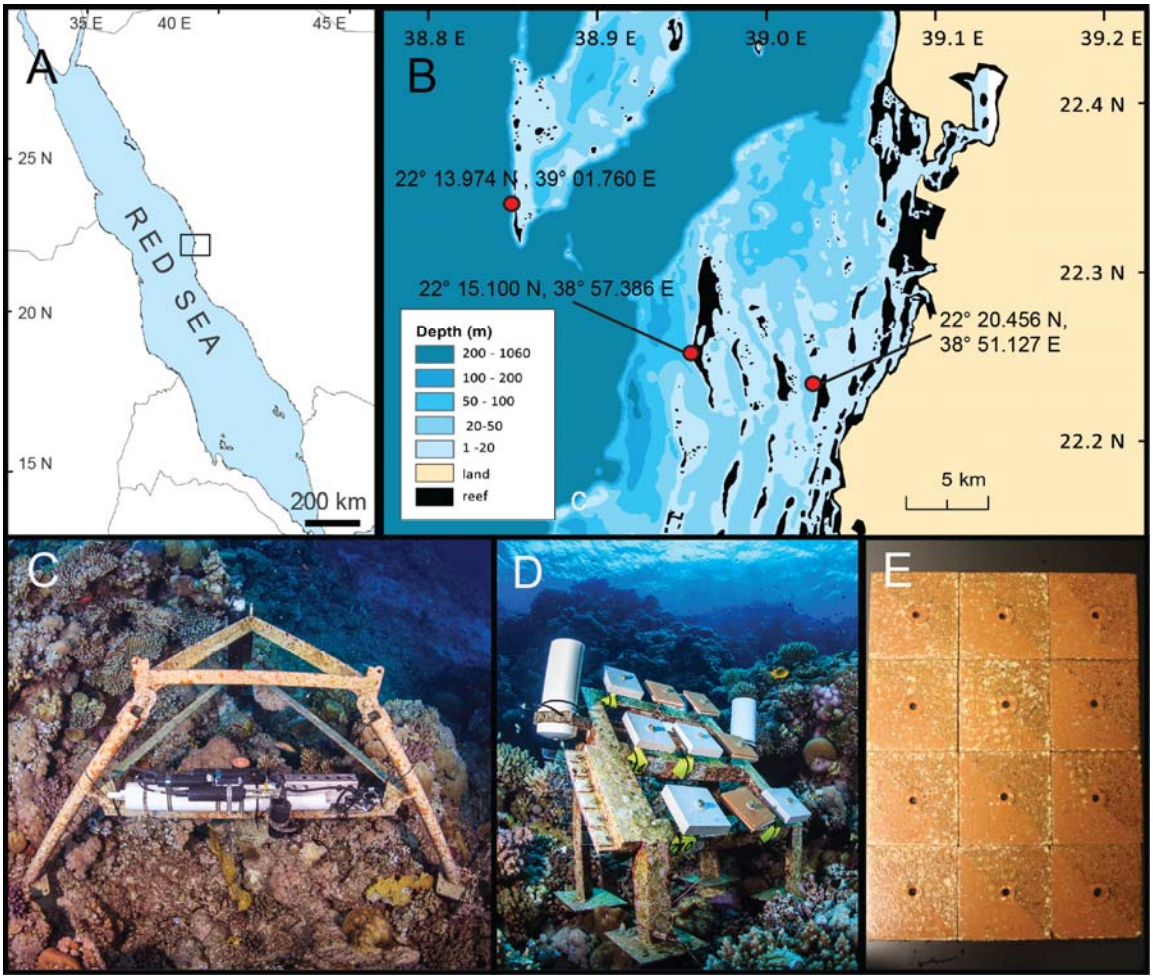

Figure 3 Map of study area and set up of coral reef monitoring sites in the central Red Sea. (A) The study area is located in the central Red Sea, (B) with three study sites (red markers) across the shelf. (C) Loggers (CTDs and ADCPs) for continuous data collection were moored to aluminum tripods fixed to the reef at 7 – 9 m depth. (D) Sediment traps and tiles were mounted on an aluminum frame fixed to the reef. (E) Sampled tiles after scraping of half of the biofilm for 16S rRNA gene amplification. Image credits: (A, B) Maha Khalil; (C, D) Tane Sinclair Taylor; (E) Stephan Kremb.

Table 1 Overview of monitoring data from three reefs along a cross-shelf gradient in the central Red Sea collected during 2012/2013.

			SPRING			SUMMER			FALL			WINTER		
Type of sampling		Variable	N	M	O	N	M	O	N	M	O	N	M	O
Current meters	Continuous	Current speed and direction	Deployment: March – June Logging Frq: 10 min;				Deployment: June – September Logging Frq: 10 min;			Deployment: September – December Logging Frq: 10 min;			Deployment: December – March Logging Frq: 10 min;	
CTDs		Temperature Salinity DO Turbidity Chlorophyll	Logging Frq: 60 min				Logging Frq: 60 min			Logging Frq: 60 min			Logging Frq: 60 min	
Reef water samples	Discrete	Phosphate Silicate Nitrate &Nitrite Ammonia					Sampling: September (2012) 6 Rep						Sampling: February (2012) 6 Rep	
		Reef water bacteria (total of 12 samples)	Sampling: June 1 Rep				Sampling: September 1 Rep			Sampling: December 1 Rep			Sampling: March 1 Rep	
Sediment traps	Seasonal	Sedi-mentation rate OC C:N ratio	Deployment: March - June 3 Rep;				Deployment: June - September 3 Rep;			Deployment: September - December 1-3 Rep;			Deployment: December - March 3 Rep;	
Terracotta tiles		Bacterial biofilm (total of 42 samples) Algal biofilm (total of 48 samples)	4 Rep				1-4 Rep			1-4 Rep			4 Rep	

This overview shows deployment months, number of data points, and replicate numbers from continuous logging and discrete/seasonal sampling events. The sampling design included a 4-season schedule (one season = three months) and three reef sites across the shelf of the central Red Sea. Continuous CTD and current data sets per reef and season contain 2000-2200 data points, apart from striped areas (900-1500 data points). Dark grey = physico-chemical data; Light grey = biotic data; White = missing data; N = nearshore, M = midshore, O = offshore, CTD = Conductivity-temperature-depth recorder; DO = Dissolved oxygen; OC = organic content of collected sediments; C:N = carbon-nitrogen ratio of collected sediments; Frq = frequency; Rep = replicates

Supplementary Table 1 Details on logging, collecting, and sampling design. See excel table.

3.3.2. Currents

Current speed (m s^{-1}) and direction were measured continuously using Nortek AS Aquadopp Doppler current meters (Vangkronken, Norway). Instruments were moored vertically to tripod frames (Figure 3 C) and exchanged every three months (Table 1). To reduce biofouling on the sensors a zinc oxide paste was applied (DESITIN®). Currents were recorded over 0.5 m bins about 1.5 m above the substrate and measurement intervals were set to 60-seconds burst-averaged current speeds at 10-minute sampling intervals (except for the midshore spring deployment with 10-seconds burst-averaged current speeds every 5-minutes). Rose plots were generated using the MATLAB (Release 2012b, The MathWorks, Inc., USA) function *wind_rose* (M MA 2010) showing frequencies of current directions and speeds (m s^{-1}) for reef and season, and for the full year. Collected data are available from the Dryad Digital Repository: http://dx.doi.org/10.5061/dryad.9mj14.

3.3.3. Temperature, salinity, dissolved oxygen, chlorophyll-a, and turbidity

Physico-chemical variables (i.e., temperature [°C], salinity [Practical Salinity Unit PSU], dissolved oxygen [DO; mg L^{-1}], turbidity [Nephelometric Turbidity Units NTU], chlorophyll-a [µg L^{-1}]) were logged continuously over three-month intervals (Table 1) using conductivity-temperature-depth (CTD) recorders (SBE 16plusV2 SEACAT, RS-232, Seabird, USA, Figure 3 C) that were equipped with a DO sensor (SBE 43, Seabird, USA) and an optical sensor for turbidity (700 nm) and chlorophyll-a fluorescence (ex/em: 470/695 nm; ECO FLNTU, WETlabs, USA). Sensors were fitted with automatic wipers counteracting biofouling on the sensor optics. Sampling frequency was set to 60-minutes intervals recording averages over 10 measurements.

Continuous data from the CTDs were plotted as time series and as density plots using R function *geom_density* (kernel density estimation, default settings) (Wickham and Chang 2015).

3.3.4. Dissolved inorganic nutrients

To report on levels of phosphate, silicate, nitrate & nitrite, and ammonia we used samples from the data set reported in Ziegler et al. (2015). Discrete water samples were collected at each of the monitoring stations, once in winter (11 and 29 February 2012) and again at the end of summer (10 and 24 September 2012) and filtered over GF/F filters (0.7 µm; Whatman, USA). We used six replicate values from samples collected at the depth of 5 m (n = 3) and 10 m (n = 3).

3.3.5. Sedimentation

Three replicate sediment traps (PVC tube traps, dimensions: D = 8.2 cm, H = 22 cm, placed 1 m above substrate, Figure 3 D) were used to measure sedimentation rates. A funnel was fixed in the opening of the traps to reduce turbulence and minimize colonization by large marine organisms. Sediment traps were replaced every three months (Table 1); they were closed under water and transported to the lab on ice. Sea water including all sediment was filtered onto 0.22 µm PVDF filters (Millipore, Billerica, MA, USA) and filters were stored at -80 °C until further processing. The samples were dried over night at 40 °C, weighed (Mettler Toledo, XS205, max 220 g, d = 0.01 g), and sedimentation rates were calculated as mg m^{-2} d^{-1}. To assess the organic content (OC), sediments were ground using mortar and pestle. From each sediment trap a subsample was muffled at 550 °C for 3 h, and the remaining ash-free

dry weight was determined. Additional subsamples were used to measure organic carbon (C) and nitrogen (N) concentrations as well as the respective isotopic signatures. Subsamples were acidified with 0.1 N HCl to remove inorganic C and CN content. Isotopic ratios ($\delta^{13}C$ and $\delta^{15}N$) were analyzed relative to Pee Dee Belemnite standard and atmospheric nitrogen using an isotope ratio mass spectrometer (Delta plus XP, Thermo Finnigan, USA).

3.3.6. Univariate analyses of physico-chemical variables

Univariate 2-factorial permutational MANOVAs (PERMANOVAs, Primer-E V6, Anderson et al. 2008) were used to characterize the differences between the factors "reef" (3 levels: nearshore, midshore, and offshore) and "season" (4 levels: spring, summer, fall, and winter) for each of the 10 physico-chemical variables, i.e., current direction, current speed, temperature, salinity, DO, chlorophyll-a, turbidity, sedimentation rate, and OC and C:N ratios of collected sediments. Analyses were performed on monthly means of the continuous variables and based on Euclidian distances, type III partial sum of squares, 9,999 unrestricted permutations of raw data.

To characterize the changes in inorganic nutrient levels (phosphate, silicate, nitrate & nitrite, and ammonia), univariate 2-factorial ANOVAs were conducted for each nutrient species, testing the factors "reef" (3 levels: nearshore, midshore, and offshore) and "season" (2 levels: summer and winter), followed by Tukey's HSD post-hoc tests where applicable (STATISTICA 10, StatSoft Inc. 2011).

3.3.7. Bacterial communities of biofilm and reef water

To assess biofilms, terracotta tiles were first sanded off on their non-glazed side to smoothen the surface, autoclaved, and then deployed at the monitoring sites (n = 4 tiles per site and season; Table 1). The tiles were attached to aluminum frames (Figure 3 D) and aligned to the angle of the reef slope with the non-glazed side facing the water column. After each recovery, tiles were rinsed with filtered sea water (0.22 µm), wrapped in aluminum foil, shock-frozen in liquid nitrogen on the boat, and stored at -80 °C. One half of each was used to characterize bacterial communities and to determine algal cover of the biofilm (see below).

Reef water bacterial communities were assessed as follows: water samples were taken with cubitainers (4 L, n = 1) in direct proximity of each monitoring setup at the end of each season on the day of recovery of the tiles. Water samples were transported on ice in the dark to the lab. From each sample, 1 L was filtered over a 0.22 µm Durapore PVDF filter (Millipore, Billerica, MA, USA) and filters were frozen at -80 °C until DNA extraction. Half of each water filter was cut into small stripes with sterile razorblades and transferred into a 2 ml vial. After adding 400 µl AP1 buffer of DNeasy plant kit (Qiagen, Hilden, Germany), the samples were incubated on a rotating wheel for 20 min and subsequently extracted following the manufacturer's protocol.

To assess bacterial biofilms present in the coral reef environment, samples were retrieved from terracotta tiles. Frozen tiles were placed on ice, unwrapped, and half of each tile was scratched off with a sterile razorblade (Figure 3 E). Each biofilm sample was transferred into a 2 ml vial, vortexed, and about 100 mg transferred into

a fresh vial. Next, 400 µl AP1 buffer (DNeasy plant kit, Qiagen) was added to each sample and DNA was extracted following the manufacturer's protocol. After extraction, DNA concentrations for each sample were quantified on a NanoDrop 2000C spectrophotometer (Thermo Fisher Scientific, Waltham, MA, USA). We used the primers 341F (5'-TCGTCGGCAGCGTCAGATGTGTATAAGAGACAGCCTACGGGNGGCWGCAG -3') and 805R 5'-(GTCTCGTGGGCTCGGAGATGTGTATAAGAGACAGGACTACHVGGGTATCTAATCC -3') that target the 16S V3 and V4 regions (Klindworth et al. 2012). The primers contained Illumina adapter overhangs used for subsequent indexing (underlined above; Illumina, San Diego, CA, USA). PCRs were performed in triplicate (with 5 - 14 ng DNA) using KAPA HiFi HotStart ReadyMix (KAPA Biosystems, Wilmington, MA, USA) with a final primer concentration of 0.2 µM and a total volume adjusted to 20 µl with RNase-free water. The amplification cycling temperatures were set to one cycle at 95 °C for 3 min, 25 cycles each at 98 °C for 30 sec, 55 °C for 30 sec, and 72 °C for 30 sec, followed by a final extension step at 72 °C for 5 min. PCR products from one of the triplicates were visually assessed via 1 % agarose gel electrophoresis with 10 µl per sample. Subsequently, triplicates were combined, PCR products were cleaned, indexed (8 cycles of indexing PCR using Nextera XT indexing adapters), and cleaned again following the Illumina 16S guidelines for MiSeq. All samples were quantified on the BioAnalyzer (Agilent Technologies, Santa Clara, CA, USA) and by Qubit (Quant-IT dsDNA Broad Range Assay Kit; Invitrogen, Carlsbad, CA, USA) and pooled in

equimolar ratios. Sequencing was performed using the Illumina SBS technology for MiSeq at 8 pM and 10 % phiX.

The software mothur (version 1.16.1, Schloss et al. 2009) was used for 16S rRNA gene analysis. Sequence reads were split according to barcodes, contigs were built, singletons (n = 1 over all samples) were removed, a pre-clustering step (2 bp difference, Huse et al. 2010) was implemented, quality-trimming was performed, and the data were aligned against SILVA (release 119, Pruesse et al. 2007). Chimeric sequences were removed using UCHIME as implemented in mothur (Edgar et al. 2011), and unwanted sequences (chloroplasts, mitochondria, archaea, eukaryotes, unknown), classified against Greengenes (McDonald et al. 2012) with a bootstrap of 60, were removed. Next, sequences of each sample were subsampled to 1,068 sequences, which eliminated six samples harboring from 7 - 207 sequences, resulting in 42 biofilm samples. Sequences determined in this study have been deposited in the NCBI Sequence Read Archive under accession number PRJNA306204 (http://www.ncbi.nlm.nih.gov/bioproject/PRJNA306204).

A 97 % similarity cutoff was chosen to obtain Operational Taxonomic Units (OTUs) using the average neighbor algorithm in mothur. OTUs were classified based on their most abundant sequences. Stacked column plots were created based on the relative abundances of OTUs in the taxonomic families for each reef and season. To characterize and compare bacterial community composition in reef water and biofilms, mothur was used to derive the numbers of shared OTUs between biofilm and water samples via Venn diagrams. mothur was further used to calculate Chao1

richness estimator (Chao 1984) and the Inverse Simpson's diversity index over each reef and season.

Due to different replication numbers for biofilm (n = 1 to 4) and water samples (n = 1), bacterial communities were evaluated using different statistical approaches. Alpha diversity indices of reef water communities were compared by two 1-way Kruskal-Wallis ANOVAs (firstly pooled for "reef", secondly for "season") followed by 2-tailed multiple comparisons tests where indicated. Two-factorial ANOVAs (for the factors "reef" and "season") were performed for biofilms comparing alpha diversity indices. Where applicable, Tukey's HSD post-hoc tests were conducted.

OTU reef water community data were ln(x + 1) transformed and tested using two 1-factorial PERMANOVAs (one each for the factors "season" and "reef"). Test designs were based on Bray-Curtis similarities, partial sum of squares type III, 9,999 permutations of residuals under a reduced model using Monte-Carlo simulations, and followed by pair-wise tests where applicable. OTU based biofilm data were ln(x + 1) transformed and tested with a 2-factorial PERMANOVA for differences within each of the factors "reef" and "season". Both data sets, i.e., bacterial communities of reef water and biofilms, were visualized in a non-Metric Multidimensional Scaling (nMDS) plot based on Bray-Curtis similarities. To test for differential abundance between "reefs" and "seasons", the OTU data set was filtered to retain all OTUs present in > 50 % of samples. This resulted in 72 reef water OTUs and 163 biofilm OTUs which were subjected to non-parametric Mack-Skillings analyses at a *p*-value cutoff of 0.01 (MeV V4.9, Saeed et al. 2003).

3.3.8. Algal biofilm communities

After each three-month deployment period, algal biofilms on recovered terracotta tiles were photographed with a stereomicroscope (Discovery.V20 SteREO and AxioCam MRm, Zeiss, Germany). To quantify the cover of functional categories overgrowing each tile, four to five randomly photographed subsections (1.4 x 1 cm) were examined using image-based analysis (CPCe software 4.1, Kohler and Gill 2006). In each subsample, the underlying organisms for 20 randomly selected points were assigned to one of nine functional categories: open space, filamentous algae, crustose coralline algae (CCA), green crusts (non-coralline light green crusts), red crusts (non-coralline red crusts), brown crusts (non-coralline dark-green and brownish crusts), cyanobacteria, red macro algae (fleshy upright red algae), and sessile invertebrates (Jessen et al. 2013a). Abundance counts for each tile were calculated as means of the subsections, converted to percent cover, and visualized in stack column plots per reef and season (n = 4).

Algae community data were ln(x + 1) transformed and tested for significant differences within each of the factors “reef” and “season” using a 2-factorial PERMANOVA and the same test design as for bacterial biofilms. To further visualize the structure of the data, an nMDS plot based on Bray-Curtis similarities was generated and a SIMilarity PERcentage (SIMPER) analysis (Primer-E V6) was conducted for “reef” and “season”. Each of the nine algal categories was tested for differential abundance between “reefs” and “seasons” by conducting non-parametric Mack-Skillings balanced design analyses at a *p*-value cutoff of 0.05.

3.3.9. Analyses of multivariate physico-chemical data and 'biological-environmental' matching

Analyses to characterize the overall physico-chemical conditions at the reef sites were based on 10 physico-chemical variables, i.e. current direction, current speed, temperature, salinity, DO, chlorophyll-a, turbidity, sedimentation rate, OC, and C:N ratio of collected sediments. Firstly, significant correlations between physico-chemical variables were determined using Spearman's rank correlation analysis (STATISTICA 10, Stat Soft Inc. 2011). Secondly, environmental data were tested for differences between "reefs" and "seasons" with a 2-factorial PERMANOVA (based on square-root transformed, normalized Euclidian distances, type III partial sum of squares and 9,999 permutations of residuals under a reduced model) and visualized using an nMDS plot.

To link multivariate physico-chemical to biotic data (i.e., reef water bacteria, bacterial biofilm, and algal biofilm), biological-environmental (BIOENV) matching was performed in Primer-E V6 (Clarke and Gorley 2006), based on Spearman's rank correlations and 999 permutations. This routine was run three times to test the match between each of the resemblance matrices of biotic data with the distance matrix of physico-chemical data, and to determine those combinations of physico-chemical variables that best explained the structure in the biotic data.

3.4. Results

We monitored three reefs along a cross-shelf gradient in the central Red Sea over an entire year and provide a detailed description of the seasonal dynamics of physico-

chemical and biotic properties in the three reef habitats (Figure 3). We organize the data according to scale, starting with physico-chemical variables and continuing with bi-annually measured inorganic nutrients and seasonal sedimentation levels. We then present data on bacterial community structure from the surrounding reef water. We further provide a first account of biotic communities, such as bacterial and algal biofilms. Our analyses explore the spatio-temporal dynamics of all physico-chemical and biotic variables and their interactions.

3.4.1. Currents

We recorded current directions and speeds in proximity (1.5 m) to the reef. Across all reefs, the main axis of current direction was parallel to the shore (NW-SE). Over the year, the offshore reef was dominated by currents from NW to SE (Figure 4 E3), whereas the flow in the nearshore reef was inverse with a main direction from SE to NW (Figure 4 E1). Variable currents from both directions and of similar frequencies characterized the midshore reef (Figure 4 E2). Current speeds reached maxima of 0.3 m s^{-1} at the offshore reef, which also experienced higher frequencies of strong currents compared to the other reef sites (

Table 2). Current directions significantly differed between reefs, but not between seasons, and current speed significantly differed between reefs and seasons

Table 3. Over all reefs, current speeds mostly ranged between 0 and 0.1 m s^{-1} and significantly increased in winter compared with current speeds in fall (

Table 3, Figure 4).

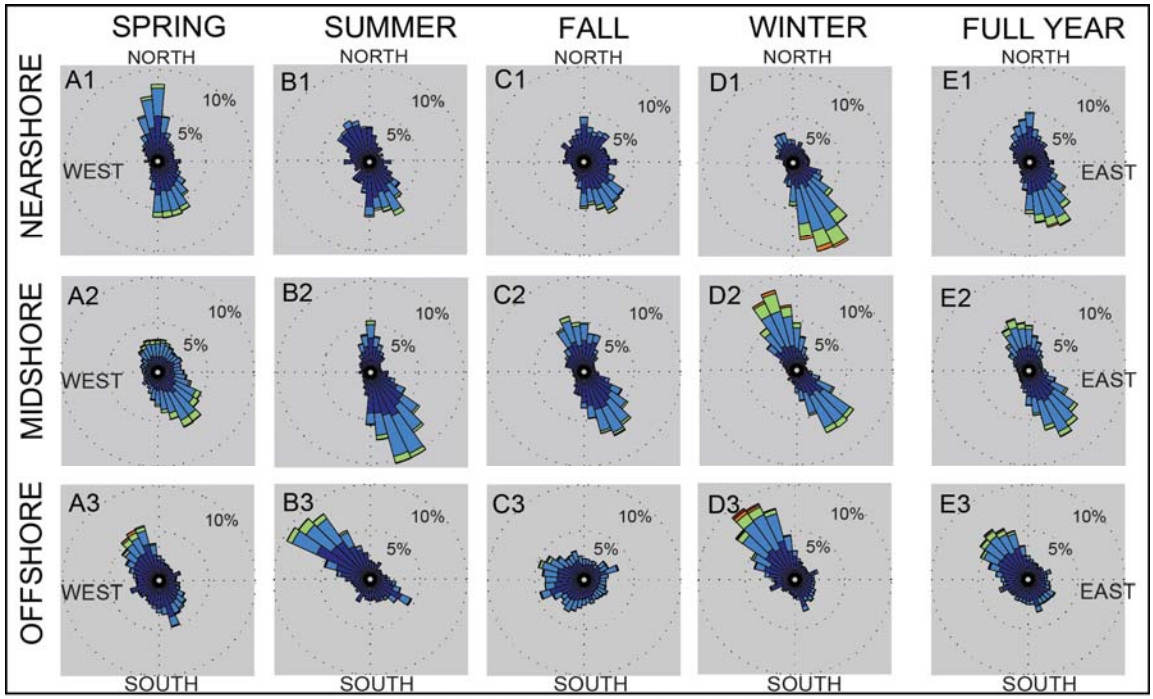

Figure 4 Current profiles of three coral reefs along a cross-shelf gradient in the central Red Sea during 2012/2013. Rose plots display seasonal current profiles and a full-year profile for each of the study sites (i.e., nearshore, midshore, and offshore). Lengths of bars show the frequencies of current directions (angle indicates the direction where currents come from), and their speeds are coded by color.

Table 2 Summary of physico-chemical variables of three coral reefs along a cross-shelf gradient in the central Red Sea during 2012/2013.

Variable	SPRING			SUMMER			FALL			WINTER		
	Near-shore	Mid-shore	Off-shore	Near-shore	Mid-shore	Off-shore	Near-shore	Mid-shore	Off-shore	Near-shore	Mid-shore	Off-shore
Current speed [m s^{-1}]												
mean	0.04	0.05	0.03	0.03	0.04	0.03	0.03	0.04	0.04	0.05	0.05	0.04
SD	0.03	0.03	0.03	0.02	0.03	0.02	0.02	0.03	0.02	0.03	0.03	0.03
Max.	0.16	0.22	0.22	0.14	0.17	0.17	0.18	0.22	0.19	0.19	0.17	0.30
Temperature [°C]												
mean	28.22	28.10	27.81	31.93	30.82	30.78	30.19	30.30	30.39	26.14	26.53	26.52
SD	1.06	1.10	1.08	0.46	0.77	0.56	1.35	1.02	1.05	0.63	0.57	0.58
Min.	26.65	26.48	26.16	31.0	28.83	29.32	27.0	28.28	27.95	24.09	24.24	25.32
Max.	30.83	30.3	30.07	33.06	32.3	32.07	32.15	31.67	31.83	27.7	28.37	28.17
Salinity [PSU]												
means	39.2	38.99	38.94	39.50	39.25	39.30	39.59	39.52	39.57	39.30	39.33	39.10
SD	0.12	0.12	0.14	0.10	0.16	0.21	0.16	0.13	0.13	016	0.17	0.20
Min.	38.96	38.73	38.44	39.19	38.92	38.99	39.14	39.04	39.02	38.89	38.9	38.75
Max.	39.56	39.27	39.33	39.7	39.54	39.86	39.87	39.77	39.77	39.56	39.67	39.52
Dissolved oxygen [mg L^{-1}]												
mean	2.86	3.52	3.86	2.22	3.45	3.44	2.96	4.11	3.65	3.12	4.04	3.61
SD	0.51	0.67	0.59	0.77	0.63	0.55	0.76	1.04	0.59	0.32	0.46	0.83
Min.	1.14	0.7	2.29	0.09	0.45	1.51	1.63	1.95	1.92	2.81	2.41	0.07
Max.	4.2	4.66	5.01	3.86	4.79	4.69	6.11	8.87	5.22	4.05	5.3	5.24
Turbidity [NTU]												
mean	0.41	0.49	0.41	0.49	0.35	0.63	0.47	0.48	0.44	0.53	0.47	0.20
SD	0.63	0.47	0.08	0.41	0.25	0.31	0.99	0.13	0.22	0.61	0.08	0.05
Min.	0	0	0.33	0.21	0.1	0.13	0.16	0	0.1	0.24	0.38	0.14
Max.	9.75	9.72	2.41	8.31	6.48	1.24	9.7	3.93	8.99	9.66	2.8	1.36
Chlorophyll-a [µg L^{-1}]												
mean	0.48	0.67	0.16	0.64	0.51	0.28	0.57	0.46	0.21	0.49	0.60	0.28
SD	0.16	0.11	0.07	0.19	0.26	0.11	0.27	0.13	0.09	0.23	0.14	0.10
Min.	0	0.31	0.07	0.3	0.16	0.03	0.12	0.11	0.06	0.09	0.24	0.11
Max.	2.03	3.4	0.65	2.67	1.53	0.75	3.18	1.86	0.69	3.4	1.32	0.93
Inorganic nutrients												
Phos. [µM] mean	-	-	-	0.05	0.05	0.06	-	-	-	0.09	0.09	0.09
SD	-	-	-	0.01	0.01	0.01	-	-	-	0.02	0.01	0.01
Silic. [µM] mean	-	-	-	0.34	0.34	0.19	-	-	-	0.63	0.52	0.57
SD	-	-	-	0.08	0.07	0.03	-	-	-	0.12	0.06	0.09
Nitr.[µM] mean	-	-	-	0.15	0.09	0.21	-	-	-	0.13	0.19	0.17
SD	-	-	-	0.08	0.07	0.13	-	-	-	0.03	0.03	0.08

Ammo. [µM] mean	-	-	-	0.12	0.19	0.20	-	-	-	0.16	0.17	0.15
SD	-	-	-	0.16	0.1	0.1	-	-	-	0.12	0.08	0.11
Sedimentation rate [mg m^{-2} day^{-1}]												
mean	72.88	100.64	155.28	126.95	57.40	59.96	75.94	100.1	61.44	192.89	69.38	88.18
SD	45.9	42.35	18.84	45.60	14.59	21.13	11.05	-	13.50	20.30	8.43	19.44
Organic content of collected sediments [mg m^{-2} day^{-1}]												
mean	12.84	14.33	18.02	18.88	9.59	12.47	13.18	15.56	6.01	28.51	10.30	10.79
SD	5.6	2.75	4.17	5.71	1.40	5.55	0.60	-	3.72	1.20	1.82	2.58
Avg.. % of total sediments	17.6	14.2	11.6	14.9	16.7	20.8	17.4	15.5	9.8	14.8	14.8	12.2
C:N ratio of collected sediments												
mean	6.17	6.59	6.26	7.44	7.30	8.12	6.01	5.81	6.81	6.15	6.83	7.38
SD	0.39	0.63	1.26	0.33	0.53	0.22	0.12	-	0.55	0.17	0.59	1.48

Means, standard deviations (SD), minima and maxima (Min./Max.) summarize physico-chemical data. Phos. = Phosphate, Silic. = Silicate, Nitr. = Nitrate and nitrite, Ammo. = Ammonia

Table 3 Differences of physico-chemical variables between three coral reefs along a cross-shelf gradient in the central Red Sea during 2012/2013.

	Univariate 2-factorial PERMANOVAs					
	Reef		Season		Reef x Season	
	Pseudo-*F*	*p*	Pseudo-*F*	*p*	Pseudo-*F*	*p*
Current direction	29.55	<0.001	0.68	0.569	6.75	<0.001
Current speed	10.07	0.001	7.97	0.001	1.86	0.133
Temperature	0.40	0.675	49.85	<0.001	0.53	0.785
Salinity	5.90	0.008	21.80	<0.001	1.52	0.222
Dissolved oxygen	21.09	<0.001	4.95	0.011	1.30	0.297
Turbidity	0.66	0.544	0.38	0.793	1.84	0.116
Chlorophyll-a	31.60	<0.001	0.43	0.744	1.91	0.118
Sedimentation rate	4.24	0.030	3.71	0.027	7.91	<0.001
OC	9.87	0.001	2.10	0.128	6.67	<0.001
C:N ratio	2.85	0.081	6.20	0.003	0.65	0.689

3.4.2. CTD variables

Physico-chemical variables were continuously logged in the three reefs along the cross-shelf gradient over the full year using CTDs. Data are displayed in time series and density plots (Figure 5). All seasonal means are summarized in (

Table 2). Differences in temperature and salinity were small between reefs and substantial over the year, whereas differences in DO, turbidity, and chlorophyll-a were pronounced between the reef sites, but not between seasons.

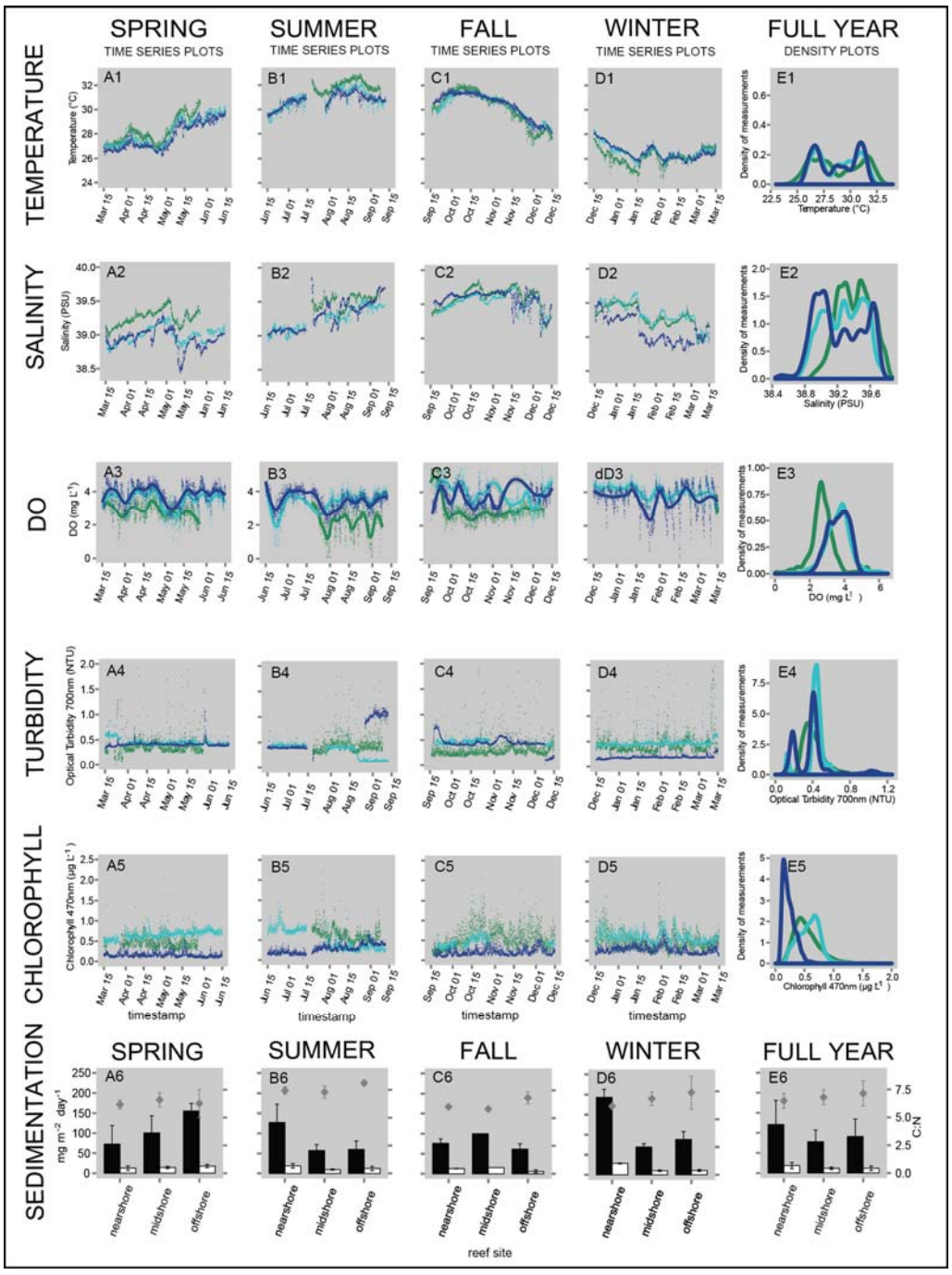

Figure 5 Physico-chemical variables of three coral reefs along a cross-shelf gradient in the central Red Sea during 2012/2013. Continuously logged data of temperature (A1-D1), salinity (A2-D2), dissolved

oxygen (DO; A3-d3), turbidity (A4-D4), and chlorophyll-a (a5–d5) is shown as time series plots over each season. The DO time series was fitted by polynomial regression (LOESS, span = 0.2). Plots in the last column (E1-E5) summarize full-year data using density plots (kernel density estimation) to display frequency densities of data points observed in each reef. In the density plot of DO, the winter data set was excluded, as data from the nearshore reef was missing for almost the entire season. Sedimentation variables (A6-E6) are presented in bar plots (means ± SD). Green = nearshore reef; light blue = midshore reef; dark blue = offshore reef; black bars = sedimentation rate; white bars = organic content of sediments; diamonds = C:N ratio of sediments.

3.4.2.1. Temperature

Highest temperatures were recorded in summer (max. 33 °C) and the lowest in winter

(min. 24 °C;

Table 2 and Figure 5 A1 - D1). In spring and fall, temperatures transitioned and spanned a range of 8.97 °C over all reefs and seasons. Density plots representing temperatures over the full year were bimodal (with two dominant frequency peaks) reflecting the substantial differences between the two seasons summer and winter (

Table 3 and Figure 5 E1). A non-significant trend in site differences was also apparent from the plots: the temperature profile in the midshore reef was widely overlapping with the offshore site. At the same time nearshore temperatures were higher than in midshore and offshore during summer, and lower during winter (Figure 5 B1 and D1).

3.4.2.2. Salinity

Salinity was lowest in spring (min. 38.4 PSU) and increased over the summer reaching the highest values in fall (max. 39.9 PSU;

Table 2 and Figure 5 A2 and C2). Most prominent seasonal differences were found in the offshore reef (spanning a range from 38.44 to 39.86, Figure 5 E2). Salinity at the nearshore site was increased compared to the other sites, except in fall when salinity values were very similar and highest across all reefs (Figure 5 C2). All site and seasonal differences were significant (

Table 3). Importantly, variability was limited to a relatively small annual range of 1.43 PSU.

3.4.2.3. Dissolved oxygen (DO)

Seasonal means for DO included day and night measurements and ranged between 2.22 ± 0.77 and 4.11 ± 1.04 mg L^{-1} (

Table 2). Seasonal differences were significant (

Table 3). The variability over the full year was similar to the variability on shorter time scales: DO range for the full year was 8.81 mg L^{-1} and the range of DO within one reef and one season was up to 6.92 mg L^{-1}. More obvious were the differences between sites, with lower DO levels at the nearshore site compared to the midshore and offshore reefs (

Table 3 and Figure 5 A3 - E3).

3.4.2.4. Turbidity and chlorophyll-a

Turbidity levels were lowest in winter (0.20 ± 0.05 NTU) and highest in summer (0.63 ± 0.31 NTU) at the offshore site. Chlorophyll-a values ranged between 0.16 ± 0.07 µg L^{-1} and 0.67 ± 0.11 µg L^{-1}, recorded during spring in the offshore and midshore site, respectively (

Table 2). Only site differences were statistically significant for chlorophyll-a (

Table 3), characterized by a larger variability and higher values in the nearshore reef and lower values of decreasing variability with distance from shore (Figure 5 A4 - E4 and A5 - E5).

3.4.2.5. Dissolved inorganic nutrients

Bi-annual measurements of phosphate, silicate, nitrate & nitrite, and ammonia revealed overall low inorganic nutrient levels (

Table 2). Nitrate & nitrite levels and ammonia did not vary significantly between reefs and seasons. The means of nitrate & nitrite were 0.16 ± 0.08 μM and 0.17 ± 0.11 μM for ammonia. Phosphate and silicate concentrations were significantly higher in winter (0.9 ± 0.01 and 0.57 ± 0.10 μM, respectively) than in summer (0.05 ± 0.01 and 0.29 ± 0.09 μM; both $p < 0.001$, ANOVA). Additionally, nearshore silicate levels were significantly higher compared to offshore (nearshore 0.48 ± 0.18 μM, offshore 0.38 ± 0.21 μM; $p < 0.05$, ANOVA).

3.4.2.6. Sedimentation

Sediment traps were used to measure sedimentation rates, organic content (OC), and C:N ratios of the collected sediments (Figure 5 A6 – E6). Rates differed significantly between reefs and seasons with a significant interaction between both factors (

Table 3). The highest seasonal sedimentation rate was measured at the nearshore reef during winter (193 ± 20 mg m^{-2} day^{-1}), and the lowest at the midshore reef during summer (57 ± 15 mg m^{-2} day^{-1};

Table 2). During summer, fall, and winter, sedimentation rates decreased with distance from shore (Figure 5 B6 –D6). Spring showed an inverse pattern with increasing sedimentation rate from nearshore to offshore (Figure 5 A6).

OC content of collected sediments also significantly differed between reef sites, but not between seasons, and we found a significant interaction between both factors (

Table 3). OC content ranged from 6.01 ± 3.72 mg m^{-2} day^{-1} to 28.51 ± 1.02 mg m^{-2} day^{-1} (

Table 2), which resulted in an average contribution of 15.03 ± 2.96 % to total collected sediments. During spring and fall, the percentage of OC in sediments significantly decreased with increasing distance to shore (from 17.6 to 11.6 %, and from 17.4 to 9.8 % of total collected sediments, respectively;

Table 2). This trend was reversed during summer: OC contribution was increasing with larger distance from shore (from 14.9 to 20.8 %). During winter OC content was similar in all reefs (12.2 – 14.8 %). The C:N ratio of collected sediments ranged between 6 – 8 across reefs and seasons (

Table 2). C:N ratios in summer (7.3 – 8.1) were significantly higher compared to all other seasons (between 5.8 and 7.4,

Table 2,

Table 3). Differences between reefs were not significant, but measurements indicate a trend of an increase in C:N ratio with distance from shore (Figure 5 A6 – E6).

3.4.3. Community composition and dynamics of reef water bacteria and bacterial biofilms

MiSeq amplicon sequencing of the 16S rRNA gene from 12 reef water and 42 biofilm samples produced a total of 4,183,963 sequences that clustered into 3,418 Operational Taxonomic Units (OTUs) at 97 % after editing (Supplementary Table 2). Good's coverage (Good 1953) ranged between 0.92 – 0.97 for water samples and 0.73 – 0.95 for biofilm samples. The average number of OTUs per sample was 144 (± 15 SD) and 355 (± 58 SD) for reef water and biofilms samples, respectively. 408 OTUs were present in reef water, 2,929 in biofilms, and only an additional 81 OTUs (i.e. 2 %) were shared between them. Average diversity (Inverse Simpson's index (ISI) 108.27 ± 35.95) and richness (Chao1 670.93 ± 178.29) were far higher in biofilm samples than in reef water samples (ISI 7.76 ± 2.72; Chao1 220.99 ± 41.82). Additional information on sequencing and OTU data of water and biofilm samples are presented in Supplementary Table 3 and Table 4.

Table 4 Summary of biotic variables (reef water bacteria, bacterial biofilms, algal biofilms) of three coral reefs along a cross-shelf gradient in the central Red Sea during 2012/2013.

	SPRING			SUMMER			FALL			WINTER		
Variable	Near-shore	Mid-shore	Off-shore	Near-shore	Mid-shore	Off-shore	Near-shore	Mid-shore	Off-shore	Near-shore	Mid-shore	Off-shore
Reef water bacteria												
#OTUs	119	139	125	121	132	122	117	132	125	99	104	154
Chao1	205	254	247	218	271	236	191	212	232	140	165	282
ISI	11	7	8	7	6	14	7	7	6	6	4	10
Bacterial biofilms												
#OTUs	415 (10)	377 (37)	346 (15)	274	446 (14)	363 (72)	319	293 (77)	311 (37)	347 (13)	316 (44)	365 (23)
Chao1	767 (61)	682 (91)	678 (70)	412	971 (63)	671 (228)	568	583 (273)	539 (170)	711 (72)	523 (152)	674 (80)
ISI	141 (21)	134 (35)	91 (7)	71	164 (38)	119 (34)	99	63 (32)	87 (14)	89 (19)	99 (19)	108 (6)
Algal biofilms												
SIMPER results (% contrib.)	Open Space 29.1%	Brown crusts 26.4%	Brown crusts 27.6%	Open Space 29.8%	Brown crusts 26.4%	Open Space 29.2%	Open Space 11.0%	Open Space 32.4%	Open Space 27.5%	Open Space 28.0%	Open Space 32.3%	Open Space 28.8%
	Brown crusts 22.1%	Open Space 22.1%	Open Space 26.7%	CCA 26.3%	Open Space 25.7%	Brown crusts 23.8	CCA 24.5%	Green crusts 21.5%	CCA 26.1%	Green crusts 20.3%	Brown crusts 28.1%	Green crusts 26.3%
	CCA 21.7%	Green crusts 17.7%	Green crusts 18.4%	Green crusts 21.2%	Green crusts 20.5%	CCA 20.8%	Green crusts 16.9%	Brown crusts 20.1%	Green crusts 24.4%	Brown crusts 19.4%	Green crusts 13.5%	Brown crusts 24.3%
Total % contrib.	72.9%	66.2%	72.8%	77.2%	72.7%	73.8%	74.4%	74.1%	77.7%	67.8%	73.9%	79.2%

Biofilm and reef water bacterial communities are represented as means (± SD) of #OTUs, and alpha diversity indices: Chao1 richness estimator and Inverse Simpson's diversity index (ISI). Values without SDs had only 1 replicate (see Supplementary Table 1). For algal biofilms, the three main contributors to similarity within each reef per season according to SIMilarity PERcentrage analysis (SIMPER) are listed; #OTUs = number of distinct operational taxonomic units; contrib. = contribution; CCA = crustose coralline algae

Supplementary Table 2 Overview of sequence abundance counts per OTU and sample, OTU taxonomic classification, and OTU 16S rRNA reference sequence for bacterial communities of seawater and biofilms. See excel table.

Supplementary Table 3 Summary statistics for sequences and OTU-based alpha-diversity measures for bacterial communities of seawater and biofilm. See excel table.

3.4.3.1. Community composition and dynamics of reef water bacteria

Reef water bacterial communities were dominated by the family Synechococcaceae (Cyanobacteria; 30 – 55 %). Together with Flavobacteriaceae (5 – 21 %),

Pelagibacteraceae (4 – 10 %), OCS15 (3 – 9 %), Halomonadaceae (1 – 10 %), Rhodospirillaceae (1 – 6 %), Rhodobacteraceae (1 – 7 %), and unclassified proteobacteria (4 – 9 %), these bacterial families comprised up to 85 % of the entire community (Figure 6 A). Alpha diversity indices (Table 4) of reef water bacterial communities were not statistically different between reefs or seasons ($p > 0.05$, Kruskal-Wallis ANOVAs), but comparisons of reef water bacterial communities based on OTU abundance showed significant differences between seasons in multivariate PERMANOVAs (Table 5, Figure 6 B). We did not identify significant differentially abundant OTUs on a spatial or seasonal scale using univariate Mack-Skillings tests, likely due to the absence of replicates for seawater bacterial communities.

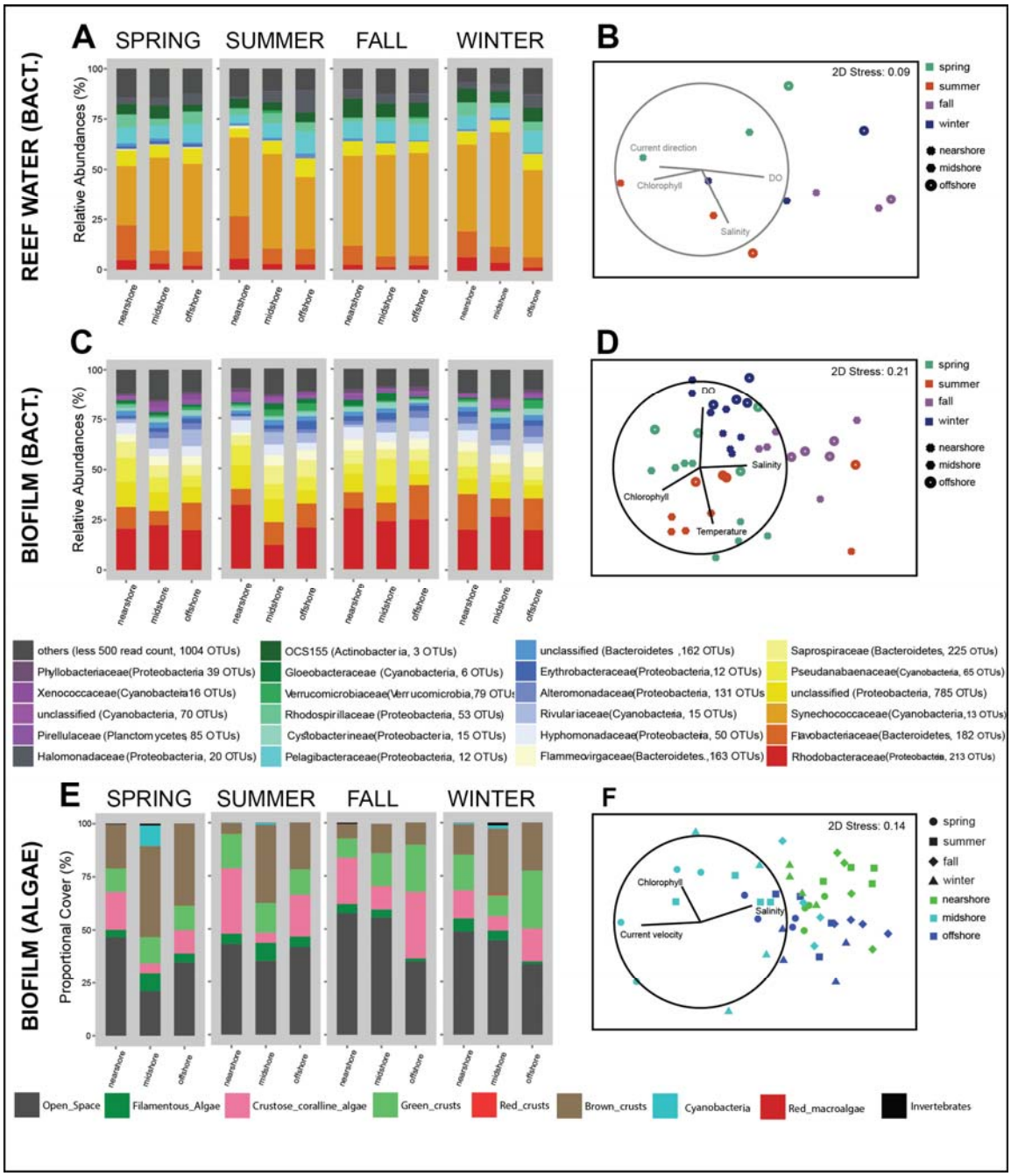

Figure 6 Community structure of reef water bacteria and bacterial and algal biofilms at three coral reefs along a cross-shelf gradient in the central Red Sea during 2012/2013. Stack column plots and non-Metric Multidimensional Scaling (nMDS) plots show the bacterial community composition of (A - B) reef water, and (C – D) bacterial biofilms. In the plots (E – F), algal composition of biofilms is illustrated. nMDS plots are based on Bray-Curtis similarities of ln(x+1) transformed data. Vectors (in B, D, F) represent combinations of physico-chemical variables, which best explain the structure of the biotic data (Biological-environmental (BIOENV) matching routine). The length of the vectors indicates their correlation coefficients with the nMDS axes. Vectors in black represent significant correlates, grey indicate statistically non-significant correlates from the BIOENV analysis.

Table 5 Spatio-seasonal structuring of biotic and physico-chemical data from three coral reefs along a cross-shelf gradient in the central Red Sea during 2012/2013.

	Reef		**Season**		**Reef x Season**	
	Pseudo-*F*	*p*	Pseudo-*F*	*p*	Pseudo-*F*	*p*
Reef water bacterial communities	1.40	0.176	2.04	**0.023**	-	-
Bacterial biofilm communities	3.27	**<0.001**	3.05	**<0.001**	1.57	**<0.001**
Algal biofilm communities	18.64	**<0.001**	8.54	**<0.001**	2.74	**0.001**
Physico-chemical variables	10.96	**<0.001**	7.34	**<0.001**	3.07	**<0.001**

Bacterial reef water communities were tested using 1-factorial permutational MANOVAs (PERMANOVAs) with Monte Carlo simulations. Bacterial biofilms, algal biofilms, and 10 physico-chemical variables were tested with multivariate 2-factorial PERMANOVAs.

3.4.3.2. Community composition and dynamics of bacterial biofilms

Dominant bacterial families were Rhodobacteraceae (11 – 31 %), Flavobacteriaceae (7 – 17 %), unclassified Proteobacteria (5 – 12 %), and Pseudanabaenaceae (3 – 12 %), which together comprised about 50 % of the biofilm communities (Figure 6 C). Further, the bacterial families Saprospiraceae, Flammeovirgaceae, Hyphomonadaceae, Rivulariaceae, Alteromonadaceae, Erythrobacteraceae (each contributing 1 – 9 %), unclassified Bacteroidetes, Cystobacterineae, Gloeobacteraceae, Verrucomicrobiaceae, Pirellulaceae, and unclassified Cyanobacteria (each with < 3 %) added up to 85% of community composition.

OTU-based alpha diversity of bacterial biofilm communities differed between seasons, with significantly lower ISI values in fall and winter and higher values in spring and summer ($p < 0.05$, Table 4). Bacterial community composition of biofilms significantly varied between reefs and seasons including a significant interaction

found by multivariate PERMANOVA (Table 5 and Figure 6 D). Pair-wise tests showed that differences were significant between almost all pairs of reefs and seasons (Table 5).

Overall, 21 OTUs were differentially abundant between reefs, while 30 OTUs were different between seasons (Table 6 and Supplementary Table 4). Among these, 5 OTUs displayed significantly different abundances between seasons and reefs. Sequence counts for these OTUs comprised 29 % of all biofilm sequences (Figure 7) and displayed the following abundance patterns: 14 OTUs gradually increased or decreased over the cross-shelf gradient, and 18 OTUs changed in abundance between the seasons. Most abundant OTUs that were significantly different between seasons belonged to the families Rhodobacteraceae (OTU00003: *Loktanella* sp*;* OTU00017 and OTU00019: unclassified Rhodobacteraceae), Cystobacterineae (OTU00030: unclassified Cystobacterineae), and Gloeobacteraceae (OTU00010: *Gloeobacter* sp). The most abundant OTU significantly varying between reefs was classified as *Halomicronema* sp in the family Pseudanabaenaceae (OTU00021), and *Muricauda* sp, a Flavobacteriaceae (OTU00015), varied between reefs and seasons. Bacterial taxa that significantly changed in abundance between the warmer and colder seasons were *Rhodovulum* sp (OTU 00122), *Rhodobaca* sp (OTU 00135), and an unclassified bacterium (OTU 00135), *Gloeobacter* sp (OTU 00010), one unclassified bacterium of Flammeovirgaceae (OTU 00161), a bacterium of the order of Myxococcales (OTU 00232), and one from the family A4b (OTU 00419). All differentially abundant OTUs in reef biofilms were highly similar (94 – 99 % identity) to sequences that had

previously been encountered in marine and hypersaline environments (BLAST results, Supplementary Table 4).

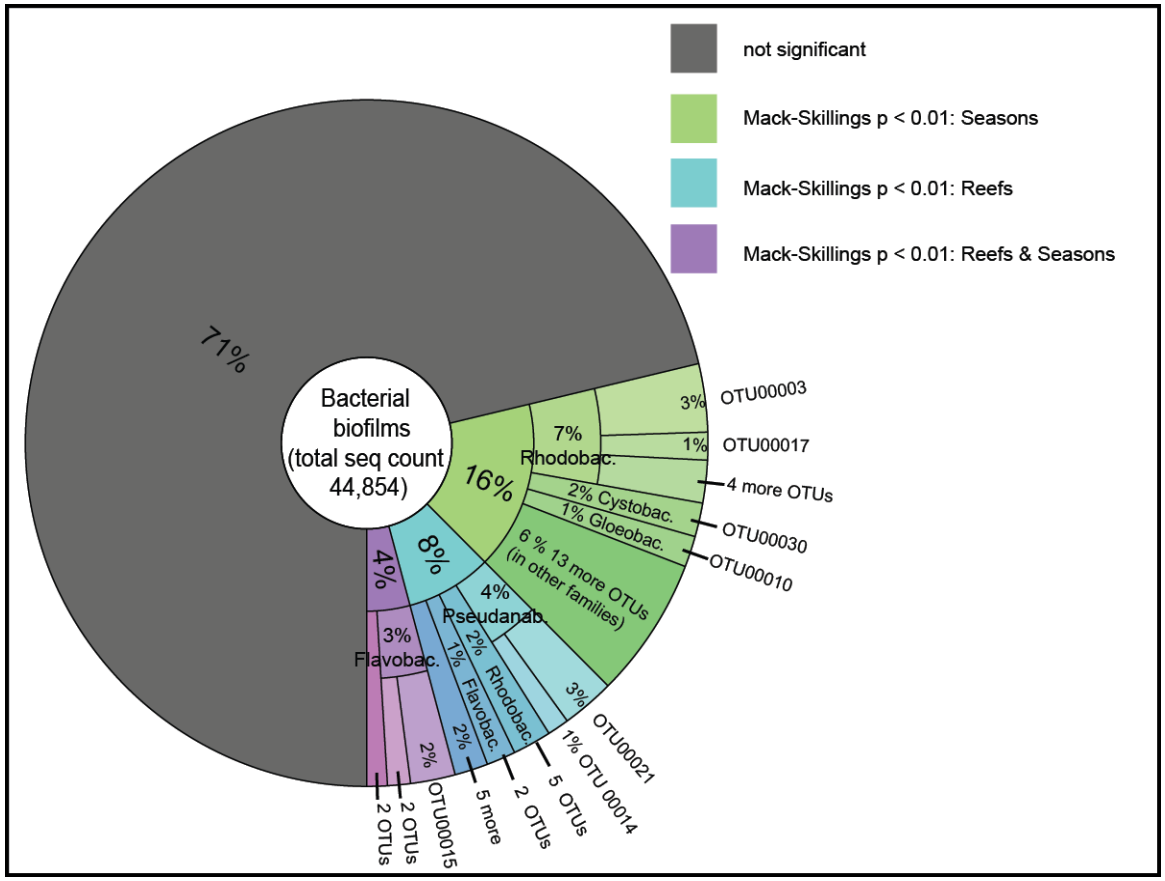

Figure 7 Proportions of sequences belonging to differentially abundant OTUs. (Rhodobac. = Rhodobacteraceae; Cystobac. = Cystobacterineae; Gloeobac. = Gloeobacteraceae; Peudanab. = Pseudanabaenaceae; Flavobac. = Flavobacteriaceae).

Table 6 Differentially abundant bacterial OTUs and algal groups of biofilms over reefs and seasons.

Bacterial family (OTU)	Sequence counts per OTU	*p* (reef)	*p* (season)	Spatial pattern	Seasonal pattern
Abundance pattern: spatial gradient					
Flavobacteriaceae(OTU00067)	301	< 0.01	0.03	increasing from NEARSHORE to OFFSHORE	-
Xenococcaceae(OTU 00048)*	286	< 0.01	< 0.01		
Rhodobacteraceae(OTU 00097)	267	< 0.01	0.14		
Flavobacteriaceae(OTU 00134)*	210	< 0.01	< 0.01		
Verrucomicrobiaceae(OTU 00206)	173	< 0.01	0.02		
Rhodobacteraceae(OTU 00145)*	151	< 0.01	< 0.01		
Rhodobacteraceae(OTU 00331)	145	< 0.01	< 0.01		
Erythrobacteraceae(OTU 00058)	61	< 0.01	0.60		
Pseudanabaenaceae(OTU 00021)	1123	< 0.01	< 0.01	decreasing from NEARSHORE to OFFSHORE	-
Flavobacteriaceae(OTU 00015)*	951	< 0.01	0.00		
Flavobacteriaceae(OTU 00062)	317	< 0.01	0.05		
Rhodobacteraceae(OTU 00074)	232	< 0.01	0.04		
Hyphomonadaceae(OTU 00061)	181	< 0.01	0.34		
Rhodobacteraceae(OTU 00090)	131	< 0.01	0.40		
Abundance pattern: other spatial					
Pseudanabaenaceae(OTU 00014)	461	< 0.01	0.35	increased in MIDSHORE	-
unclassified Alphaproteobacteria(OTU 00065)	205	< 0.01	0.21		
Rhodobacteraceae(OTU 00259)	48	< 0.01	0.45		
Flavobacteriaceae(OTU 00031)*	276	< 0.01	< 0.01	decreased in MIDSHORE	-
Flammeovirgaceae(OTU 00179)	88	< 0.01	0.04		
Abundance pattern: increased during warmer seasons					
Gloeobacteraceae(OTU 00010)	656	0.15	< 0.01	-	increased in SUMMER and FALL
Rhodobacteraceae(OTU 00122)	125	0.66	< 0.01		
unclassified Deltaproteobacteria (Myxococcales)(OTU 00232)	101	0.04	< 0.01		
Pseudanabaenaceae(OTU 00032)	78	0.94	< 0.01		
A4b(OTU 00419)	50	0.25	< 0.01		
Rhodobacteraceae(OTU 00019)	500	0.02	< 0.01	-	increased in FALL
Flammeovirgaceae(OTU 00161)	143	0.02	< 0.01		
Rhodobacteraceae(OTU 00135)	103	0.49	< 0.01		
Abundance pattern: decreased during warmer seasons					
Cystobacterineae(OTU 00030)	713	0.04	< 0.01	-	increased in SPRING and WINTER
Cohaesibacteraceae(OTU 00004)	412	0.21	< 0.01		
Xenococcaceae(OTU 00048)*	286	< 0.01	< 0.01	-	increased in SPRING
Kiloniellaceae(OTU 00249)	214	< 0.01	< 0.01		
unclassified Alpharoteobacteria(OTU 00131)	170	0.20	< 0.01	-	increased in WINTER
Rhodobacteraceae(OTU 00145)*	151	0.01	< 0.01		
Flammeovirgaceae(OTU 00155)	86	0.41	< 0.01		
Flavobacteriaceae(OTU 00201)	70	0.75	< 0.01		
Flammeovirgaceae(OTU 00137)	69	0.02	< 0.01		
Phycisphaeraceae(OTU 00083)	61	0.96	< 0.01		
Abundance pattern: other seasonal					
Alteromonadaceae(OTU 00093)	287	0.02	< 0.01	-	increased in FALL and WINTER
Flavobacteriaceae(OTU 00031)*	276	< 0.01	< 0.01		
Abundance pattern: temporal succession					
Rhodobacteraceae(OTU 00003)	1441	0.04	< 0.01	-	increasing from SPRING to WINTER
Flavobacteriaceae(OTU 00015)*	951	< 0.01	< 0.01		
Rhodobacteraceae(OTU 00017)	585	0.28	< 0.01		

Hyphomonadaceae(OTU 00016)	498	0.10	< 0.01		
Rivulariaceae(OTU 00059)	353	0.09	< 0.01		
Flavobacteriaceae(OTU 00134)*	210	< 0.01	< 0.01		
Rhodobacteraceae(OTU 00053)	172	0.19	< 0.01	-	decreasing from SPRING to WINTER
Trueperaceae(OTU 00091)	163	0.02	< 0.01		
Pseudanabaenaceae(OTU u00055)	119	0.29	< 0.01		
Pseudanabaenaceae(OTU 00147)	109	0.74	< 0.01		
Algal group	Count per group	*p* (reef)	*p* (season)	Spatial pattern	Seasonal pattern
Abundance pattern: spatial					
Green crusts	712	0.03	0.08	increased in OFFSHORE	-
Cyanobacteria	55	0.02	0.46	increased in MIDSHORE	-
Filamentous Algae	225	0.04	0.35	decreased in OFFSHORE	-
Abundance pattern: spatial and temporal					
CCA	751	< 0.01	< 0.01	decreased in MIDSHORE	increased in SUMMER and FALL
Brown crusts	1056	< 0.01	< 0.01	increased in MIDSHORE	increased in SPRING and WINTER
Open Space	1985	< 0.01	0.02	decreasing from NEARSHORE to OFFSHORE	increased in FALL

All significant results (Mack-Skillings tests; $p < 0.01$ for bacterial OTUs and $p < 0.05$ for algal groups) are denoted with a description of spatial and/or seasonal abundance pattern.

Supplementary Table 4 Differentially abundant bacterial OTUs and algal groups of biofilms over reefs and seasons. See excel table.

3.4.3.3. Community composition and dynamics of algal biofilms

We assessed the composition of algal biofilms based on a total of 4,797 counts from 48 terracotta tiles. After three months exposure in the reefs, epilithic algae on average covered > 50 % of each tile surface. The lowest algal cover (40 – 55 %) occurred nearshore and midshore during fall and winter, whereas the highest algal cover (79 %) occurred in the midshore reef during spring. Dominant algal categories were brown crusts (5 – 40 %), CCA (5 – 30 %), and green crusts (10 – 30 %). Filamentous algae were present at low proportions (1 – 9 %). Other rare categories, such as cyanobacteria (< 2 %) and sessile invertebrates (~1 %) were only found on tiles in nearshore and midshore reefs. We did not encounter red macro algae. Red crusts

were widely absent as well, except for the midshore reef during winter where the cover was < 1 % (Figure 6 E).

Brown crusts, CCA, green crusts, and open space, each contributed about 20 to 30 % to the similarity within each reef and season, cumulatively explaining about 65 to 80 % of the variability in algal communities (SIMPER, Table 4). Algal biofilm communities from the midshore reef had a larger variation over seasons (Bray-Curtis similarity 87.27, SIMPER; Figure 6 F) compared to algal communities from the nearshore and offshore reefs (92.99 and 91.89, respectively, SIMPER). Algal community composition was significantly different between reefs and seasons, including a significant interaction component (Table 5). The algal community of each reef in each season was significantly different from all others (pairwise comparisons, $p < 0.05$), except summer and winter in the nearshore reef, and spring and summer in the offshore reef ($p > 0.05$) (Table 6, Supplementary Table 4). Algal cover significantly increased with distance to shore. Seasonal variability of algal biofilms was characterized by a higher occurrence of brown crusts in the spring and winter, and of CCA in fall, which coincided with a decrease of total algal cover.

3.4.4. Physico-chemical environment and drivers of biotic communities in coral reefs

Physico-chemical conditions structured reefs and seasons and were most different between summer and winter and the geographically most distant reefs, nearshore and offshore, as visualized in the nMDS plot (all $p < 0.001$; Table 5 and Figure 8).

Several pairs of physico-chemical variables varied jointly or inversely between reefs and seasons (

Table 7): Current speeds and directions significantly correlated with chlorophyll-a. Current speeds were inversely correlated with temperature. Temperature significantly correlated with salinity and DO, while DO correlated with chlorophyll-a. We found significant correlation of chlorophyll-a with turbidity and sedimentation rates with OC content of sediments.

Differences in multivariate physico-chemical data correlated with differences in biotic communities. A combination of salinity, chlorophyll-a, DO, and current direction best explained variations in reef water bacterial communities, but this correlation was not significant (

Table 7, Figure 6 B). The matching of physico-chemical properties with bacterial biofilm communities resulted in a significant correlation, and the patterns were best explained by a combination of temperature, salinity, chlorophyll-a, and DO (Figure 6 D). Differences in physico-chemical data and algal biofilm composition were best explained by the variables salinity, chlorophyll-a, and current speed that were also statistically significant (Figure 6 F).

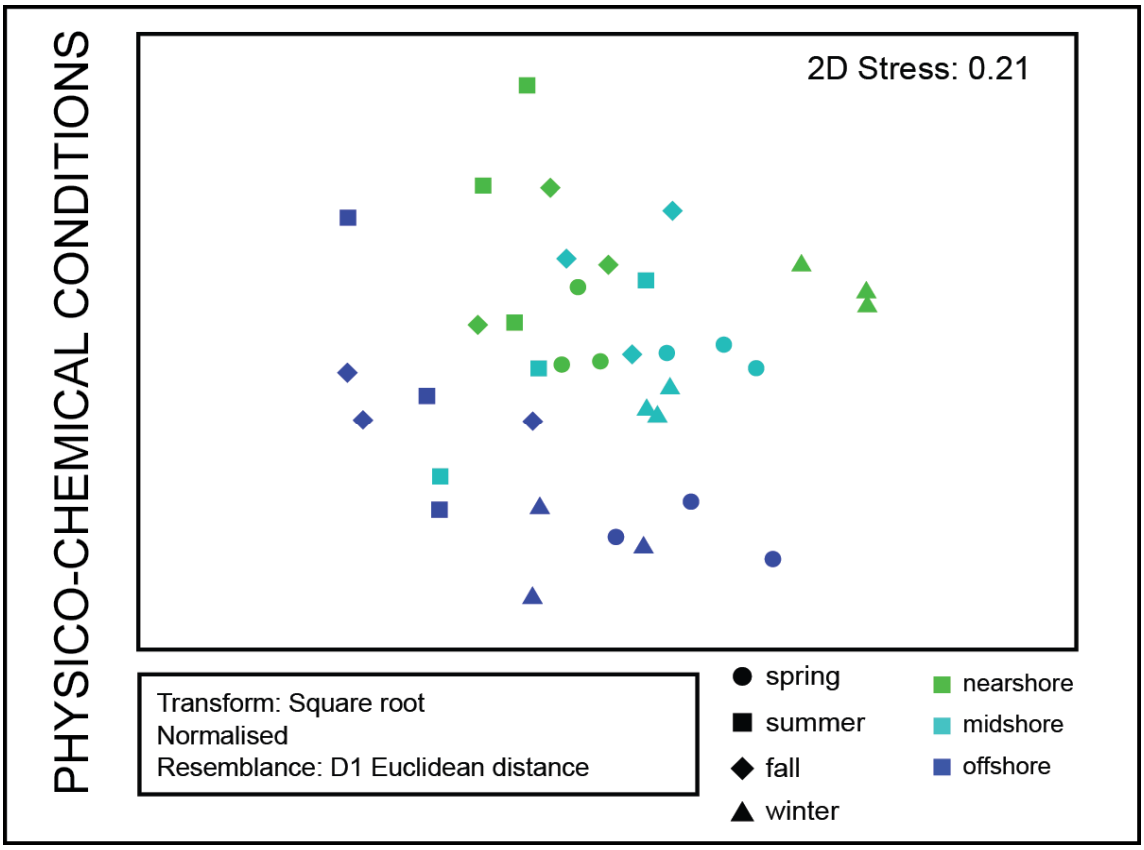

Figure 8 Structuring of reef habitats by physico-chemical conditions. Non-Metric Multidimensional Scaling (nMDS) plot illustrates the structure of reef environments based on 10 physico-chemical variables (current direction, current speed, temperature, salinity, dissolved oxygen (DO), chlorophyll-a, turbidity, sedimentation rate, and organic content (OC) and C:N ratio of collected sediments).

Table 7 Correlations between physico-chemical variables and biological-environmental (BIOENV) matching.

Physico-chemical variables (Spearman's correlations)				
Variable 1	Variable 2	R	t(n-2)	*p*
Current speed	Current directions	0.41	2.55	0.016
Current speed	Temperature	-0.51	-3.36	0.002
Current speed	Chlorophyll-a	0.34	2.05	0.048
Current directions	Chlorophyll-a	0.59	4.09	<0.001
Temperature	Salinity	0.50	3.34	0.002
Temperature	DO	-0.35	-2.07	0.047
DO	Chlorophyll-a	-0.40	-2.39	0.023
Chlorophyll-a	Turbidity	0.45	2.93	0.006
Sedimentation rate	OC	0.83	8.19	<0.001
Biological-environmental correlations (BIOENV)				
Biotic similarity matrix	ρ	*p*	Correlated combination of variables	
Reef water bacterial communities	0.37	0.196	Salinity, Chlorophyll-a, DO, Current direction	
Biofilm bacterial communities	0.47	0.001	Temperature, Salinity, Chlorophyll-a, DO	
Biofilm algal communities	0.35	0.001	Salinity, Chlorophyll-a, Current speed	

All significant results from Spearman's rank correlations on pairs of physico-chemical variables are presented. BIOENV routine measured the match between combinations of the physico-chemical distance matrix and the biotic resemblance matrices (reef water bacteria, bacterial biofilm, and algal biofilm) using Spearman's correlation on ranks. The combinations of physico-chemical variables correlated to the biotic data structures with the highest ρ are reported for each biotic data set. R = Spearman's correlation coefficient; t(n-2) = Spearman's rank correlation t-statistic; DO = dissolved oxygen; OC = organic content of collected sediments, ρ = Spearman's correlation coefficient (BIOENV routine).

3.5. I. Discussion

In this study we present a first account of physical, chemical, and biotic *in situ* data acquired simultaneously in coral reefs of the central Red Sea over the course of a full year. Our data revealed that the comparatively unexplored reefs in this region are exposed to a high degree of spatial (cross-shelf) and temporal (seasonal) variability. We uncovered connections between physico-chemical conditions and community

structure of bacterial and algal biofilms, contributing valuable information on the major drivers of biotic coral reef processes in this naturally variable environment. Importantly, we predominantly identified environmental variables that are predicted to change due to ocean warming (i.e., temperature, salinity, dissolved oxygen [DO]) and increased coastal pollution (chlorophyll-a).

3.5.1. Physico-chemical baseline data of coral reefs in the central Red Sea

Our physico-chemical data show that coral reefs in the central Red Sea are subjected to summer temperature and salinity levels that exceed coral reef global average maxima (Kleypas et al. 1999b) and to comparably low DO levels (Ohde and van Woesik 1999; Manasrah et al. 2006). Turbidity and sedimentation rates were far below levels reported from coral reefs elsewhere (e.g. Great Barrier Reef [GBR]), whereas chlorophyll-a and nutrients were mostly comparable to measurements from other coral reef regions (Rogers 1990; Schaffelke et al. 2012). Further, our data reveal a high degree of spatio-temporal variability: seasonality was primarily reflected in temperature and salinity levels, whereas DO, chlorophyll-a, and sedimentation varied over the spatial scale.

3.5.1.1. Currents

Derived from ocean model simulations, currents on the eastern coast of the central Red Sea are influenced by strong seasonal or permanent gyres and by the eastern boundary current that carries water masses from the south (Sofianos and Johns 2003). However, around reef platforms bathymetry and atmospheric forcing may be the strongest determinants for current properties (Monismith 2007; Bower and

Farrar 2015). Accordingly, the main current direction (NW to SE) at our offshore site was likely driven by NW-winds (Bower and Farrar 2015), while the reversed direction (SE to NW) in the nearshore reef may be related to the eastern boundary current (travelling northward) (Sofianos and Johns 2003). The currents around our study site are likely to transport nutrients and influence heat budgets, as indicated by the significant correlations of currents with chlorophyll-a and temperature. The offshore site receives water masses form the Red Sea basin, whereas water exchange between the nearshore reef and the basin may be limited. Elevated salinity levels in the nearshore reef support this assumption, as they are likely caused by the longer residency time of water, resulting in higher relative evaporation rates. Water exchange between coral reefs and the open sea can play an important role in mediating stress events, such as rising salinity or excessive summer warming (Nakamura and Van Woesik 2001). Hence, nearshore reefs in the central Red Sea may be at higher risk to experience episodes of environmental stress compared to the more distant reefs. Higher prevalence of bleached corals in nearshore than in offshore reef sites during a coral bleaching event in 2010 and 2015 confirms this assumption (Furby et al. 2013; Roik et al. 2015c).

3.5.1.2. Temperature and salinity

During summer we measured high seasonal temperature means of up to 31.9 °C (maxima of 33 °C). These exceed the typical average maximum for coral reefs (29.5 °C, Kleypas et al. 1999) by 1.5 °C and reflect conditions that are predicted for reefs worldwide by the mid to end of this century given an increase of average temperatures (28 °C) by 1.8 - 4.0 °C (IPCC 2007). Seasonally averaged salinity levels

from our study sites (38 - 39 PSU), while typical for the Red Sea (Rasul et al. 2015), also by far exceed global averages (34 - 35 PSU) (Kleypas et al. 1999b; Guan et al. 2015).

In regard to temperature and salinity, the Red Sea can be considered a marginal coral reef environment where reef biota may live close to their physiological limits (Sawall et al. 2015). Yet, coral communities are abundant and diverse along the central Red Sea coast (Sawall et al. 2014; Klaus 2015). Consequently, environments such as the Red Sea are highly valuable to study thermo-tolerant adaptations that may be key to survival of coral reef organisms facing environmental change (Fine et al. 2013; Sawall and Al-Sofyani 2015).

Among all measured physico-chemical variables, temperature and salinity fluctuated most pronouncedly between seasons. For instance, the annual temperature range (9 °C) was 2- to 4-fold higher than in most equatorial reefs (2 - 4 °C in coral reefs in the Caribbean, Indo-pacific, and Pacific Ocean), and comparable to temperature ranges from more extreme regions that support coral habitats, such as the Sea of Oman (7 °C) and the Persian/Arabian Gulf (12 – 20 °C) (Hume et al. 2013). Despite high salinity levels, salinity fluctuation was low (range: 1.43 PSU) compared to tropical reefs with regular riverine and precipitation input (e.g. GBR salinity varies by 5 to 10 PSU, Muthiga and Szmant 1987), and putatively driven by evaporation processes related to temperature as deduced from the correlation of both variables. The Red Sea is a semi-enclosed basin located in between arid landmasses (Rasul et al. 2015) that may be particularly affected by ocean warming, leading to even higher temperatures and

salinity levels. Coral bleaching events in the last decade are an indication that thermal limits of many coral species have already been reached (Furby et al. 2013). The here presented environmental data will be an important contribution to quantify long-term effects of ocean warming in the central Red Sea.

3.5.1.3. Dissolved oxygen (DO)

DO levels in coral reefs are primarily driven by biological processes such as respiration and photosynthesis (Ohde and van Woesik 1999). Differences in these processes may result in large spatial differences in DO compared to seasonal changes. Lower DO levels in the nearshore reef suggests a predominance of heterotrophic organisms, such as sponges, other filter feeders, or heterotrophic bacteria, but also reduced water mixing close to shore. Seasonal DO averages in our study were derived from continuous data, including diurnal (elevated DO due to photosynthesis) and nocturnal (lowered DO due to respiration) values. The majority of studies report averages only from day-time measurements, impeding comparison with our values. One study that considered day- and night-time values showed a variation of DO values on a range from 1.3 to 11.1 mg L^{-1} in a high-latitude coral reef of Japan (Ohde and van Woesik 1999). Within the Red Sea, offshore shallow waters in the northern part had relatively high DO levels (6 – 7 mg L^{-1}, Manasrah et al. 2006). In comparison, DO levels in our study (2.2 - 4.1 mg L^{-1}) were low. This reduction in DO between north and central Red Sea is likely driven by higher temperatures in the central Red Sea that decreases oxygen solubility.

Globally, DO levels are predicted to decrease and hypoxic environments to spread as a consequence of climate change (Keeling et al. 2010). Levels of 2 mg L^{-1} DO and below had been characterized as hypoxic in the majority of studies, mostly for temperate regions (Vaquer-Sunyer and Duarte 2008). As DO levels in the central Red Sea occasionally reach such levels, hypoxia may represent another challenge for Red Sea organisms facing climate change.

3.5.1.4. Chlorophyll-a and dissolved inorganic nutrients

Chlorophyll-a concentration is frequently used as a proxy for primary production and nutrient availability in the water column (Spencer 1985). The waters of the Red Sea are among the most oligotrophic worldwide (Sheppard et al. 1992). Chlorophyll-a levels derived from remote sensing data show that surface water concentrations range from extreme oligotrophy (< 0.01 to 0.4 mg m^{-3}) in the northern and northern-central Red Sea to chlorophyll-a concentrations exceeding characteristic coral reef conditions by an order of magnitude in the southern Red Sea (0.5 - 5.0 mg m^{-3}) (Raitsos et al. 2013). Accordingly, in the central Red Sea we found *in situ* chlorophyll-a levels and concentrations of dissolved inorganic nutrients mostly in the range of values from other oligotrophic coral reef regions. Chlorophyll-a seasonal averages were at the lower end (0.16 to 0.67 µg L^{-1}) of the range of concentrations observed in other coral reefs (0.17 - 4.67 µg L^{-1}, Szmant 2002). Conditions at the nearshore and midshore reefs in our study area were comparable to inshore reefs of the GBR (up to 0.7 µg L^{-1} over the full year, Schaffelke et al. 2012), while concentrations in the offshore reef were lower (0.16 to 0.28 µg L^{-1}) and comparable to more oligotrophic reef sites such as reef systems in Hawaii (up to 0.31 µg L^{-1}, Silbiger et al. 2014).

Low chlorophyll-a concentrations in our study area also reflect the limited availability of inorganic nutrients. Nitrogen species concentrations (nitrate & nitrite 0.16 µM; ammonia 0.17 µM) were comparably low (Hawaii, Phoenix islands, GBR, and Western Australia; 0.04 - 2.5 µM and 0.05 – 5.52 µM for nitrate & nitrite and ammonia, respectively, Szmant 2002). Phosphate levels (0.07 µM) were among the lowest values reported for coral reefs (0.08 - 0.6 µM) (Szmant 2002). While our collected data (bi-annual sampling) does not resolve seasonal patterns, it indicates enrichment of nutrients during winter. This trend has previously been reported for the Red Sea based on remote sensing data and was attributed to an increased vertical mixing and the intrusion of nutrient-rich waters from the Gulf of Aden (Raitsos et al. 2013).

3.5.1.5. Sedimentation and Turbidity

Sedimentation rates and turbidity were very low in the study area and decreased from nearshore to offshore following a common pattern of land-based sedimentation (Edinger et al. 2000; Brodie et al. 2007; Cooper et al. 2007; Mallela 2007). Turbidity indicates suspended particulates in the water column that, depending on their organic content, are filtered or ingested by heterotrophic biota serving as a source of nutrition (Anthony and Fabricius 2000). On the other hand, high abundance of suspended particles inhibit light penetration, which impacts photosynthesis or can smother benthic organisms, hence, high sedimentation levels are commonly regarded as stressors to coral reefs (Rouzé et al. 2015). Sedimentation rates on Caribbean and Pacific coral reef habitats are considered ‘natural’ at 1 - 10 mg cm^{-2} day^{-1} (Rogers 1990), while stressful conditions start at around 70 mg cm^{-2} day^{-1} (Browne et al. 2015). Our data show that sedimentation rates in the central Red Sea reefs are far

from such conditions. Seasonal rates ranged between 0.0057 - 0.0193 mg cm^{-2} day^{-1}, which is only ~ 2 % of the lowest natural sedimentation rate recorded elsewhere (Rogers 1990). Seasonal averages of turbidity from the central Red Sea (0.20 - 0.63 NTU) range well below recordings from the GBR (0.6 – 7.0 NTU) (Schaffelke et al. 2012).

Similar to chlorophyll-a, OC of collected sediments and turbidity showed no significant seasonal pattern that would indicate a period of higher productivity in the water column. However, our data revealed that the typical decrease of sedimentation rates from nearshore to offshore was inversed in spring. Hence, in this period heterotrophic biota in the offshore reef environments may benefit from more particulates and higher OC content. This observation may be related to the Arabian Ocean monsoon, which causes dust storms and/or increase mixing in the water column during spring and fall (Acker et al. 2008). Further monitoring is required in order to confirm if this pattern is re-occurring every year.

All C:N ratios of sediments were above the Redfield ratio (6.6) (Redfield et al. 1963), which confirms that primary production in the central Red Sea is nitrogen limited (Healey and Hendzel 1979). This is also evident from low concentrations of nitrogen species in the study area. C:N ratios of particulates were significantly higher (7.3 - 8.1) during summer compared to other seasons, indicating a higher rate of carbon assimilation of planktonic organisms that constitute these particulates in this season (Williams 1995).

3.5.2. Biotic baseline data of coral reefs in the central Red Sea: reef water bacteria and bacterial and algal biofilms

We present a first account of key biotic variables of coral reefs in the central Red Sea, including reef water bacteria, bacterial biofilms, and algal biofilms. The catalogue of bacterial taxa (Supplementary Table 2) and algal groups represents a first assessment of microscopic communities in naturally variable reef environments of the central Red Sea. Coral reef bacterial biofilms were much more diverse compared to reef water and other Red Sea coral microbiomes (Bayer et al. 2013; Jessen et al. 2013b; Roder et al. 2015; Ziegler et al. 2016). Bacterial and algal biofilms were variable (29 % of bacterial and 99 % of algal communities significantly differed between reefs and seasons), and an increase in bacterial diversity during spring and summer coincided with significantly increased algal growth, supporting the notion of interaction of algal and bacterial communities via exudates (Barott et al. 2011a; Haas et al. 2013). Furthermore, significant variability between the warm and cool season provides insight into potential community changes with regard to ocean warming. In the following the findings are discussed in detail.

3.5.2.1. Composition and dynamics of reef water bacteria

Reef water at our study sites comprised bacterial communities that were similar to those reported from other oceans (Pommier et al. 2007; Sunagawa et al. 2015). A feature of reef water bacterial communities over all sites and seasons was the dominance of the cyanobacterial family Synechococcaceae, which is characteristic for open-sea surface water across the Red Sea (Ngugi et al. 2012; Shibl et al. 2014). Synechococcaceae are particularly adapted to oligotrophic environments and are a

major primary producer in oligotrophic waters (Palenik et al. 2003). Similarly, Pelagibacteracaea that constitute another abundant group in our samples are associated with oligotrophic conditions (Morris et al. 2002),.

Reef water bacterial community structure differed between seasons, but remained stable across reefs despite physico-chemical differences. The lack of spatial changes may indicate only little land-based influences in our study area, considering that reef water bacterial communities are shown to change strongly along gradients of acute pollution compared to seasonal changes (Campbell et al. 2015).

3.5.2.2. Composition and dynamics of bacterial biofilms

Biofilms in coral reefs have received attention due to their importance in controlling recruitment of reef-building corals (Webster et al. 2004; Jessen et al. 2014) with far-reaching consequences for benthic community structuring (Marhaver et al. 2013). To our knowledge bacterial biofilms in coral reefs have been studied only in Sulawesi, Indonesia (Sawall et al. 2012) and in the GBR (Webster et al. 2004, 2011, Witt et al. 2011, 2012a). These studies focused on CCA associated bacteria or epilithic biofilm communities along a gradient of eutrophication or terrestrial run-off. To date, only little is known about bacterial biofilm and reef water community structure and their responses to natural environmental fluctuations in less impacted environments.

We show that in the central Red Sea five bacterial phyla dominate biofilms over all reef sites and seasons. Of these, Proteobacteria, Bacteroidetes, and Cyanobacteria were previously described from coral reef biofilms in the GBR, and Verrucomicrobia was previously found in coral reef sediments (Uthicke and McGuire 2007; Witt et al.

2012a). Verrucomicrobia was also found in marine biofilms from temperate and polar regions (Webster and Negri 2006; Bengtsson et al. 2010). The last bacterial phylum Planctomycetes was identified in estuarine biofilms (Moss et al. 2006) and on the surface of red algae (Miranda et al. 2013). On the family level, Rhodobacteraceae (Proteobacteria) and Flavobacteriaceae (Bacteroidetes) were most prevalent in Red Sea biofilms. Both families were found in coral reef biofilms before (Webster et al. 2004, 2011; Sharp et al. 2015) and associated with community shifts along a water quality gradient (Witt et al. 2012a). Members of the family Rhodobacteraceae are known as rapid surface colonizers and are considered to be involved in the formation of marine biofilms (Dang et al. 2008). Their roles in benthic community structuring are diverse, with a few species of this family enhancing coral recruitment (Sharp et al. 2015), but other species being pathogenic opportunists in coral disease (Sunagawa et al. 2009; Roder et al. 2014a, 2014b).

Bacterial biofilm diversity in this study was at least 10-fold higher (average Inverse Simpson's index (ISI) of 108) compared to bacterial diversity in reef water (ISI of 8), and also in comparison to reef water and coral microbiomes reported in other Red Sea studies (ISI of 2 – 23 and 1 – 2, respectively, Bayer et al. 2013; Jessen et al. 2013b; Ziegler et al. 2016). Implications of this high bacterial diversity are still unknown and warrant further study of bacterial biofilms.

Similar to findings for reef water bacterial communities, studies showed that seasonality of biofilm communities was minor or not detectable along nutrient or pollution gradients in coral reef systems, while the spatial variability was high (Sawall

et al. 2012; Witt et al. 2012a). This is in contrast to bacterial biofilms in our study area that displayed high seasonality and low spatial dynamics. The prominent seasonal response may be interpreted as a natural pattern in a putatively less impacted reef area. This is corroborated by the observation that all differentially abundant OTUs were previously encountered in marine environments (see Supplementary Table 4) without any apparent link to anthropogenic sources (Ansari et al. 2015). Lastly, this study identified several bacterial OTUs that were significantly increased or decreased in the warmer seasons. These OTUs may be comparably temperature-sensitive and can presumably indicate community shifts caused by temperature changes.

3.5.2.3. Composition and dynamics of algal biofilms

Our biofilm data includes algal assemblages following a three-month succession from a cross-shelf gradient over four seasons. Composition of algal biofilms plays an essential role in coral and other invertebrates settlement and the survival of recruits (Heyward and Negri 1999; Kuffner et al. 2006). Brown or green algal crusts or turfs, which contributed up to 70 % to algal communities in this study, are typically negatively associated with coral larval recruitment (Barott et al. 2011b). CCA have a beneficial effect on coral recruitment and survival (Barott et al. 2011b), but were less abundant in this study. CCA commonly dominate offshore environments, but in our data offshore and midshore environments showed similar amounts of CCA (Ateweberhan et al. 2006; Dean et al. 2015). Our data represent algal settlement patterns on smooth and light exposed surfaces, where brown and green algae may have an advantage over CCA, which are known to better proliferate in low light environments (Gattuso et al. 2006; Jessen et al. 2013a). Other less abundant algal

groups such as red algae and red crusts were almost absent from the exposed settlement tiles, presumably because they also favor sheltered environments (Jessen et al. 2013a), which the exposed tiles did not provide.

In our study, algal community composition significantly differed between reefs and seasons, confirming that algal communities and their biomass are highly dynamic on spatial and seasonal scales (Ateweberhan et al. 2006; Diaz-Pulido et al. 2007; Ferrari et al. 2012). The community changes were determined by the most abundant components of the assemblages: brown crusts, green crusts, CCA, and open space. Algal cover and bacterial diversity were highest during spring and summer coinciding with the timing of coral reproduction. This overlap with the coral spawning season in the Red Sea (April to June) (Bouwmeester et al. 2014a) indicates that algal community patterns may potentially influence the settlement behavior and success of coral larvae.

3.5.3. Physico-chemical drivers of biotic communities in the central Red Sea

Increasing the understanding of environmental variability in coral reefs is essential to predicting ecosystem response to environmental change (Hughes et al. 2003; Koch et al. 2009). While addressing single physico-chemical variables in isolation may provide some insight, the analysis of cumulative effects from multiple variables are of relevance to gain a more complete understanding of complex ecological systems (Crain et al. 2008). Our study provided an opportunity to match the simultaneously collected physico-chemical and biotic data and to explore interactions between

physico-chemical conditions and the biotic realm *in situ*, the results of which are discussed in the following.

Although nutrient enrichment or pollution related factors were shown to be the only drivers of bacterial communities in coral reefs elsewhere (Sawall et al. 2012; Witt et al. 2012a; Kelly et al. 2014; Campbell et al. 2015), our results suggest that in less disturbed environmental settings, bacterial biofilms are influenced by a combination of temperature, salinity, DO, but also chlorophyll-a. *Ex situ* experiments confirmed a temperature-induced regulation of bacterial biofilm composition and physiology (Webster et al. 2011; Witt et al. 2012b; Stratil et al. 2013). Also, salinity and DO levels were shown to influence biofilm and water column bacteria in estuaries (Bouvier and del Giorgio 2002; Magalhães et al. 2005; Nocker et al. 2007).

The spatio-temporal structuring of algal biofilm communities at our sites were best explained by salinity, chlorophyll-a, and current speed. We expected chlorophyll-a levels to be associated with differences in algal composition, given that irradiance together with nutrient availability (both variables that are related to chlorophyll-a) are considered the most important requirements for algal growth (Diaz-Pulido and McCook 2005; Diaz-Pulido et al. 2007). Salinity has been shown to affect physiology, growth, and community shifts in marine algae, especially in estuaries, where salinity differences are high (McLachlan 1961; Fong et al. 1996; Martins et al. 1999). However, salinity has been rarely considered as a variable controlling algal settlement and growth in coral reefs (Diaz-Pulido and McCook 2005; Ateweberhan et al. 2006; Ferrari et al. 2012). Our data indicate that in the high salinity levels of the

central Red Sea already small differences can influence algal biofilm assemblages. It is important to note though, that our results represent the best match of the variables investigated. For algal biofilm settlement and succession, grazing is usually another highly influential driver (Lefèvre and Bellwood 2010; Ferrari et al. 2012), and herbivory may therefore have had a contribution in our study area as well.

3.5.4. Conclusions

The Red Sea is known as a highly variable, oligotrophic, and still sparsely studied region that maintains coral reefs of high coral cover under comparably high temperature and salinity. Therefore it provides a suitable area to study spatio-temporal dynamics and to investigate coral reef functioning under environmental conditions that deviate from most other coral reefs. Here we present a first account of year-long *in situ* baseline data on physico-chemical variables and key biotic factors to provide insights into coral reef functioning and natural levels of variability. As such, our data provide a comparative foundation for future coral reef studies assessing effects of environmental change. Our analyses highlight the prevalence of spatio-temporal dynamics of physico-chemical and biotic variables. For instance, variability of bacterial and algal biofilms in regard to temperature and salinity differences between summer and winter, may guide further research on potential biofilm community changes in response to future warming. Our data show that temperature and salinity, but also dissolved oxygen levels in the Red Sea are comparable to projected 'future ocean' conditions. Importantly, these variables were also identified among the major drivers of biotic community dynamics, and are projected to be even further affected by the progression of global climate change. This suggests additive

bottom-up effects on Red Sea benthic communities as a result of future climate change.

3.6. References

Achituv Y, Dubinsky Z (1990) Evolution and zoogeography of coral reefs. Ecosystems of the world. Elsevier, Amsterdam, pp 1–9

Acker J, Leptoukh G, Shen S, Zhu T, Kempler S (2008) Remotely-sensed chlorophyll a observations of the northern Red Sea indicate seasonal variability and influence of coastal reefs. J Mar Syst 69:191–204

Afeworki Y, Videler JJ, Bruggemann JH (2013) Seasonally changing habitat use patterns among roving herbivorous fishes in the southern Red Sea: the role of temperature and algal community structure. Coral Reefs 32:475–485

Ainsworth TD, Thurber RV, Gates RD (2010) The future of coral reefs: a microbial perspective. Trends Ecol Evol 25:233–240

Anderson MJ, Gorley RN, Clarke KR (2008) PERMANOVA+ for PRIMER: Guide to software and statistical methods.

Ansari MI, Harb M, Jones B, Hong P-Y (2015) Molecular-based approaches to characterize coastal microbial community and their potential relation to the trophic state of Red Sea. Sci Rep 5:9001

Anthony KR., Fabricius KE (2000) Shifting roles of heterotrophy and autotrophy in coral energetics under varying turbidity. J Exp Mar Biol Ecol 252:221–253

Arnold S, Steneck R, Mumby P (2010) Running the Gauntlet: Inhibitory Effects of Algal Turfs on the Processes of Coral Recruitment. Mar Ecol-Prog Ser 91–105

Ateweberhan M, Bruggemann JH, Breeman AM (2006) Effects of extreme seasonality on community structure and functional group dynamics of coral reef algae in the southern Red Sea (Eritrea). Coral Reefs 25:391–406

Ban SS, Graham NAJ, Connolly SR (2014) Evidence for multiple stressor interactions and effects on coral reefs. Glob Change Biol 20:681–697

Barott KL, Rodriguez-Brito B, Janouškovec J, Marhaver KL, Smith JE, Keeling P, Rohwer FL (2011a) Microbial diversity associated with four functional groups of benthic reef algae and the reef-building coral Montastraea annularis. Environ Microbiol 13:1192–1204

Barott KL, Rodriguez-Mueller B, Youle M, Marhaver KL, Vermeij MJA, Smith JE, Rohwer FL (2011b) Microbial to reef scale interactions between the reef-building coral Montastraea annularis and benthic algae. Proc R Soc B Biol Sci 279:1655–1664

Battin TJ, Kaplan LA, Denis Newbold J, Hansen CME (2003) Contributions of microbial biofilms to ecosystem processes in stream mesocosms. Nature 426:439–442

Bauman AG, Feary DA, Heron SF, Pratchett MS, Burt JA (2013) Multiple environmental factors influence the spatial distribution and structure of reef communities in the northeastern Arabian Peninsula. Mar Pollut Bull 72:302–312

Bayer T, Neave MJ, Alsheikh-Hussain A, Aranda M, Yum LK, Mincer T, Hughen K, Apprill A, Voolstra CR (2013) The microbiome of the Red Sea coral *Stylophora pistillata* is dominated by tissue-associated Endozoicomonas bacteria. Appl Environ Microbiol

Bengtsson M, Sjøtun K, Øvreås L (2010) Seasonal dynamics of bacterial biofilms on the kelp Laminaria hyperborea. Aquat Microb Ecol 60:71–83

Bonaldo RM, Bellwood DR (2010) Spatial variation in the effects of grazing on epilithic algal turfs on the Great Barrier Reef, Australia. Coral Reefs 30:381–390

Bourne DG, Webster NS (2013) Coral Reef Bacterial Communities. In: Rosenberg E., DeLong E.F., Lory S., Stackebrandt E., Thompson F. (eds) The Prokaryotes. Springer Berlin Heidelberg, Berlin, Heidelberg, pp 163–187

Bouvier TC, del Giorgio PA (2002) Compositional changes in free-living bacterial communities along a salinity gradient in two temperate estuaries. Limnol Oceanogr 47:453–470

Bouwmeester J, Baird AH, Chen CJ, Guest JR, Vicentuan KC, Berumen ML (2014) Multi-species spawning synchrony within scleractinian coral assemblages in the Red Sea. Coral Reefs 1–13

Bower AS, Farrar JT (2015) Air–Sea Interaction and Horizontal Circulation in the Red Sea. In: Rasul N.M.A., Stewart I.C.F. (eds) The Red Sea. Springer Berlin Heidelberg, pp 329–342

Boyd P, Hutchins D (2012) Understanding the responses of ocean biota to a complex matrix of cumulative anthropogenic change. Mar Ecol Prog Ser 470:125–135

Brodie J, De'ath G, Devlin M, Furnas M, Wright M (2007) Spatial and temporal patterns of near-surface chlorophyll *a* in the Great Barrier Reef lagoon. Mar Freshw Res 58:342

Browne NK, Tay J, Todd PA (2015) Recreating pulsed turbidity events to determine coral–sediment thresholds for active management. J Exp Mar Biol Ecol 466:98–109

Campbell AM, Fleisher J, Sinigalliano C, White JR, Lopez JV (2015) Dynamics of marine bacterial community diversity of the coastal waters of the reefs, inlets, and wastewater outfalls of southeast Florida. MicrobiologyOpen

Cantin NE, Cohen AL, Karnauskas KB, Tarrant AM, McCorkle DC (2010) Ocean Warming Slows Coral Growth in the Central Red Sea. Science 329:322–325

Chao A (1984) Nonparametric estimation of the number of classes in a population. Scand J Stat 265–270

Clarke KR, Gorley RN (2006) PRIMER v6: User Manual / Tutorial.

Cooper TF, Uthicke S, Humphrey C, Fabricius KE (2007) Gradients in water column nutrients, sediment parameters, irradiance and coral reef development in the Whitsunday Region, central Great Barrier Reef. Estuar Coast Shelf Sci 74:458–470

Crain CM, Kroeker K, Halpern BS (2008) Interactive and cumulative effects of multiple human stressors in marine systems. Ecol Lett 11:1304–1315

Dang H, Li T, Chen M, Huang G (2008) Cross-Ocean Distribution of Rhodobacterales Bacteria as Primary Surface Colonizers in Temperate Coastal Marine Waters. Appl Environ Microbiol 74:52–60

Davis KA, Lentz SJ, Pineda J, Farrar JT, Starczak VR, Churchill JH (2011) Observations of the thermal environment on Red Sea platform reefs: a heat budget analysis. Coral Reefs 30:25–36

Dean AJ, Steneck RS, Tager D, Pandolfi JM (2015) Distribution, abundance and diversity of crustose coralline algae on the Great Barrier Reef. Coral Reefs 1–14

Diaz-Pulido G, McCook LJ (2005) Effects of nutrient enhancement on the fecundity of a coral reef macroalga. J Exp Mar Biol Ecol 317:13–24

Diaz-Pulido G, McCook LJ, Larkum AWD, Lotze HK, Raven JA, Schaffelke B, Smith JE, Steneck RS (2007) Vulnerability of macroalgae of the Great Barrier Reef to climate change. Climate change and the Great Barrier Reef: a vulnerability assessment. Great Barrier Reef Marine Park Authority and the Australian Greenhouse Office,

Diez I, Secilla A, Santolaria A, Gorostiaga JM (1999) Phytobenthic Intertidal Community Structure Along an Environmental Pollution Gradient. Mar Pollut Bull 38:463–472

Dinsdale EA, Rohwer F (2011) Fish or Germs? Microbial Dynamics Associated with Changing Trophic Structures on Coral Reefs. In: Dubinsky Z., Stambler N. (eds)

Coral Reefs: An Ecosystem in Transition. Springer Netherlands, Dordrecht, pp 231–240

Edgar RC, Haas BJ, Clemente JC, Quince C, Knight R (2011) UCHIME improves sensitivity and speed of chimera detection. Bioinformatics 27:2194–2200

Edinger EN, Limmon GV, Jompa J, Widjatmoko W, Heikoop JM, Risk MJ (2000) Normal coral growth rates on dying reefs: Are coral growth rates good indicators of reef health? Mar Pollut Bull 40:404–425

Eidens C, Bayraktarov E, Hauffe T, Pizarro V, Wilke T, Wild C (2014) Benthic primary production in an upwelling-influenced coral reef, Colombian Caribbean. PeerJ 2:e554

Fabricius K, De'ath G, McCook L, Turak E, Williams DM (2005) Changes in algal, coral and fish assemblages along water quality gradients on the inshore Great Barrier Reef. Mar Pollut Bull 51:384–398

Fabricius KE (2005) Effects of terrestrial runoff on the ecology of corals and coral reefs: review and synthesis. Mar Pollut Bull 50:125–146

Falter JL, Lowe RJ, Atkinson MJ, Cuet P (2012) Seasonal coupling and de-coupling of net calcification rates from coral reef metabolism and carbonate chemistry at Ningaloo Reef, Western Australia. J Geophys Res Oceans 117:C05003

Ferrari R, Gonzalez-Rivero M, Ortiz JC, Mumby PJ (2012) Interaction of herbivory and seasonality on the dynamics of Caribbean macroalgae. Coral Reefs 31:683–692

Fine M, Gildor H, Genin A (2013) A coral reef refuge in the Red Sea. Glob Change Biol n/a–n/a

Fong P, Boyer KE, Desmond JS, Zedler JB (1996) Salinity stress, nitrogen competition, and facilitation: what controls seasonal succession of two opportunistic green macroalgae? J Exp Mar Biol Ecol 206:203–221

Furby KA, Bouwmeester J, Berumen ML (2013) Susceptibility of central Red Sea corals during a major bleaching event. Coral Reefs 32:505–513

Gattuso J-P, Gentili B, Duarte CM, Kleypas JA, Middelburg JJ, Antoine D, others (2006) Light availability in the coastal ocean: impact on the distribution of benthic photosynthetic organisms and their contribution to primary production. Biogeosciences 3:489–513

Good IJ (1953) The polulation frequencies of species and the estimation of population parameters. Biometrika 40:237–264

Guadayol Ò, Silbiger NJ, Donahue MJ, Thomas FIM (2014) Patterns in Temporal Variability of Temperature, Oxygen and pH along an Environmental Gradient in a Coral Reef. PLoS ONE 9:e85213

Guan Y, Hohn S, Merico A (2015) Suitable Environmental Ranges for Potential Coral Reef Habitats in the Tropical Ocean. PLoS ONE 10:e0128831

Haas AF, Nelson CE, Rohwer F, Wegley-Kelly L, Quistad SD, Carlson CA, Leichter JJ, Hatay M, Smith JE (2013) Influence of coral and algal exudates on microbially mediated reef metabolism. PeerJ 1:e108

Hadfield MG (2011) Biofilms and Marine Invertebrate Larvae: What Bacteria Produce That Larvae Use to Choose Settlement Sites. Annu Rev Mar Sci 3:453–470

Hatcher BG, Larkum AWD (1983) An experimental analysis of factors controlling the standing crop of the epilithic algal community on a coral reef. J Exp Mar Biol Ecol 69:61–84

Healey FP, Hendzel LL (1979) Indicators of Phosphorus and Nitrogen Deficiency in Five Algae in Culture. J Fish Res Board Can 36:1364–1369

Helmuth B, Russell BD, Connell SD, Dong Y, Harley CD, Lima FP, Sará G, Williams GA, Mieszkowska N (2014) Beyond long-term averages: making biological sense of a rapidly changing world. Clim Change Responses 1:

Hentschel U, Piel J, Degnan SM, Taylor MW (2012) Genomic insights into the marine sponge microbiome. Nat Rev Microbiol 10:641–654

Heyward AJ, Negri AP (1999) Natural inducers for coral larval metamorphosis. Coral Reefs 18:273–279

Hoegh-Guldberg O, et al. (2015) Reviving the Ocean Economy: the case for action 2015. 60pp

Hughes TP, Baird AH, Bellwood DR, Card M, Connolly SR, Folke C, Grosberg R, Hoegh-Guldberg O, Jackson JBC, Kleypas J, Lough JM, Marshall P, Nyström M, Palumbi SR, Pandolfi JM, Rosen B, Roughgarden J (2003) Climate Change, Human Impacts, and the Resilience of Coral Reefs. Science 301:929–933

Hughes TP, Rodrigues MJ, Bellwood DR, Ceccarelli D, Hoegh-Guldberg O, McCook L, Moltschaniwskyj N, Pratchett MS, Steneck RS, Willis B (2007) Phase Shifts, Herbivory, and the Resilience of Coral Reefs to Climate Change. Curr Biol 17:360–365

Hume B, D'Angelo C, Burt J, Baker AC, Riegl B, Wiedenmann J (2013) Corals from the Persian/Arabian Gulf as models for thermotolerant reef-builders: Prevalence

of clade C3 Symbiodinium, host fluorescence and ex situ temperature tolerance. Mar Pollut Bull 72:313–322

Huse SM, Welch DM, Morrison HG, Sogin ML (2010) Ironing out the wrinkles in the rare biosphere through improved OTU clustering. Environ Microbiol 12:1889–1898

IPCC (2007) Synthesis Report. An Assessment of the Intergovernmental Panel on Climate Change. Intergovernmental Panel on Climate Change, Valencia, Spain

Jessen C, Roder C, Villa Lizcano JF, Voolstra CR, Wild C (2013a) In-Situ Effects of Simulated Overfishing and Eutrophication on Benthic Coral Reef Algae Growth, Succession, and Composition in the Central Red Sea. PLoS ONE 8:e66992

Jessen C, Villa Lizcano JF, Bayer T, Roder C, Aranda M, Wild C, Voolstra CR (2013b) In-situ Effects of Eutrophication and Overfishing on Physiology and Bacterial Diversity of the Red Sea Coral *Acropora hemprichii*. PLoS ONE 8:e62091

Jessen C, Voolstra CR, Wild C (2014) *In situ* effects of simulated overfishing and eutrophication on settlement of benthic coral reef invertebrates in the Central Red Sea. PeerJ 2:e339

Jouffray J-B, Nyström M, Norström AV, Williams ID, Wedding LM, Kittinger JN, Williams GJ (2015) Identifying multiple coral reef regimes and their drivers across the Hawaiian archipelago. Philos Trans R Soc B Biol Sci 370:20130268

Keeling RF, Körtzinger A, Gruber N (2010) Ocean Deoxygenation in a Warming World. Annu Rev Mar Sci 2:199–229

Kelly LW, Williams GJ, Barott KL, Carlson CA, Dinsdale EA, Edwards RA, Haas AF, Haynes M, Lim YW, McDole T, Nelson CE, Sala E, Sandin SA, Smith JE, Vermeij MJA, Youle M, Rohwer F (2014) Local genomic adaptation of coral reef-associated microbiomes to gradients of natural variability and anthropogenic stressors. Proc Natl Acad Sci 201403319

Khalil MT, Cochran JEM, Berumen ML (2013) The abundance of herbivorous fish on an inshore Red Sea reef following a mass coral bleaching event. Environ Biol Fishes 96:1065–1072

Klaus R (2015a) Coral Reefs and Communities of the Central and Southern Red Sea (Sudan, Eritrea, Djibouti, and Yemen). In: Rasul N.M.A., Stewart I.C.F. (eds) The Red Sea. Springer Berlin Heidelberg, pp 409–451

Klaus R (2015b) Coral Reefs and Communities of the Central and Southern Red Sea (Sudan, Eritrea, Djibouti, and Yemen). In: Rasul N.M.A., Stewart I.C.F. (eds) The Red Sea. Springer Berlin Heidelberg, pp 409–451

Kleypas JA, McManus JW, Menez LAB (1999) Environmental Limits to Coral Reef Development: Where Do We Draw the Line? Am Zool 39:146–159

Klindworth A, Pruesse E, Schweer T, Peplies J, Quast C, Horn M, Glöckner FO (2012) Evaluation of general 16S ribosomal RNA gene PCR primers for classical and next-generation sequencing-based diversity studies. Nucleic Acids Res gks808

Koch EW, Barbier EB, Silliman BR, Reed DJ, Perillo GM, Hacker SD, Granek EF, Primavera JH, Muthiga N, Polasky S, Halpern BS, Kennedy CJ, Kappel CV, Wolanski E (2009) Non-linearity in ecosystem services: temporal and spatial variability in coastal protection. Front Ecol Environ 7:29–37

Kohler KE, Gill SM (2006) Coral Point Count with Excel extensions (CPCe): A Visual Basic program for the determination of coral and substrate coverage using random point count methodology. Comput Geosci 32:1259–1269

Kuffner IB, Walters LJ, Becerro MA, Paul VJ, RitsonWilliams R, Beach KS (2006) Inhibition of coral recruitment by macroalgae and cyanobacteria. Mar Ecol Prog Ser 323:107–117

Kürten B, Al-Aidaroos AM, Struck U, Khomayis HS, Gharbawi WY, Sommer U (2014) Influence of environmental gradients on C and N stable isotope ratios in coral reef biota of the Red Sea, Saudi Arabia. J Sea Res 85:379–394

Lefèvre CD, Bellwood DR (2010) Seasonality and dynamics in coral reef macroalgae: variation in condition and susceptibility to herbivory. Mar Biol 157:955–965

Lowe RJ, Falter JL (2015) Oceanic Forcing of Coral Reefs. Annu Rev Mar Sci 7:null

Magalhães CM, Joye SB, Moreira RM, Wiebe WJ, Bordalo AA (2005) Effect of salinity and inorganic nitrogen concentrations on nitrification and denitrification rates in intertidal sediments and rocky biofilms of the Douro River estuary, Portugal. Water Res 39:1783–1794

Mallela J (2007) Coral reef encruster communities and carbonate production in cryptic and exposed coral reef habitats along a gradient of terrestrial disturbance. Coral Reefs 26:775–785

Manasrah R, Raheed M, Badran MI (2006) Relationships between water temperature, nutrients and dissolved oxygen in the northern Gulf of Aqaba, Red Sea. Oceanologia 48:237–253

Marhaver KL, Vermeij MJA, Rohwer F, Sandin SA (2013) Janzen-Connell effects in a broadcast-spawning Caribbean coral: distance-dependent survival of larvae and settlers. Ecology 94:146–160

Martins I, Oliveira JM, Flindt MR, Marques JC (1999) The effect of salinity on the growth rate of the macroalgae *Enteromorpha intestinalis* (Chlorophyta) in the Mondego estuary (west Portugal). Acta Oecologica 20:259–265

McCook L, Jompa J, Diaz-Pulido G (2014) Competition between corals and algae on coral reefs: a review of evidence and mechanisms. Coral Reefs 19:400–417

McDonald D, Price MN, Goodrich J, Nawrocki EP, DeSantis TZ, Probst A, Andersen GL, Knight R, Hugenholtz P (2012) An improved Greengenes taxonomy with explicit ranks for ecological and evolutionary analyses of bacteria and archaea. ISME J 6:610–618

McLachlan J (1961) The Effect of Salinity on Growth and Chlorophyll Content in Representative Classes of Unicellular Marine Algae. Can J Microbiol 7:399–406

Miranda LN, Hutchison K, Grossman AR, Brawley SH (2013) Diversity and Abundance of the Bacterial Community of the Red Macroalga *Porphyra umbilicalis*: Did Bacterial Farmers Produce Macroalgae? PLoS ONE 8:e58269

M MA (2010) Wind_rose - File Exchange - MATLAB Central. http://www.mathworks.com/matlabcentral/fileexchange/17748-wind-rose

Monismith SG (2007) Hydrodynamics of Coral Reefs. Annu Rev Fluid Mech 39:37–55

Morris RM, Rappé MS, Connon SA, Vergin KL, Siebold WA, Carlson CA, Giovannoni SJ (2002) SAR11 clade dominates ocean surface bacterioplankton communities. Nature 420:806–810

Moss JA, Nocker A, Lepo JE, Snyder RA (2006) Stability and Change in Estuarine Biofilm Bacterial Community Diversity. Appl Environ Microbiol 72:5679–5688

Muthiga NA, Szmant AM (1987) The effects of salinity stress on the rates of aerobic respiration and photosynthesis in the hermatypic coral Siderastrea siderea. Biol Bull 173:539–551

Nakamura T, Van Woesik R (2001) Water-flow rates and passive diffusion partially explain differential survival of corals during the 1998 bleaching event. Mar Ecol Prog Ser 212:301–304

Ngugi DK, Antunes A, Brune A, Stingl U (2012) Biogeography of pelagic bacterioplankton across an antagonistic temperature–salinity gradient in the Red Sea. Mol Ecol 21:388–405

Nocker A, Lepo JE, Martin LL, Snyder RA (2007) Response of Estuarine Biofilm Microbial Community Development to Changes in Dissolved Oxygen and Nutrient Concentrations. Microb Ecol 54:532–542

Ohde S, van Woesik R (1999) Carbon dioxide flux and metabolic processes of a coral reef, Okinawa. Bull Mar Sci 65:559–576

Palenik B, Brahamsha B, Larimer FW, Land M, Hauser L, Chain P, Lamerdin J, Regala W, Allen EE, McCarren J, Paulsen I, Dufresne A, Partensky F, Webb EA, Waterbury J (2003) The genome of a motile marine Synechococcus. Nature 424:1037–1042

Pineda J, Starczak V, Tarrant A, Blythe J, Davis K, Farrar T, Berumen M, da Silva JCB (2013) Two spatial scales in a bleaching event: Corals from the mildest and the most extreme thermal environments escape mortality. Limnol Oceanogr 58:1531–1545

Pommier T, Canbäck B, Riemann L, Boström KH, Simu K, Lundberg P, Tunlid A, Hagström Å (2007) Global patterns of diversity and community structure in marine bacterioplankton. Mol Ecol 16:867–880

Pruesse E, Quast C, Knittel K, Fuchs BM, Ludwig W, Peplies J, Glöckner FO (2007) SILVA: a comprehensive online resource for quality checked and aligned ribosomal RNA sequence data compatible with ARB. Nucleic Acids Res 35:7188–7196

Raitsos DE, Hoteit I, Prihartato PK, Chronis T, Triantafyllou G, Abualnaja Y (2011) Abrupt warming of the Red Sea. Geophys Res Lett 38:L14601

Raitsos DE, Pradhan Y, Brewin RJW, Stenchikov G, Hoteit I (2013) Remote Sensing the Phytoplankton Seasonal Succession of the Red Sea. PLoS ONE 8:e64909

Rasul NMA, Stewart ICF, Nawab ZA (2015) Introduction to the Red Sea: Its Origin, Structure, and Environment. In: Rasul N.M.A., Stewart I.C.F. (eds) The Red Sea. Springer Berlin Heidelberg, pp 1–28

Redfield AC, B. H. Ketchum, Richards FA (1963) The influence of organisms on the composition of sea-water. In: Hill M.N. (eds) The sea, ideas and observations on progress in the study of seas. Interscience, New York, pp 26–77

Riegl B, Berumen M, Bruckner A (2013) Coral population trajectories, increased disturbance and management intervention: a sensitivity analysis. Ecol Evol 3:1050–1064

Roder C, Arif C, Bayer T, Aranda M, Daniels C, Shibl A, Chavanich S, Voolstra CR (2014a) Bacterial profiling of White Plague Disease in a comparative coral species framework. ISME J 8:31–39

Roder C, Arif C, Daniels C, Weil E, Voolstra CR (2014b) Bacterial profiling of White Plague Disease across corals and oceans indicates a conserved and distinct disease microbiome. Mol Ecol 23:965–974

Roder C, Bayer T, Aranda M, Kruse M, Voolstra CR (2015) Microbiome structure of the fungid coral Ctenactis echinata aligns with environmental differences. Mol Ecol 24:3501–3511

Rogers CS (1990) Responses of coral reefs and reef organisms to sedimentation. Mar Ecol Prog Ser Oldendorf 62:185–202

Roik A, Roder C, Röthig T, Voolstra CR (2015a) Spatial and seasonal reef calcification in corals and calcareous crusts in the central Red Sea. Coral Reefs

Roik A, Röthig, Till, Ziegler, Maren, Voolstra, Christian R (2015b) Coral bleaching event in the central Red Sea. MIDEAST CORAL REEF Soc MCRS Newsl 3

Rosenberg E, Ben-Haim Y (2002) Microbial diseases of corals and global warming. Environ Microbiol 4:318–326

Rosenberg E, Koren O, Reshef L, Efrony R, Zilber-Rosenberg I (2007) The role of microorganisms in coral health, disease and evolution. Nat Rev Microbiol 5:355–362

Röthig T, Ochsenkühn MA, Roik A, van der Merwe R, Voolstra CR (2016) Long-term salinity tolerance is accompanied by major restructuring of the coral bacterial microbiome. Mol Ecol 25:1308–1323

Rouzé H, Lecellier G, Langlade MJ, Planes S, Berteaux-Lecellier V (2015) Fringing reefs exposed to different levels of eutrophication and sedimentation can support similar benthic communities. Marine Pollution Bulletin 92:212–221

Saeed AI, Sharov V, White J, Li J, Liang W, Bhagabati N, Braisted J, Klapa M, Currier T, Thiagarajan M, Sturn A, Snuffin M, Rezantsev A, Popov D, Ryltsov A, Kostukovich E, Borisovsky I, Liu Z, Vinsavich A, Trush V, Quackenbush J (2003) TM4: a free, open-source system for microarray data management and analysis. BioTechniques 34:374–378

Sawall Y, Al-Sofyani A (2015) Biology of Red Sea Corals: Metabolism, Reproduction, Acclimatization, and Adaptation. In: Rasul N.M.A., Stewart I.C.F. (eds) The Red Sea. Springer Berlin Heidelberg, pp 487–509

Sawall Y, Al-Sofyani A, Hohn S, Banguera-Hinestroza E, Voolstra CR, Wahl M (2015) Extensive phenotypic plasticity of a Red Sea coral over a strong latitudinal temperature gradient suggests limited acclimatization potential to warming. Sci Rep 5:8940

Sawall Y, Kürten B, Hoang BX, Sommer U, Wahl M, Al-Sofyani A, Al-Aidaroos AM, Marimuthu N, Khomayis HS, Gharbawi WY (2014) Coral Communities, in Contrast to Fish Communities, Maintain a High Assembly Similarity along the

Large Latitudinal Gradient along the Saudi Red Sea Coast. J Ecosys Ecograph S4:10.4172/2157–7625.1000s4–003

Sawall Y, Richter C, Ramette A (2012) Effects of Eutrophication, Seasonality and Macrofouling on the Diversity of Bacterial Biofilms in Equatorial Coral Reefs. PLoS ONE 7:e39951

Schaffelke B, Carleton J, Skuza M, Zagorskis I, Furnas MJ (2012) Water quality in the inshore Great Barrier Reef lagoon: Implications for long-term monitoring and management. Mar Pollut Bull 65:249–260

Schloss PD, Westcott SL, Ryabin T, Hall JR, Hartmann M, Hollister EB, Lesniewski RA, Oakley BB, Parks DH, Robinson CJ, Sahl JW, Stres B, Thallinger GG, Horn DJV, Weber CF (2009) Introducing mothur: Open-Source, Platform-Independent, Community-Supported Software for Describing and Comparing Microbial Communities. Appl Environ Microbiol 75:7537–7541

Sharp KH, Sneed JM, Ritchie KB, Mcdaniel L, Paul VJ (2015) Induction of Larval Settlement in the Reef Coral *Porites astreoides* by a Cultivated Marine Roseobacter Strain. Biol Bull 228:98–107

Sheppard C, Price A, Roberts C (1992) Marine Ecology of the Arabian Region. Acad Press San Diego Calif 358pp

Shibl AA, Thompson LR, Ngugi DK, Stingl U (2014) Distribution and diversity of Prochlorococcus ecotypes in the Red Sea. FEMS Microbiol Lett 356:118–126

Silbiger NJ, Guadayol scar, Thomas FIM, Donahue MJ (2014) Reefs shift from net accretion to net erosion along a natural environmental gradient. Mar Ecol Prog Ser 515:33–44

Sneed JM, Ritson-Williams R, Paul VJ (2015) Crustose coralline algal species host distinct bacterial assemblages on their surfaces. ISME J 9:2527–2536

Sofianos SS, Johns WE (2003) An Oceanic General Circulation Model (OGCM) investigation of the Red Sea circulation: 2. Three-dimensional circulation in the Red Sea. J Geophys Res Oceans 108:3066

Spencer CP (1985) The use of plant micro-nutrient and chlorophyll records as indices of eutrophication in inshore waters. Neth J Sea Res 19:269–275

Stratil SB, Neulinger SC, Knecht H, Friedrichs AK, Wahl M (2013) Temperature-driven shifts in the epibiotic bacterial community composition of the brown macroalga *Fucus vesiculosus*. MicrobiologyOpen 2:338–349

Sunagawa S, Coelho LP, Chaffron S, Kultima JR, Labadie K, Salazar G, Djahanschiri B, Zeller G, Mende DR, Alberti A, Cornejo-Castillo FM, Costea PI, Cruaud C,

d'Ovidio F, Engelen S, Ferrera I, Gasol JM, Guidi L, Hildebrand F, Kokoszka F, Lepoivre C, Lima-Mendez G, Poulain J, Poulos BT, Royo-Llonch M, Sarmento H, Vieira-Silva S, Dimier C, Picheral M, Searson S, Kandels-Lewis S, Tara Oceans coordinators, Bowler C, de Vargas C, Gorsky G, Grimsley N, Hingamp P, Iudicone D, Jaillon O, Not F, Ogata H, Pesant S, Speich S, Stemmann L, Sullivan MB, Weissenbach J, Wincker P, Karsenti E, Raes J, Acinas SG, Bork P, Boss E, Bowler C, Follows M, Karp-Boss L, Krzic U, Reynaud EG, Sardet C, Sieracki M, Velayoudon D (2015) Structure and function of the global ocean microbiome. Science 348:1261359–1261359

Sunagawa S, DeSantis TZ, Piceno YM, Brodie EL, DeSalvo MK, Voolstra CR, Weil E, Andersen GL, Medina M (2009) Bacterial diversity and White Plague Disease-associated community changes in the Caribbean coral Montastraea faveolata. ISME J 3:512–521

Sunagawa S, Woodley CM, Medina M (2010) Threatened Corals Provide Underexplored Microbial Habitats. PLoS ONE 5:e9554

Szmant AM (2002) Nutrient enrichment on coral reefs: is it a major cause of coral reef decline? Estuaries Coasts 25:743–766

Uthicke S, McGuire K (2007) Bacterial communities in Great Barrier Reef calcareous sediments: Contrasting 16S rDNA libraries from nearshore and outer shelf reefs. Estuar Coast Shelf Sci 72:188–200

Vaquer-Sunyer R, Duarte CM (2008) Thresholds of hypoxia for marine biodiversity. Proc Natl Acad Sci 105:15452–15457

Wall M, Putchim L, Schmidt GM, Jantzen C, Khokiattiwong S, Richter C (2015) Large-amplitude internal waves benefit corals during thermal stress. Proc R Soc Lond B Biol Sci 282:20140650

Webster FJ, Babcock RC, Van Keulen M, Loneragan NR (2015) Macroalgae Inhibits Larval Settlement and Increases Recruit Mortality at Ningaloo Reef, Western Australia. PLoS ONE 10:e0124162

Webster NS, Luter HM, Soo RM, Botté ES, Simister RL, Abdo D, Whalan S (2013) Same, same but different: symbiotic bacterial associations in GBR sponges. Aquat Microbiol 3:444

Webster NS, Negri AP (2006) Site-specific variation in Antarctic marine biofilms established on artificial surfaces. Environ Microbiol 8:1177–1190

Webster NS, Smith LD, Heyward AJ, Watts JEM, Webb RI, Blackall LL, Negri AP (2004) Metamorphosis of a Scleractinian Coral in Response to Microbial Biofilms. Appl Environ Microbiol 70:1213–1221

Webster NS, Soo R, Cobb R, Negri AP (2011) Elevated seawater temperature causes a microbial shift on crustose coralline algae with implications for the recruitment of coral larvae. ISME J 5:759–770

Wickham H, Chang W (2015) ggplot2: An Implementation of the Grammar of Graphics.

Williams PJ leB. (1995) Evidence for the seasonal accumulation of carbon-rich dissolved organic material, its scale in comparison with changes in particulate material and the consequential effect on net CN assimilation ratios. Mar Chem 51:17–29

Wilson SK, Bellwood DR, Choat JH, Furnas MJ (2003) Detritus in the epilithic algal matrix and its use by coral reef fishes. Oceanogr Mar Biol 41:279–310

Witt V, Wild C, Anthony KRN, Diaz-Pulido G, Uthicke S (2011a) Effects of ocean acidification on microbial community composition of, and oxygen fluxes through, biofilms from the Great Barrier Reef. Environ Microbiol 13:2976–2989

Witt V, Wild C, Uthicke S (2011b) Effect of substrate type on bacterial community composition in biofilms from the Great Barrier Reef. FEMS Microbiol Lett 323:188–195

Witt V, Wild C, Uthicke S (2012a) Terrestrial Runoff Controls the Bacterial Community Composition of Biofilms along a Water Quality Gradient in the Great Barrier Reef. Appl Environ Microbiol 78:7786–7791

Witt V, Wild C, Uthicke S (2012b) Interactive climate change and runoff effects alter O2 fluxes and bacterial community composition of coastal biofilms from the Great Barrier Reef. Aquat Microb Ecol 66:117–131

van Woesik R, Tomascik T, Blake S (1999) Coral assemblages and physico-chemical characteristics of the Whitsunday Islands: evidence of recent community changes. Mar Freshw Res 50:427–440

Ziegler M, Roder C, Bchel C, Voolstra CR (2015) Niche acclimatization in Red Sea corals is dependent on flexibility of host-symbiont association. Mar Ecol Prog Ser 533:149–161

Ziegler M, Roik A, Porter A, Zubier K, Mudarris MS, Ormond R, Voolstra CR (2016) Coral microbial community dynamics in response to anthropogenic impacts near a major city in the central Red Sea. Mar Pollut Bull 105:629–640

CHAPTER II

4. Spatial and seasonal reef calcification in corals and calcareous crusts in the central Red Sea

Anna Roik[1], Cornelia Roder[1], Till Röthig[1], Christian R Voolstra[1]

[1]Red Sea Research Center, Division of Biological and Environmental Science and Engineering, King Abdullah University of Science and Technology, Thuwal, Saudi Arabia

This manuscript has been published with Springer, *Coral Reefs* Journal

(Accepted, 27th November 2015; online on 14th December 2015)

Roik A, Roder C, Röthig T, Voolstra CR (2015) Spatial and seasonal reef calcification in corals and calcareous crusts in the central Red Sea. Coral Reefs 1–13, DOI: 10.1007/s00338-015-1383-y

4.1. Abstract

The existence of coral reef ecosystems critically relies on the reef carbonate framework produced by scleractinian corals and calcareous crusts (i.e., crustose coralline algae). While the Red Sea harbors one of the longest connected reef systems in the world, detailed calcification data is only available from the northernmost part. To fill this knowledge gap, we measured *in situ* calcification rates of primary and secondary reef-builders in the central Red Sea. We collected data on the major habitat-forming coral genera *Porites*, *Acropora*, and *Pocillopora*, and also on calcareous crusts (CC) in a spatio-seasonal framework. The scope of the study comprised sheltered and exposed sites of three reefs along a cross-shelf gradient and over four seasons of the year. Calcification of all coral genera was consistent across the shelf and highest in spring. In addition, *Pocillopora* showed increased calcification at exposed reef sites. In contrast, CC calcification increased from nearshore, sheltered to offshore, exposed reef sites, but also varied over seasons. Comparing our data to other reef locations, calcification in the Red Sea was in the range of data collected from reefs in the Caribbean and Indo-Pacific, however, *Acropora* calcification estimates were at the lower end of worldwide rates. Our study shows that the increasing coral cover from nearshore to offshore environments aligned with CC calcification but not coral calcification, highlighting the potentially important role of CC in structuring reef cover and habitats. While coral calcification maxima have been typically observed during summer in many reef locations worldwide, calcification maxima during spring in the central Red Sea indicate that summer temperatures exceeded the optima of reef calcifiers in this region. This study provides a foundation

for comparative efforts and sets a baseline to quantify impact of future environmental change in the central Red Sea.

4.2. Introduction

Tropical coral reefs are of unique value with regard to ecosystem productivity as well as species diversity (Wilkinson 2008). Their ecological importance is intimately linked to the structural complexity of the habitat (Goreau 1963), which is essential for the existence of most reef organisms (Graham 2014). Biogenic reef calcification, which is limited to tropical shorelines of warm, clear, sunlit waters and relatively stable physical conditions (Kleypas et al. 1999), is a key process contributing to reef habitat complexity. Scleractinian corals are the primary reef-builders that deposit calcium carbonate ($CaCO_3$) to give rise to the three-dimensional reef framework. Secondary reef-builders, composed predominantly of crustose coralline algae (Corallinales), form calcareous crusts (CC) and fortify the reef framework through cementation, counteracting its disintegration through erosion processes (Mallela and Perry 2007; Perry and Hepburn 2008).

In scleractinian corals, calcification depends on the productivity of the intracellular dinoflagellate algal symbionts (commonly referred to as zooxanthellae) that supply energy to the coral host through photosynthesis (Muscatine 1990). In addition, calcification rates in corals can further increase through heterotrophic feeding on plankton and suspended matter in the water column (Houlbrèque and Ferrier-Pagès 2009). CC calcification (considering Corallinales), in comparison, is directly based on the algae's physiology and depends on factors that support photosynthesis (reviewed

in Borowitzka and Larkum 1987) such as availability of light and inorganic nutrients (Chalker 1981; Chisholm 2000; Ferrier-Pagès et al. 2000).

Calcification rates are considered to be most sensitive to changes in temperature (Castillo et al. 2014), although the aragonite saturation state is also a determining factor (Gattuso et al. 1998; Martin and Gattuso 2009). High temperatures have been shown to positively impact coral growth leading to calcification maxima during summer conditions (Crossland 1984; Hibino and van Woesik 2000; Kuffner et al. 2013) and to higher calcification at warmer, lower latitudes compared to cooler, higher latitudes (Lough and Barnes 2000; Carricart-Ganivet 2004). Yet calcification rates can be fitted to a Gaussian distribution with a calcification maximum indicating the optimal temperature and calcification limits towards high and low temperature values (Marshall and Clode 2004). Indeed, reduced calcification has been shown to be associated with a rise in sea surface temperatures (SST), even when bleaching is not present (Cooper et al. 2008; Cantin et al. 2010; Carricart-Ganivet et al. 2012). Hence, coral growth and calcification rates are considered a diagnostic tool to provide insight into the performance and health status of corals (Edinger et al. 2000; Wooldridge 2014).

The majority of coral reefs thrive in stable physical environments with temperatures typically not exceeding 29 °C and salinity around 36 PSU (Kleypas et al. 1999), which is typically most favorable to coral growth. The Red Sea deviates from these environmental settings, with sea surface temperatures (SSTs) reaching 32 °C in the summer, temperature differences of up to 10 °C throughout the annual cycle (Davis

et al. 2011), and a relatively high salinity of 40 PSU or higher (Abu-Ghararah 1997). Yet the Red Sea features a high $CaCO_3$ saturation state (Steiner et al. 2014) and low sediment loads (Abu-Ghararah 1997), both of which can be considered beneficial for calcification. Indeed, pelagic $CaCO_3$ precipitation rates in the Red Sea were estimated to be higher than in the Gulf of Aden or the Indian Ocean (Steiner et al. 2014), but a comprehensive study collecting *in situ* reef calcification rates is missing.

To provide a baseline of reef calcification data for the reefs in the central Red Sea, we quantified *in situ* calcification rates as mass increments over time using the buoyant weight technique (Davies 1989) in a multispecies framework including primary and secondary reef-builders and spanning different reef locations across the shelf and across four seasons. Further, using spatial calcification rates of different calcifiers, we investigated whether and how their calcification performance relates to their benthic abundance in reef sites. Moreover, we explored the relationship of temperature and seasonal calcification rates using *in situ* temperature records. By comparing resulting annual average calcification rates from the central Red Sea with data from the Caribbean and the Indo-Pacific, we examined whether the unique environmental setting encountered in the Red Sea (warm, clear, sunlit and highly carbonate saturated) potentially maintains higher reef calcification compared to other coral reef regions.

4.3. Material and Methods

4.3.1. Study sites and seasons

Data for this study were collected at the exposed (fore reef) and sheltered (back reef) sites of three reefs, comprising six sites along a cross-shelf gradient off the Saudi Arabian coast (Figure 9): offshore exposed and sheltered (Shi'b Nazar reef, 22°20.456 N, 38°51.127 E); midshore exposed and sheltered (Al Fahal reef, 22°15.100 N, 38°57.386 E); and inshore exposed and sheltered (Inner Fsar reef, 22°13.974 N, 39°01.760 E). All study sites were located between 7.5 and 9 m depth. The study sites represented reefs of different environmental conditions, ranging from well-mixed habitats exposed to the open sea to turbid lagoonal inshore waters (Figure 10 A).

Four seasons were measured consecutively over 3-month intervals during one full year from mid-September 2012 to mid-September 2013 for corals and from mid-December 2012 to mid-December 2013 for CC. Seasons were defined as follows: spring from 15 March 2013 to 15 June 2013; summer from 15 June 2013 to 15 September 2013; fall from 15 September 2012 to 15 December 2012 (for coral assessment) or 15 September 2013 to 15 December 2013 (for CC assessment); and winter from 15 December 2012 to 15 March 2013.

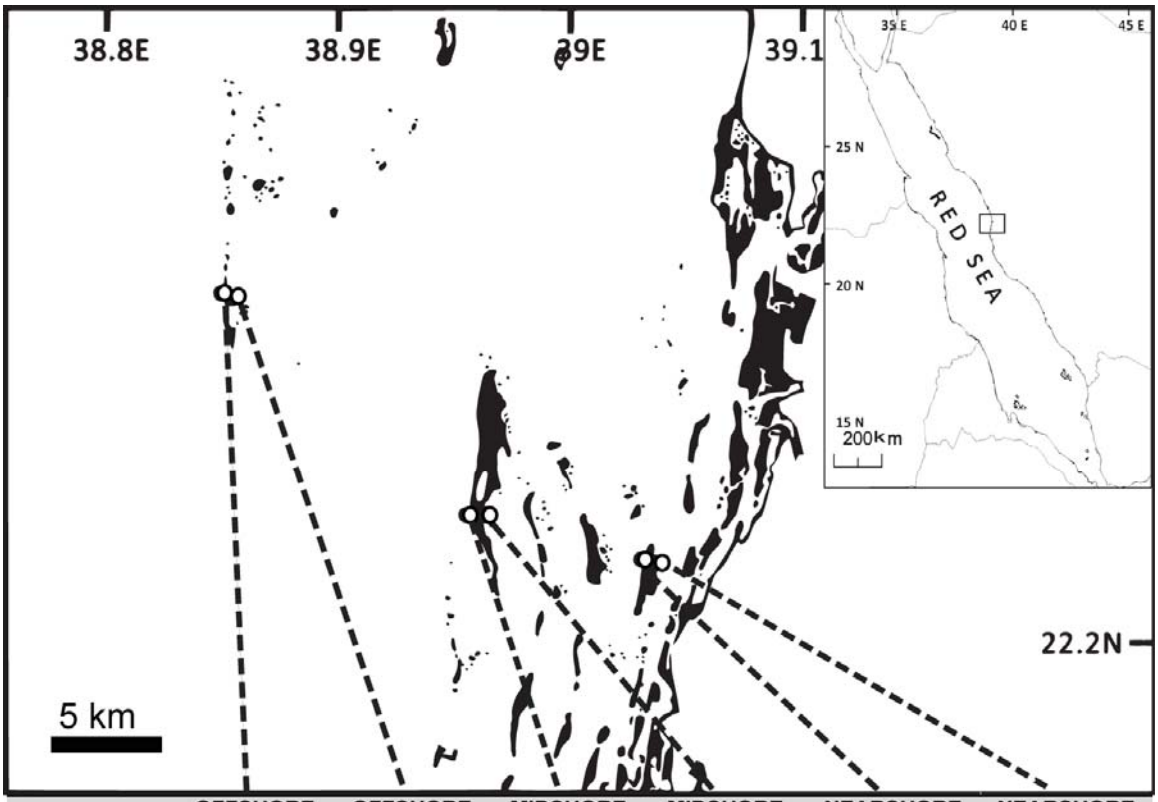

	OFFSHORE EXPOSED	OFFSHORE SHELTERED	MIDSHORE EXPOSED	MIDSHORE SHELTERED	NEARSHORE EXPOSED	NEARSHORE SHELTERED
coordinates	22°20.456 N 38°51.127 E	22°20.502 N 38°51.245 E	22°15.100 N 38°57.386 E	22°15.119 N 38°57.761 E	22°13.974 N 39°01.760 E	22°13.850 N 39°02.216 E
distance from shore	25 km	25 km	10 km	10 km	3 km	3 km
	replicates per season					
SPRING	POR (5) ACR (6) POC (6) CC (5)	POR (4) ACR (7) POC (6) CC (5)	POR (5) ACR (6) POC (5) CC (5)	POR (6) ACR (10) POC (7) CC (6)	POR (8) ACR (7) CC (3)	POR (8) ACR (6) CC (5)
SUMMER	POR (5) ACR (6) POC (6) CC (2)	POR (4) ACR (7) POC (6) CC (5)	POR (7) ACR (4) POC (4) CC (5)	POR (6) ACR (10) POC (6) CC (4)	POR (8) ACR (6) CC (4)	POR (7) ACR (5) CC (5)
FALL	POR (5) ACR (6) POC (5) CC (0)	POR (6) ACR (7) POC (5) CC (1)	POR (3) ACR (6) POC (5) CC (1)	POR (4) ACR (4) POC (2) CC (5)	POR (1) ACR (4) CC (5)	POR (6) ACR (4) CC (6)
WINTER	POR (5) ACR (5) POC (5) CC (6)	POR (6) ACR (4) POC (5) CC (5)	POR (5) ACR (4) POC (6) CC (6)	POR (4) ACR (5) POC (3) CC (6)	POR (7) ACR (4) CC (5)	POR (2) ACR (6) CC (6)

Figure 9 Overview of spatio-seasonal study design. The reef map provides location of the six study sites along the cross-shelf gradient. The table includes the site coordinates, site distance from shore, and replicate numbers (in brackets) for each calcifier group in each reef site (POR = *Porites*; ACR = *Acropora*; POC = *Pocillopora;* CC = calcareous crusts)

Figure 10 Study sites and *in situ* set up of moored frames. Photo panel (A) shows the study sites along the cross-shelf gradient, which represent reefs ranging from exposed fore-reef, well-mixed habitats to turbid back-reef lagoonal waters. Photo panel (B) presents a moored frame deployed at a study site and demonstrates how coral fragments (top) and plastic microscope slides (red box, bottom) were attached. (Photos: Anna Roik)

4.3.2. Benthic reef composition

To characterize the study sites, benthic reef composition was surveyed between October and December 2013. We followed a modified rugosity transect methodology from Perry et al. (2012). While standard line-intercept methods may underestimate the coverage of cryptic benthic components (e.g., coralline algae), the rugosity transect provides better resolution in this regard (Goatley and Bellwood 2011) as it follows reef topography. Six replicate transects (10 m long, spaced 10 m apart) at depths of 7.5–9 m were sampled parallel to the reef front. We considered the following benthic categories: sand/silt; rubble; rock; recently dead coral; macro- and turf algae; sponges; soft coral; other non-calcifying benthic reef organisms; and CC. Further, we recorded subcategories for the major reef-building taxa *Porites* spp., *Acropora* spp. and *Pocillopora* spp. and categorized other corals according to major growth forms as other branching, other massive corals, encrusting, and plate/foliose

corals. Data were prepared as mean and standard deviation of six replicate transects per reef (

Supplementary Table 5).

4.3.3. Temperature profiles

Temperature loggers (SBE 16plusV2 SEACAT, RS-232, Sea-Bird Electronics, Bellevue WA, USA) were deployed at the exposed study sites of each shelf section within the four seasons of the year in parallel with the assessment of coral calcification (see details above). For logistical reasons and due to battery life times of available loggers, sheltered sites were equipped with temperature loggers (TidbiT v2 temp, resolution 0.02 °C, accuracy 0.2 °C, Onset, Bourne MA USA) only during summer and winter seasons (summer deployment: 22 July 2013 to 11 September 2013; winter deployment: 25 November 2012 to 2 February 2013). For the time series plot, hourly logged data was smoothed through a weekly moving average filter. Additionally, the overall annual mean and standard deviation were determined. Moreover, we provide temperature averages, standard deviations, minima, maxima and the range per reef site and season (

Supplementary Table 6).

4.3.4. Seasonal calcification rates of reef-building corals

We measured seasonal calcification rates in fragments of the three dominant coral genera between September 2012 and September 2013. *Porites* spp. fragments (massive growing *P. lobata* and *P. lutea* morphotypes) were included as representatives of the massive coral genus *Porites*, three acroporid morphotypes (*A. squarrosa, A. plantaginea, A. hemprichii*) were sampled to represent the branching coral genus *Acropora*, and fragments of the branching coral morphotype *Pocillopora verrucosa* were collected to represent the genus *Pocillopora* (in nearshore reef sites this genus was not sufficiently present to assess calcification). In the following we pool species into *Porites*, *Acropora*, and *Pocillopora* groups.

Coral fragments of similar size (5–10 cm) were collected from distinct colonies growing at least 5 m apart using hammer and chisel for massive corals or a dive knife for branching corals. Six to ten fragments were selected (avoiding fragments infested by endo- and epilithic organisms via visual inspection) and attached to a PVC frame using fishing line; each coral fragment was mounted between two bars of the frame, leaving a distance of ~25 cm to the bottom and top PVC bar (Figure 10 B). Fragments were acclimated *in situ* for 1–2 weeks before calcification measurements were started. Within this period, the tissue and skeleton of coral fragments overgrew the fishing line with no apparent tissue damage or health impact. Only visually healthy fragments at the beginning and end of the measuring periods were considered.

Therefore, replicate numbers were reduced in some cases after the three-month period of deployment (see final replicate numbers in Figure 9 and

Supplementary Table 7).

Buoyant weight of fragments (Davies 1989) was measured at the beginning and end of each season: spring (10–13 and 24 March 2013 and 15–17 June 2013); summer (15–17 June 2013 and 9–11 September 2013); fall (16–18 and 25–26 September 2012 and 8–11 December 2012) and winter (8–11 December 2012 and 10–13 and 24 March 2013). Coral fragments were weighed *in situ* using a stainless-steel spring scale (Pesola, Switzerland, division 1 g, precision ±0.3%) and weight increases over seasons were determined. Over the course of seasonal measurements, missing or otherwise impacted coral colony fragments were replaced for the following season with newly collected fragments. Seasonal rates (G_{Coral}) were expressed as percent accretion of carbonate per day (

Equation 1, adopted from Ferrier-Pagès et al. 2000) using buoyant weight (Bw) increments over the calcification interval (season), normalized to the pre-season buoyant weight (Bw1) for each coral fragment, and divided by the days of the calcification interval (t).

$$G_{Coral}\ (\%\ day^{-1}) = \frac{\left[\left(\frac{Bw2-Bw1}{Bw1}\right)*100\right]}{t}$$

Equation 1 Calculation of coral calcification rates as %-accretion per day using buoyant weight measurements

4.3.5. Seasonal calcification rates of calcareous crusts (CC)

Calcification rates for CC were measured on seasonally sampled disposable microscope plastic slides (2.5cm x 6cm, Thermo Scientific Nunc Microscope Slides, USA) between December 2012 and December 2013. Deployment and sampling were

conducted at the beginning and end of each season: spring (11–13 March 2013 to 15–18 June 2013); summer (15–18 June 2013 to 11–12 September 2013); fall (11–12 September 2013 to 9–11 December 2013); winter (8–11 December 2012 to 11–13 March 2013).

Plastic/polyvinyl chloride (PVC) surfaces are commonly employed substrates for the measurement of carbonate accretion (Bak 1976; Kuffner et al. 2013). We used small slides due to their light weight, which allowed higher resolution and increased accuracy of the carbonate accretion measurements over relatively short periods of time (three months). Prior to deployment, the clear and smooth slides were sandpapered resulting in a whitish, frosted surface. Six slides were deployed on an aluminum frame at every site (Figure 10 B). Some slides were lost during the deployment (see replicate numbers in Figure 9 and

Supplementary Table 7). Visual inspection of the recovered plastic slides indicated that CC were composed of green algae, brown algae, and coralline crusts. In a few cases bryozoans were present, but neither coral recruits nor any other calcifying invertebrates were visually apparent. Upon recovery, slides were bleached for 12–14 h to remove organic material, dried for 48 h at 40 °C in an incubator (BINDER, Tuttlingen, Germany) and the dry mass (Dw1) comprising slide weight and carbonate accretion on both sides was obtained gravimetrically (Mettler Toledo XS 205, d = 0.01 mg/0.1 mg). Subsequently, slides were acidified in a 1:8 dilution of synthetic vinegar for 12–24 h to remove the entire carbonate crust, dried again (48 h at 40 °C), and weights of slides without carbonate (Dw2) were measured. Seasonally measured calcification rates were expressed as G_{CC} (mg cm^{-2} day^{-1}) by subtracting Dw2 from Dw1 and normalizing carbonate accretion to the slide surface area (cm^2) and the number of deployment days (t) following

Equation 2.

$$G_{CC}\ (\text{mg cm}^{-2}\text{day}^{-1}) = \frac{(\text{Dw1}-\text{Dw2})}{\text{cm}^2 \times \text{t}}$$

Equation 2 Calculation of calcareous crust calcification rates as $CaCO_3$ accretion per cm per day

4.3.6. Statistical analyses

Non-parametric multifactorial PERMANOVAs were employed to test for differences in coral seasonal calcification rates. Where calcification rates were repeatedly measured on one coral fragment across the seasons, tests for autocorrelation were performed to account for independence (Ljung and Box 1978; not significant for all repeated measurements). Next, coral calcification rates were square root-

transformed and data from all corals were subjected to a multifactorial PERMANOVA (based on Euclidean distances and 999 permutations). Additionally, tests were run for each coral genus separately. Post-hoc pair-wise tests were conducted for each significant factor independently. Further, we characterized the seasonal pattern in coral calcification rates; the increase in spring was quantified by calculating differences (as percentage increase) between the mean calcification rates in spring and the mean rates of the other seasons for each site.

The CC data were tested similarly to coral data using the same transformation, PERMANOVA design, and specifications. Additionally, we characterized the seasonal pattern in CC calcification rates; the significant decrease in spring and summer was quantified by calculating differences (as percentage decrease) between mean calcification rates in spring and summer and mean rates in fall/winter.

Linear regressions were applied in each calcifier group to explore the relationships between calcification rates and the calcifiers' percent cover at the reef sites. Additionally, linear regressions were performed between the calcification rates of CC and the percent cover of the coral genera and between the percent cover of CC and percent cover of corals. Multifactorial analyses were conducted using the software package PRIMER-E v6 (PERMANOVA+). Statistica (StatSoft Inc. 2011, version 10) and SigmaPlot (Systat Software, version 11.0) were used for autocorrelation tests and linear regression.

4.3.7. Global comparison of calcification rates

For a comparative presentation of the calcification rates from our study, we compiled calcification data from coral reef regions around the globe (see Supplementary Appendix 1 for comparison of calcification data obtained with different measures). The most common metric reported in other studies is carbonate accretion normalized to surface area. In order to compare CC calcification, we compared highest and lowest seasonal G_{CC} (mg cm^{-2} day^{-1}) values (Supplementary Table 7). For coral, calcification rates, G_{Coral} (mg cm^{-2} day^{-1}), were generated for a subset of samples, which represented all reef sites and were measured over two adjacent seasons (i.e., fall and winter; spring and summer; *Porites*, n = 13; *Acropora*, n = 22; *Pocillopora*, n = 23). Buoyant weight (Bw) increments over the two seasons were converted to dry weight increments (Dw) following

Equation **3** (Davies 1989):

$$\text{Dw (mg)} = \frac{\text{Bw (mg)}}{1-\left(\frac{\rho\text{Seawater}}{\rho\text{Coral}}\right)}$$

Equation 3 Calculation of dry weight increments using buoyant weight measurements

We determined the surface area (cm^2) by wax dipping (Veal et al. 2010) and calculated overall calcification rates as dry weight increment per surface and day (mg cm^{-2} day^{-1}). Coral skeletal density values (ρ_{Coral}) of these coral fragments were determined according to Davies (1989) (

Equation 4) resulting in the mean densities of 2.72 ± 0.10, 2.87 ± 0.21 and 2.77 ± 0.14 g cm^{-3} (±SD) for *Porites*, *Acropora* and *Pocillopora*, respectively. Further, for each reef at each sampling time seawater density values ($\rho_{Seawater}$) were taken from the CTDs

moored at the exposed sites (monthly means $\rho_{Seawater}$ ranged between 1.023 and 1.026 g cm^{-3}).

$$\rho Coral\ (g\ cm^{-3}) = \frac{\rho Seawater}{1-\left(\frac{Bw}{Dw}\right)}$$

Equation 4 Calculation of coral skeletal density

4.4. Results

In this study we assessed spatio-seasonal patterns of calcification for primary and secondary reef-builders in the central Red Sea. The chosen study sites represent open sea exposed and sheltered lagoonal environments (see locations in Figure 9; visual representation of habitats in Figure 10 A). We characterized the cross-shelf gradient by benthic cover assessment (Figure 11) and measurements of water temperatures during the seasons (Figure 12).

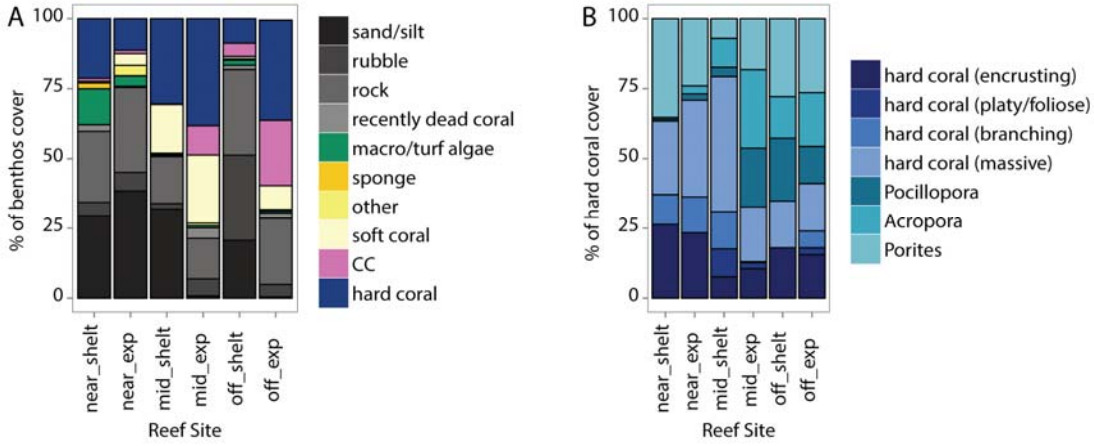

Figure 11 Benthic composition at the six study sites depicted as means from six replicate rugosity transects per site. (A) Benthic categories as proportion of benthos cover (%). The category 'hard coral' sums all coral categories assessed. (B) The composition of hard coral cover is expressed as percent of total hard coral cover and includes the major reef-building coral taxa (*Porites* spp., *Acropora* spp., *Pocillopora* spp.) as well as other corals categorized to major morphological groups. Abbreviations: CC = calcareous crusts; near = nearshore; mid = midshore; off = offshore; shelt = sheltered; exp = exposed

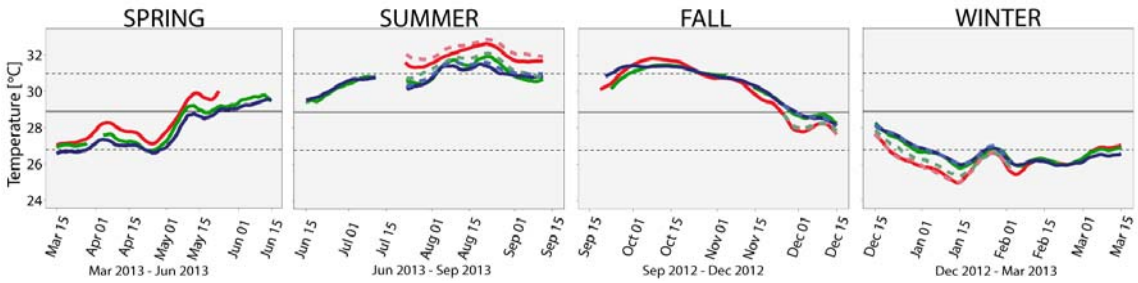

Figure 12 Seasonal temperature profiles in the central Red Sea across study sites. Data are plotted for all study sites using a weekly moving average (red = nearshore; green = midshore; blue = offshore; continuous line = exposed; dashed line = sheltered). All plots depict the annual mean temperature (black line) and the annual standard deviation (±SD: black dashed lines)

4.4.1. Benthic reef composition

Benthic transect data revealed differences between locations along the cross-shelf gradient (Figure 11 A; Supplementary Table 5); all sheltered sites were dominated by sandy bottom, rubble, and rock surface and characterized by a low percentage of live substrate (benthic organisms) (<40%). Exposed sites in offshore and midshore reefs had the highest percentage of live benthos (>68%) and the highest abundance (>35%) of calcifying biota (hard coral and CC). The cover of calcareous crusts increased with distance from shore, from ~1% in both nearshore sites and in the sheltered midshore site to 10% and 23% in the midshore and offshore exposed sites, where coral cover was also greatest. In the offshore sheltered reef site, CC abundance was comparatively low (5%).

Major scleractinian coral taxa belong to the genera of *Acropora*, *Pocillopora*, *Porites* constituted 32–56% of the total hard coral cover in the study sites (Figure 11). Among the major taxa, the most widely abundant coral genus across the reefs was *Porites* (about >20% of the total hard coral cover on most reefs). *Acropora* and *Pocillopora*

were comparatively rare in nearshore reefs (both taxa present at 0.6– 3%), but prevalent in midshore exposed and offshore exposed and sheltered sites (13–27%). Both genera increased in abundance with increasing distance from shore; while *Acropora* constituted 10% in the midshore sheltered site, *Pocillopora* was only present at 3%. In the midshore exposed site, both genera made up a larger percentage of the total coral cover (*Acropora*: 21%, *Pocillopora*: 27%).

4.4.2. Temperature profile

Data records from 7.5 to 9 m depth revealed increasing temperatures from spring onwards (mid-March), with maxima in summer (July and August), decreasing again during fall (late-September) and winter (December), and a minimum from January to early March (Figure 12 ; Supplementary Table 6). The coldest season was winter (mid-December until mid-March) with a seasonal mean temperature of 26.4 ± 0.7 °C across sites (spanning a temperature range of 24.1–28.4 °C). The warmest season was summer (mid-June until mid-September) with a seasonal mean of 31.1 ± 0.7 °C across all sites (spanning a temperature range of 28.6–33.3 °C). The seasons representing rising and falling temperatures were spring (mid-March until mid-June; seasonal mean: 28.0 ± 1.1 °C, range: 26.2–30.8 °C) and fall (mid-September until mid-December; seasonal mean: 30.0 ± 1.2 °C; range: 27.0–32.2 °C). Standard deviations between 0.7 and 1.2 °C calculated per season pooled over the reef sites indicate smaller temperature differences between the sites, in comparison to the differences per site over the year (i.e., seasonal differences) that were characterized by higher standard deviations of 1.9 to 2.9 °C (Supplementary Table 6). The seasonal

temperature differences between the lowest and highest temperature over the year recorded for each of the reef sites across the shelf were 6.6 to 9.0 °C.

4.4.3. Seasonal calcification of reef-building corals

Multifactorial PERMANOVAs were used to determine seasonal and spatial differences in calcification rates. The analysis on all seasonal coral rates revealed that coral 'genus' was the strongest source of variation (Pseudo-F = 88.2, $p_{(perm)}$ = 0.001; Table 8, Supplementary Table 8). Further, a PERMANOVA on each coral genus separately revealed two patterns of coral calcification: calcification rates for *Porites* and *Acropora* significantly differed among seasons ($p_{(perm)} < 0.05$ for both genera), but not among reefs or between exposures. *Pocillopora* calcification rates were different among seasons as well as between exposures (both factors $p_{(perm)}$ = 0.001), but not among reefs. Common to all coral genera, highest calcification rates were observed during spring (Figure 13, Supplementary Table 7). On average, spring calcification was 72% higher in *Porites*, 74% in *Acropora*, and 58% higher in *Pocillopora* compared to the other seasons. There were only few cases when spring calcification was similar to, but still higher than, the other seasons (increase was <5%, Supplementary Table 9). Of the three coral genera, only *Pocillopora* showed a significant difference in calcification rates between exposed and sheltered sites with rates higher at exposed sites (pair-wise test results for midshore: $p_{(perm)}$ = 0.001; offshore: $p_{(perm)} > 0.05$). Rates at most reefs were 8–55% higher at the exposed sites than at sheltered sites, but the differences were largest at the exposed site of the midshore reef during winter and fall, with rates increased by up to 170% and 270%, respectively. In addition, among all coral genera only calcification for *Pocillopora* had a significant linear

relationship to cover of benthos (R^2 = 0.40, p = 0.009; Table 9, Supplementary Figure 1 A).

Table 8 PERMANOVA (fixed factors) results of seasonal calcification data.

PERMANOVA design	p (perm) all corals	PERMANOVA design	p (perm) *POR*	p (perm) *ACR*	p (perm) *POC*	p (perm) CC
coralgenus	0.001	-	-	-	-	-
reef(coralgenus)	0.365	reef	0.096	0.615	0.314	0.001
exposure(reef(coralgenus))	0.001	exposure(reef)	0.06	0.094	0.001	0.001
season(exposure(reef(coralgenus)))	0.001	season(exposure(reef))	0.017	0.033	0.001	0.001

POR = *Porites*; ACR = *Acropora*; POC = *Pocillopora*; CC = calcareous crusts; p(perm) = p-value PERMANOVA

Table 9 Relationships between calcification rates and percent cover of calcifiers in the reef. (A) Linear regressions explore the relationships between calcification rates and percent cover of each calcifier. (B) Results of the linear regressions between calcification rates of CC and percent cover of each coral genus. (C) Results of the linear regressions between percent cover of CC and percent cover of the corals.

Dependent variable	Explanatory variable	Linear regression	
A. Calcification rates	Percent cover of benthos	R^2	p
POR	POR	0.07	0.221
ACR	ACR	0.03	0.452
POC	POC	0.40	0.009
B. calcification rates	Percent cover of benthos	R^2	p
CC	CC	0.82	<0.001
CC	POR	0.28	0.010
CC	ACR	0.41	0.001
CC	POC	0.43	<0.001
C. Percent cover of benthos	Percent cover of benthos	R^2	p
CC	POR	0.54	<0.001
CC	ACR	0.44	<0.001
CC	POC	0.45	<0.001

POR = *Porites*; ACR = *Acropora*; POC = *Pocillopora*; CC = calcareous crusts

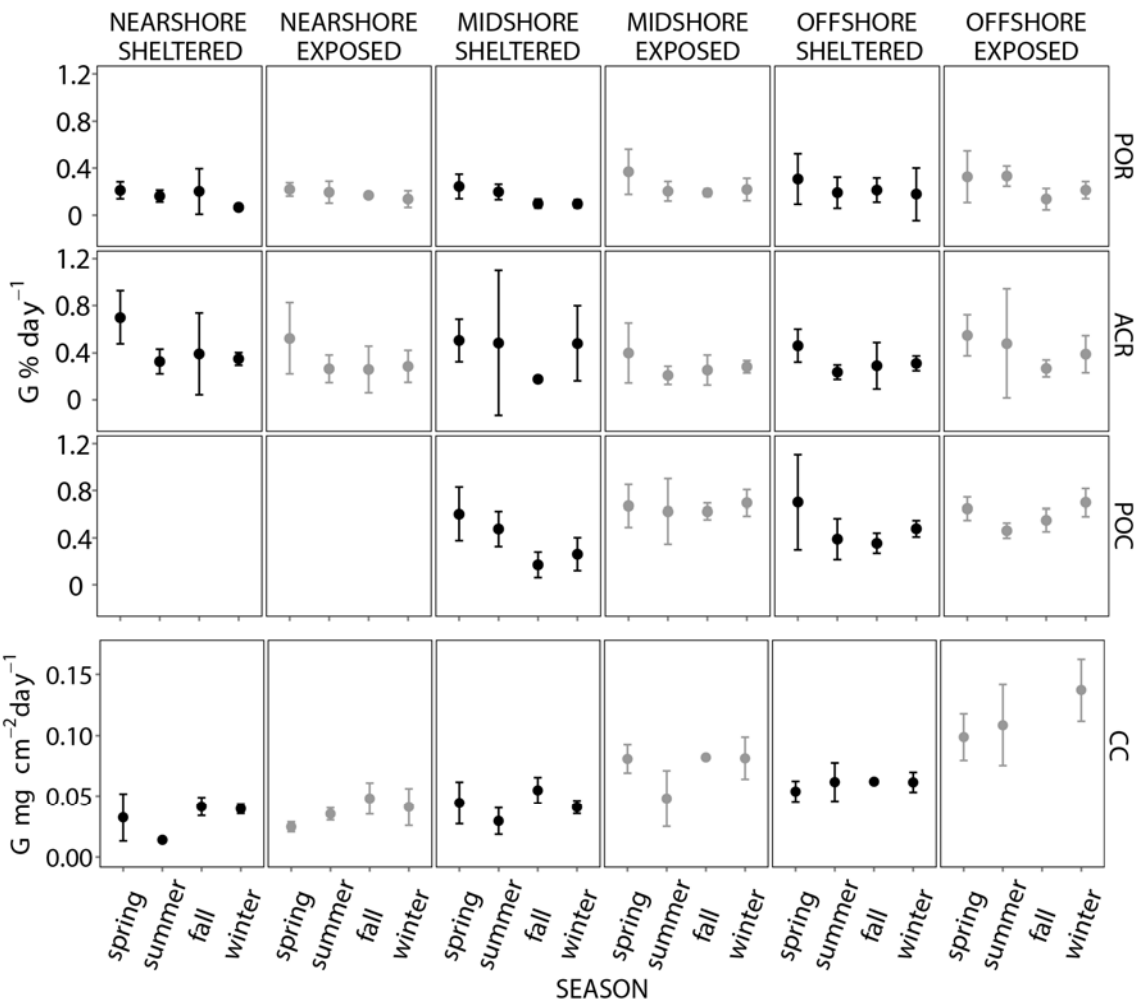

Figure 13 Spatio-seasonal patterns of reef calcification for corals and calcareous crusts (CC). Plots are separated according to reef location (columns) with further subdivision for seasons on the x-axis. The first three rows show seasonal coral calcification rates as percent accretion per day (G_{Coral} [% day^{-1}]) with each row showing one coral genus (POR = *Porites*, ACR = *Acropora*, POC = *Pocillopora*). Calcification for pocilloporid corals was not measured in nearshore reef sites. The fourth row shows CC calcification rates as dry weight accretion per surface area per day (G_{CC} [mg cm^{-2} day^{-1}]). Filled circle = means, error bars = standard deviation; color code: grey = exposed, black = sheltered

4.4.4. Seasonal calcification of calcareous crusts (CC)

Calcification patterns of CC (Figure 13, Supplementary Table 7) differed from those of corals. Significant differences in CC calcification rates were found for factors season, reef, and exposure (all: $p_{(perm)}$ = 0.001; Table 8, Supplementary Table 10). Calcification rates of CC significantly increased with distance to shore and further

increased at exposed sites compared to sheltered reef sites in the midshore and offshore reefs (both: pair-wise test $p_{(perm)}$ = 0.001). The highest seasonal mean calcification rate was measured at the exposed offshore site during winter (0.137 ± 0.025 mg cm^{-2} day^{-1}), while the lowest was at the sheltered nearshore site during summer (0.014 ± 0.002 mg cm^{-2} day^{-1}). Regarding the cross-shelf gradient, calcification at the offshore exposed site was 8.8-fold higher than at the nearshore sheltered site. Calcification rates were 50–123% higher at the exposed reef sites (midshore and offshore reefs), but there was no significant difference between the exposed and sheltered site at the nearshore reef. Seasonality in CC was characterized by lower seasonal mean calcification rates during spring and summer at all sites (Supplementary Table 11). Spring and summer mean calcification rates were reduced by 13–66% compared to the highest seasonal means in fall/winter for each respective site.

CC calcification rates and benthic cover were significantly linearly correlated (R^2 = 0.82 $p < 0.001$; Table 9, Supplementary Figure 1 B). Further, CC calcification was significantly correlated to the percent cover of the three coral taxa (*Porites*: R^2 = 0.28, p = 0.01; *Acropora*: R^2 = 0.41 p = 0.001; *Pocillopora*: R^2 = 0.43 $p < 0.001$, Supplementary Figure 1 C - E). Accordingly, CC percent cover correlated significantly with the coverage by coral taxa (*Porites*: R^2 = 0.54, $p < 0.001$; *Acropora*: R^2 = 0.44 $p < 0.001$; *Pocillopora*: R^2 = 0.45 $p < 0.001$; Supplementary Figure 1 F – H).

4.4.5. Global comparison of calcification rates

Annual average calcification rates for *Porites* and *Pocillopora* from the central Red Sea were in the range of calcification rates from other regions (Table 10), while *Acropora* calcification rates were lower. In detail, *Porites* in the central Red Sea (1.46 ± 0.52 mg cm^{-2} day^{-1} ±SD) was intermediate in the range of values between 0.24 and 2.16 mg cm^{-2} day^{-1} from other regions (see below). *Pocillopora* calcified at an annual average rate of 0.92 ± 0.21 mg cm^{-2} day^{-1} in the central Red Sea and was at the higher end of the commonly measured range of 0.09–1.18 mg cm^{-2} day^{-1} reported from other studies. *Acropora* from the central Red Sea calcified at an average rate of 0.72 ± 0.17 mg cm^{-2} day^{-1}, and was at the low end of the range reported by Goreau and Goreau (1959) for the Caribbean (0.84–3.06 mg cm^{-2} day^{-1}) and below the calcification reported from French Polynesia and Western Australia (around 1.0 mg cm^{-2} day^{-1}; Comeau et al. 2013; Foster et al. 2014). Calcification rates for *Acropora* and *Pocillopora* from aquaculture were far lower than field-based measurements (0.04–0.07 and 0.07–0.15 mg cm^{-2} day^{-1}, respectively). CC calcification rates from the central Red Sea (0.014–0.137 mg cm^{-2} day^{-1}) were in line with the rates measured elsewhere (lowest and highest reported values: 0.019 and 0.130 mg cm^{-2} day^{-1} both from the Caribbean), only Pari et al. (1998) reported a 3-fold higher maximum (0.310 mg cm^{-2} day^{-1}) measured in French Polynesia.

Table 10 Global comparison of annual calcification rates (G). Locations from the central Red Sea (this study), the Indo-Pacific, and the Caribbean are considered.

Calcifier	Region	G (mg cm^{-2} day^{-1})	Study	Method
POR (*Porites* spp.)	Central Red Sea	1.46 (0.52)	This study	Buoyant weight
POR (*Porites furcata*)	Caribbean	0.24–2.16 [1)]	Goreau and Goreau (1959)	$Ca^{45}Cl_2$-incubations
POR (*Porites* sp.)	Japan	1.89	Comeau et al. (2014b)	Buoyant weight
POR (*Porites* sp.)	Hawaii	1.1	Comeau et al. (2014b)	Buoyant weight
POR (*Porites rus*)	French Polynesia	1.53 (0.07)	Comeau et al. (2013)	Buoyant weight
POR (*Porites* sp.)	French Polynesia	1.2	Comeau et al. (2014b)	Buoyant weight
ACR (*Acropora* spp).	Central Red Sea	0.72 (0.17)	This study	Buoyant weight
ACR (*Acropora eurystoma*)	Red Sea (Gulf of Aqaba)	0.96 [2)]	Schneider and Erez (2006)	TA depletion
ACR (*Acropora palmata*)	Caribbean	3.06 [1)]	Goreau and Goreau (1959)	$Ca^{45}Cl_2$-incubations
ACR (*Acropora cervicornis*)	Caribbean	0.84 [1)]	Goreau and Goreau (1959)	$Ca^{45}Cl_2$-incubations
ACR (*Acropora pulchra*)	Indian Ocean (Western Australia)	1.15	Foster et al. (2014)	Buoyant weight
ACR (*Acropora yongei*)	Indian Ocean (Western Australia)	1.31–2.02	Ross et al. (2015)	Buoyant weight
ACR (*Acropora pulchra*)	French Polynesia	1.41 (0.08)	Comeau et al. (2013)	Buoyant weight
ACR (*Acropora pulchra*)	French Polynesia	1.02 (0.05)$^+$	Comeau et al. (2014a)	Buoyant weight
ACR (*Acropora millepora*)	Aqua culture	0.04–0.07	Schoepf et al. (2013)	Buoyant weight
POC (*Pocillopora* spp.)	Central Red Sea	0.92 (0.19)	This study	Buoyant weight
POC (*Pocillopora verrucosa*)	Red Sea	0.09–0.97 [3)]	Sawall et al. (2015)	TA depletion
POC (*Pocillopora damicornis*)	Indian Ocean (Western Australia)	0.66	Foster et al. (2014)	Buoyant weight
POC (*Pocillopora damicornis*)	Indian Ocean (Western Australia)	0.34–0.90	Ross et al. (2015)	Buoyant weight
POC (*Pocillopora damicornis*)	Japan	1.18	Comeau et al. (2014b)	Buoyant weight
POC (*Pocillopora damicornis*)	Hawaii	0.75	Comeau et al. (2014b)	Buoyant weight
POC (*Pocillopora damicornis*)	Hawaii	0.17–0.38 [4)]	Clausen and Roth (1975)	$Ca^{45}Cl_2$-incubations
POC (*Pocillopora damicornis*)	French Polynesia	0.69 (0.08)	Comeau et al. (2013)	Buoyant weight
POC (*Pocillopora damicornis*)	French Polynesia	0.6	Comeau et al. (2014b)	Buoyant weight
POC (*Pocillopora damicornis*)	Aqua culture	0.07–0.15	Schoepf et al. (2013)	Buoyant weight
CC	Central Red Sea	0.014–0.137	This study	Dry weight
CC	Caribbean	0.036	Bak (1976)	Dry weight
CC	Caribbean	0.130	Kuffner et al. (2013)	Dry weight
CC	Caribbean	0.019–0.035 [5)]	Mallela and Perry (2007)	Dry weight
CC	Caribbean	0.029 (0.019) [5)]	Mallela (2013)	Dry weight
CC	French Polynesia	0.05–0.310	Pari et al. (1998)	Dry weight

Values are reported as a regional range, as an average value as mean (SD), or if labelled $^+$ as an average value mean (SE). Values were converted to mg cm^{-2} day^{-1} from: [1)]µg Ca cm^{-2} h^{-1}, [2)]µmol $CaCO_3$ cm^{-2} h^{-1}, [3)]µmol $CaCO_3$ cm^{-2} d^{-1}, [4)]ng $CaCO_3$ mm^{-2} h^{-1}, [5)]g m^{-2} $year^{-1}$. POR = *Porites*, ACR = *Acropora*, POC = *Pocillopora*, CC = calcareous crusts

4.5. Discussion

Coral reef ecosystems critically rely on the reef carbonate framework produced by calcifying biota. In this study, we assessed spatial and seasonal reef calcification in corals and calcareous algae in the central Red Sea. We found that calcification in reef-building corals from the genus *Porites* and *Acropora* varied seasonally, while calcification in *Pocillopora* was influenced by season and site exposure. Importantly, calcification in secondary reef-builders (CC) differed along the cross-shelf gradient and also with site exposure and season.

4.5.1. Spatial calcification and coral reef benthic composition

It has been rarely tested whether or how calcification rates play a role in structuring the benthic composition (Pratchett et al. 2015). In our study, we collected data on calcification rates and benthic reef abundance for selected coral genera to further understand how calcification performance related to coral abundance in nearshore, midshore, and offshore reef sites. Among the corals in our study, only pocilloporid calcification rates were different among reef sites and were significantly related ($R^2 = 0.40$, $p < 0.01$) to their benthic abundances. *Pocillopora* is characterized as a 'weedy' and competitive taxon, often dominant in benthic assemblages (Darling et al. 2012). In our study, pocilloporids were less dominant and their calcification rates were also lower in sheltered than at exposed sites. This observation suggests that pocilloporid calcification rates may be a contributing factor to explain the taxon's dominance in exposed reef sites. In contrast, calcification rates in *Porites* and *Acropora* did not differ among sites and did correlate to their benthic abundance. In particular for *Acropora,* it is most evident that calcification rates, which were similar from nearshore to

offshore reefs, cannot explain the increasing abundances from nearshore towards offshore reefs. Based on these data, we argue that benthic abundance of corals studied here is less determined by their calcification performance than by other aspects such as limited coral settlement in nearshore locations. Lower settlement and recruitment rates may be a consequence of increased sedimentation or other coastal disturbances (Gilmour 1999), which are typical for nearshore reef sites (Cooper et al. 2007).

CC, aside from their role as secondary reef-builders contributing to reef carbonate production and fortification of the reef framework (Mallela 2007; Perry and Hepburn 2008), and fulfil another crucial ecological role by providing settlement cues and substrate for the larvae of reef-building corals (Heyward and Negri 1999). Our data support this argument by showing a significant positive relationship of CC calcification rates and percent cover with the abundances of the three important reef-builders *Porites*, *Acropora* and *Pocillopora*. Since studies focusing on CC are scarce (Mallela 2013), our conclusions emphasize the importance of incorporating the assessment of CC calcification and community dynamics in future coral reefs studies and monitoring efforts.

4.5.2. Seasonal calcification and temperature dependency

Among various physico-chemical factors that can influence calcification in corals and CC (e.g., aragonite saturation state, nutrient and light availability) (Chalker 1981; Gattuso et al. 1998; Chisholm 2000; Ferrier-Pagès et al. 2000), temperature has been demonstrated to be a dominant driver (Borowitzka and Larkum 1987; Martin and Gattuso 2009; Cooper et al. 2012; Castillo et al. 2014). In this study, calcification in

corals and CC from the central Red Sea were significantly driven by season. Further, temperature differences on the seasonal scale were larger than differences among sites across the shelf (i.e., nearshore, midshore, offshore). Consequently, we consider seasonal temperature differences an essential component of the seasonal variation in calcification rates. In the Gulf of Aqaba (northern Red Sea region), temperatures and community net calcification were found to be positively correlated at a temperature range of 23 – 27 °C, but not for temperatures above 27 °C (Silverman et al. 2007). Our long-term measurements of seasonal calcification rates do not allow deduction of exact temperature optima for these calcifiers. More importantly, our data indicate that the optimal conditions for calcification may be similar in the three coral genera (*Porites*, *Acropora,* and *Pocillopora*) and lie within the temperature range of spring (min–max: 26.2 – 30.8 °C). Further, for CC we can show that both spring and summer (min–max. 26.2 – 33.3 °C), are associated with reduced seasonal calcification rates, which implies that temperatures in this range may be detrimental to CC calcification.

Calcification maxima are observed when local seawater temperatures meet the temperature optimum of the local calcifiers. Typically calcification maxima have been reported for the warmest season of the year (summer), for example for *Siderastrea siderea* from the northern Caribbean (Kuffner et al. 2013), *Acropora formosa* from Western Australia (Crossland 1984), CC from Japan (Hibino and van Woesik 2000) and net community calcification in Hawaii (Atkinson and Grigg 1984). Importantly, in the northern Red Sea, calcification maxima were reported for summer (Silverman et al. 2007; Sawall et al. 2015), whereas in the southern region highest calcification rates were measured in *Pocillopora verrucosa* during winter, the coldest season of the year

(Sawall et al. 2015) indicating that calcification peaks are determined by optimal prevailing temperature profiles. Here, we demonstrate that in the central Red Sea calcification maxima of three coral genera (*Porites*, *Acropora*, *Pocillopora*) were not observed during the warmest season of the year (summer), but during spring. This is in accordance with the recently reported north to south calcification patterns observed for *Pocillopora verrucosa* in the Red Sea where Sawall et al. (2015) found that calcification maxima occurred during summer in the north and during winter in the south. Our results can be interpreted as an indication that summer temperatures in the central Red Sea exceed the optimum local calcification temperature of three coral species and CC. A similar observation was recently reported from Western Australia (Foster et al. 2014), where the absence of a summer peak in calcification has been interpreted as a consequence of anomalously high summer temperatures in that region.

4.5.3. Calcification in corals vs. calcareous crusts (CC)

Our measurement of calcification rates revealed different trends for corals and CC. We showed that coral calcification rates varied mainly with season. By contrast, CC calcification rates were strongly influenced by cross-shelf position, site exposure, and seasonality. This may be attributable to physiological differences between corals (Tambutté et al. 2011) and CC (Borowitzka and Larkum 1987) and also shows that environmental parameters other than temperature are important. Putatively, increased turbidity and decreased irradiance in nearshore reef locations (Cooper et al. 2007) might explain the highly reduced nearshore calcification rates of CC, which rely solely on photosynthesis (Chisholm 2000; Edinger et al. 2000; Fabricius and

De'ath 2001). Coral calcification, by comparison, seemed to be less affected by the higher turbidity and lower irradiance in nearshore sites. Taken together, our results show that CC calcification is much more variable over distance to shore and seasons in comparison to coral calcification. This suggests that CC calcification is more sensitive to spatio-temporal differences in environmental conditions, and may thus be more susceptible to environmental change. Considering the importance of CC in shaping the reef structure, their sensitivity to changing environmental conditions may have substantial consequences for coral reef benthic communities.

4.5.4. Global comparison of calcification rates from the central Red Sea

Although calcification studies are numerous and cover many locations globally, our effort towards a global comparison of calcification rates indicated that it remains difficult to make accurate comparisons, due to inconsistencies in methodologies or the normalization of measurements (see Supplementary Appendix 1). Our comparative evaluation based on annual average calcification rates from studies using a similar approach to ours showed that the range of calcification in two major coral genera (*Porites* and *Pocillopora*) and CC were very similar between the Red Sea and the Caribbean or Indo-Pacific (Table 10). For the coral *Acropora*, we demonstrated that calcification rates in our study were at the lower end of the global range, although Red Sea conditions, i.e., high light penetration and high carbonate saturation, are anticipated to be beneficial for calcification. We conclude that Red Sea coral reef calcifiers are neither more nor less productive in terms of carbonate accretion, despite these favorable conditions. Indications that summer temperatures exceed the optima of reef calcifiers in this region (this study; Sawall et al. 2015) in

conjunction with increasing temperatures as a result of environmental change (Raitsos et al. 2011) pose detrimental effects to calcifiers, which may be counterbalancing the presumably beneficial effects of the Red Sea environment for calcification. The future persistence of coral reefs depends, besides other factors, on the rate of calcification in reef-building biota. Therefore, monitoring and evaluation of calcification rates in the Red Sea is crucial for the assessment of ecosystem stability. We hope that our study provides a baseline for calcification rates in primary and secondary reef builders in this region and serves as a foundation for comparative efforts to quantify impact of future environmental change.

4.6. References

Abu-Ghararah ZH (1997) Assessment of land-based sources and activities affecting the marine environment in the Red Sea and Gulf of Aden. UNEP Regional Seas Reports and Studies No 166

Atkinson MJ, Grigg RW (1984) Model of a coral reef ecosystem. II. Gross and net benthic primary production at French Frigate Shoals, Hawaii. Coral Reefs 3:13–22

Bak RPM (1976) The growth of coral colonies and the importance of crustose coralline algae and burrowing sponges in relation with carbonate accumulation. Neth J Sea Res 10:285–337

Borowitzka MA, Larkum AWD (1987) Calcification in algae: mechanisms and the role of metabolism. Crit Rev Plant Sci 6:1–45

Cantin NE, Cohen AL, Karnauskas KB, Tarrant AM, McCorkle DC (2010) Ocean warming slows coral growth in the central Red Sea. Science 329:322–325

Carricart-Ganivet JP (2004) Sea surface temperature and the growth of the West Atlantic reef-building coral *Montastraea annularis*. J Exp Mar Bio Ecol 302:249–260

Carricart-Ganivet JP, Cabanillas-Terán N, Cruz-Ortega I, Blanchon P (2012) Sensitivity of calcification to thermal stress varies among genera of massive reef-building corals. PLoS One 7:e32859

Castillo KD, Ries JB, Bruno JF, Westfield IT (2014) The reef-building coral *Siderastrea siderea* exhibits parabolic responses to ocean acidification and warming. Proc R Soc Lond B Biol Sci 281:20141856

Chalker BE (1981) Simulating light-saturation curves for photosynthesis and calcification by reef-building corals. Mar Biol 63:135–141

Chisholm JRM (2000) Calcification by crustose coralline algae on the northern Great Barrier Reef, Australia. Limnol Oceanogr 45:1476–1484

Clausen CD, Roth AA (1975) Estimation of coral growth-rates from laboratory 45Ca-incorporation rates. Marine Biology 33:85–91

Comeau S, Carpenter RC, Edmunds PJ (2014a) Effects of irradiance on the response of the coral *Acropora pulchra* and the calcifying alga *Hydrolithon reinboldii* to temperature elevation and ocean acidification. J Exp Mar Bio Ecol 453:28–35

Comeau S, Edmunds PJ, Spindel NB, Carpenter RC (2013) The responses of eight coral reef calcifiers to increasing partial pressure of CO_2 do not exhibit a tipping point. Limnol Oceanogr 58:388–398

Comeau S, Carpenter RC, Nojiri Y, Putnam HM, Sakai K, Edmunds PJ (2014b) Pacific-wide contrast highlights resistance of reef calcifiers to ocean acidification. Proc R Soc Lond B Biol Sci 281:20141339

Cooper TF, O'Leary RA, Lough JM (2012) Growth of Western Australian corals in the Anthropocene. Science 335:593–596

Cooper TF, Uthicke S, Humphrey C, Fabricius KE (2007) Gradients in water column nutrients, sediment parameters, irradiance and coral reef development in the Whitsunday region, central Great Barrier Reef. Estuar Coast Shelf Sci 74:458–470

Cooper TF, De'ath G, Fabricius KE, Lough JM (2008) Declining coral calcification in massive *Porites* in two nearshore regions of the northern Great Barrier Reef. Glob Chang Biol 14:529–538

Crossland CJ (1984) Seasonal variations in the rates of calcification and productivity in the coral *Acropora formosa* on a high-latitude reef. Mar Ecol Prog Ser 15:135–140

Darling ES, Alvarez-Filip L, Oliver TA, McClanahan TR, Côté IM (2012) Evaluating life-history strategies of reef corals from species traits. Ecol Lett 15:1378–1386

Davies PS (1989) Short-term growth measurements of corals using an accurate buoyant weighing technique. Mar Biol 101:389–395

Davis KA, Lentz SJ, Pineda J, Farrar JT, Starczak VR, Churchill JH (2011) Observations of the thermal environment on Red Sea platform reefs: a heat budget analysis. Coral Reefs 30:25–36

Edinger EN, Limmon GV, Jompa J, Widjatmoko W, Heikoop JM, Risk MJ (2000) Normal coral growth rates on dying reefs: are coral growth rates good indicators of reef health? Mar Pollut Bull 40:404–425

Fabricius K, De'ath G (2001) Environmental factors associated with the spatial distribution of crustose coralline algae on the Great Barrier Reef. Coral Reefs 19:303–309

Ferrier-Pagès C, Gattuso JP, Dallot S, Jaubert J (2000) Effect of nutrient enrichment on growth and photosynthesis of the zooxanthellate coral *Stylophora pistillata*. Coral Reefs 19:103–113

Foster T, Short JA, Falter JL, Ross C, McCulloch MT (2014) Reduced calcification in Western Australian corals during anomalously high summer water temperatures. J Exp Mar Bio Ecol 461:133–143

Gattuso J-P, Frankignoulle M, Bourge I, Romaine S, Buddemeier RW (1998) Effect of calcium carbonate saturation of seawater on coral calcification. Glob Planet Change 18:37–46

Gilmour J (1999) Experimental investigation into the effects of suspended sediment on fertilisation, larval survival and settlement in a scleractinian coral. Mar Biol 135:451–462

Goatley CHR, Bellwood DR (2011) The roles of dimensionality, canopies and complexity in ecosystem monitoring. PLoS One 6:e27307

Goreau TF (1963) Calcium carbonate deposition by coralline algae and corals in relation to their roles as reef-builders. Ann N Y Acad Sci 109:127–167

Goreau TF, Goreau NI (1959) The physiology of skeleton formation in corals. II. Calcium deposition by hermatypic corals under various conditions in the reef. Biol Bull 117:239–250

Graham NAJ (2014) Habitat complexity: coral structural loss leads to fisheries declines. Curr Biol 24:R359–R361

Heyward AJ, Negri AP (1999) Natural inducers for coral larval metamorphosis. Coral Reefs 18:273–279

Hibino K, van Woesik R (2000) Spatial differences and seasonal changes of net carbonate accumulation on some coral reefs of the Ryukyu Islands, Japan. J Exp Mar Bio Ecol 252:1–14

Houlbrèque F, Ferrier-Pagès C (2009) Heterotrophy in tropical scleractinian corals. Biol Rev 84:1–17

Kleypas JA, McManus JW, Menez LAB (1999) Environmental limits to coral reef development: where do we draw the line? Am Zool 39:146–159

Kuffner IB, Hickey TD, Morrison JM (2013) Calcification rates of the massive coral *Siderastrea siderea* and crustose coralline algae along the Florida Keys (USA) outer-reef tract. Coral Reefs 32:987–997

Ljung GM, Box GEP (1978) On a measure of lack of fit in time series models. Biometrika 65:297–303

Lough JM, Barnes DJ (2000) Environmental controls on growth of the massive coral *Porites*. J Exp Mar Bio Ecol 245:225–243

Mallela J (2007) Coral reef encruster communities and carbonate production in cryptic and exposed coral reef habitats along a gradient of terrestrial disturbance. Coral Reefs 26:775–785

Mallela J (2013) Calcification by reef-building sclerobionts. PLoS One 8:e60010

Mallela J, Perry C (2007) Calcium carbonate budgets for two coral reefs affected by different terrestrial runoff regimes, Rio Bueno, Jamaica. Coral Reefs 26:129–145

Marshall AT, Clode P (2004) Calcification rate and the effect of temperature in a zooxanthellate and an azooxanthellate scleractinian reef coral. Coral Reefs 23:218–224

Martin S, Gattuso J-P (2009) Response of Mediterranean coralline algae to ocean acidification and elevated temperature. Glob Chang Biol 15:2089–2100

Muscatine L (1990) The role of symbiotic algae in carbon and energy flux in reef corals. In: Dubinsky Z (ed.) Coral reefs, Ecosystems of the world vol. 25, Elsevier, Amsterdam, pp 75–87

Pari N, Peyrot-Clausade M, Le Champion-Alsumard T, Hutchings P, Chazottes V, Gobulic S, Le Champion J, Fontaine MF (1998) Bioerosion of experimental substrates on high islands and on atoll lagoons (French Polynesia) after two years of exposure. Mar Ecol Prog Ser 166:119–130

Perry C, Edinger E, Kench P, Murphy G, Smithers S, Steneck R, Mumby P (2012) Estimating rates of biologically driven coral reef framework production and erosion: a new census-based carbonate budget methodology and applications to the reefs of Bonaire. Coral Reefs 31:853–868

Perry CT, Hepburn LJ (2008) Syn-depositional alteration of coral reef framework through bioerosion, encrustation and cementation: taphonomic signatures of reef accretion and reef depositional events. Earth Sci Rev 86:106–144

Pratchett MS, Anderson KD, Hoogenboom MO, Widman E, Baird AH, Pandolfi JM, Edmunds PJ, Lough JM (2015) Spatial, temporal and taxonomic variation in coral growth—implications for the structure and function of coral reef ecosystems. Oceanogr Mar Biol Annu Rev 53:215–295

Raitsos DE, Hoteit I, Prihartato PK, Chronis T, Triantafyllou G, Abualnaja Y (2011) Abrupt warming of the Red Sea. Geophys Res Lett 38:L14601

Ross CL, Falter JL, Schoepf V, McCulloch MT (2015) Perennial growth of hermatypic corals at Rottnest Island, Western Australia (32°S). PeerJ 3:e781

Sawall Y, Al-Sofyani A, Hohn S, Banguera-Hinestroza E, Voolstra CR, Wahl M (2015) Extensive phenotypic plasticity of a Red Sea coral over a strong latitudinal temperature gradient suggests limited acclimatization potential to warming. Sci Rep 5:8940

Schneider K, Erez J (2006) The effect of carbonate chemistry on calcification and photosynthesis in the hermatypic coral *Acropora eurystoma*. Limnol Oceanogr 1284–1293

Schoepf V, Grottoli AG, Warner ME, Cai W-J, Melman TF, Hoadley KD, Pettay DT, Hu X, Li Q, Xu H, Wang Y, Matsui Y, Baumann JH (2013) Coral energy reserves and calcification in a high-CO_2 world at two temperatures. PLoS One 8:e75049

Silverman J, Lazar B, Erez J (2007) Effect of aragonite saturation, temperature, and nutrients on the community calcification rate of a coral reef. J Geophys Res 112:C05004

Steiner Z, Erez J, Shemesh A, Yam R, Katz A, Lazar B (2014) Basin-scale estimates of pelagic and coral reef calcification in the Red Sea and Western Indian Ocean. Proc Natl Acad Sci U S A 111:16303–16308

Tambutté S, Holcomb M, Ferrier-Pagès C, Reynaud S, Tambutté É, Zoccola D, Allemand D (2011) Coral biomineralization: from the gene to the environment. J Exp Mar Biol Eco 408:58–78

Veal CJ, Carmi M, Fine M, Hoegh-Guldberg O (2010) Increasing the accuracy of surface area estimation using single wax dipping of coral fragments. Coral Reefs 29:893–897

Wilkinson C (2008) Status of coral reefs of the world: 2008. Global Coral Reef Monitoring Network and Reef and Rainforest Research Centre, Townsville, Australia

Wooldridge SA (2014) Assessing coral health and resilience in a warming ocean: why looks can be deceptive. Bioessays 36:201400074

4.7. Supplementary Materials

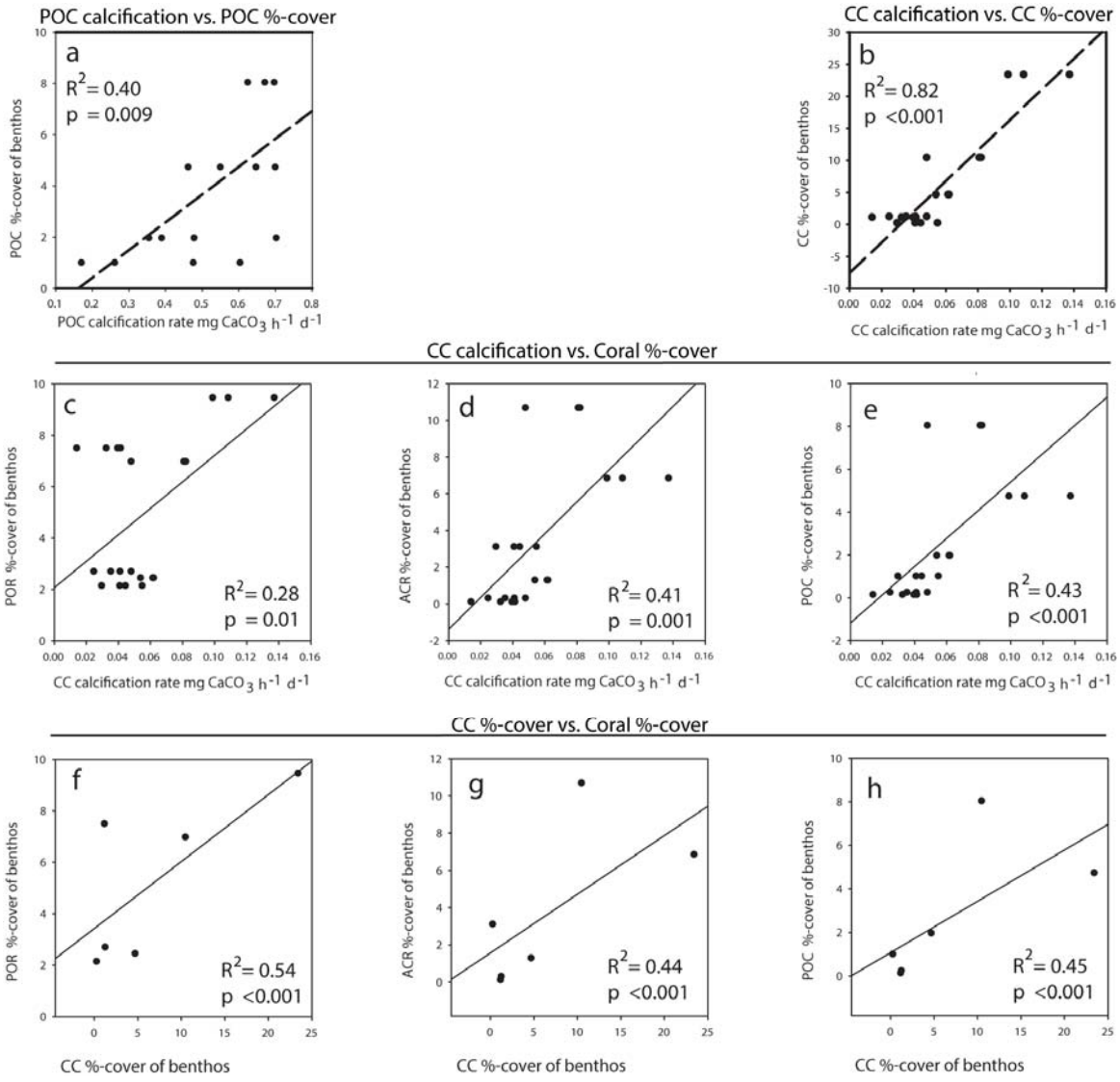

Supplementary Figure 1 Linear regressions of calcification rates and calcifier %-cover of benthos. Scatterplots of significant results ($p < 0.05$) are shown. (a) Linear regression of *Pocillopora* calcification rates vs percent cover; (b) linear regressions of calcareous crusts (CC) calcification rates vs percent cover; (c–e) linear regression of CC calcification rates vs percent cover of coral groups; (f–h) linear regressions of CC percent cover and percent cover of coral groups (POR = *Porites*; ACR = *Acropora*; POC = *Pocillopora*)

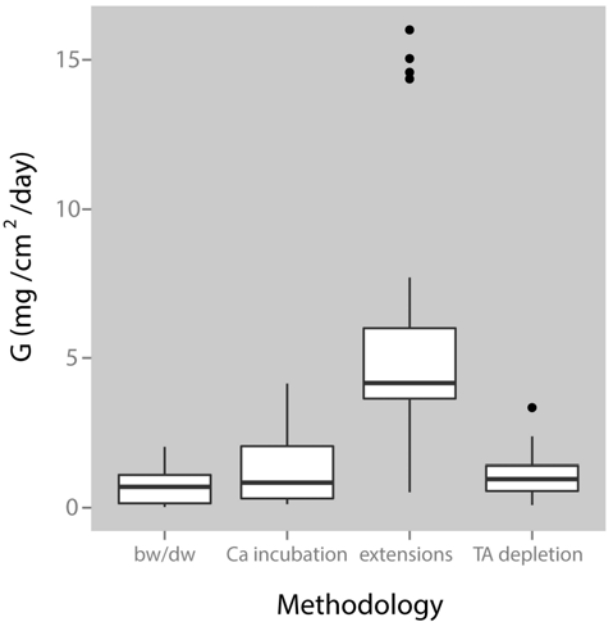

Supplementary Figure 2 Comparison of calcification data obtained with different methodologies. Box plots represent inter-study comparisons between calcification rates (G, mg cm-2 d-1) obtained for reef calcifiers (corals and calcareous crusts) using various methods. First and third quartiles, and the 1.5-fold inter-quartile range are marked by the boxes and whiskers, respectively. Points represent data beyond this range. Abbreviations: bw/dw = buoyant weight or dry weight measurements (n = 44), Ca incubation = Ca45Cl2-incubations (n = 11), extensions = linear extension rate and density estimates (n = 37), TA depletion = total alkalinity depletion method (n = 11).

Supplementary Table 5 Benthos composition at the study sites. Table of benthic percent cover showing the means (±SD) of six replicate rugosity transects per study site at a depth of 7.5–9 m. 'Total hard coral' is the sum of all coral categories assessed.

Transect % cover	offshore exposed		offshore sheltered		midshore exposed		midshore sheltered		nearshore exposed		nearshore sheltered	
Category	Mean	±SD	Mean	±SD	Mean	±SD	Mean	±SD	Mean	±SD	Mean	±SD
calcareous crusts	23.42	6.13	4.68	3.03	10.47	8.33	0.25	0.62	1.24	1.02	1.15	1.29
macro/turf algae	0.71	0.60	1.84	2.53	0.78	0.84	0.47	0.49	3.66	2.28	12.82	5.78
soft coral	8.58	5.30	0.92	1.30	24.53	10.87	17.40	3.34	4.17	3.06	0.12	0.18
sponge	0.16	0.39	0.00	0.00	0.00	0.00	0.42	0.67	0.13	0.32	2.08	2.26
other	0.36	0.74	0.40	0.79	0.91	1.18	0.00	0.00	3.70	1.40	0.43	0.55
rubble	4.43	4.05	30.61	29.69	6.08	6.58	1.96	2.18	6.64	9.39	4.84	4.23
sand/silt	0.47	0.55	20.65	17.81	0.83	1.04	31.94	11.12	38.41	15.73	29.50	19.40
recently dead coral	2.01	1.94	1.55	1.92	3.73	2.00	0.31	0.76	0.39	0.65	2.38	1.76
rock	23.60	7.37	30.57	22.30	14.45	5.54	16.87	7.82	30.40	12.75	25.42	9.53
hard coral (branching)	2.15	3.55	0.00	0.00	0.12	0.30	4.08	3.37	1.46	1.67	2.30	3.54
hard coral (encrusting)	5.52	3.14	1.58	2.46	4.02	3.85	2.31	2.28	2.63	1.80	5.59	3.27
hard coral (massive)	6.12	5.30	1.48	2.30	7.53	6.43	14.67	5.81	3.89	1.38	5.59	1.85
hard coral (plate/foliose)	0.90	1.92	0.00	0.00	0.82	1.52	3.03	7.42	0.00	0.00	0.00	0.00
Acropora spp.	6.86	10.64	1.30	2.11	10.69	5.76	3.13	5.98	0.32	0.78	0.13	0.20
Pocillopora spp.	4.75	3.80	1.98	2.16	8.05	5.50	1.01	0.89	0.25	0.31	0.15	0.36
Porites spp.	9.46	7.07	2.45	2.61	6.98	4.00	2.14	1.33	2.70	1.81	7.50	4.08
total hard coral	35.76	9.57	8.79	6.53	38.21	7.97	30.37	5.62	11.25	4.32	21.26	9.72

SD = standard deviation

Supplementary Table 6 Temperatures in the study sites. Table of mean seasonal and annual *in situ* temperatures (°C) at study sites at a depth of 7.5–9 m.

Reef	Site exposure	Season	N	Mean	±SD	Min	Max	Range
offshore	exposed	spring	2208	27.8	1.1	26.2	30.1	3.9
offshore	exposed	summer	2098	30.7	0.6	28.6	32.1	3.5
offshore	exposed	fall	2126	30.4	1.1	28.0	31.8	3.9
offshore	exposed	winter	2160	26.5	0.6	25.3	28.2	2.9
offshore	sheltered	spring	0	n.a.	n.a.	n.a.	n.a.	n.a.
offshore	sheltered	summer	1392	31.1	0.5	29.1	32.1	3.0
offshore	sheltered	fall	552	28.8	0.4	28.1	29.9	1.8
offshore	sheltered	winter	1274	26.8	0.6	25.6	28.3	2.7
midshore	exposed	spring	2207	28.1	1.1	26.5	30.3	3.8
midshore	exposed	summer	2098	30.8	0.7	28.8	32.3	3.5
midshore	exposed	fall	2076	30.3	1.0	28.3	31.7	3.4
midshore	exposed	winter	2160	26.5	0.6	24.2	28.4	4.1
midshore	sheltered	spring	0	n.a.	n.a.	n.a.	n.a.	n.a.
midshore	sheltered	summer	1392	31.4	0.6	30.0	32.6	2.6
midshore	sheltered	fall	552	28.3	0.5	27.2	29.4	2.2
midshore	sheltered	winter	1274	26.3	0.7	24.8	28.0	3.2
nearshore	exposed	spring	1751	28.2	1.1	26.7	30.8	4.2
nearshore	exposed	summer	1403	31.9	0.4	31.0	33.1	2.1
nearshore	exposed	fall	2174	30.2	1.3	27.0	32.2	5.2
nearshore	exposed	winter	2160	26.1	0.6	24.1	27.7	3.6
nearshore	sheltered	spring	0	n.a.	n.a.	n.a.	n.a.	n.a.
nearshore	sheltered	summer	1392	32.2	0.4	31.3	33.3	2.0
nearshore	sheltered	fall	552	28.3	0.4	27.4	29.4	2.0
nearshore	sheltered	winter	1274	26.0	0.7	24.5	27.8	3.3
offshore	exposed	annual	8592	28.8	2.0	25.3	32.1	6.7
offshore	sheltered	annual	3218	29.0	2.0	25.6	32.1	6.6
midshore	exposed	annual	8541	28.9	1.9	24.2	32.3	8.1
midshore	sheltered	annual	3218	28.8	2.4	24.8	32.6	7.8
nearshore	exposed	annual	7488	28.9	2.3	24.1	33.1	9.0
nearshore	sheltered	annual	3218	29.1	2.9	24.5	33.3	8.8
all sites	all sites	spring	6166	28.0	1.1			
all sites	all sites	summer	9775	31.1	0.7			
all sites	all sites	fall	8032	30.0	1.2			
all sites	all sites	winter	10302	26.4	0.7			

N = number of measurements; SD = standard deviation; n.a. = value not available

Supplementary Table 7 Seasonal mean calcification rates for corals and calcareous crusts (CC). Coral calcification rates as G_{Coral} % day^{-1}; CC calcification rates as G_{CC} mg cm^{-2} day^{-1} (N = number of replicates; SD = standard deviation; SE = standard error; n.a .= value not available; * = fewer than 3 replicates; + = fewer than 4 replicates; ACR = *Acropora*; POR = *Porites*; POC = *Pocillopora*)

Calcifier	Reef site	Site exposure	Season	N	Mean	±SD	±SE	Min	Max
POR	offshore	exposed	spring	5	0.326	0.221	0.099	0.19	0.707
POR	offshore	exposed	summer	5	0.331	0.087	0.039	0.206	0.432
POR	offshore	exposed	fall	5	0.136	0.09	0.04	0.038	0.256
POR	offshore	exposed	winter	5	0.211	0.073	0.033	0.12	0.296
POR	offshore	sheltered	spring	4	0.307	0.216	0.108	0.133	0.578
POR	offshore	sheltered	summer	4	0.191	0.132	0.066	0.079	0.351
POR	offshore	sheltered	fall	6	0.212	0.103	0.042	0.058	0.37
POR	offshore	sheltered	winter	6	0.177	0.223	0.091	0.046	0.625
POR	midshore	exposed	spring	5	0.369	0.193	0.086	0.162	0.556
POR	midshore	exposed	summer	7	0.202	0.084	0.032	0.103	0.347
POR	midshore	exposed	fall	3	0.190+	0.033	0.019	0.171	0.228
POR	midshore	exposed	winter	5	0.217	0.096	0.043	0.111	0.37
POR	midshore	sheltered	spring	6	0.243	0.105	0.043	0.117	0.397
POR	midshore	sheltered	summer	6	0.196	0.066	0.027	0.079	0.259
POR	midshore	sheltered	fall	4	0.098	0.037	0.019	0.065	0.143
POR	midshore	sheltered	winter	4	0.096	0.034	0.017	0.065	0.144
POR	nearshore	exposed	spring	8	0.218	0.058	0.02	0.12	0.306
POR	nearshore	exposed	summer	8	0.194	0.094	0.033	0.072	0.389
POR	nearshore	exposed	fall	1	0.168*	n.a.	n.a.	0.168	0.168
POR	nearshore	exposed	winter	7	0.136	0.07	0.026	0.058	0.229
POR	nearshore	sheltered	spring	8	0.21	0.073	0.026	0.142	0.347
POR	nearshore	sheltered	summer	7	0.161	0.051	0.019	0.072	0.212
POR	nearshore	sheltered	fall	6	0.202	0.193	0.079	0.076	0.586
POR	nearshore	sheltered	winter	2	0.067*	0.006	0.004	0.063	0.071
ACR	offshore	exposed	spring	6	0.551	0.176	0.072	0.337	0.864
ACR	offshore	exposed	summer	6	0.48	0.464	0.189	0.123	1.389
ACR	offshore	exposed	fall	6	0.269	0.072	0.03	0.192	0.37
ACR	offshore	exposed	winter	5	0.389	0.159	0.071	0.247	0.661
ACR	offshore	sheltered	spring	7	0.462	0.141	0.053	0.21	0.643
ACR	offshore	sheltered	summer	7	0.236	0.062	0.023	0.152	0.335
ACR	offshore	sheltered	fall	7	0.291	0.199	0.075	0.062	0.582
ACR	offshore	sheltered	winter	4	0.311	0.063	0.032	0.254	0.382
ACR	midshore	exposed	spring	6	0.4	0.256	0.105	0.202	0.913
ACR	midshore	exposed	summer	4	0.209	0.077	0.039	0.115	0.303
ACR	midshore	exposed	fall	6	0.254	0.128	0.052	0.048	0.409
ACR	midshore	exposed	winter	4	0.283	0.053	0.026	0.215	0.342
ACR	midshore	sheltered	spring	10	0.507	0.182	0.058	0.259	0.821
ACR	midshore	sheltered	summer	10	0.486	0.616	0.195	0.148	2.222

Calcifier	Reef site	Site exposure	Season	N	Mean	±SD	±SE	Min	Max
ACR	midshore	sheltered	fall	4	0.176	0.012	0.006	0.164	0.193
ACR	midshore	sheltered	winter	5	0.48	0.318	0.142	0.209	1.029
ACR	nearshore	exposed	spring	7	0.524	0.302	0.114	0.185	1.026
ACR	nearshore	exposed	summer	6	0.265	0.118	0.048	0.159	0.476
ACR	nearshore	exposed	fall	4	0.26	0.199	0.1	0.131	0.556
ACR	nearshore	exposed	winter	4	0.286	0.137	0.068	0.093	0.409
ACR	nearshore	sheltered	spring	6	0.703	0.224	0.092	0.501	1.111
ACR	nearshore	sheltered	summer	5	0.327	0.105	0.047	0.175	0.444
ACR	nearshore	sheltered	fall	4	0.393	0.349	0.175	0.139	0.899
ACR	nearshore	sheltered	winter	6	0.35	0.054	0.022	0.247	0.397
POC	offshore	exposed	spring	5	0.647	0.099	0.044	0.541	0.806
POC	offshore	exposed	summer	6	0.461	0.065	0.027	0.345	0.53
POC	offshore	exposed	fall	6	0.549	0.098	0.04	0.394	0.648
POC	offshore	exposed	winter	6	0.699	0.119	0.049	0.568	0.881
POC	offshore	sheltered	spring	6	0.702	0.404	0.165	0.38	1.481
POC	offshore	sheltered	summer	6	0.389	0.174	0.071	0.218	0.714
POC	offshore	sheltered	fall	5	0.354	0.086	0.038	0.242	0.476
POC	offshore	sheltered	winter	5	0.478	0.07	0.031	0.376	0.556
POC	midshore	exposed	spring	5	0.671	0.182	0.082	0.556	0.994
POC	midshore	exposed	summer	4	0.624	0.279	0.139	0.401	0.988
POC	midshore	exposed	fall	5	0.624	0.071	0.032	0.556	0.719
POC	midshore	exposed	winter	6	0.696	0.112	0.046	0.556	0.864
POC	midshore	sheltered	spring	7	0.603	0.227	0.086	0.417	1.061
POC	midshore	sheltered	summer	6	0.476	0.15	0.061	0.278	0.724
POC	midshore	sheltered	fall	2	0.170*	0.109	0.077	0.093	0.247
POC	midshore	sheltered	winter	3	0.261	0.141	0.081	0.123	0.404
CC	offshore	exposed	spring	5	0.099	0.019	0.009	0.074	0.12
CC	offshore	exposed	summer	2	0.109*	0.033	0.024	0.085	0.132
CC	offshore	exposed	winter	6	0.137	0.025	0.01	0.108	0.184
CC	offshore	sheltered	spring	5	0.054	0.008	0.004	0.04	0.063
CC	offshore	sheltered	summer	5	0.062	0.016	0.007	0.049	0.088
CC	offshore	sheltered	fall	1	0.062*	n.a.	n.a.	0.062	0.062
CC	offshore	sheltered	winter	5	0.061	0.008	0.004	0.049	0.069
CC	midshore	exposed	spring	5	0.081	0.012	0.005	0.062	0.094
CC	midshore	exposed	summer	5	0.048	0.023	0.01	0.027	0.084
CC	midshore	exposed	fall	1	0.082*	n.a.	n.a.	0.082	0.082
CC	midshore	exposed	winter	6	0.081	0.017	0.007	0.055	0.105
CC	midshore	sheltered	spring	6	0.044	0.017	0.007	0.032	0.078
CC	midshore	sheltered	summer	4	0.03	0.011	0.005	0.017	0.042
CC	midshore	sheltered	fall	5	0.055	0.011	0.005	0.041	0.069
CC	midshore	sheltered	winter	6	0.041	0.005	0.002	0.033	0.048
CC	nearshore	exposed	spring	3	0.025+	0.004	0.002	0.021	0.029

Calcifier	Reef site	Site exposure	Season	N	Mean	±SD	±SE	Min	Max
CC	nearshore	exposed	summer	4	0.035	0.005	0.002	0.031	0.042
CC	nearshore	exposed	fall	5	0.048	0.013	0.006	0.026	0.058
CC	nearshore	exposed	winter	5	0.041	0.015	0.007	0.03	0.066
CC	nearshore	sheltered	spring	5	0.032	0.019	0.009	0.017	0.066
CC	nearshore	sheltered	summer	5	0.014	0.002	0.001	0.012	0.016
CC	nearshore	sheltered	fall	6	0.041	0.007	0.003	0.033	0.052
CC	nearshore	sheltered	winter	6	0.04	0.004	0.002	0.035	0.044

N = number of replicates; SD = standard deviation; SE = standard error; n.a .= value not available; * = fewer than 3 replicates; + = fewer than 4 replicates; ACR = *Acropora*; POR = *Porites*; POC = *Pocillopora*

Supplementary Table 8 PERMANOVA results for coral calcification data. PERMANOVA (fixed factors, nested design) full result table of seasonal coral calcification data.

Source	*df*	SS	MS	Pseudo-*F*	$p_{(perm)}$	Unique Permutations
Calcification rates: all corals						
coralgenus	2	305.92	152.96	88.62	0.001	999
reef(coralgenus)	5	9.34	1.87	1.08	0.365	998
exposure(reef(coralgenus))	8	68.61	8.58	4.97	0.001	999
season(exposure(reef(coralgenus)))	48	180.32	3.76	2.18	0.001	998
Residual	282	486.71	1.73			
Total	345	1119.60				
Calcification rates: *Porites*						
reef	2	5.76	2.88	2.29	0.096	999
exposure(reef)	3	10.02	3.34	2.65	0.06	999
season(exposure(reef))	18	46.11	2.56	2.03	0.017	998
Residual	103	129.84	1.26			
Total	126	187.89				
Calcification rates: *Acropora*						
reef	2	2.48	1.24	0.49	0.615	998
exposure(reef)	3	16.91	5.64	2.23	0.094	999
season(exposure(reef))	18	83.50	4.64	1.83	0.033	999
Residual	112	283.39	2.53			
Total	135	387.42				
Calcification rates: *Pocillopora*						
reef	1	1.10	1.10	1.00	0.314	993
exposure(reef)	2	41.68	20.84	19.00	0.001	998
season(exposure(reef))	12	50.71	4.23	3.85	0.001	999
Residual	67	73.49	1.10			
Total	82	150.92				

df = degrees of freedom; SS = sum of squares; MS = mean squares

Supplementary Table 9 Seasonal differences in coral calcification. Changes (as percentage increase) between the mean coral calcification rates in spring and the mean rates of the other seasons (i.e., summer, fall, winter) for each site. Percentages quantify the increase in spring calcification compared to the rates of the other seasons; the spring calcification was increased by >5% and up to 250% for the majority of sites.

Calcifier	Reef site	Site exposure	Spring increase in relation to other seasons	Percentage increase (%)
POR	offshore	exposed	summer	-2*
POR	offshore	exposed	fall	139
POR	offshore	exposed	winter	54
POR	offshore	sheltered	summer	61
POR	offshore	sheltered	fall	45
POR	offshore	sheltered	winter	73
POR	midshore	exposed	summer	82
POR	midshore	exposed	fall	94
POR	midshore	exposed	winter	70
POR	midshore	sheltered	summer	24
POR	midshore	sheltered	fall	149
POR	midshore	sheltered	winter	153
POR	nearshore	exposed	summer	12
POR	nearshore	exposed	fall	30
POR	nearshore	exposed	winter	60
POR	nearshore	sheltered	summer	30
POR	nearshore	sheltered	fall	4*
POR	nearshore	sheltered	winter	213
ACR	offshore	exposed	summer	15
ACR	offshore	exposed	fall	105
ACR	offshore	exposed	winter	41
ACR	offshore	sheltered	summer	96
ACR	offshore	sheltered	fall	59
ACR	offshore	sheltered	winter	49
ACR	midshore	exposed	summer	91
ACR	midshore	exposed	fall	57
ACR	midshore	exposed	winter	41
ACR	midshore	sheltered	summer	4*
ACR	midshore	sheltered	fall	188
ACR	midshore	sheltered	winter	6
ACR	nearshore	exposed	summer	98
ACR	nearshore	exposed	fall	102
ACR	nearshore	exposed	winter	83
ACR	nearshore	sheltered	summer	115
ACR	nearshore	sheltered	fall	79

Calcifier	Reef site	Site exposure	Spring increase in relation to other seasons	Percentage increase (%)
ACR	nearshore	sheltered	winter	101
POC	offshore	exposed	summer	40
POC	offshore	exposed	fall	18
POC	offshore	exposed	winter	-7*
POC	offshore	sheltered	summer	80
POC	offshore	sheltered	fall	98
POC	offshore	sheltered	winter	47
POC	midshore	exposed	summer	7
POC	midshore	exposed	fall	7
POC	midshore	exposed	winter	-4*
POC	midshore	sheltered	summer	27
POC	midshore	sheltered	fall	255
POC	midshore	sheltered	winter	131

POR = *Porites*; ACR = *Acropora*; POC = *Pocillopora*; cases where percentage of increase was <5% are marked with an asterisk *

Supplementary Table 10 PERMANOVA results for calcareous crusts calcification data. PERMANOVA (fixed factors, nested design) full result table of seasonal calcification data from calcareous crusts.

Source	*df*	SS	MS	Pseudo-*F*	$p_{(perm)}$	Unique Permutations
reef	2	14.27	7.13	95.16	0.001	999
exposure(reef)	3	6.70	2.23	29.79	0.001	999
season(exposure(reef))	17	6.04	0.36	4.74	0.001	998
Residual	83	6.22	0.07			
Total	105	37.51				

df = degrees of freedom; SS = sum of squares; MS = mean squares

Supplementary Table 11 Seasonal differences in calcareous crusts (CC) calcification. Changes (as percentage decrease) between the spring and summer mean CC calcification rates and the highest rate in fall or winter at each reef site; spring and summer calcification was decreased by 13–66% in the majority of sites.

Calcifier	Reef	Site exposure	Season	Percentage decrease (%) (in relation to the highest rate in fall or winter)
CC	offshore	exposed	spring	-28
CC	offshore	exposed	summer	-21
CC	offshore	sheltered	spring	-13
CC	offshore	sheltered	summer	-1*
CC	midshore	exposed	spring	-1*
CC	midshore	exposed	summer	-41
CC	midshore	sheltered	spring	-19
CC	midshore	sheltered	summer	-46
CC	nearshore	exposed	spring	-49
CC	nearshore	exposed	summer	-27
CC	nearshore	sheltered	spring	-22
CC	nearshore	sheltered	summer	-66

cases where decrease was <5% are marked with an asterisk *

Supplementary Appendix 1 Comparability of calcification data obtained with different measures

To compare calcification rates, we compiled data for corals (*Porites*, *Acropora,* and *Pocillopora*) and calcareous crusts (CC) from studies in the Caribbean and Indo-Pacific that used a variety of methodologies to quantify calcification (buoyant weight technique, total alkalinity depletion method, calcium-45 labelling technique, and estimates from linear extension and skeletal density). We collected calcification rates only from those studies that reported calcification as carbonate accretion normalized to surface area. Initially, we extracted 103 calcification rates (coral: n = 85; CC: n = 18) from 38 studies (see References) measured *in situ* or under ambient conditions in aquaculture. We used box plots to visualize the distribution of all calcification data collected. Box plots grouped by methodology showed a remarkable difference between calcification estimated from linear extension rates and skeletal densities in comparison to other methods (Supplementary Figure 2). Based on these observations, we compared and tested for differences between different methodologies using Kruskal–Wallis test by ranks (in Statistica 10).

The comparison of calcification rates (coral and CC) across different studies indicate a methodological bias; values obtained from linear extension measurements significantly differed from other methods (Kruskal–Wallis test by ranks, multiple comparisons: $p < 0.001$): they were on average 4–7-fold higher and had higher variability (3.84 SD) compared to the other techniques (0.72–1.35 SD). As a consequence, we excluded calcification rates based on linear extension rates from our global comparison and compared our data from the central Red Sea to the calcification rates from studies using the buoyant weight technique, total alkalinity

depletion method, or calcium-45 labelling technique. We conclude that, although calcification studies are numerous, comparisons between different geographic regions remain problematic due to the differences of methodologies and metrics used to quantify calcification.

A recent review by Pratchett et al. (2015) approached this issue in a comprehensive synthesis evaluating coral growth studies from the past decades. Since measurements of linear extensions (from alizarin staining, tagging, or X-radiography) have been the most common method to assess growth in corals, the review focused on growth rates expressed as annual linear extensions (mm yr^{-1}) and as calcification rates (carbonate accretion per unit surface area) estimated from these linear extension values and skeletal density. In comparison, our comparative approach included calcification rates based on direct measurements of carbonate accretion, such as buoyant/dry weight measurements or the total alkalinity depletion method. Based on our collection of these calcification data, we provide evidence of a methodological bias in the quantification of calcification. Our data suggest that the estimates based on linear extension rates may overestimate calcification compared to the direct measurements of carbonate accretion. A larger compilation of calcification data with more detailed and specific comparative analyses of calcification rates across studies will be needed to provide further insight into this problem.

Appendix 1 References

Bak RPM (1976) The growth of coral colonies and the importance of crustose coralline algae and burrowing sponges in relation with carbonate accumulation. Neth J Sea Res 10:285–337

Bessat F, Buigues D (2001) Two centuries of variation in coral growth in a massive *Porites* colony from Moorea (French Polynesia): a response of ocean-atmosphere variability from south central Pacific. Palaeogeogr Palaeoclimatol Palaeoecol 175:381–392

Chisholm JRM (2000) Calcification by crustose coralline algae on the northern Great Barrier Reef, Australia. Limnol Oceanogr 45:1476–1484

Comeau S, Carpenter RC, Edmunds PJ (2014a) Effects of irradiance on the response of the coral *Acropora pulchra* and the calcifying alga *Hydrolithon reinboldii* to temperature elevation and ocean acidification. J Exp Mar Bio Ecol 453:28–35

Comeau S, Edmunds PJ, Spindel NB, Carpenter RC (2013) The responses of eight coral reef calcifiers to increasing partial pressure of CO2 do not exhibit a tipping point. Limnol Oceanogr 58:388–398

Comeau S, Carpenter RC, Nojiri Y, Putnam HM, Sakai K, Edmunds PJ (2014b) Pacific-wide contrast highlights resistance of reef calcifiers to ocean acidification. Proc Roy Soc Lond B Biol Sci 281:20141339

Cooper TF, Death G, Fabricius KE, Lough JM (2008) Declining coral calcification in massive *Porites* in two nearshore regions of the northern Great Barrier Reef. Glob Chang Biol 14:529–538

De'ath G, Lough JM, Fabricius KE (2009) Declining coral calcification on the Great Barrier Reef. Science 323:116–119

Edinger EN, Limmon GV, Jompa J, Widjatmoko W, Heikoop JM, Risk MJ (2000) Normal coral growth rates on dying reefs: Are coral growth rates good indicators of reef health? Mar Pollut Bull 40:404–425

Foster T, Short JA, Falter JL, Ross C, McCulloch MT (2014) Reduced calcification in Western Australian corals during anomalously high summer water temperatures. J Exp Mar Bio Ecol 461:133–143

Gladfelter EH, Monahan RK, Gladfelter WB (1978) Growth rates of five reef-building corals in the northeastern Caribbean. Bull Mar Sci 28:728–734

Goreau TF, Goreau NI (1959) The Physiology Of Skeleton Formation In Corals. II. Calcium Deposition By Hermatypic Corals Under Various Conditions In The Reef. Biol Bull 117:239–250

Holcomb M, Tambutté E, Allemand D, Tambutté S (2014) Light enhanced calcification in *Stylophora pistillata*: effects of glucose, glycerol and oxygen. PeerJ 2:e375

Johnson MD, Moriarty VW, Carpenter RC (2014) Acclimatization of the crustose coralline alga Porolithon onkodes to variable pCO2. PLoS One 9:e87678

Kuffner IB, Hickey TD, Morrison JM (2013) Calcification rates of the massive coral Siderastrea siderea and crustose coralline algae along the Florida Keys (USA) outer-reef tract. Coral Reefs 32:987–997

Lough JM, Barnes DJ (1992) Comparisons of skeletal density variations in *Porites* from the central Great Barrier Reef. J Exp Mar Bio Ecol 155:1–25

Lough JM, Barnes DJ (1997) Several centuries of variation in skeletal extension, density and calcification in massive *Porites* colonies from the Great Barrier Reef: a proxy for seawater temperature and a background of variability against which to identify unnatural change. J Exp Mar Bio Ecol 211:29–67

Lough JM, Cantin NE (2014) Perspectives on massive coral growth rates in a changing ocean. Biol Bull 226:187–202

Mallela J (2013) Calcification by reef-building sclerobionts. PLoS One 8:e60010

Mallela J, Perry C (2007) Calcium carbonate budgets for two coral reefs affected by different terrestrial runoff regimes, Rio Bueno, Jamaica. Coral Reefs 26:129–145

Manzello DP (2010) Coral growth with thermal stress and ocean acidification: lessons from the eastern tropical Pacific. Coral Reefs 29:749–758

Mass T, Einbinder S, Brokovich E, Shashar N, Vago R, Erez J, Dubinsky Z (2007) Photoacclimation of *Stylophora pistillata* to light extremes: metabolism and calcification. Mar Ecol Prog Ser 334:93–102

Morgan KM, Kench PS (2012) Skeletal extension and calcification of reef-building corals in the central Indian Ocean. Mar Environ Res 81:78 – 82

Pari N, Peyrot-Clausade M, Le Champion-Alsumard T, Hutchings P, Chazottes V, Gobulic S, Le Champion J, Fontaine MF (1998) Bioerosion of experimental substrates on high islands and on atoll lagoons (French Polynesia) after two years of exposure. Mar Ecol Prog Ser 166:119–130

Pratchett MS, Anderson KD, Hoogenboom MO, Widman E, Baird AH, Pandolfi JM, Edmunds PJ, Lough JM (2015) Spatial, temporal and taxonomic variation in coral growth — Implications for the structure and function of coral reef ecosystems. Oceanogr Mar Biol Annu Rev 53:215–295

Risk MJ, Sammarco PW (1991) Cross-shelf trends in skeletal density of the massive coral *Porites lobata* from the Great Barrier Reef. Mar Ecol Prog Ser 69:195–200

Ross CL, Falter JL, Schoepf V, McCulloch MT (2015) Perennial growth of hermatypic corals at Rottnest Island, Western Australia (32°S). PeerJ 3:e781

Sawall Y, Al-Sofyani A, Hohn S, Banguera-Hinestroza E, Voolstra CR, Wahl M (2015) Extensive phenotypic plasticity of a Red Sea coral over a strong latitudinal temperature gradient suggests limited acclimatization potential to warming. Sci Rep 5:8940

Sawall Y, Teichberg MC, Seemann J, Litaay M, Jompa J, Richter C (2011) Nutritional status and metabolism of the coral *Stylophora subseriata* along a eutrophication gradient in Spermonde Archipelago (Indonesia). Coral Reefs 30:841–853

Schneider K, Erez J (2006) The effect of carbonate chemistry on calcification and photosynthesis in the hermatypic coral *Acropora eurystoma*. Limnol Oceanogr 51:1284–1293

Schneider RC, Smith SV (1982) Skeletal Sr content and density in *Porites* spp. in relation to environmental factors. Mar Biol 66:121–131

Schoepf V, Grottoli AG, Warner ME, Cai W-J, Melman TF, Hoadley KD, Pettay DT, Hu X, Li Q, Xu H, Wang Y, Matsui Y, Baumann JH (2013) Coral energy reserves and calcification in a high-CO2 world at two temperatures. PLoS One 8:e75049

Scoffin TP, Tudhope AW, Brown BE, Chansang H, Cheeney RF (1992) Patterns and possible environmental controls of skeletogenesis of *Porites lutea*, South Thailand. Coral Reefs 11:1–11

Smith LW, Barshis D, Birkeland C (2007) Phenotypic plasticity for skeletal growth, density and calcification of *Porites lobata* in response to habitat type. Coral Reefs 26:559–567

Tanzil JTI, Brown BE, Dunne RP, Lee JN, Kaandorp JA, Todd PA (2013) Regional decline in growth rates of massive *Porites* corals in Southeast Asia. Glob Chang Biol 19:3011–3023

Tanzil JTI, Brown BE, Tudhope AW, Dunne RP (2009) Decline in skeletal growth of the coral *Porites lutea* from the Andaman Sea, South Thailand between 1984 and 2005. Coral Reefs 28:519–528

Tudhope, AW, Allison, N, LeTissier, MDA, Scoffin, TP (1993) Growth characteristics and susceptibility to bleaching in massive *Porites* corals, south Thailand. Proc 7th Int Coral Reef Symp 1:64–69

CHAPTER III

5. Abiotic and biotic drivers of carbonate budgets in the central Red Sea provide insights into present-day coral reef growth in a naturally high temperature and high alkalinity sea

Anna Roik[1], Till Röthig[1], Claudia Pogoreutz[1,2], Christian R. Voolstra[1]

[1]Red Sea Research Center, Division of Biological and Environmental Science and Engineering, King Abdullah University of Science and Technology, Thuwal, Saudi Arabia

[2]Coral Reef Ecology Group (CORE), Leibniz Center for Tropical Marine Ecology, 28359 Bremen, Germany

This manuscript is prepared for the submission to

Biogeosciences (Copernicus publications)

Roik A, Röthig T, Pogoreutz C, Voolstra CR (in preparation) Abiotic and biotic drivers of carbonate budgets in the central Red Sea provide insights into present-day coral reef growth in a naturally high temperature and high alkalinity sea.

5.1. Abstract

The growth of a coral reef framework relies on warm, alkaline, and well sunlit tropical ocean conditions and is crucial for maintaining ecosystem functioning and services. In the central Red Sea, alkalinity is naturally high, but increasing temperature already impairs capacities of reef-building calcifiers. It is unknown how this combination of beneficial and detrimental abiotic factors affects the balance between calcification and erosion and thereby the overall reef growth. To provide insight into present-day reef growth dynamics in the central Red Sea, we assessed the baseline variability of temperature, pH, and total alkalinity (A_T), among others in four reef sites along a cross-shelf gradient (25 km). We measured net-accretion/erosion rates (G_{net}) using *in situ* deployed limestone blocks, and estimated community calcification and bioerosion rates (sea urchins and parrotfish) in order to determine census-based carbonate budgets (G_{budget}). On average, A_T (2346 – 2431 μmol kg^{-1}), aragonite saturation state (4.5 - 5.2 Ω_a), and pCO_2 (283 -315 μatm) were close to estimates of preindustrial global ocean surface water. Continuously measured pH revealed diel ranges that were particularly high in the protected nearshore and lagoonal sites (~0.55 pH) and associated with negative or low G_{net} and G_{budget} states. Central Red Sea $G_{budgets}$ spanned from negative to positive net-production states between nearshore and offshore. G_{net} was ranging from -0.96 to 0.37 kg $CaCO_3$ $m^{-2}yr^{-1}$, and $G_{budgets}$ from -1.48 to 2.44 kg $CaCO_3$ $m^{-2}yr^{-1}$. Temperature and pH variability were negatively correlated with G_{net} and G_{budget}, while A_T and Ω_a were positively related. In the best fitting distance-based linear models, A_T explained > 50 % of G_{net} and G_{budget}. Parrotfish abundances explained an additional ~20 % in the G_{budget} model. High levels of A_T and

Ω_a observed in the central Red Sea reefs may buffer against the effects of ocean acidification and delay the arrival of low thresholds that are critical for reef growth. However, relatively small changes of these variables may already change reef growth processes, as indicated by the relationship of small cross-shelf differences of 32 µmol A_T kg^{-1} and 0.2 Ω_a with G_{net} and G_{budget}. Despite present-day offshore G_{budget} was lower compared to remote Indian Ocean reefs, comparison with historical data from the northern Red Sea suggests that overall reef growth in the Red Sea might have remained similar since 1995. Our data present a baseline for future studies and will be particularly useful to quantify the impact of destructive events, such as the most recent Third Global Bleaching event (2015-2016), on the reef growth potential in the central Red Sea.

5.2. Introduction

Reef growth is limited to warm and aragonite saturated tropical oceans (Buddemeier 1997; Kleypas et al. 1999b) and is essential for coral reef functioning. The coral reef framework not only maintains a remarkable biodiversity, but also valuable ecosystem services that include food supply, coastal protection, among others (Reaka-Kudla 1997; Moberg and Folke 1999). Biogenic calcification, erosion, and dissolution cumulatively contribute to the formation of the reef framework constructed of calcium carbonate ($CaCO_3$, mainly aragonite) (Glynn 1997; Perry et al. 2008). The balance of carbonate loss and accretion are controlled by abiotic and biotic factors: temperature, properties of the carbonate chemistry (e.g. pH, total alkalinity A_T, and aragonite saturation state [Ω_a]), calcifying benthic communities (scleractinian corals and coralline algal crusts), as well as grazing and endolithic bioeroders (e.g.

parrotfish, sea urchins, and boring sponges) (Kleypas et al. 2001; Glynn and Manzello 2015). Positive carbonate budgets (G_{budget}) are maintained when reef calcification produces more $CaCO_3$ than is being removed, and rely in a great part on the ability of benthic calcifiers to precipitate calcium carbonate from seawater ($Ca^{2+} + CO_3^{2-} \leftrightarrow CaCO_3$, Tambutté et al. (2011). Calcification increases with higher temperature, but has an upper thermal limit (Jokiel and Coles 1990; Marshall and Clode 2004). In addition, higher availability of the carbonate ion and its tendency to precipitate (e.g., a higher total A_T and Ω_a) is positively correlated with calcification rates (Schneider and Erez 2006; Marubini et al. 2008).

Today's oceans are warming, which is a danger to reef calcifiers, as temperatures start exceeding their thermal optima and slowing down calcification (Death et al. 2009; Carricart-Ganivet et al. 2012). Simultaneously, calcification may become more energetically costly (Cohen and Holcomb 2009; Cai et al. 2016; Waldbusser et al. 2016) with ocean acidification, as manifested by a decrease in ocean's pH and hence a decrease of Ω_a (Orr et al. 2005). Further, ocean acidification will counteract reef growth by stimulating destructive processes, e.g. the proliferation and erosive activity of endolithic organisms (Tribollet et al. 2009; Fang et al. 2013; Enochs 2015).

Low and negative $G_{budgets}$ are generally associated with a disturbance of natural abiotic conditions that are known to support coral reef growth, i.e. certain ranges of temperature, nutrients, pH, and Ω_a (Buddemeier 1997; Kleypas et al. 1999b). In most tropical coral reefs, negative $G_{budgets}$ are a hallmark of reef degradation due to an increased intensity or frequency of extreme climate events (Eakin 2001;

Schuhmacher et al. 2005) or local human impacts, such as pollution and eutrophication (Edinger et al. 2000; Chazottes et al. 2002). Resulting degradation of reef habitat is most obviously linked to shifts in ecological structures, for instance loss of coral cover or expansions in bioeroder abundances, e.g. grazing sea urchins can rapidly lead to negative $G_{budgets}$ (Alvarez-Filip et al. 2009; Bronstein and Loya 2014). Census-based $G_{budgets}$ are a powerful tool to assess reef persistence and degradation allowing to compare states of coral reef systems regionally and globally (Perry et al. 2012, 2015; Kennedy et al. 2013). In most recent years, G_{budget} studies demonstrated that reef growth in the Caribbean has decreased by 50% compared to historical mid- to late-Holocene reef growth and 37% of the reefs are reported to be in a net-erosional state (Perry et al. 2013).

In regions, such as the eastern tropical Pacific or the Persian/Arabian Gulf (PAG), abiotic conditions naturally deviate from the 'typical' coral reef conditions and support only low abundances of reef-building corals, but high rates of bioerosion, hence neutral or partly negative $G_{budgets}$ (Perry and Larcombe 2003; Manzello et al. 2008; Bauman et al. 2013). These marginal coral reef communities have been estimated to be most susceptible to ocean warming and acidification (Couce et al. 2012), as they already live at their environmental limits (e.g., high temperatures and/or low pH). In Bermuda and the Eastern Pacific, marginal reefs have been identified as particularly threatened by the effects of ocean acidification due to their already comparably low pH levels (Bates et al. 2010; Manzello 2010). On the other hand, ocean warming is the greater threat to coral communities in the PAG, as they

live within the globally warmest climate zone that is warming at a high rate (Sheppard and Loughland 2002; Riegl 2003).

Red Sea coral reefs are exposed to challenging conditions in terms of high temperature and salinity regimes (Kleypas et al. 1999b), but in contrast to the PAG, the Red Sea supports remarkable reef ecosystems with coral reef framework along its entire coastline (Riegl et al. 2012). Over the past decades however, calcification rates as derived from coral cores indicate a decline in response to ocean warming as shown for the Great Barrier reef, the Caribbean, and also the central Red Sea (Cooper et al. 2008; Bak et al. 2009; Cantin et al. 2010). In the central and southern Red Sea, present-day data indicate reduced calcification rates of corals and calcifying crusts during summer when exposed to the warmest temperatures of the year (Roik et al. 2015b; Sawall et al. 2015). While increasing temperatures are seemingly stressful for calcifiers, high A_T values (~ 2400 µmol kg^{-1}, Metzl et al. 1989) are putatively beneficial for carbonate accretion in the Red Sea (Tambutté et al. 2011). It is yet unknown how these present-day stressors and drivers of reef growth influence the overall net-carbonate production in the Red Sea. Availability of G_{budget} data for Red Sea coral reefs is poor (Jones et al. 2015). Aside from one early census-based assessment of the G_{budget} for a reef in the Gulf of Aqaba, northern Red Sea (Dullo et al. 1996a), where calcification and erosion/dissolution rates were considered, few other studies that exist only reported calcification rates (Heiss 1995; Cantin et al. 2010; Roik et al. 2015b; Sawall and Al-Sofyani 2015).

In this study we assessed the abiotic and biotic drivers of reef growth, and determined the G_{budget} for the central Red Sea coral reefs. In this effort we examined sites along an environmental cross-shelf gradient during winter and summer, firstly providing an account of temperature and seawater chemistry parameters, focusing on pH and A_T measurements, to reveal the present-day carbonate chemistry exposures. Secondly, we followed the census-based G_{budget} approach to estimate net carbonate production states using reef site-specific biotic parameters that cumulatively contribute to reef growth. Specifically, we use the calcification rates of major reef-building coral taxa (*Porites*, *Pocillopora*, and *Acropora*) and of calcerous crusts. Further, net-accretion/erosion rates of bare reef substrate (G_{net}), assessed via limestone blocks deployed in the reefs and the erosion rates of external bioeroders, such as parrotfish and sea urchins were collected. Finally, we explore the correlations of potential drivers on G_{net} and the overall $G_{budgets}$ using the abiotic and biotic datasets. These data provide an insight into reef growth dynamics and a comparative baseline to assess the effects of ongoing environmental change to reef growth in the central Red Sea.

5.3. Materials and Methods

5.3.1. Study sites and environmental monitoring

Study sites were located in the Saudi Arabian central Red Sea along an environmental cross-shelf gradient, which was previously described in Roik et al. (in revision) and Roik et al. (2015). Briefly, along this gradient from nearshore to offshore dissolved oxygen increase, but chlorophyll-a, turbidity, and sedimentation decrease and were influenced by seasonal variation. Overall, the reefs are exposed to high salinity (38 - 39 PSU), and high summer temperatures (29 – 33 °C) that exceed average maxima for

coral reefs globally (29 °C, (Kleypas et al. 1999b). Also, dissolved oxygen is temporarily low (0.1 – 5.2 mg L^{-1}) reaching levels, which on a global range is defined as "hypoxic" in a majority of studies (Vaquer-Sunyer and Duarte 2008).

Data for this study were collected at four sites: one offshore forereef at ~25 km distance from the coastline (22° 20.456 N, 38° 51.127 E, "Shi'b Nazar"), two midshore sites (forereef and lagoon) at ~10 km distance (22° 15.100 N, 38° 57.386 E, "Al Fahal"), and a nearshore forereef at ~3km distance (22° 13.974 N, 39° 01.760 E, "Inner Fsar"). All stations were located between 7.5 and 9 m depth. In the following, reef sites are referred to as "offshore", "midshore", "midshore lagoon", and "nearshore", respectively. Abiotic variables were measured in the study sites during two seasons in 2014. Continuous data of temperature and pH were recorded during "winter" (10th February – 6th April 2014) and "summer" (20th June – 20th September 2014). Additionally, for 5 – 6 consecutive weeks during each of the two seasons, seawater samples were collected at each station on SCUBA to measure inorganic nutrient content (nitrate and nitrite "NO_3^-&NO_2^-", ammonia "NH_4^+", and phosphate "PO_4^{3-}") and two carbonate chemistry parameters, total alkalinity (A_T) and pH (Supplementary Table 12).

5.3.2. Abiotic parameters: continuous data

Conductivity-Temperature-Depth loggers (CTDs, SBE 16plusV2 SEACAT, RS-232, Sea-Bird Electronics, Bellevue, WA, USA) equipped with pH probes (SBE 18/27, Sea-Bird) were deployed to collect times series data of temperature (°C) and pH_{CTD} at hourly intervals. Both sensors were factory calibrated. To control for drift of the pH

probes, sensor were tested before and after deployment using certified standard buffers (pH-7 “38746” and pH-10 “38749”, Fluka Analystics, Sigma-Aldrich, Germany). Data corrections were applied where necessary. Diel profiles of continuous data were plotted per reef and season including smoothing polynomial regression lines fitted by *geom_smooth* in R package *ggplot2* (LOESS, span = 0.1). To visualize the seasonal temperature and pH regimes in the reef sites, histograms were created using the function *stat_bin*, as implemented in the R package *ggplot2* (R Core Team 2013; Wickham and Chang 2015).

5.3.3. Abiotic parameters: seawater samples

Seawater samples were collected in the reef sites using cubitainers (Supplementary Table 12). At the same time 60 mL seawater samples were taken over a 0.45 µm filter on a syringe for A_T measurements. Immediately after sampling, pH_{SWS} (= pH of seawater samples) was measured onboard in subsamples taken from the cubitainers (n = 3, precision of ± 0.05 pH units) using a portable pH probe with an integrated temperature sensor (Orion 4 Star Plus, Thermo Fisher Scientific, MA, USA). The probe was previously calibrated with certified standard buffers (pH-4 “38743,” pH-7 “38746” and pH-10 “38749”, Fluka Analystics, Sigma-Aldrich). Seawater samples were transported on ice in the dark and were processed on the same day. Samples were filtered over GF/F filters (0.7 µm, Whatman, UK) and filtrates were frozen at -20 °C until further analysis. The inorganic nutrient content (NO_3^-&NO_2^-, NH_4^+, and PO_4^{3-}) was determined using standard colorimetric tests and a Quick-Chem 8000 AutoAnalyzer (Zellweger Analysis, Inc.). A_T samples were analyzed within 2 – 4 h after collection using an automated acidimetric titration system (Titrando 888,Metrohm

AG, Switzerland). Gran-type titrations were performed with a 0.01 M HCl certified standard solution (prepared from 0.1 HCl, Fluka Analytics) at a precision of ± 9 µmol kg^{-1}. Using A_T, pH_{SWS} (seawater samples), salinity, and temperature (from CTD) carbonate chemistry parameters were calculated using the R package *seacarb* (Gattuso et al. 2015). Carbonic acid dissociation constants were employed as recommended in (Dickson et al. 2007): K1 & K2 (Lueker et al. 2000), Kf (Perez and Fraga 1987), and Ks (Dickson 1990).

5.3.4. Net-accretion/erosion rates measurements using limestone blocks

Net-accretion/erosion rates were measured using limestone blocks (100 x 100 x 21 mm, ρ = 2.3 kg L^{-1}, n = 4) that were weighed (Mettler Toledo XS2002S, readability = 10 mg) before and after deployment on the reefs. Before weighing, blocks were autoclaved and dried for a week in a climate chamber at 40°C (BINDER, Tuttlingen, Germany). Sets of blocks were deployed for 0.5 years (September 2012 – March 2013), and for 1 year (June 2013 – June 2014) at six sites, including the four reef sites and the offshore and nearshore backreefs. Another set of blocks was deployed for 2.5 years from January 2013 – June 2015 in the four reef sites. Upon recovery, blocks were treated with bleach for 24 – 36 h to remove all organic material. Net-accretion rates were based on the normalized differences of pre-deployment and post-deployment weights and expressed as G_{net} (kg m^{-2} yr^{-1}).

5.3.5. Reef carbonate budget estimates

Reef carbonate budgets (G_{budget}, kg m^{-1} yr^{-1}) were estimated following the census-based *ReefBudget* approach (Perry et al. 2012), which was adjusted for the central

Red Sea. Site specific benthic calcification rates ($G_{benthos}$, kg m^{-1} yr^{-1}), net-accretion/erosion rates of hard substrate ($G_{netbenthos}$, kg m^{-1} yr^{-1}), and erosion rates of crucial bioeroders such as sea urchins (E_{echino}, kg m^{-1} yr^{-1}) and parrotfishes (E_{parrot}, kg m^{-1} yr^{-1}) were incorporated in the G_{budget} estimates (see Figure 14).

First, $G_{benthos}$ was estimated using locally measured calcification rates of corals and calcareous crusts as reported by (Roik et al. 2015b) (Supplementary Table 13). These calcification rates ($G_{calcifier}$) were extrapolated over the percentage cover of respective calcifiers assessed in six 10 m rugosity transects per site (Supplementary equations 1 A,

Supplementary Table 14). Transects were performed following (Perry et al. 2012) and data were previously reported in detail in (Roik et al. 2015b). In the lagoonal midshore site all transects were performed in hard substrate dominated areas. Next, to account for the carbonate net-accretion/erosion of hard substrate, $G_{netbenthos}$ rates were calculated for each reef site using G_{net} rates from limestone blocks (see above) that were extrapolated over the percentage cover of "rock" and "recently dead coral" from rugosity transects (Supplementary equations 1 B, Supplementary Table 13). To estimate echinoid erosion rates (E_{echino}) abundances of major sea urchin genera and their size classes per reef site were considered. Sea urchin census was conducted along the same benthic rugosity transects between 9.00 and 14.00 h, and included the most common bioerosive genera *Diadema*, *Echinometra*, *Echinostrephus*, *Eucidaris* in the size classes 0 – 20, 21 – 40, 41 – 60, 61 – 80, 81 – 100 mm. Genus and size specific erosion rates for sea urchins were employed in equations *sensu* (Perry et al. 2012) to

estimate erosion rates per individual echinoid genus (Supplementary equations 2 A – C,

Supplementary Table 15). Parrotfish abundances per species and fork length (FL: 5-14, 15-24, 25-34, 35-44, 45 -70, and > 70 cm) were recorded in stationary visual census point count surveys (n = 6, plot Ø = 15 m, duration = 10 min, 9.30 am – 12.00 pm, distance between plots 20 m, Bannerot and Bohnsack 1986). Parrotfish species- or genus-specific abundance data were normalized to survey time and plot area, and converted into erosion rates via calculations based on size-specific estimates for bite rate and volume for several Red Sea taxa, under the assumption of 10 h of feeding activity per day; shown in Supplementary Table 17 (Alwany et al. 2009; Hoey et al. 2015). Specifically, bite rates and volumes were adjusted according to the percentage of bites leaving scars, and to fish size using the relationship between bite volume and average fork length, using Supplementary equations 3 C and D (Bruggemann et al. 1994, 1996) as recommended in (Perry et al. 2012). These specific erosion rates as well as abundances were used to calculate parrotfish erosion rates (E_{parrot}) per site (Supplementary equations 3 A - B, Supplementary Table 16).

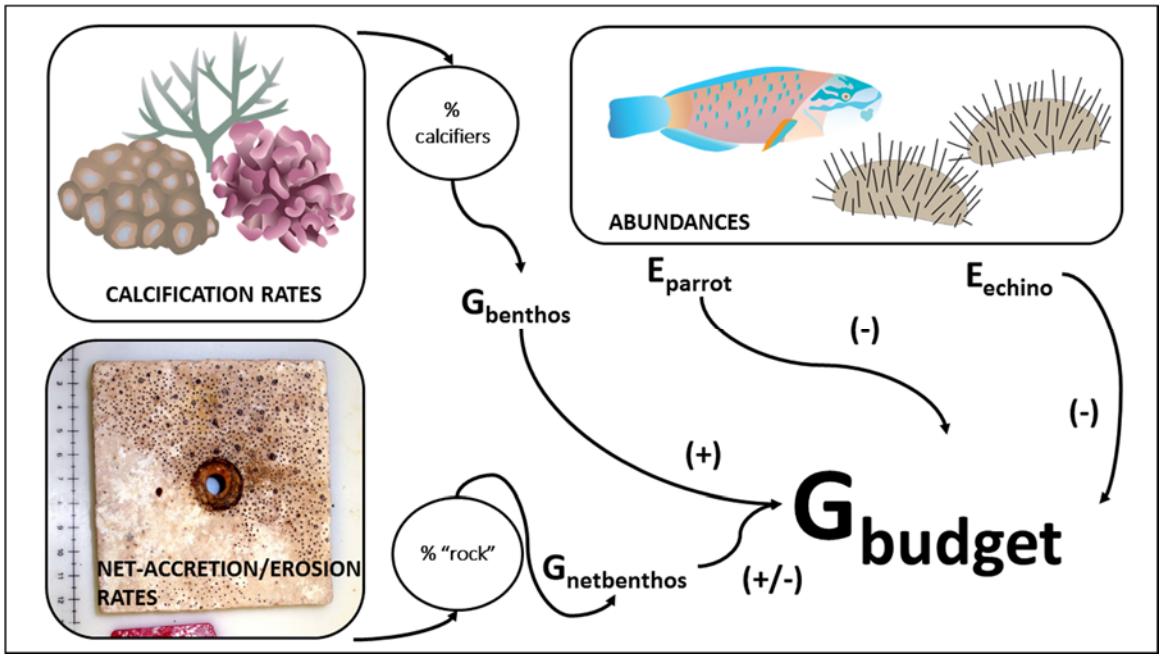

Figure 14 Procedure for carbonate budget estimation in this study. Values and equations that were used in the calculations of carbonate budgets are deposited in the Supplementary Materials (5.7). $G_{benthos}$ = benthic community calcification rate, $G_{netbenthos}$ = net-accretion/erosion rate of bare reef substrate, E_{parrot} = parrotfish erosion rate, E_{echino} = sea urchin erosion rate, G_{budget} = carbonate budget of a reef.

5.3.6. Statistical analyses: Abiotic parameters

Continuous data (temperature and pH) were summarized as daily means, daily standard deviations (SD), daily minima and maxima. Since some data did not fulfill the assumptions of normal distribution and homoscedascity (Kolmogorov-Smirnov and Levene's test), univariate 2-factorial permutational ANOVAs (PERMANOVAs) were used. The factors "reef" (nearshore, midshore lagoon, midshore, and offshore) and "season" (winter and summer) were tested using PERMANOVAS based on 999 permutations of residuals under a reduced model and type II partial sums of squares, performed on Euclidian resemblance matrices that were calculated from $\log_2 (x+1)$ transformed data (Anderson et al. 2008). Within each significant factor post-hoc pair-wise tests followed.

Inorganic nutrients (NO_3^-&NO_2^-, NH_4^+, and PO_4^{3-}) and carbonate chemistry (pH_{SWS}, A_T, C_T, Ω_a, HCO_3^- , CO_3^{2-}) were first evaluated using multivariate PERMANOVAs and principal coordinate ordination (PCO) according to the continuous data test design. Multivariate 2-factorial PERMANOVAs on Euclidian resemblance matrices created from normalized data were run under same specifications as above. Next, univariate 2-factorial ANOVAs were employed to evaluate the parameters separately under the same test design. For this, inorganic nutrients and carbonate chemistry parameters

were transformed (log_2 (x+1): pH_{SWS}, A_T, Ω_a; square-root: C_T, CO_3^{2-} ; box-cox: HCO_3^-) to meet assumptions of normality and homoscedascity.

5.3.7. Statistical analyses: Net-accretion/erosion rates and carbonate budgets

G_{net} data were tested for effects of the factors "reef" (nearshore, midshore, and offshore), "site exposure" (fore- and backreef), and "deployment time" (0.5, 1, and 2.5 years). Because of missing measurements in the nearshore and offshore backreef sites for the deployment time of 2.5 years, a univariate 3-factorial PERMANOVA was conducted using Euclidian distance matrix 999 permutations of residuals under a reduced model and type II partial sum of squares.

G_{budget} were tested for statistical differences between the four "reef sites" (nearshore, midshore lagoon, midshore, and offshore) using a 1-factorial ANOVA, after box-cox transforming the data to meet the assumptions. In parallel, biotic variables were tested using a 1-factorial ANOVA for square-root transformed $G_{benthos}$, and non-parametric Kruskal-Wallis tests for non-transformed $G_{netbenthos}$, E_{echino}, and E_{parrot}. Tukey's HSD post-hoc tests followed where applicable.

5.3.8. Statistical analyses: Abiotic and biotic drivers

To evaluate the influence of abiotic and biotic predictors on G_{net} and G_{budget}, a multivariate statistics approach was applied. Distance-based linear models (DistLM) were performed including biotic and abiotic predictor variables. Models were tested for (a) G_{net} and (b) G_{budget} data. G_{net} encompassed data of pooled 1-year and 2.5-year measurements from four reef sites (nearshore, midshore lagoon, midshore, and offshore). Predictor variables for (a) were reef growth relevant abiotic parameters,

comprising means and SDs from continuous measurements of temperature and pH_{CTD} per reef site, and the means of inorganic nutrients (NO_3^-&NO_2^-, NH_4^+, and PO_4^3) and carbonate chemistry parameters (A_T, C_T, Ω_a, HCO_3^-, and CO_3^{2-}) (

Table 11). Biotic variables that can potentially influence G_{net} on limestone blocks were added to the models, i.e. parrotfish abundances and percentage cover (%) of calcareous crusts, both derived from the reef surveys. For (b) predictor variables were the same abiotic parameters as used for (a), but the list of biotic predictors was extended by adding variables available from reef surveys that presumably have influence on the carbonate budget in a reef site, i.e. % total hard corals, % hard coral morphs (branching, encrusting, massive, and platy/foliose), % major reef-building coral families (Poritidae, Acroporidae, and Pocilloporidae), % calcareous crusts, % algae & sponges, benthos rugosity, and echinoid and parrotfish abundances. Prior to DistLM, some predictor variables (i.e. echinoid and parrotfish abundances, % platy/foliose corals, and % Poritidae) were $\log_{10}$ (x+1) transformed to improve the symmetry in their distributions following (Anderson et al. 2008). Both DistLM routines were performed on Euclidian resemblance matrices, implementing the step-wise forward procedure with 9999 permutations and adjusted R^2 criterion. Additionally, Spearman rank correlation coefficients were obtained for the response variables and their predictors.

Statistica (StatSoft Inc. 2011, version 10) was used for Kolmogorov-Smirnov and Levene's test of normality and homoscedascity, data transformations, to perform ANOVAs, Kruskal-Wallis tests, and Spearman rank correlations. Uni- and multivariate PERMANOVAs and DistLM routines were conducted using the software package PRIMER-E v6 (PERMANOVA+) (Anderson et al. 2008).

5.4. Results

5.4.1. Abiotic parameters relevant for reef growth

The seasonal mean temperature varied between 26.0 ± 0.6°C in winter and 30.9 ± 0.7°C in summer across all reefs (

Table 11, Table 12). The difference across the shelf was on the average ~0.4°C. Seasonal and spatial differences in all temperature data (daily means, daily SDs, daily minima and maxima) were significant (Figure 15 A, Supplementary Table 18). At all sites, daily means were significantly separated between the seasons ($p < 0.001$). The nearshore and midshore reef experienced the lowest temperature (both ~26°C in winter), and the nearshore reef the highest temperatures (31.5 ± 0.6°C in summer). In addition compared to all other sites, the nearshore reef had significantly higher daily maxima during summer ("daily max.", $p = 0.01$, Figure 15 B, Table 12), as well as the significantly lower minima during winter ($p < 0.01$) compared to other sites.

Across all reef sites, seasonal means for pH were 8.13 ± 0.19 in winter and 8.10 ± 0.22 in summer (

Table 11). Seasonal pH means were intermediate on the midshore and offshore (8.10 ± 0.05 to 8.16 ± 0.09), and highest on the nearshore reef (8.25 ± 0.27 to 8.32 ± 0.12). Lowest seasonal means were recorded on the midshore lagoon with 8.00 ± 0.19 in winter and 7.96 ± 0.32 in summer, where also significantly lowest daily minima were recorded (occasionally as low as ~7.00 pH). Overall, continuous pH data show that spatial differences were pronounced, while the effect of seasonality was very minor. All daily pH data differed between reef sites ($p < 0.01$, Supplementary Table 18, Figure 15 D), whereas only daily pH SDs and maxima were significantly different between the seasons ($p < 0.01$ and $p < 0.05$, respectively, Figure 15 C). The nearshore reef exhibited the highest daily maxima (occasionally reaching up to ~9.00 pH) which significantly decreased across the shelf from nearshore to offshore ($p < 0.01$). On all sites, pH followed a diel pattern with peak values around noon (12:00 h). Daily SDs were significantly larger in nearshore (0.12 – 0.27,

Table 11) and in the midshore lagoon (0.19 – 0.32) compared to the smaller variation at midshore and offshore sites (0.05 - 0.09, $p < 0.01$). The daily pH range was on the average spanning a range of ~0.55 pH units (8.06 – 8.60 pH) at the nearshore site and ~0.15 pH units (8.06 – 8.20) at the offshore site (Table 12).

Table 11 Reef growth relevant abiotic parameters measured in coral reefs along a cross-shelf gradient in the central Red Sea. Temperature (Temp) and pH were continuously measured using *in situ* loggers (CTDs). Weekly collected seawater samples were used for the determination of inorganic nutrient concentrations, i.e. nitrate and nitrite (NO_3^-&NO_2^-), ammonia (NH_4^+), and phosphate (PO_4^{3-}). Carbonate chemistry parameters were measured as total alkalinity (A_T) and pH in the same samples and used to calculate the carbonate ion concentration (CO_3^{2-}), aragonite saturation state (Ω_a), total inorganic carbon (C_T), bicarbonate ion (HCO_3^-), and partial pressure of carbon dioxide (pCO_2).

	Continuous data		Seawater samples									
Site and Season	Temp	pH_{CTD}	NO_3^- &NO_2^-	NH_4^+	PO_4^{3-}	pH_{SWS}	A_T	HCO_3^{-*}	CO_3^{2-*}	Ωa^*	C_T^*	pCO_2^*
	°C		µmol L^{-1}				µmol L^{-1}				µmol kg^{-1}	µatm
Central Red Sea	26.0	8.13	0.36	0.35	0.07	8.16	2423	1683	299	4.62	1990	292
reefs winter	(0.6)	(0.19)	(0.25)	(0.2)	(0.02)	(0.02)	(18)	(24)	(7)	(0.12)	(21)	(14)
Central Red Sea	31.0	8.10	0.61	0.5	0.03	8.13	2369	1588	314	4.95	1910	303
reefs summer	(0.7)	(0.22)	(0.25)	(0.22)	(0.02)	(0.03)	(38)	(41)	(17)	(0.28)	(36)	(25)
Nearshore	26.1	8.25	0.31	0.34	0.06	8.15	2414	1678	297	4.6	1983	295
exposed winter	(0.7)	(0.27)	(0.17)	(0.19)	(0.02)	(0.02)	(21)	(36)	(6)	(0.11)	(31)	(16)
Nearshore	31.5	8.31	0.6	0.42	0.02	8.11	2346	1576	309	4.88	1892	311
exposed summer	(0.6)	(0.12)	(0.28)	(0.17)	(0.01)	(0.03)	(31)	(37)	(14)	(0.23)	(32)	(22)
Midshore	25.9	8.00	0.41	0.46	0.07	8.15	2421	1695	294	4.54	1997	301
sheltered winter	(0.6)	(0.19)	(0.31)	(0.28)	(0.02)	(0.02)	(21)	(19)	(10)	(0.14)	(16)	(17)
Midshore	30.9	7.96	0.68	0.58	0.04	8.11	2365	1603	306	4.83	1917	315
sheltered summer	(0.6)	(0.32)	(0.26)	(0.28)	(0.03)	(0.03)	(40)	(47)	(18)	(0.29)	(40)	(31)
Midshore exposed	26.1	8.15	0.32	0.34	0.06	8.17	2431	1679	304	4.7	1991	286
winter	(0.5)	(0.07)	(0.3)	(0.19)	(0.02)	(0.02)	(14)	(27)	(8)	(0.13)	(21)	(15)
Midshore exposed	30.7	8.17	0.58	0.5	0.02	8.13	2373	1594	313	4.93	1915	300
summer	(0.7)	(0.09)	(0.26)	(0.26)	(0.01)	(0.02)	(38)	(37)	(15)	(0.24)	(34)	(16)
Offshore exposed	26.0	8.10	0.4	0.26	0.08	8.16	2425	1679	302	4.66	1988	285
winter	(0.4)	(0.05)	(0.24)	(0.15)	(0.02)	(0.01)	(20)	(18)	(2)	(0.03)	(19)	(5)
Offshore exposed	30.8	8.13	0.59	0.51	0.03	8.15	2393	1579	328	5.17	1914	283
summer	(0.7)	(0.08)	(0.25)	(0.18)	(0.03)	(0.02)	(35)	(47)	(16)	(0.26)	(39)	(19)

All values as mean (SD); pH_{CTD} = pH from CTD; pH_{SWS} = pH from seawater samples # day-time measurements (7:00 – 19:00); * parameters calculated using *seacarb* implemented in R (R Core Team 2013; Gattuso et al. 2015)

Table 12 Temperature and carbonate chemistry ranges in coral reefs along a cross-shelf gradient in the central Red Sea. Daily ranges, seasonal and cross-shelf differences.

	winter	summer	nearshore	offshore	cross-shelf Δ
Temperature (°C)					
avg, daily mean	26.0	30.9	29.4	29.0	~0.4
avg, daily SD	0.1	0.2	0.2	0.2	-
avg. daily min. – max.	25.8 – 26.2	30.6 – 31.3	29.2 – 29.7	28.7 – 29.2	-
absolute min. – max.	23.8 – 27.4	28.2 – 32.7	23.8 – 32.7	25.2 – 32.2	-
pH					
avg. daily mean	8.13	8.10	8.27	8.12	~0.05
avg. daily SD	0.12	0.10	0.19	0.04	-
avg. daily min. – max.	7.99 – 8.36	7.99 – 8.28	8.06 – 8.60	8.06 – 8.20	-
absolute min. – max.	7.57 – 9.08	6.88 – 9.02	7.54 – 9.08	7.86 – 8. 61	-
A_T (µmol kg^{-1})					
mean	2422	2369	2373	2405	~32
Ω_a					
mean	4.62	4.95	4.76	4.96	~0.2

avg. = average, SD = standard deviation, min. = minimum, max. = maximum, Δ = cross-shelf difference between avg. daily means in nearshore and offshore

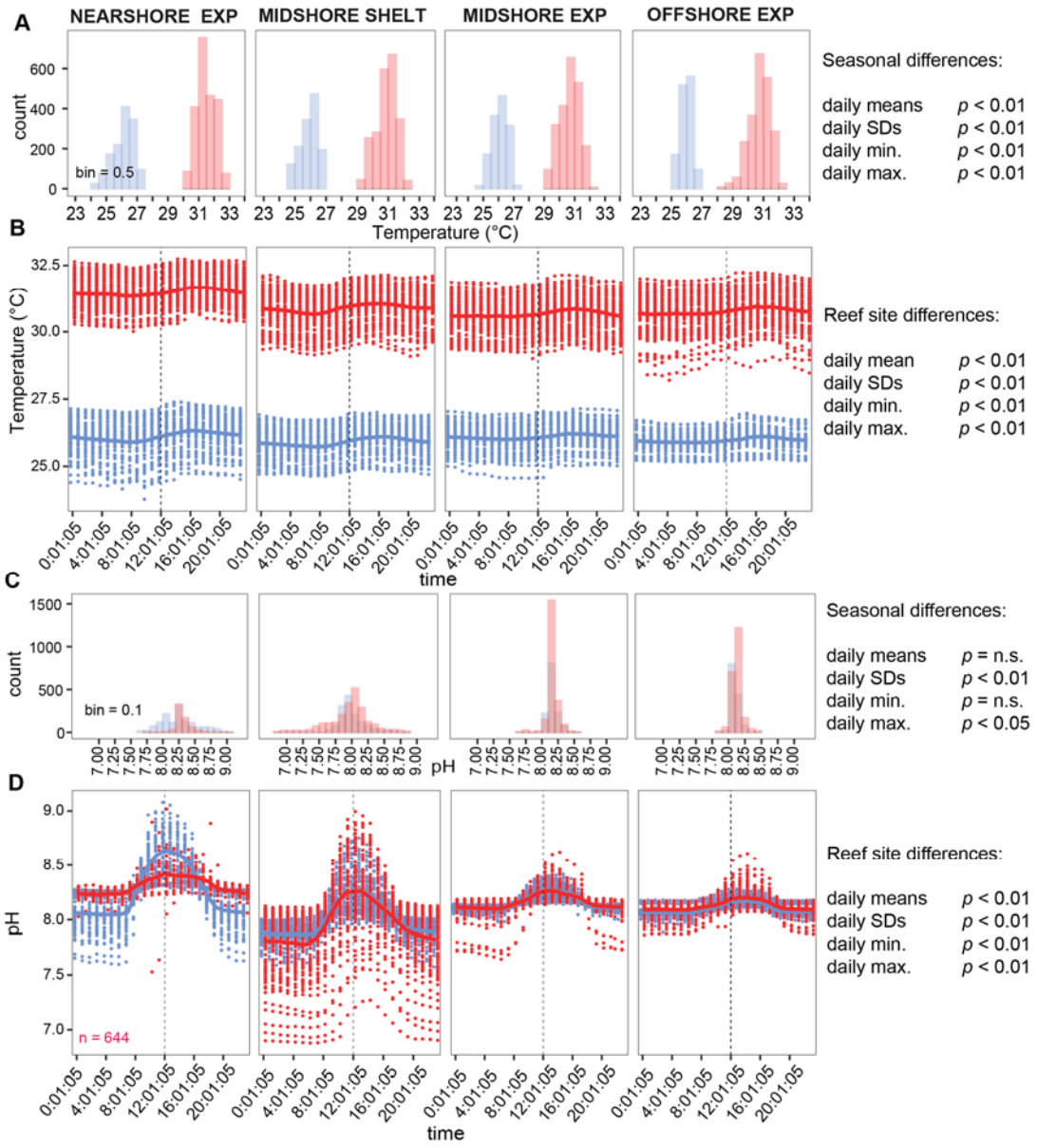

Figure 15 Temperature and pH regimes in coral reefs along a cross-shelf gradient in the central Red Sea. Continuous data of temperature (A - B) and pH_{CTD} (C - D) collected during winter (blue) and summer (red) are presented in histograms (A, C) and diel profiles (B, D). Data points per reef site in winter comprise n = 1344, and n = 2231 in summer. The pH data set in summer includes only n = 644. Diel profiles show raw data points and local polynomial regression lines (LOESS, span = 0.1). A dotted vertical line marks the midday time. Univariate PERMANOVA results indicate significant differences between reefs and seasons. (EXP = exposed, shelt SHELT = sheltered, univar. = univariate, n.s. = not significant)

Multivariate analyses of inorganic nutrients and carbonate chemistry show main variation between the seasons (both $p < 0.001$, Supplementary Table 18, Figure 16 A

- B). Specifically, nitrate and nitrite and ammonia levels almost doubled from winter (0.36 ± 0.25 μmol L^{-1} and 0.35 ± 0.20 μmol L^{-1},

Table 11) to summer (0.61 ± 0.25 µmol L^{-1} and 0.50 ± 0.22 µmol L^{-1}). In contrast, phosphate was higher in winter compared to summer (0.07 ± 0.02 vs. 0.03 ± 0.02 µmol L^{-1}, Supplementary Table 18 and Figure 16 C). Highest inorganic nutrient contents were measured in the midshore lagoon with up to 0.68 µmol NO_3^-&NO_2^- L^{-1}, 0.58 µmol NH_4^+ L^{-1} in summer, and 0.07 µmol PO_4^{3-} L^{-1} in winter, but phosphate was also high in offshore during winter (0.08 µmol $PO_4^{3-}L^{-1}$), which was a significant compared to the other sites ($p < 0.05$).

Table 11 and Figure 16 D present carbonate chemistry parameters that show overall elevated A_T, C_T and HCO_3^- concentrations in winter (2423 ± 18 μmol A_T L^{-1}, 1990 ± 21 μmol C_T L^{-1}, and 1683 ± 24 μmol HCO_3^- $L^{-1,}$

Table 11) compared to summer (2369 ± 38 A_T µmol L^{-1}, 1910 ± 36 µmol C_T L^{-1}, and 1588 ± 41 µmol HCO_3^- L^{-1}, Supplementary Table 18). Our pCO_2 estimates for the central Red Sea reefs ranged between 285 - 315 µatm across reef and seasons. Tests within each reef site showed that higher A_T during winter was significant at the nearshore reef ($p < 0.05$), while C_T and HCO_3^- were significantly higher at all sites ($p < 0.05$). Conversely, Ω_a and CO_3^{2-} were overall reduced during winter (winter: 4.62 ± 0.12 Ω_a and 299 ± 7 µmol CO_3^{2-} L^{-1}; summer: 4.95 ± 0.28 Ω_a and 314 ± 17 µmol CO_3^{2-} L^{-1}). Within sites, seasonal differences of Ω_a were only significant in the offshore site ($p < 0.05$). By trend, A_T and Ω_a increased from nearshore to offshore with average differences of 32 µmol kg^{-1} and Ω_a 0.2 (Figure 16 D, Table 12).

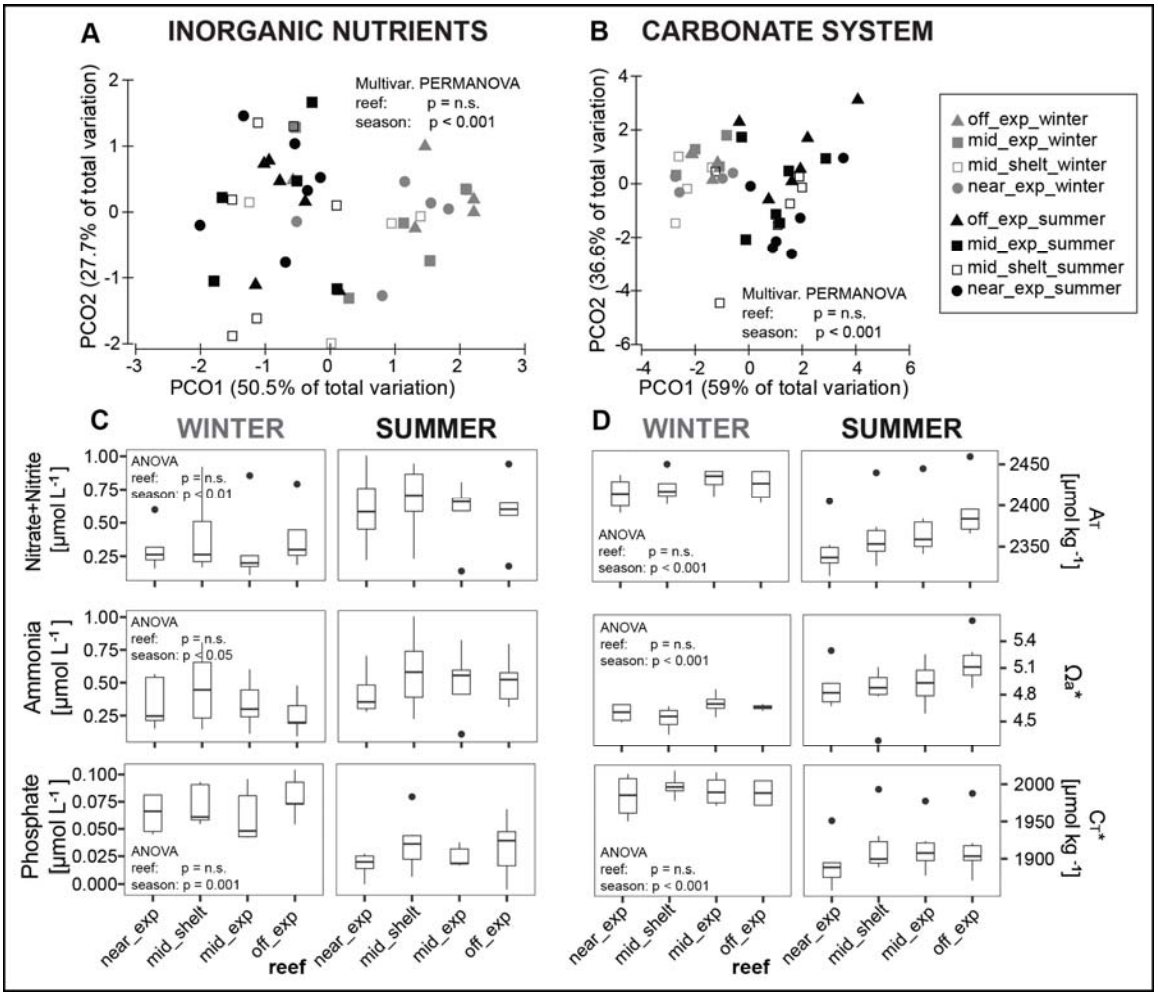

Figure 16 Coral reef inorganic nutrients and carbonate chemistry parameters along a cross-shelf gradient in the central Red Sea. Principal coordinates analyses (PCO) in A – B to visualize differences between reef sites and seasons (winter and summer) in the multivariate data structure of inorganic nutrients and the carbonate chemistry parameters. PCO analyses are based on Euclidian resemblances of normalized variables. Inorganic nutrient conditions are represented by the variables nitrate and nitrite (NO_3^-&NO_2^-), ammonia (NH_4^+), and phosphate (PO_4^{3-}). Multivariate carbonate chemistry data contain pH of seawater samples (pH_{SWS}), total alkalinity (A_T), total dissolved inorganic carbon (C_T), aragonite saturation state (Ω_a), bicarbonate (HCO_3^-), and carbonate (CO_3^{2-}). Boxplots C – D illustrate the differences of single parameters between the reefs within each season (box: 1st and 3rd quartiles, whiskers: 1.5-fold inter-quartile range, points: data beyond this range). Among the carbonate chemistry parameters only A_T, C_T, and Ω_a were plotted. Grey = winter, black = summer, off = offshore, mid = midshore, near = nearshore, exp = exposed forereef, shelt = sheltered lagoon, n.s. = not significant

5.4.2. Net-accretion/erosion rates along a cross-shelf gradient

Net accretion/erosion rates (G_{net}) for limestone blocks in the reef sites along the cross shelf gradient were between -0.96 and 0.37 kg m^{-2} yr^{-1} (both values measured in the

2.5 year deployment, Figure 17, Table 13). Only limestone blocks recovered from the reefs after 1 and 2.5 years deployment had visual signs of boring activity by endolithic bioeroders (e.g., worms or sponges, see examples in Figure 17 A - H). G_{net} (1 and 2.5 year) were negative in nearshore (between -0.96 and -0.2 kg m^{-2} yr^{-1}), around zero in the midshore exposed site (0.01 - 0.06 kg m^{-2} yr^{-1}), and positive in offshore (up to 0.37 kg m^{-2} yr^{-1}). Reef sites and the deployment times had a significant effect on the variability of G_{net} (Figure 17, Supplementary Table 19). G_{net} was generally increased by longer deployment periods ($p < 0.001$).

Table 13 Temporal succession of net-accretion/erosion rates (G_{net}) in coral reefs along a cross-shelf gradient in the central Red Sea. G_{net} (kg m^{-2} yr^{-1}) was calculated using weight gain/loss of limestone blocks deployed in the reef sites for 0.5, 1, and 2.5 years. Means per site are shown and standard deviations are in brackets. yr = year

G_{net} (kg m^{-2} yr^{-1})	Deployment time (yr)		
Reef site	0.5	1	2.5
Nearshore sheltered	0.16 (0.09)	-0.2 (0.35)	-
Nearshore exposed	0.11 (0.07)	-0.61 (0.49)	-0.96 (0.75)
Midshore sheltered	0.13 (0.09)	0.06 (0.03)	-0.29 (0.12)
Midshore exposed	0.11 (0.16)	0.01 (0.07)	0.06 (0.12)
Offshore sheltered	0.03 (0.02)	-0.07 (0.07)	-
Offshore exposed	0.14 (0.11)	0.08 (0.09)	0.37 (0.08)

yr = year

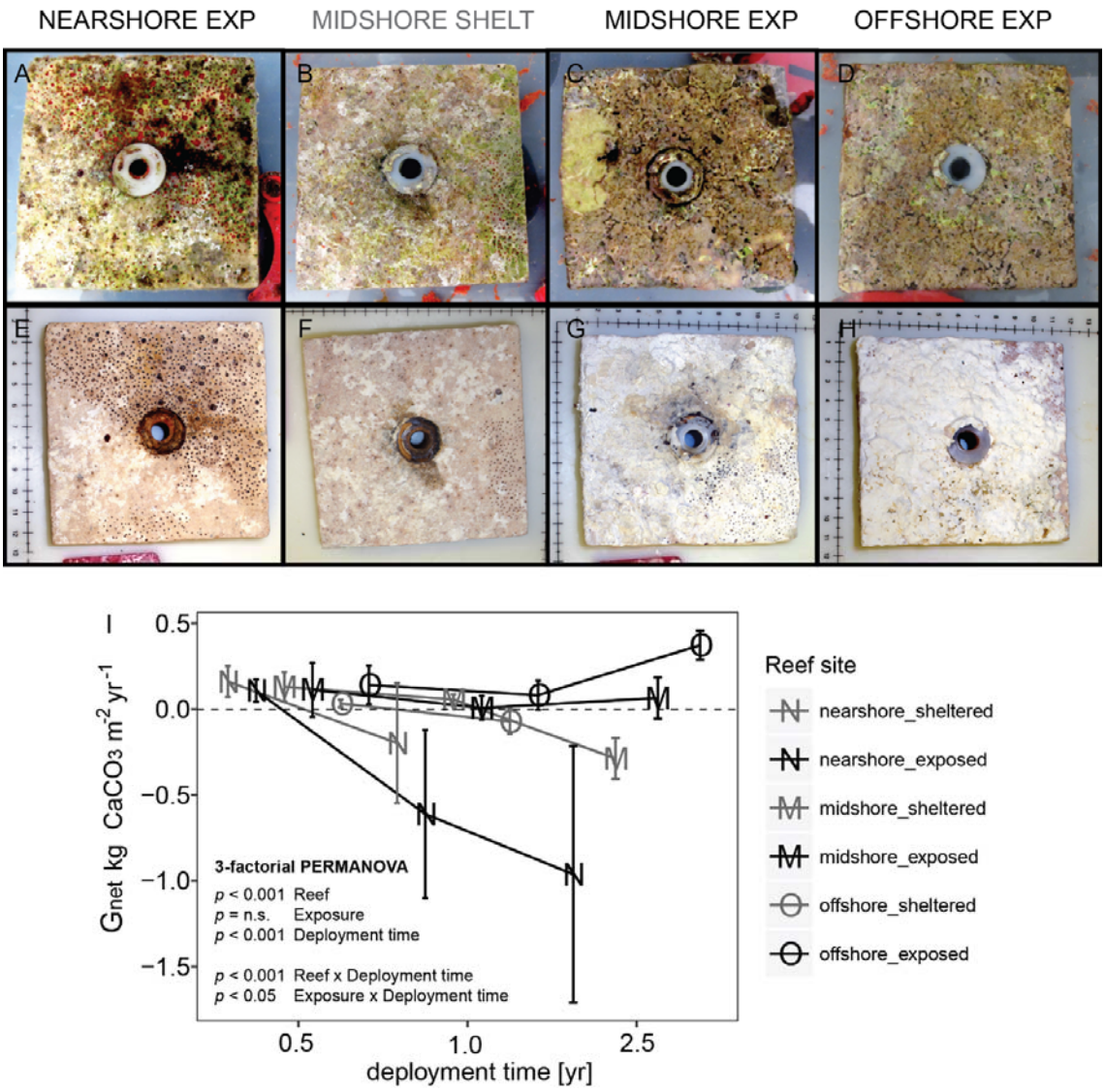

Figure 17 Limestone blocks after 2.5 years deployment in the reef sites and net-accretion/erosion rates (G_{net}) measured in the central Red Sea. Photos show (A – D) freshly collected limestone blocks that were recovered after 2.5 years, and the same blocks (E – H) after bleaching and drying. Boring holes of endolithic sponges are clearly noticeable in the nearshore exposed and both midshore reef sites. In the midshore and offshore exposed reefs blocks were covered with crusts of biogenic carbonate mostly accreted by coralline algae assemblages. Plot (I) illustrates the temporal succession of G_{net} in limestone blocks deployed in different reef sites for 0.5, 1 and 2.5 years along the cross-shelf gradient. Only significant interactions are shown. (EXP = exposed [in black], SHELT = sheltered [in grey], scales in E – H in cm)

5.4.3. Carbonate budgets along a cross-shelf gradient

The carbonate budgets ($G_{budgets}$) for the entire cross-shelf gradient was highly variable and on average 0.65 ± 1.73 kg m^{-2} yr^{-1}. This encompasses values from the negative nearshore budget -1.48 ± 1.75 kg m^{-2} yr^{-1} up to the positive offshore budget 2.44 ± 1.03 kg m^{-2} yr^{-1} (Table 14). Differences were significant between reef sites ($p < 0.05$, Figure 18 A), except budgets for both midshore sites. Among the biotic variables contributing to the carbonate budget (Figure 18 B – E), reef sites were a significant factor for community calcification rates ($G_{benthos}$) and net-accretion/erosion of bare substrate ($G_{netbenthos}$). $G_{benthos}$ differed between all sites ($p < 0.05$, Figure 18 B), while $G_{netbenthos}$ differed between all sites except each pair of neighboring sites ($p < 0.001$, Figure 18 C). Differences of parrot fish and sea urchin erosion rates (E_{echino} and E_{parrot}) were not significant (Figure 18 D -E). Within-site variation of E_{parrot} was high compared to the full range of values (e.g. SDs between 0.3 and 1.9 kg m^{-2} yr^{-1}, Table 14).

Table 14 Reef carbonate budget estimates and contributing biotic variables (kg m^{-2} yr^{-1}) along a cross shelf gradient in the central Red Sea. Calcification rates of benthic calcifiers ($G_{benthos}$), net-accretion/erosion rates of reef substrate ($G_{netbenthos}$), and the erosion rates of echinoids and parrotfishes (E_{echino}, E_{parrot}) contribute to the total carbonate budget (G_{budget}) in a reef site. Means per site are shown and standard deviations are in brackets. The last row gives the means and standard deviations across all sites.

Reef	$G_{benthos}$	$G_{netbenthos}$	E_{echino}	E_{parrot}	G_{budget}
Nearshore exposed	0.426 (0.149)	-0.315 (0.129)	-0.228 (0.189)	-1.36 (1.886)	-1.477 (1.748)
Midshore sheltered	1.15 (0.222)	-0.027 (0.014)	-0.187 (0.193)	-0.338 (0.271)	0.598 (0.368)
Midshore exposed	1.762 (0.242)	0.009 (0.003)	-0.024 (0.04)	-0.727 (0.307)	1.02 (0.353)
Offshore exposed	2.812 (0.646)	0.094 (0.022)	-0.019 (0.003)	-0.444 (0.701)	2.443 (1.033)
Cross-shelf gradient	1.538 (0.958)	-0.06 (0.168)	-0.114 (0.159)	-0.717 (1.04)	0.646 (1.734)

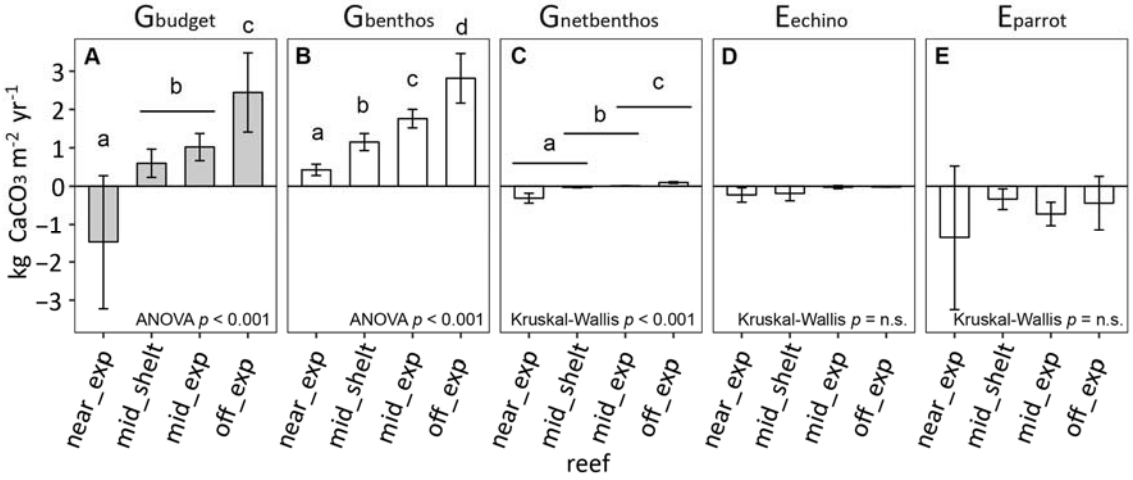

Figure 18 Reef carbonate budget estimates and contributing biotic variables along a cross-shelf gradient in the central Red Sea. Benthos accretion ($G_{benthos}$, $G_{netbenthos}$), and the erosion rates of echinoids and parrotfishes (E_{echino}, E_{parrot}) contribute to the total reef carbonate budget (G_{budget}) at each reef site. Bars indicate means and errorbars show standard deviations of (A) G_{budget} and (B – E) biotic variables ($G_{benthos}$, $G_{netbenthos}$, E_{echino}, E_{parrot}). Letters a – d indicate significantly different groups. Near_exp = nearshore exposed, mid_shelt = midshore sheltered (lagoon), mid_exp = midshore exposed, off_exp = offshore exposed.

5.4.4. Abiotic and biotic drivers related to net-accretion rates and carbonate budgets

Results from correlations and distance based linear models were similar for G_{net} and G_{budget}. First, temperature means, temperature SDs, and pH SDs negatively correlated, while A_T, Ω_a, CO_3^{2-}, and phosphate positively correlated with G_{net} ($\rho \geq |0.59|$, Table 15). The best model for G_{net} data accounted for 56% (adjusted R^2) of the total variation. Here, A_T alone explained 54% of the data and is the only statistically valid predictor of two abiotic variables in the model (the second being Ω_a accounting for only 2% more, Table 16).

In parallel, temperature means, temperature SDs, and pH SDs were the strongest negative abiotic correlates of G_{budget}, while A_T, Ω_a, CO_3^{2-}, and phosphate were positively correlated ($\rho \geq |0.59|$, Table 15). Among biotic variables, % total hard coral

and calcareous crusts were positively correlated. The best model for G_{budget} fitted six biotic and abiotic predictors and explained total variation of 87% (adjusted R^2). Again, A_T was the major predictor explaining 65% alone. Additionally, one biotic variable, specifically parrotfish abundances, added up to 85% of explained variation. Both variables were significant in the test. The remaining four predictors included in the model (nitrate and nitrite, % total hard coral, % encrusting coral, % of total hard coral, and % Acroporidae) were non-significant and of minute relevance (altogether contributing only 3%, Table 16).

Table 15 Coefficients from Spearman rank order correlations for predictor variables vs. G_{net} and G_{budget}. 12 abiotic and 13 biotic variables were correlated with G_{net} (= net-accretion/erosion rates of limestone blocks) and G_{budget} (= carbonate budget estimates). Biotic variables encompassed 2 bioeroder (abundances), and 11 relevant benthic categories (%-cover). Correlations that have a Spearman's correlation coefficient $\rho \geq |0.59|$ are shown.

	G_{net}		G_{budget}	
Abiotic variables	ρ	*p*	ρ	*p*
Temperature(ctd) mean	-0.65	< 0.05	-0.71	< 0.05
Temperature(ctd) SD	-0.65	< 0.05	-0.71	< 0.05
pH(ctd) mean	-0.39	< 0.05	-0.45	< 0.05
pH(ctd) SD	-0.59	< 0.05	-0.65	< 0.05
A_T mean	0.80	< 0.05	0.89	< 0.05
Ωa mean	0.59	< 0.05	0.65	< 0.05
C_T mean	0.24	n.s.	0.27	n.s
CO_3^2 mean	0.59	< 0.05	0.65	< 0.05
HCO_3^- mean	0.24	n.s.	0.27	n.s
Nitrite and nitrate mean	0.39	< 0.05	0.45	< 0.05
Ammonia mean	0.37	< 0.05	0.40	n.s
Phosphate mean	0.65	< 0.05	0.71	< 0.05
Biotic variables	ρ	*p*	ρ	*p*
Parrotfish abundance	-0.39	< 0.05	-0.26	n.s
Echinoid abundance	-	-	-0.51	< 0.05
Rugosity	-	-	0.67	< 0.05
% total hard coral	-	-	0.70	< 0.05
% Poritidae	-	-	0.43	< 0.05
% Acroporidae	-	-	0.31	n.s
% Pocilloporidae	-	-	0.57	< 0.05
% platy/foliose coral	-	-	0.52	< 0.05
% encrusting coral	-	-	0.28	n.s
% massive coral	-	-	0.28	n.s
% encrusting coral	-	-	0.28	n.s
% branching coral	-	-	-0.20	n.s
% calcareous crusts	0.59	< 0.05	0.69	< 0.05
%-cover algae & sponges	-	-	0.20	n.s

Table 16 Distance based linear models (DistLM) and sequential tests. Response variables were G_{net} (= net-accretion/erosion rates of limestone blocks) and G_{budget} (= reef carbonate budget estimates). Predictor variables were 12 abiotic variables, bioeroder abundances (1 variable for G_{net}, 2 for G_{budget}), and %-cover of relevant benthic categories (1 for G_{net}, 11 for G_{budget}).

Response variable: G_{net}							
Best Model	Adj R^2	R^2	RSS	# of fitted Variables			
	0.56	0.59	3.21	2			
Sequential test							
Variable	Cumul. Adj R^2	SS (trace)	Pseudo-F	*p*	R^2.	Cumul. R^2	res.df
+A_T mean	0.54	4.39	37.84	0.00	0.56	0.56	30
+ Ω_a mean	0.56	0.27	2.48	0.12	0.03	0.59	29
Response variables: G_{budget}							
Best Model	Adj R^2	R^2	RSS	# of fitted Variables			
	0.87	0.9	6.67	6			
Sequential test							
Variable	Cumul. Adj. R^2	SS (trace)	Pseudo-*F*	*p*	R^2	Cumul. R^2	res.df
+A_T mean	0.65	46.18	44.13	0.000	0.67	0.67	22
+Parrotfish abundance	0.82	11.75	21.89	0.000	0.17	0.84	21
+Nitrite and nitrate mean	0.84	1.67	3.48	0.078	0.02	0.86	20
+% encrusting coral	0.85	1.27	2.89	0.102	0.02	0.88	19
+% hard coral	0.86	0.80	1.91	0.181	0.01	0.89	18
+% Acroporidae	0.87	0.86	2.19	0.154	0.01	0.90	17

Cumul. Adj. R^2 = Cumulative adjusted R^2, Cumul. R^2 = Cumulative R^2, res.df = residual degrees of freedom, A_T = total alkalinity

5.5. Discussion

Our study presents data on reef growth in the central Red Sea, a geographic region that is governed by high salinities and temperatures. Additionally, the Red Sea is already impacted by ocean warming (Cantin et al. 2010; Raitsos et al. 2011). Here we investigated the present-day baseline of reef growth along an environmental cross-shelf gradient in the central Red Sea. We summarize reef growth processes by net-accretion/erosion rates (G_{net}) using limestone blocks deployed in reef sites, as well as

by applying a census-based carbonate budget (G_{budget}) approach (Perry et al. 2012). Our data show that carbonate chemistry parameters (i.e., total alkalinity [A_T], aragonite saturation state [Ω_a], and pCO_2) differed in comparison to reef sites in other locations. Hourly measurements reveal a comparably larger variability spanning ~0.55 pH units on a diel scale in the nearshore and midshore lagoon habitats, which co-occurred with negative G_{net} and $G_{budgets}$. In the following, we discuss central Red Sea reef growth rates that ranged from net-erosion in the nearshore to net-accretion in the midshore and offshore reefs, and the underlying biotic drivers, such as community calcification and bioerosion rates. We compare our results with trends from other coral reef locations and historical estimates.

5.5.1. Abiotic parameters governing reef growth in the central Red Sea

High resolution data that reveals natural variability of abiotic conditions on diel, seasonal, and spatial scales are critical for our understanding of spatio-temporal patterns of physiological stress of marine organisms (Helmuth et al. 2010, 2014). Our sampling effort of *in situ* temperature, carbonate chemistry, and inorganic nutrients characterizes the present-day conditions that reef calcifiers and bioeroders experience in our study sites. Our data show that A_T, Ω_a, and pCO_2 were on average closer to the estimates of preindustrial global ocean surface water, rather than to most recent measurements on other coral reef systems, such as the Great Barrier Reef (GBR, Uthicke et al. 2014) or off Puerto Rico (Gray et al. 2012). This implies that Red Sea waters have a high buffering capacity with regard to ocean acidification, and may reach critically low Ω_a levels for reef calcification at a later time point than other tropical coral reef locations. As a consequence, coral reefs in the Red Sea constitute a

stark contrast to locations of low A_T and Ω_a that are critically threatened by ocean acidification, such as the marginal coral habitats of Bermuda (Yeakel et al. 2015), Table 17) or the eastern tropical Pacific, e.g. Galápagos and upwelling sites off Panama (Manzello et al. 2008).

We found seasonal variation in carbonate chemistry similar to observations from the Gulf of Aqaba (GoA) (Silverman et al. 2007a) featuring a decrease of A_T and C_T and increase of Ω_a in summer. A nutrient enrichment period has been previously described during winter for the entire Red Sea (Raitsos et al. 2013). Affirmatively, in our study sites we found phosphate enrichment during winter. But at the same time nitrate and nitrite and ammonia were slightly decreased, unlike in the GoA (Silverman et al. 2007a).

Hourly recordings of temperature and pH allowed us to demonstrate remarkable diel fluctuations (Table 12). The data show that diel range was more than double in nearshore (~0.55 pH units) compared to the offshore forereef (~0.15 pH units). Data also shows also that extreme events occur in the nearshore and midshore lagoonal sites (e.g., lowest temperatures during winter and highest during summer, but also lowest night-time and highest day-time pH). The pH in coral reef ecosystems often displays consistent diel fluctuation (Hofmann et al. 2011), however variability reported from other locations was smaller than on the nearshore and midshore lagoon in the central Red Sea. For comparison, the pH on a fringing reef in Hawaii (Kaneʻohe Bay) ranges within 0.08 - 0.33 pH units, spanning from 7.83 to 8.03 pH at the most variable site (Silbiger et al. 2014), on a reef flat in the GBR pH ranges within

0.25 pH units from 7.92 to 8.17 pH (Albright et al. 2013), and on a Palmyra reef terrace within the same range from 7.85 to 8.10 (Hofmann et al. 2011).

Especially in coastal environments, spatio-temporal variations in parameters such as dissolved oxygen, C_T, and pH are often the consequence of biotic ecosystem feedbacks driven by photosynthetic production and respiratory consumption (Drupp et al. 2011). In our study area nearshore reefs are surrounded by relatively shallow waters, and are likely exposed to less water exchange compared to midshore and offshore forereefs. This leads to more pronounced signatures of biotic feedback in nearshore reefs such as observed for dissolved oxygen dynamics (Roik et al. in revision), and for pH in this study. Diel variability of pH suggests that also A_T will fluctuate in the reefs, which is associated with feedbacks of calcification that removes CO_3^{2-}, and dissolution that contributes CO_3^{2-} back to the water column (Silverman et al. 2007a; Zundelevich et al. 2007; Bates et al. 2010). Further study is required to explore these remarkable diel cycles of biotic feedback in the protected nearshore and lagoonal habitats.

By trend, A_T and Ω_a increased from nearshore to offshore by 32 µmol kg^{-1} and 0.2 Ω_a on average (Table 12). Similar spatial gradients were observed along a fringing reef in the GoA (Silverman et al. 2007b), and also in Bermuda, where nearshore values were 20 – 40 µmol kg^{-1} lower than offshore (Bates et al. 2010). In our study area, current circulation patterns may explain these gradients. The offshore reef and midshore receive most currents from the Red Sea basin supplying A_T richer water to the reefs, whereas the nearshore reef and midshore lagoon is increasingly supplied with the boundary current from the south (Roik et al. in revision), which passes

through the reef systems along the coast and hence may carry A_T depleted waters. Differences in seawater chemistry between offshore and nearshore reefs were related to reef growth processes, which is discussed later.

Table 17 Global comparison of carbonate chemistry.

	A_T (µmol kg^{-1})	Ω_a	pCO_2 (µatm)
Central Red Sea (this study)[1]	2346 – 2431	4.5 - 5.2	283 – 315
Global preindustrial values (Manzello et al. 2008)[2]	~2315	~4.3	~280
Great Barrier Reef (Uthicke et al. 2014)[3]	2069 – 2315	2.6 - 3.8	340 - 554
Puerto Rico, Caribbean (Gray et al. 2012)[4]	2223 - 2315	3.4– 3.9	356 – 460
Bermuda (Yeakel et al. 2015)[5]	2300 – 2400	2.7 - 3.6	300 -450
Panama, upwelling sites (Manzello et al. 2008)[2]	1869.5	2.96	368
Galapagos (Manzello et al. 2008) [2]	2299	2.49	636

[1] lowest and highest means per reef site and season; [2] estimated averages, for details see referenced study; [3] lowest and highest means from reef sites during wet and dry seasons; [4] lowest and highest seasonal means from one site; [5] minimum and maximum from time series plots

5.5.2. Net-accretion/erosion rates (Gnet) and carbonate budgets (Gbudgets) along a cross-shelf gradient

Limestone blocks, used to measure G_{net}, were exposed to biotic $CaCO_3$ accretion (mainly by encrusting calcifiers such as coralline algae), endolithic erosion by boring organisms, and surface abrasion by grazing fish (Tribollet and Golubic 2005). G_{net} was subject to a succession pattern in our study sites, reflecting the colonization progress on the limestone blocks (Chazottes et al. 1995; Tribollet and Golubic 2005). Clear differences in G_{net} along the environmental gradient only arose after an exposure time of greater than 1 year, when established epilithic and endolithic communities were apparent (e.g. **Figure 17**). Measurements from 2.5 years deployment show net-erosion rates in nearshore and net-accretion rates in offshore. On a global scale, the majority of reef sites had similar G_{net} (e.g. Moorea, -0.49 - 0.63 kg m^{-2} yr^{-1}, (Pari et al. 1998). The lowest net-erosion rate from our nearshore sites was on the average only

¼ lower compared to the highest rates determined in the Thai Andaman Sea reefs (~ -4 kg m^{-2} yr^{-1}), and Moorea, French Polynesia, (~ -7 kg m^{-2} yr^{-1},Pari et al. 1998; Schmidt and Richter 2013).

The G_{budget} estimates represent the cumulative contribution of the major biotic drivers of reef growth, such $G_{benthos}$, $G_{netbenthos}$, E_{echino} and E_{parrot} (Glynn 1997; Perry et al. 2012). Overall, these biotic drivers increased from nearshore to offshore, resulting in a net-erosive budget in the nearshore reef, low net-accretion budgets in the midshore reef, up to highest net-accretion in offshore. According to this estimates, currently the central Red Sea nearshore reefs disintegrate at half the rate that the offshore reefs grow.

There is a disparity between the the cross-shelf patterns of G_{budget} and its biotic drivers ($G_{benthos}$, $G_{netbenthos}$, E_{echino}, and E_{parrot}) from this study and the patterns found in other coral reefs. For instance, while the G_{budget} is reported to be high in protected, turbid inshore reefs in the GBR (Browne et al 2013), our similarly structured nearshore study site, was net-erosive. Accordingly, parrotfish erosion was highest in the nearshore area in the central Red Sea, whereas the lowest rates were reported for the inshore reefs in the GBR (Tribollet et al. 2002; Hoey and Bellwood 2007). On Caribbean islands, parrotfish erosion rates are also generally increased in protected leeward reefs, but these sites are typically characterized by a high coral cover which drives a positive G_{budget} (Perry et al. 2012, 2014). In comparison, our nearshore site had the highest parrotfish erosion, but a negative G_{budget} due to low coral cover. Similarly, echinoid erosion in Zanzibar, which is higher on exposed forereefs

compared with protected reefs (Bronstein and Loya 2014), is in contrast to the increased sea urchin erosion in the protected nearshore site in our study. These regional difference strongly suggest that coral reef habitats in the Red Sea are unique environments, and extrapolating findings from other regions to the Red Sea is mostly not feasible.

5.5.3. Global and historical perspective on carbonate budgets (Gbudgets) in the Red Sea

$G_{budgets}$ measured in the central Red Sea were comparable with a majority of coral reef sites in the Caribbean, eastern tropical Pacific, and Java Sea that ranged from -0.8 to 4.5 kg m^{-2} yr^{-1} (Mallela and Perry 2007), and lower than the highest $G_{budgets}$ for remote reefs of the Chagos Archipelago of up to 9.8 kg m^{-2} yr^{-1} (Perry et al. 2015). It remains more difficult to draw a historical perspective on $G_{budgets}$ in the Red Sea. Pelagic and reefal net-accretion rates of carbonates were estimated based on basin-scale historical measurements of A_T from 1998 (Steiner et al. 2014). This broad 1998 baseline for coral reef net-accretion (0.9 kg $m^{-2}yr^{-1}$) is in accordance with its contemporaneous census-based budget approach from a fringing reef in GoA from 1994 –1996 (0.7 – 0.9 kg $m^{-2}yr^{-1}$, (Dullo et al. 1996a). Notably, the $G_{budgets}$ presented in this current study on average fit into this range, and are even slightly higher in the offshore reef. Additionally, when disregarding bioerosion, the gross calcification rate of benthic communities from our offshore site compares very well with the highest gross calcification from the GoA in 1994 (2.7 kg m^{-2} yr^{-1}, Heiss 1995) Both comparisons imply that reef growth may have not changed over the past 20 years despite the ongoing warming trend. This contradicts more recent studies. In the

90ies, warming rates of sea surface temperatures abruptly increased in the entire Red Sea (Raitsos et al. 2011), decreasing coral calcification rates in the central part (Cantin et al. 2010). In order to understand if this event had an influence on the total $G_{budgets}$, it is necessary to compare present-day budgets with (pre-90ies) estimates. (Dullo et al. 1996a) provide a Holocene net reef production rate of 0.8 kg m^{-2} yr^{-1} assessed from reef cores from the GoA, which compares well with our present day G_{budget}, and again supports the notion that reef growth has remained stable over even larger temporal scales. However, more and better comparable data will be required to confirm this assertion. Due to the strong latitudinal gradient of temperature and salinity reef growth dynamics may differ between GoA and the central Red Sea which may bias this comparison. Also, the GoA Holocene net reef production could be an underestimation compared to the net reef production for Caribbean fossil reefs (1.21 kg m^{-2} yr^{-1}, Hubbard et al. 1990), or the preindustrial budget for in the Florida Reef in the Caribbean (8.3 kg m^{-2} yr^{-1}, Enochs 2015).

Our data may serve as a new baseline for comparative future studies in the region. Importantly, these data have been collected before the "Third Global Bleaching Event" (Witze 2015), which during summer 2015 has impacted reef communities in our study area (Monroe et al., in prepatation). Our pre-bleaching G_{budget} will be valuable to determine if and how G_{budget} states of Red Sea coral reefs will have changed after this disturbance.

5.5.4. Abiotic drivers related to reef growth in the central Red Sea

Our study explored the linkage between abiotic and biotic variables and coral reef growth along a cross-shelf environmental gradient. In our study sites, significant negative correlates for both, G_{net} and $G_{budgets}$, were temperature means and pH variation, while positive correlates were A_T, Ω_a, CO_3^{2-}, and phosphate.

The negative correlates suggest that habitats governed by higher temperature and larger pH variability support only low budgets or net-erosion states, which is apparent for the nearshore and midshore lagoonal habitats. Assumedly, also lower levels of dissolved oxygen and higher turbidity as demonstrated for the same nearshore site in a previous study (Roik et al. in revision) may contribute to a comparably challenging habitat for recruitment and performance of calcifiers. Calcification has been shown to be less efficient at exceedingly high temperatures, low pH levels, and under turbid conditions (Marshall and Clode 2004; Fabricius 2005; Marubini et al. 2008; Castillo et al. 2014). At the same time, activity of endolithic bioeroders can be supported by temporarily low pH at nearshore and lagoonal sites leading to low or negative budgets (Fang et al. 2013). Recently, (Silbiger et al. 2014) showed that differences in pH variability between micro-habitats already significantly influenced accretion and erosion.

The positive correlates of G_{net} and $G_{budgets}$, i.e. A_T, Ω_a, CO_3^{2-}, are mostly directly linked to the calcification process. A positive relationship between A_T, pH, and Ω_a with calcification had been established in many laboratory and mesocosm experiments (e.g., (Langdon et al. 2000; Schneider and Erez 2006), and this relationship was also

identified for Ω_a and CO_3^{2-} concentration *in situ* on reef community scale (Silverman et al. 2007b; Bates et al. 2010). In our study, among all measured abiotic and biotic variables, the best predictors in both, G_{net} and G_{budget}, was A_T, alone explaining more than half of the data variation.

Another, driver for reef growth in our study area is phosphate. It is an essential nutrient in photosynthesis which is an important source of energy for calcification in the most important reef builders, symbiotic corals and coralline algae. While an overload of nutrients is detrimental for calcification and the reef-building communities (Fabricius 2005; Tambutté et al. 2011), our results show that in a very oligotrophic system, such as the Red Sea, reef growth can positively respond to an increase in phosphate levels. It has been demonstrated that an increased nitrogen:phosphorous ratio has a negative effect on reef-building corals raising the stress-susceptibility of the coral-dinoflagellate symbiosis in aquaria experiments (Wiedenmann et al. 2013). Our results may reflect this negative effect of phosphate depletion on reef building corals. It will be of interest to study inorganic nutrient ratios in the central Red Sea and their impact on coral physiology in more detail.

To this end, in the Red Sea high temperatures have been described to influence calcification seasonally and on the long-term (Silverman et al. 2007b; Cantin et al. 2010; Roik et al. 2015b; Sawall et al. 2015). Accordingly, future coral growth in the Red Sea has been modelled based on this relationship of calcification rates with temperatures (Cantin et al. 2010). Our study now shows that additionally significant relations of reef growth processes with inorganic nutrient variability and carbonate

chemistry exist. Using the here presented relationships of multi-variable data with reef growth could be a basis for modelling future reef growth predictions for the Red Sea.

5.5.5. Biotic drivers related to reef growth in the central Red Sea

Calcifying communities (i.e. coral cover) and carbonate production are the most decisive drivers for Gbudgets on global scale (Franco et al. 2016). Loss of coral cover gives way to bioeroders that become the critical force leading to degradation of reef framework. This has become particularly apparent in the Caribbean, where Gbudgets were reported to shift into negative production states when live coral cover was below 10% (Perry et al. 2013). The relevance of calcifying communities becomes also highly apparent in our dataset: % total hard coral and calcareous crusts were the strongest positive correlates for Gbudget, and the latter one also for Gnet. Additionally, our analyses show that parrotfish erosion is a considerable driving force across our study sites. Parrot fish abundances and erosion were higher in the Red Sea (on the average -1.57 kg m^{-2} yr^{-1}) compared to the neighboring PAG (Hoey et al. 2015). Here, we show that in the central Red Sea, parrotfish abundances explained ~20% of Gbudget data in the best distance-based linear model, reflecting high parrotfish erosion in the nearshore reef driving the carbonate production state into a net erosion state.

Grazing parrotfishes are considered dominant bioeroders that are associated with sediment production and degradation of reef framework (Bruggemann et al. 1996; Bellwood et al. 2003). Despite their high carbonate removal activity, parrotfishes are

vital components to the ecosystem for their secondary controls on the natural accretion and erosion balance. Parrotfish grazing activity is vital to maintain a coral dominated state by regulating benthic algal growth. Diverse functional groups of parrotfishes remove algae in different successional stages (e.g., turfs and macroalgae), and thereby create space for coral and coralline algae recruitment (Mumby 2006). An absence of parrotfishes can promote a phase-shift in coral reefs including the reduction of coral cover to communities dominated by non-calcifying organisms (Hughes et al 2007), and hence a decrease in gross carbonate production. Moreover, overfishing of parrotfishes and other fish species can also result in a loss of feeding pressure on bioeroders or their larvae (e.g., sea urchins) resulting in a uncontrolled population increase leading reefs on a trajectory of degradation (e.g. (McClanahan and Shafir 1990; Edgar et al. 2010).

5.5.6. Conclusions

The Red Sea represents a geographic region where coral reefs thrive in high temperature and high alkalinity waters. Baseline datasets on reef growth from this region are valuable as they provide insight into reef functioning under remarkably variable abiotic conditions that deviate from the global averages for coral reefs. In this study we show that carbonate chemistry parameters relevant for reef growth are comparable to estimates of preindustrial global ocean surface water, suggesting that the Red Sea will be less sensitive to ocean acidification than most other reef locations. However, A_T in the reefs was significantly related to net carbonate production rates, and it remains to be further investigated how already small changes in carbonate chemistry can affect reef growth in the central Red Sea. Despite present-day offshore

carbonate budget in the central Red Sea being lower than highest net-production states on remote reefs in the Indian Ocean, comparison with historical Red Sea data suggests that reef growth may have remained mostly stable since 1995. Since carbonate budgets are a powerful tool to track the trajectories of modern-day and future reef states, we ancitipate that our dataset will be particularly valuable when evaluating the impact of recent disturbances, such as the "Third Global Bleaching Event", on the reef building communities and the overall reef growth potential in the central Red Sea.

5.6. References

Albright R, Langdon C, Anthony KRN (2013) Dynamics of seawater carbonate chemistry, production, and calcification of a coral reef flat, Central Great Barrier Reef. Biogeosciences Discuss 10:7641–7676

Alvarez-Filip L, Dulvy NK, Gill JA, Côté IM, Watkinson AR (2009) Flattening of Caribbean coral reefs: region-wide declines in architectural complexity. Proc R Soc Lond B Biol Sci 276:3019–3025

Alwany MA, Thaler E, Stachowitsch M (2009) Parrotfish bioerosion on Egyptian Red Sea reefs. J Exp Mar Biol Ecol 371:170–176

Anderson MJ, Gorley RN, Clarke KR (2008) PERMANOVA+ for PRIMER: Guide to software and statistical methods.

Bak RPM, Nieuwland G, Meesters EH (2009) Coral Growth Rates Revisited after 31 Years: What is Causing Lower Extension Rates in *Acropora Palmata*? Bull Mar Sci 84:287–294

Bannerot SP, Bohnsack JA (1986) A stationary visual census technique for quantitatively assessing community structure of coral reef fishes. NOAA,

Bates NR, Amat A, Andersson AJ (2010) Feedbacks and responses of coral calcification on the Bermuda reef system to seasonal changes in biological processes and ocean acidification. Biogeosciences 7:2509–2530

Bauman AG, Feary DA, Heron SF, Pratchett MS, Burt JA (2013) Multiple environmental factors influence the spatial distribution and structure of reef communities in the northeastern Arabian Peninsula. Mar Pollut Bull 72:302–312

Bellwood DR, Hoey AS, Choat JH (2003) Limited functional redundancy in high diversity systems: resilience and ecosystem function on coral reefs. Ecol Lett 6:281–285

Bronstein O, Loya Y (2014) Echinoid community structure and rates of herbivory and bioerosion on exposed and sheltered reefs. J Exp Mar Biol Ecol 456:8–17

Bruggemann J, van Kessel A, van Rooij J, Breeman A (1996) Bioerosion and sediment ingestion by the Caribbean parrotfish Scarus vetula and Sparisoma viride:implications of fish size, feeding mode and habitat use. Mar Ecol Prog Ser 134:59–71

Bruggemann J, van Oppen M, Breeman A (1994) Foraging by the stoplight parrotfish Sparisoma viride. I. Food selection in different, socially determined habitats. Mar Ecol Prog Ser 106:41–55

Buddemeier RW (1997) Symbiosis: Making light work of adaptation. Nature 388:229–230

Cai W-J, Ma Y, Hopkinson BM, Grottoli AG, Warner ME, Ding Q, Hu X, Yuan X, Schoepf V, Xu H, Han C, Melman TF, Hoadley KD, Pettay DT, Matsui Y, Baumann JH, Levas S, Ying Y, Wang Y (2016) Microelectrode characterization of coral daytime interior pH and carbonate chemistry. Nat Commun 7:11144

Cantin NE, Cohen AL, Karnauskas KB, Tarrant AM, McCorkle DC (2010) Ocean Warming Slows Coral Growth in the Central Red Sea. Science 329:322–325

Carricart-Ganivet JP, Cabanillas-Terán N, Cruz-Ortega I, Blanchon P (2012) Sensitivity of Calcification to Thermal Stress Varies among Genera of Massive Reef-Building Corals. PLoS ONE 7:e32859

Castillo KD, Ries JB, Bruno JF, Westfield IT (2014) The reef-building coral Siderastrea siderea exhibits parabolic responses to ocean acidification and warming. Proc R Soc B Biol Sci 281:20141856

Chazottes V, Campion-Alsumard TL, Peyrot-Clausade M (1995) Bioerosion rates on coral reefs: interactions between macroborers, microborers and grazers (Moorea, French Polynesia). Palaeogeogr Palaeoclimatol Palaeoecol 113:189–198

Chazottes V, Le Campion-Alsumard T, Peyrot-Clausade M, Cuet P (2002) The effects of eutrophication-related alterations to coral reef communities on agents and rates of bioerosion (Reunion Island, Indian Ocean). Coral Reefs 21:375–390

Cohen AL, Holcomb M (2009) Why corals care about ocean acidification: uncovering the mechanism. Oceanography 22:118–127

Cooper TF, Death G, Fabricius KE, Lough JM (2008) Declining coral calcification in massive *Porites* in two nearshore regions of the northern Great Barrier Reef. Glob Change Biol 14:529–538

Couce E, Ridgwell A, Hendy EJ (2012) Environmental controls on the global distribution of shallow-water coral reefs. J Biogeogr 39:1508–1523

Death G, Lough JM, Fabricius KE (2009) Declining Coral Calcification on the Great Barrier Reef. Science 323:116–119

Dickson AG (1990) Standard potential of the reaction: AgCl(s) + 12H2(g) = Ag(s) + HCl(aq), and and the standard acidity constant of the ion HSO4− in synthetic sea water from 273.15 to 318.15 K. J Chem Thermodyn 22:113–127

Dickson AG, Sabine CL, Christian JR (2007) Guide to best practices for ocean CO2 measurements. PICES Special Publication 3:pp 191

Drupp P, Carlo EHD, Mackenzie FT, Bienfang P, Sabine CL (2011) Nutrient Inputs, Phytoplankton Response, and CO2 Variations in a Semi-Enclosed Subtropical Embayment, Kaneohe Bay, Hawaii. Aquat Geochem 17:473–498

Dullo W-C, Reijmer J, Schuhmacher H, Eisenhauer A, Hassan M, Heiss G (1996) Holocene reef growth and recent carbonate production in the Red Sea. Global and Regional Controls of Biodenic Sedimentation. Gottinger Arb. Geol. Palaont., Gottingen, pp 13–17

Eakin CM (2001) A tale of two Enso Events: carbonate budgets and the influence of two warming disturbances and intervening variability, Uva Island, Panama. Bull Mar Sci 69:171–186

Edgar GJ, Banks SA, Brandt M, Bustamante RH, Chiriboga A, Earle SA, Garske LE, Glynn PW, Grove JS, Henderson S, Hickman CP, Miller KA, Rivera F, Wellington GM (2010) El Niño, grazers and fisheries interact to greatly elevate extinction risk for Galapagos marine species. Glob Change Biol 16:2876–2890

Edinger EN, Limmon GV, Jompa J, Widjatmoko W, Heikoop JM, Risk MJ (2000) Normal coral growth rates on dying reefs: Are coral growth rates good indicators of reef health? Mar Pollut Bull 40:404–425

Enochs IC (2015) Ocean acidification enhances the bioerosion of a common coral reef sponge: implications for the persistence of the Florida Reef Tract. Bulletin of Marine Science 91:271–290

Fabricius KE (2005) Effects of terrestrial runoff on the ecology of corals and coral reefs: review and synthesis. Mar Pollut Bull 50:125–146

Fang JKH, Mello-Athayde MA, Schönberg CHL, Kline DI, Hoegh-Guldberg O, Dove S (2013) Sponge biomass and bioerosion rates increase under ocean warming and acidification. Glob Change Biol 19:3581–3591

Franco C, Hepburn LA, Smith DJ, Nimrod S, Tucker A (2016) A Bayesian Belief Network to assess rate of changes in coral reef ecosystems. Environ Model Softw 80:132–142

Gattuso JP, Epitalon JM, Lavigne (2015) seacarb: seawater carbonate chemistry with R. R package version 3.0.

Glynn PW (1997) Bioerosion and coral-reef growth: a dynamic balance. Chapman and Hall, USA

Glynn PW, Manzello DP (2015) Bioerosion and Coral Reef Growth: A Dynamic Balance. In: Birkeland C. (eds) Coral Reefs in the Anthropocene. Springer Netherlands, pp 67–97

Gray SEC, DeGrandpre MD, Langdon C, Corredor JE (2012) Short-term and seasonal pH, pCO_2 and saturation state variability in a coral-reef ecosystem. Glob Biogeochem Cycles 26:3

Heiss GA (1995) Carbonate production by scleractinian corals at Aqaba, Gulf of Aqaba, Red Sea. Facies 33:19–34

Helmuth B, Broitman BR, Yamane L, Gilman SE, Mach K, Mislan K a. S, Denny MW (2010) Organismal climatology: analyzing environmental variability at scales relevant to physiological stress. J Exp Biol 213:995–1003

Helmuth B, Russell BD, Connell SD, Dong Y, Harley CD, Lima FP, Sará G, Williams GA, Mieszkowska N (2014) Beyond long-term averages: making biological sense of a rapidly changing world. Clim Change Responses 1:6

Hoey AS, Bellwood DR (2007) Cross-shelf variation in the role of parrotfishes on the Great Barrier Reef. Coral Reefs 27:37–47

Hoey AS, Feary DA, Burt JA, Vaughan G, Pratchett MS, Berumen ML (2015) Regional variation in the structure and function of parrotfishes on Arabian reefs. Mar Pollut Bull: 10.1016/j.marpolbul.2015.11.035

Hofmann GE, Smith JE, Johnson KS, Send U, Levin LA, Micheli F, Paytan A, Price NN, Peterson B, Takeshita Y, Matson PG, Crook ED, Kroeker KJ, Gambi MC, Rivest EB, Frieder CA, Yu PC, Martz TR (2011) High-Frequency Dynamics of Ocean pH: A Multi-Ecosystem Comparison. PLoS ONE 6:e28983

Hubbard DK, Miller AI, Scaturo D (1990) Production and Cycling of Calcium Carbonate in a Shelf-Edge Reef System (St. Croix, U.S. Virgin Islands): Applications to the Nature of Reef Systems in the Fossil Record. J Sediment Res 60:3

Jokiel PL, Coles SL (1990) Response of Hawaiian and other Indo-Pacific reef corals to elevated temperature. Coral Reefs 8:155–162

Jones NS, Ridgwell A, Hendy EJ (2015) Evaluation of coral reef carbonate production models at a global scale. Biogeosciences 12:1339–1356

Kennedy EV, Perry CT, Halloran PR, Iglesias-Prieto R, Schönberg CHL, Wisshak M, Form AU, Carricart-Ganivet JP, Fine M, Eakin CM, Mumby PJ (2013) Avoiding Coral Reef Functional Collapse Requires Local and Global Action. Curr Biol 23:912–918

Kleypas JA, McManus JW, Menez LAB (1999) Environmental Limits to Coral Reef Development: Where Do We Draw the Line? Am Zool 39:146–159

Kleypas J, Buddemeier R, Gattuso J-P (2001) The future of coral reefs in an age of global change. Int J Earth Sci 90:426–437

Langdon C, Takahashi T, Sweeney C, Chipman D, Goddard J, Marubini F, Aceves H, Barnett H, Atkinson MJ (2000) Effect of calcium carbonate saturation state on the calcification rate of an experimental coral reef. Glob Biogeochem Cycles 14:639–654

Lueker TJ, Dickson AG, Keeling CD (2000) Ocean pCO_2 calculated from dissolved inorganic carbon, alkalinity, and equations for K_1 and K_2: validation based on laboratory measurements of CO_2 in gas and seawater at equilibrium. Mar Chem 70:105–119

Mallela J, Perry C (2007) Calcium carbonate budgets for two coral reefs affected by different terrestrial runoff regimes, Rio Bueno, Jamaica. Coral Reefs 26:129–145

Manzello DP (2010) Ocean acidification hotspots: Spatiotemporal dynamics of the seawater CO2 system of eastern Pacific coral reefs. Limnol Oceanogr 55:239–248

Manzello DP, Kleypas JA, Budd DA, Eakin CM, Glynn PW, Langdon C (2008) Poorly cemented coral reefs of the eastern tropical Pacific: Possible insights into reef development in a high-CO2 world. Proc Natl Acad Sci 105:10450–10455

Marshall AT, Clode P (2004) Calcification rate and the effect of temperature in a zooxanthellate and an azooxanthellate scleractinian reef coral. Coral Reefs 23:218–224

Marubini F, Ferrier-Pagès C, Furla P, Allemand D (2008) Coral calcification responds to seawater acidification: a working hypothesis towards a physiological mechanism. Coral Reefs 27:491–499

McClanahan TR, Shafir SH (1990) Causes and consequences of sea urchin abundance and diversity in Kenyan coral reef lagoons. Oecologia 83:362–370

Metzl N, Moore B, Papaud A, Poisson A (1989) Transport and carbon exchanges in Red Sea Inverse Methodology. Glob Biogeochem Cycles 3:1–26

Moberg F, Folke C (1999) Ecological goods and services of coral reef ecosystems. Ecol Econ 29:215–233

Monroe AA, Ziegler M, Roik A, Röthig T, Hardenstin R, Emms M, Jensen T, Voolstra CR, Berumen ML (in preparation) *In situ* observations of coral bleaching in the central Saudi Arabian Red Sea during the 2015/2016 global coral bleaching event.

Mumby PJ (2006) The Impact Of Exploiting Grazers (Scaridae) On The Dynamics Of Caribbean Coral Reefs. Ecol Appl 16:747–769

Orr JC, Fabry VJ, Aumont O, Bopp L, Doney SC, Feely RA, Gnanadesikan A, Gruber N, Ishida A, Joos F, Key RM, Lindsay K, Maier-Reimer E, Matear R, Monfray P, Mouchet A, Najjar RG, Plattner G-K, Rodgers KB, Sabine CL, Sarmiento JL, Schlitzer R, Slater RD, Totterdell IJ, Weirig M-F, Yamanaka Y, Yool A (2005) Anthropogenic ocean acidification over the twenty-first century and its impact on calcifying organisms. Nature 437:681–686

Pari N, Peyrot-Clausade M, Le Champion-Alsumard T, Hutchings P, Chazottes V, Gobulic S, Le Champion J, Fontaine MF (1998) Bioerosion of experimental substrates on high islands and on atoll lagoons (French Polynesia) after two years of exposure. Mar Ecol Prog Ser 166:119–130

Perez FF, Fraga F (1987) The pH measurements in seawater on the NBS scale. Mar Chem 21:315–327

Perry C, Edinger E, Kench P, Murphy G, Smithers S, Steneck R, Mumby P (2012) Estimating rates of biologically driven coral reef framework production and erosion: a new census-based carbonate budget methodology and applications to the reefs of Bonaire. Coral Reefs 31:853–868

Perry CT, Larcombe P (2003) Marginal and non-reef-building coral environments. Coral Reefs 22:427–432

Perry CT, Murphy GN, Graham NAJ, Wilson SK, Januchowski-Hartley FA, East HK (2015) Remote coral reefs can sustain high growth potential and may match future sea-level trends. Sci Rep 5:18289

Perry CT, Murphy GN, Kench PS, Edinger EN, Smithers SG, Steneck RS, Mumby PJ (2014) Changing dynamics of Caribbean reef carbonate budgets: emergence of reef bioeroders as critical controls on present and future reef growth potential. Proc R Soc B Biol Sci 281:20142018–20142018

Perry CT, Murphy GN, Kench PS, Smithers SG, Edinger EN, Steneck RS, Mumby PJ (2013) Caribbean-wide decline in carbonate production threatens coral reef growth. Nat Commun 4:1402

Perry CT, Spencer T, Kench PS (2008) Carbonate budgets and reef production states: a geomorphic perspective on the ecological phase-shift concept. Coral Reefs 27:853–866

Raitsos DE, Hoteit I, Prihartato PK, Chronis T, Triantafyllou G, Abualnaja Y (2011) Abrupt warming of the Red Sea. Geophys Res Lett 38:L14601

Raitsos DE, Pradhan Y, Brewin RJW, Stenchikov G, Hoteit I (2013) Remote Sensing the Phytoplankton Seasonal Succession of the Red Sea. PLoS ONE 8:e64909

R Core Team (2013) R: A language and environment for statistical computing. R Foundation for Statistical Computing, Vienna, Austria

Reaka-Kudla ML (1997) The Global Biodiversity of Coral Reefs: A Comparison with Rainforests. In: Reaka-Kudla M.L., Wilson D.E., Wilson E.O. (eds) Biodiversity II: Understanding and Protecting Our Biological Resources. The Joseph Henry Press, USA, pp 83 – 106

Riegl B (2003) Climate change and coral reefs: different effects in two high-latitude areas (Arabian Gulf, South Africa). Coral Reefs 22:433–446

Riegl BM, Bruckner AW, Rowlands GP, Purkis SJ, Renaud P (2012) Red Sea Coral Reef Trajectories over 2 Decades Suggest Increasing Community Homogenization and Decline in Coral Size. PLoS ONE 7:e38396

Roik A, Roder C, Röthig T, Voolstra CR (2015) Spatial and seasonal reef calcification in corals and calcareous crusts in the central Red Sea. Coral Reefs 1–13

Roik A, Röthig T, Roder C, Ziegler M, Kremb SG, Voolstra CR (in revision) Year-long monitoring of physico-chemical and biological variables provide a comparative baseline of coral reef functioning in the central Red Sea. PLOS ONE PONE–S–15–69229

Sawall Y, Al-Sofyani A (2015) Biology of Red Sea Corals: Metabolism, Reproduction, Acclimatization, and Adaptation. In: Rasul N.M.A., Stewart I.C.F. (eds) The Red Sea. Springer Berlin Heidelberg, pp 487–509

Sawall Y, Al-Sofyani A, Hohn S, Banguera-Hinestroza E, Voolstra CR, Wahl M (2015) Extensive phenotypic plasticity of a Red Sea coral over a strong latitudinal temperature gradient suggests limited acclimatization potential to warming. Sci Rep 5:8940

Schmidt GM, Richter C (2013) Coral Growth and Bioerosion of *Porites lutea* in Response to Large Amplitude Internal Waves. PLoS ONE 8:e73236

Schneider K, Erez J (2006) The effect of carbonate chemistry on calcification and photosynthesis in the hermatypic coral *Acropora eurystoma*. Limnol Oceanogr 51:1284–1293

Schuhmacher H, Loch K, Loch W, See WR (2005) The aftermath of coral bleaching on a Maldivian reef—a quantitative study. Facies 51:80–92

Sheppard C, Loughland R (2002) Coral mortality and recovery in response to increasing temperature in the southern Arabian Gulf. Aquat Ecosyst Health Manag 5:395–402

Silbiger NJ, Guadayol scar, Thomas FIM, Donahue MJ (2014) Reefs shift from net accretion to net erosion along a natural environmental gradient. Mar Ecol Prog Ser 515:33–44

Silverman J, Lazar B, Erez J (2007a) Community metabolism of a coral reef exposed to naturally varying dissolved inorganic nutrient loads. Biogeochemistry 84:67–82

Silverman J, Lazar B, Erez J (2007b) Effect of aragonite saturation, temperature, and nutrients on the community calcification rate of a coral reef. J Geophys Res 112:C05004

Steiner Z, Erez J, Shemesh A, Yam R, Katz A, Lazar B (2014) Basin-scale estimates of pelagic and coral reef calcification in the Red Sea and Western Indian Ocean. Proc Natl Acad Sci 1414323111

Tambutté S, Holcomb M, Ferrier-Pagès C, Reynaud S, Tambutté É, Zoccola D, Allemand D (2011) Coral biomineralization: From the gene to the environment. J Exp Mar Biol Ecol 408:58–78

Tribollet A, Decherf G, Hutchings P, Peyrot-Clausade M (2002) Large-scale spatial variability in bioerosion of experimental coral substrates on the Great Barrier Reef (Australia): importance of microborers. Coral Reefs 21:424–432

Tribollet A, Godinot C, Atkinson M, Langdon C (2009) Effects of elevated pCO2 on dissolution of coral carbonates by microbial euendoliths. Glob Biogeochem Cycles 23:3

Tribollet A, Golubic S (2005) Cross-shelf differences in the pattern and pace of bioerosion of experimental carbonate substrates exposed for 3 years on the northern Great Barrier Reef, Australia. Coral Reefs 24:422–434

Uthicke S, Furnas M, Lønborg C (2014) Coral Reefs on the Edge? Carbon Chemistry on Inshore Reefs of the Great Barrier Reef. PLoS ONE 9:e109092

Vaquer-Sunyer R, Duarte CM (2008) Thresholds of hypoxia for marine biodiversity. Proc Natl Acad Sci 105:15452–15457

Waldbusser GG, Hales B, Haley BA (2016) Calcium carbonate saturation state: on myths and this or that stories. ICES J Mar Sci J Cons 73:563–568

Wickham H, Chang W (2015) ggplot2: An Implementation of the Grammar of Graphics.

Wiedenmann J, D'Angelo C, Smith EG, Hunt AN, Legiret F-E, Postle AD, Achterberg EP (2013) Nutrient enrichment can increase the susceptibility of reef corals to bleaching. Nat Clim Change 3:160–164

Witze A (2015) Corals worldwide hit by bleaching. Nature: http://www.nature.com/doifinder/10.1038/nature.2015.18527 (accessed: April 2016)

Yeakel KL, Andersson AJ, Bates NR, Noyes TJ, Collins A, Garley R (2015) Shifts in coral reef biogeochemistry and resulting acidification linked to offshore productivity. Proc Natl Acad Sci 112:14512–14517

Zundelevich A, Lazar B, Ilan M (2007) Chemical versus mechanical bioerosion of coral reefs by boring sponges - lessons from *Pione cf. vastifica*. J Exp Biol 210:91–96

5.7. Supplementary Materials

Supplementary equations 1 Benthic community calcification and net-accretion/erosion of bare reef substrate ($G_{benthos}$ and $G_{netbenthos}$)

Legend:

Rugosity:	R
Transect planar length:	d1 [m]
Rugosity length:	d2 [m]
Percentage cover of a category in a transect:	COV [%]
Calcifier transect category:	CAT
Sum of *Rock* and *Recently dead coral* (transect categories):	RCDC
Accretion/calcification per benthos category:	$G_{Calcifier}$ (CAT)#
	G_{net} (CAT)#

Equations:

(a) $G_{benthos} = \sum_{k=CAL} G_{Calcifier}(k) * R * COV$

(b) $G_{netbenthos} = G_{net}(RCDC) * R * COV$

(c) $R = d2/d1$

#see Supplementary Table 13

Supplementary equations 2 Sea urchin bioerosion (E_{echino})

Legend:

Bioerosion rate per individual *Diadema*#:	$E_{echinoIndvD}$ [kg individuals^{-1} yr^{-1}]
Bioerosion rate per individual *Echinometra*#:	$E_{echinoIndvE}$ [kg individuals^{-1} yr^{-1}]
Bioerosion rate per individual *Other*#:	$E_{echinoIndvO}$ [kg individuals^{-1} yr^{-1}]
Size class averages:	S [mm] {10, 30, 50, 70, 90}
Echinoid abundance per reef site (census based):	$Abund_{echino}$ [individials m^{-2}]
Echinoid bioerosion rate per reef site:	E_{echino} [kg m^{-2} yr^{-1}]

Equations:

(a) $E_{echino} = E_{echinoIndv} * Abund_{echino}$

(b) $E_{echinoIndvD}(S) = 0.0029 * S^{1.6624} * 0.001 * 365$

(c) $E_{echinoIndvE}(S) = 0.0007 * S^{1.7309} * 0.001 * 365$

(d) $E_{echinoIndvO}(S) = 0.00008 * S^{2.4537} * 0.001 * 365$

#from *ReefBudget* (Perry et al. 2012)

Supplementary equations 3 Parrotfish bioerosion (E_{parrot})

Legend:

Average fork length averages:	FL [cm] {10, 20, 30, 40, 57, 100}
Species specific bite volume (from Table S6):	$BVol_{species}$ [cm^3]
Species specific bite rate (from Table S6):	Brate [b $minute^{-1}$]
Fork length specific bite volume (Bruggemann et al. 1994):	$BVol_{Bruggemann}$ [cm^3]
Fork size adjustment factor# ((Bruggemann et al. 1994):	$factor_{Bruggemann}$
% of bites leaving scars (Bruggemann et al. 1996):	B%
Adjusted species and fork size specific bite volume:	$BVol_{adj}$ [cm^3]
Size Adjusted bite rate:	$Brate_{adj}$ [b $minute^{-1}$]
Reef carbonate density (Alwany et al. 2009):	$\rho = 1.4$ [g cm^{-3}]
Hour of active feeding y per day (Alwany et al. 2009):	$h_{Feed} = 10$ [h]
Bioerosion rate per individual:	$E_{parrotIndv}$ [kg $individual^{-1}$ yr^{-1}]
Parrot fish abundance (census based):	$Abund_{parrot}$ [individuals m^{-2}]
Parrot fish bioerosion rate per reef site:	E_{Parrot} [kg m^{-2} yr^{-1}]

#Relative to FL = 40

Equations:

(a) $E_{Parrot} = E_{ParrotIndv} * Abund_{Parrot}$

(b) $E_{ParrotIndv} = Brate_{Adj} * BVol_{Adj} * \rho * 60min * h_{Feed} * 365 * 0.001$

(c) $BVol_{Adj}(FL) = BVol_{Species} * factor_{Bruggeman}(FL)$

(d) $Brate_{Adj}(FL) = B\%/100 * Brate$

(e) $factor_{Bruggeman}(FL) = BVol_{Bruggemann}(FL) / BVolBruggemann(40)$

(f) $B_{VolBruggemann} = 1.362 * 10^{-6} * FL^3$

Supplementary Table 12 Sampling schedule for seawater samples

Inorganic nutrients	Total alkalinity and pH	Season
08.12.2013, n = 1	-	winter
05.03.2014, n = 1	05.03.2014, n = 3	winter
10.03.2014, n = 1	10.03.2014, n = 3	winter
17.03.2014, n = 1	17.03.2014, n = 3	winter
26.03.2014, n =1	26.03.2014, n = 3	winter
23.06.2014, n = 1	23.06.2014, n = 3	summer
16.07.2014, n = 1	16.07.2014, n = 3	summer
20.08.2014, n = 1	20.08.2014, n = 3	summer
28.08.2014, n = 1	28.08.2014, n = 3	summer
04.09.2014, n = 1	04.09.2014, n = 3	summer
10.09.2014, n = 1	10.09.2014, n = 3	Summer

Dates = dd.mm.yyyy

Supplementary Table 13 Site specific calcification and net-accretion/erosion rates assigned to benthic transect categories.

Transect Code	Benthos category	Assigned calcification rate ($G_{calcifier}$)	Nearshore exposed*	Midshore Sheltered	Midshore exposed	Offshore exposed
HCB	Other Hard Coral (branching)	G_{HCB} = avg ACR POC	1.753 (0.021)	2.514 (0.928)	3.119 (0.886)	3.598 (1.257)
HCE	Other Hard Coral (encrusting)	G_{HCE} = avg ACR POC POR	2.842 (1.295)	2.888 (1.39)	3.341 (2.339)	4.246 (1.78)
HCM	Other Hard Coral (massive)	G_{HCM} = avg POC	2.732 (0.608)	2.732 (0.608)	3.469 (0.901)	4.11 (1.247)
HCP	Other Hard Coral (platy/foliose)	G_{HCP} = avg ACR POC POR	2.842 (1.295)	2.888 (1.39)	3.341 (2.339)	4.246 (1.78)
ACR	Acroporidae	G_{ACR} = avg ACR	1.753 (0.021)	2.362 (1.105)	2.699 (0.737)	3.151 (1.156)
POC	Pocilloporidae	G_{POC} = avg POC	2.732 (0.608)	2.732 (0.608)	3.469 (0.901)	4.11 (1.247)
POR	Poritidae	G_{POR} = avg POR	3.93 (0.537)	4.16 (2.021)	3.83 (4.257)	6.673 (1.299)
CC	Calcareous crusts (coralline algae)	G_{CC} = avg CC	0.138 (0.042)	0.151 (0.042)	0.263 (0.084)	0.411 (0.08)
		Assigned accretion/erosion rate (G_{net})				
DC	Recently Dead Coral	G_{DC} = avg G_{net}	-0.787 (-0.16)	-0.116 (0.615)	0.036 (0.201)	0.227 (0.096)
RC	Rock	G_{RC} = avg G_{net}	-0.787 (-0.16)	-0.116 (0.615)	0.036 (0.201)	0.227 (0.096)

Calcification rates $G_{calcifier}$ (kg m^{-2} yr^{-1}) are averaged per reef site from (Roik et al. 2015b). Average net-accretion rates G_{net} (kg m^{-2} yr^{-1}) are based on the deployment of limestone blocks in this study. *Since calcification rate for Pocilloporidae (POC) was not measured for the nearshore exposed reef, the average from the midshore sheltered site is used. Avg = average; standard deviations in bracket

Supplementary Table 14 Census-based benthos community calcification ($G_{benthos}$) and benthos net-accretion/erosion rates ($G_{netbenthos}$ kg m^{-2} yr^{-1})

Reef	G_{HCB}	G_{HCE}	G_{HCM}	G_{HCP}	G_{ACR}	G_{POC}	G_{POR}	G_{CC}	$G_{benthos}$	G_{DC}	G_{RC}	$G_{netbenthos}$
Nearshore exposed	0.034 (0.038)	0.097 (0.066)	0.139 (0.05)	0 (0)	0.007 (0.018)	0.009 (0.011)	0.138 (0.091)	0.002 (0.002)	0.426 (0.149)	-0.004 (0.007)	-0.311 (0.128)	-0.315 (0.129)
Midshore sheltered	0.136 (0.115)	0.094 (0.092)	0.531 (0.178)	0.116 (0.283)	0.11 (0.217)	0.039 (0.033)	0.125 (0.078)	0.001 (0.001)	1.15 (0.222)	0 (0.001)	-0.027 (0.014)	-0.027 (0.014)
Midshore exposed	0.005 (0.013)	0.181 (0.171)	0.367 (0.321)	0.042 (0.08)	0.385 (0.174)	0.37 (0.234)	0.373 (0.216)	0.039 (0.034)	1.762 (0.242)	0.002 (0.001)	0.007 (0.003)	0.009 (0.003)
Offshore exposed	0.12 (0.198)	0.382 (0.226)	0.408 (0.353)	0.064 (0.136)	0.352 (0.546)	0.315 (0.246)	1.018 (0.76)	0.155 (0.039)	2.812 (0.646)	0.007 (0.007)	0.086 (0.027)	0.094 (0.022)

Means over six replicates; standard deviations in brackets

Supplementary Table 15 Census-based sea urchin bioerosion rates E_{echino} (kg m^{-2} yr^{-1})

Reef	$E_{Diadema}$	$E_{Echinometra}$	$E_{Echinostrephus}$	$E_{Eucidaris}$	E_{Other}	E_{echino}
Nearshore exposed	0.217 (0.184)	0.011 (0.018)	0 (0)	0 (0)	0 (0)	0.228 (0.189)
Midshore sheltered	0.168 (0.185)	0 (0)	0.015 (0.037)	0.004 (0.009)	0 (0)	0.187 (0.193)
Midshore exposed	0.022 (0.038)	0.002 (0.002)	0.001 (0.003)	0 (0)	0 (0)	0.024 (0.04)
Offshore exposed	0.016 (0.001)	0.002 (0.004)	0 (0)	0 (0)	0 (0)	0.019 (0.003)

Means over six replicates; standard deviations in brackets

Supplementary Table 16 Census-based parrotfish bioerosion rates E_{parrot} (kg m^{-2} yr^{-1})

Reef	$E_{Cbicolor}$	$E_{Cgibbus}$	$E_{Csordidus}$	E_{Hharid}	$E_{Scaridae}$	$E_{Sferrugineus}$	$E_{Sfrenatus}$	$E_{Sghobban}$	E_{Sniger}	E_{Parrot}
Nearshore exposed	0 (0)	0 (0)	-0.256 (0.176)	-0.112 (0.091)	-0.272 (0.138)	-0.067 (0.067)	-0.02 (0.048)	0 (0)	-0.047 (0.024)	-1.36 (1.886)
Midshore sheltered	0 (0)	0 (0)	0 (0)	-0.229 (0.254)	-0.1 (0.144)	-0.01 (0.014)	0 (0)	0 (0)	-0.005 (0.009)	-0.338 (0.271)
Midshore exposed	0 (0.001)	-0.098 (0.23)	-0.033 (0.038)	-1.07 (1.827)	-0.103 (0.136)	-0.005 (0.011)	0 (0)	-0.05 (0.078)	-0.014 (0.014)	-0.727 (0.307)
Offshore exposed	-0.108 (0.203)	-0.098 (0.23)	-0.046 (0.038)	-0.001 (0.002)	-0.078 (0.123)	-0.023 (0.044)	-0.001 (0.001)	-0.09 (0.219)	-0.015 (0.012)	-0.444 (0.701)

Means over six replicates; standard deviations in brackets

Supplementary Table 17 Parrotfish species specific bite rates and bite volumes employed in Eparrot estimation

Species	**Bite rate [b $minute^{-1}$]**	**Bite volume [cm^3]**	**Reference**
Cetoscarus bicolor	5.88	0.110	Alwany et al. 2009
Chlorurus gibbus	6.38	0.114	Alwany et al. 2009
Chlorurus sordidus	15.30	0.008	Alwany et al. 2009
Scarus ferrugenius	11.88	0.009	Alwany et al. 2009
Scarus frenatus	10.72	0.011	Alwany et al. 2009
Scarus ghobban	10.92	0.063	Alwany et al. 2009
Scarus niger	19.78	0.002	Alwany et al. 2009
Hipposcarus harid	9.00	0.021	Hoey et al. 2015*
Other Scaridae	11.23	0.040	average of all values used here

* bite volume is an average of "scraper" bite volumes from (Alwany et al. 2009)

Supplementary Table 18 Statistical tests characterizing the spatio-seasonal variation in abiotic parameters

	Reef *p*	Season *p*	Season x Reef *p*	Test
		Continuous data		
Temperature daily means	0.001	0.001	0.001	Univariate PERMANOVA (on $log_{10}(x+1)$ data)
Temp daily SDs	0.003	0.001	0.001	Univariate PERMANOVA (on log_{10} (x+1) data)
Temp daily min.	0.001	0.001	0.001	Univariate PERMANOVA (on log_{10} (x+1) data)
Temp daily max	0.001	0.001	0.001	Univariate PERMANOVA (on log_{10} (x+1) data)
pH_{CTD} daily means	0.001	0.343	0.01	Univariate PERMANOVA (on log_{10} (x+1) data)
pH_{CTD} daily SDs	0.001	0.002	0.01	Univariate PERMANOVA (on log_{10} (x+1) data)
pH_{CTD} daily min.	0.001	0.274	0.001	Univariate PERMANOVA (on log_{10} (x+1) data)
pH_{CTD} daily max.	0.001	0.032	0.002	Univariate PERMANOVA (on log_{10} (x+1) data)
		Seawater sampling		
Inorganic nutrients	0.578	< 0.001	0.990	Multivariate PERMANOVA (non-transformed, normalized data)
NO_3^-&NO_2^-	0.825	0.003	0.973	Univariate 2-way ANOVA (boxcox (x+1) transformed)
NH_4^+	0.478	0.024	0.775	Univariate 2-way ANOVA (non-transformed)
PO_4^{3-}	0.208	< 0.001	0.853	Univariate 2-way ANOVA (log_2(x+1) transformed)
Carbonate system	0.084	< 0.001	0.730	Multivariate PERMANOVA (non-transformed, normalized data)
pH_{SWS}	0.022	< 0.001	0.560	Univariate ANOVA (log_2(x) transformed data)
A_T	0.211	< 0.001	0.604	Univariate ANOVA (log_2(x) transformed data)
C_T	0.585	< 0.001	0.935	Univariate ANOVA (sqrt(x) transformed data)
Ω_a	0.113	< 0.001	0.533	Univariate ANOVA (log_2(x) transformed data)
HCO_{3-}	0.541	< 0.001	0.961	Univariate ANOVA (boxcox (x) transformed data)
CO_3^{2-}	0.090	< 0.001	0.508	Univariate ANOVA (sqrt(x) transformed data)

Supplementary Table 19 Statistical tests for the effect of different reef sites and temporal succession on net-accretion rates (G_{net}) measured using limestone blocks.

3-factorial PERMANOVA	Pseudo-*F*	Unique permutations	*p*
Reef	19.21	9940	< 0.001
Exposure	2.02	9841	0.166
Deployment time	19.32	9947	< 0.001
Reef x Exposure	2.82	9955	0.066
Reef x Deployment	11.54	9944	< 0.001
Exposure x Deployment	4.29	9942	0.021
Reef x Exposure x Deployment	1.90	9851	0.172
Pair-wise tests	*t*	Unique permutations	*p*
midshore, offshore	1.28	9940	0.205
midshore, nearshore	4.21	9833	< 0.001
offshore, nearshore	5.72	9819	< 0.001
0.5year, 2.5years	5.47	9838	< 0.001
0.5year, 1year	4.36	9837	< 0.001
2.5years, 1year	no test over all reef sites#		

Pair-wise comparison could not be performed over all sites because of missing data for 2.5 years in nearshore and offshore sheltered sites. However, pair-wise comparisons between 2.5 years and 1year were all significant within the other four sites ($p < 0.01$).

5.7.1. References (Supplementary Materials)

Alwany, M. A., Thaler, E. and Stachowitsch, M.: Parrotfish bioerosion on Egyptian Red Sea reefs, J. Exp. Mar. Biol. Ecol., 371(2), 170–176, doi:10.1016/j.jembe.2009.01.019, 2009.

Bruggemann, J., van Oppen, M. and Breeman, A.: Foraging by the stoplight parrotfish Sparisoma viride. I. Food selection in different, socially determined habitats, Mar. Ecol. Prog. Ser., 106, 41–55, doi:10.3354/meps106041, 1994.

Bruggemann, J., van Kessel, A., van Rooij, J. and Breeman, A.: Bioerosion and sediment ingestion by the Caribbean parrotfish Scarus vetula and Sparisoma viride:implications of fish size, feeding mode and habitat use, Mar. Ecol. Prog. Ser., 134, 59–71, doi:10.3354/meps134059, 1996.

Perry, C., Edinger, E., Kench, P., Murphy, G., Smithers, S., Steneck, R. and Mumby, P.: Estimating rates of biologically driven coral reef framework production and erosion: a new census-based carbonate budget methodology and applications to the reefs of Bonaire, Coral Reefs, 31(3), 853–868, doi:10.1007/s00338-012-0901-4, 2012.

Roik, A., Roder, C., Röthig, T. and Voolstra, C. R.: Spatial and seasonal reef calcification in corals and calcareous crusts in the central Red Sea, Coral Reefs, 1–13, doi:10.1007/s00338-015-1383-y, 2015.

6. SYNTHESIS

The Red Sea is as an important region for coral reef research, but coral reefs in the central and southern part are sparsely studied. This dissertation not only assesses the *in situ* environmental regimes and biotic variability of coral reef habitats in the central Red Sea, but also highlights these coral reefs in a global context and in relation to climate change, providing abiotic parameters that potentially drive the three pivotal aspects of coral reef functioning, i.e., benthic communities, calcification, and reef carbonate budgets.

Abiotic data in this dissertation was collected between 2012 and 2014 and represent the present-day environmental conditions in the central Red Sea coral reefs. Data show that not only challenging summer temperatures and salinity levels in the reef habitats deviate from the global averages for coral reefs (Table 18), reflecting future predictions of ocean warming (IPCC Working Group I 2013), but also that dissolved oxygen levels are relatively low, reflecting the trend of deoxygenation in marine habitats with the progression of ocean warming (Keeling et al. 2010). In contrast to these stress-related variables, carbonate chemistry in the reefs is beneficial for reef-building, since on the average it resembles and even exceeds preindustrial estimates of global ocean surface water (Kleypas et al. 1999a), suggesting a high buffering capacity of Red Sea waters against ocean acidification. Overall very low levels of inorganic nutrients measured in the reefs are on the one hand beneficial to the success of symbiotic reef-building corals (Muscatine and Porter 1977). On the other hand, the here presented nutrient data also suggest a phosphate depletion especially in the summer season, while nitrate and nitrate levels remain almost unchanged. Such

a shift in the nitrogen:phosphorus balance towards a higher ratio has been previously demonstrated to decrease the heat and light stress tolerance of symbiotic reef-building corals in aquarium experiments (Wiedenmann et al. 2013). In the study area this could result in a synergistic effect with high summer temperatures, explaining the decreased efficiency of calcifiers during the summer. It will be of interest to further look into the naturally occurring inorganic nutrient ratios in the central Red Sea and explore their impact on coral physiology in more detail.

The full-year monitoring of a coral reef system in the central Red Sea shows that abiotic drivers structure coral reef habitats in space and time, separating distant offshore reefs from nearshore and midshore habitats, and further separating between the summer and winter season (Figure 19 A). In particular, the patterns of hydrodynamics, salinity, dissolved oxygen levels, and pH suggest that water exchange between the Red Sea basin and the nearshore reefs is reduced (Figure 19 B). As a consequence, habitats in the nearshore area are more isolated and demonstrate stronger signatures of biotic feedbacks on, e.g. dissolved oxygen and pH, caused by community photosynthesis, respiration, and calcification (Bates et al. 2010; Drupp et al. 2011). This larger physico-chemical variability on diel scales and the lack of offshore water influx, that could alleviate summer warming, expose these habitats to an increased environmental stress compared to the more distant offshore reefs. Extreme and highly variable temperatures, dissolved oxygen, and pH may compromise physiological processes of reef organisms (Pörtner 2010; Bopp et al. 2013). The herein presented data of spatio-temporal dynamics in the study area shows that the here studied coral reef system is an ideal location for the investigation

of how marine communities and individual organisms respond to different environmental regimes, including environmentally challenging habitats.

Table 18 *In situ* environmental regimes in coral reef habitats of the central Red Sea. The table shows the annual minimum, maximum, and mean in brackets for the central Red Sea and for coral reefs worldwide.

Environmental variable	Central Red Sea coral reefs	Coral reefs global
Temperature °C	24 – 33 [29] (a)	21 -29.5 [27.6] (c)
Salinity PSU	38.4 – 39.8 [39.3] (a)	23.3 – 40.0 [34.3] (c)
Aragonite saturation state	4.3 – 5.6 [4.8] (b)	3.28 – 4.06 [3.83] (c)
Total alkalinity µmol kg^{-1}	2315 – 2459 [2391] b)	~ 2315 (d)
Dissolved oxygen mg L^{-1}	0.1 – 8.9 [3.5] (a)	2.1 – 10.8 [6.66 / 7.03] (e)
Nitrate and nitrite µmol L^{-1}	0.1 – 1 [0.5] (a)	0 – 3.34 [0.25] (c)
Phosphate µmol L^{-1}	0 – 0.1 [0.05] (a)	0 -0.54 [0.13] (c)
Chlorophyll a fluorescence µg L^{-1}	0 – 3.4 [0.4] (a)	~ 0 - 4 [0.22 / 0.62] (f)

References: (a) based on continuous year-long measurements on reefs across the shelf (this dissertation); (b) based on continuous winter and summer measurements on reefs across the shelf (this dissertation); (c) estimated global averages for coral reefs (Kleypas et al. 1999b); (d) tropical surface ocean estimate for 1990 (Manzello et al. 2008); (e) measurements on reefs in Heron island, Great Barrier Reef, means from two sites are shown in brackets (Kinsey and Kinsey 1967); (f) minimum and maximum derived from time series plots, the lowest and the highest mean from different reefs are shown in brackets, Great Barrier Reef (Schaffelke et al. 2012)

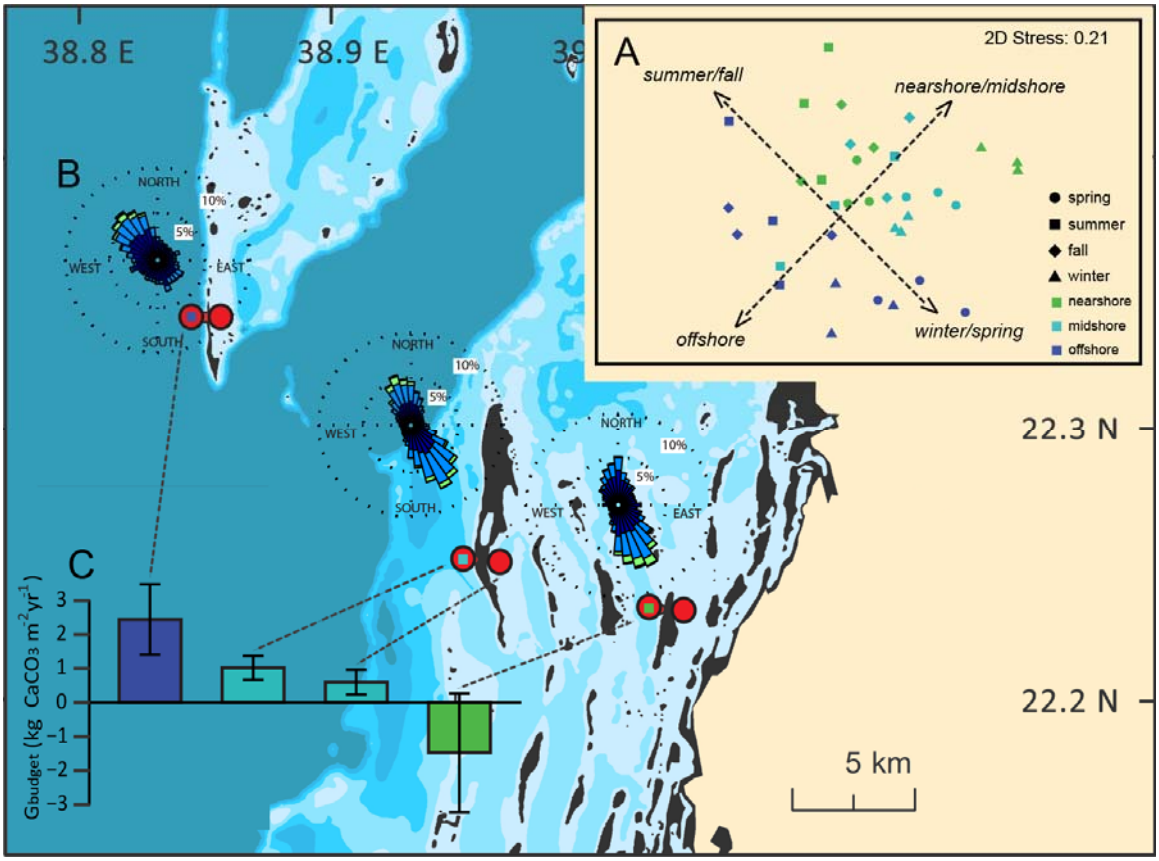

Figure 19 The map shows the study area in central Red Sea, summarizing some of the environmental properties that were assessed in this dissertation. A. shows the spatio-seasonal structuring of forereef habitats by physico-chemical conditions (nearshore, midshore, and offshore). A non-metric multidimensional scaling (nMDS) plot illustrates the structure of reef environments based on 10 physico-chemical variables (current direction, current speed, temperature, salinity, dissolved oxygen, chlorophyll-a, turbidity, sedimentation rate, and organic content, and C:N ratio of collected sediments). Arrows were added to visualize the axes along which the data separate on the spatial and seasonal scales. B. displays the hydrodynamics in the three forereef sites. Current profiles display full-year data as frequencies of current direction (bars) and the current speeds (colors). Directions are indicated by the angle of the bars. C. Census-based reef carbonate budgets (G_{budget}, means and standard deviations) in the three forereef sites from nearshore to offshore, including the midshore lagoonal back reef, span from net-erosion to positive net-accretion.

Epilithic bacterial and algal communities, are increasingly recognized as pivotal components in coral reef functioning, particularly for their function in controlling recruitment of reef-building corals, which can have far-reaching consequences for benthic community structure (Negri and Heyward 2000; Webster et al. 2004; Jessen et al. 2012; Marhaver et al. 2013). This dissertation provides a first account of the full-

year diversity and dynamics of bacterial and algal biofilm communities. Data show that coral reef biofilms allow for a remarkable diversification of bacterial communities in comparison to other bacterial habitats in coral reefs, such as the water column, corals, or sponges which are rather selective habitats exhibiting a lower diversity and evenness (

Table 19). Coral reef bacterial communities are being most extensively studied in nutrient cycling related to coral and sponge holobionts (Raina et al. 2009; Hentschel et al. 2012; Lema et al. 2012) and with regard to health and disease of reef-building corals (Rosenberg et al. 2007). However, the implications of a high bacterial diversity in biofilms are still unknown and deserve further research. Potentially, biofilms may be a reservoir of bacteria and may play a role in maintaining health and transmitting disease to e.g. reef-building corals. The herein presented comparative study of winter and summer specific community shifts is a first step potentially guiding towards insights about the community dynamics which can be expected under ocean warming scenarios. Also, the outcome showing that algal cover and bacterial diversity were highest during spring and summer, and coincide with the timing of coral reproduction (Bouwmeester et al. 2014b), deserves further specific investigation to understand the implications for coral recruitment.

Table 19 Comparison of OTU richness and diversity of coral reef bacterial communities in the central Red Sea.

Bacterial habitat	Region of 16 S rRNA gene	OTU richness estimate (Chao 1)	OTU diversity estimate (Inversed Simpson's Index)
Biofilm	16 S V 3-4 *	400 – 900 (a)	6 - 160 (a)
Seawater	16 S V 3-4 *	140 – 270 (a)	4 - 13 (a)
Seawater	16S V 5-6 #	160 – 590 (b)	2.5 -7.8 (b)
Coral	16S V 5-6 #	80 -300 (b)	1.3 – 5.9 (b)
Sponge	16S V 5-6 $	300 – 700 (c)	1.0 - 1.3 (c)

OTU= operation taxonomic units, clustered at a similarity cut-off of 3%; (*) Klindworth et al. 2012; (#) Andersson et al. 2008; ($) Simister et al. 2012; (a) minimum and maximum per sample, data from this dissertation; (b) minimum and maximum per sample, data from Röthig et al. (2016) and Ziegler et al. (2016), only data from undisturbed sites are shown, coral species: *Acropora hemprichii, Pocillopora verrucosa, Fungia granulosa;* (c) lowest and highest means from Moitinho-Silva et al. (2014), sponge species: *Xestospongia testudinaria, Stylissa carteri*

The dissertation presents data on reef growth in the central Red Sea, a geographic region which maintains a carbonate chemistry comparable or above the estimates of coral reef preindustrial values (see discussion above). Although this is expected to strongly support reef-building, annual average calcification rates for the major reef-building coral genera *Porites*, *Acropora*, and *Pocillopora* (1 – 1.5 mg cm^{-2} d^{-1}) were not higher than in other parts of the world (Figure 20). Equally, the overall reef growth, measured via census-based carbonate budgets, was in the range of budget estimates from the majority of coral reefs worldwide, but below the highest recorded budgets for remote and mostly unimpacted tropical reefs in the Indian Ocean (Pari et al. 1998; Perry et al. 2013, 2015).

It may be assumed that the capacity of calcifiers in the central Red Sea, though supported by beneficial carbonate chemistry, is temporarily compromised by the challenging conditions of high temperature. Indeed the data presented here show that reef-building corals in the study area exhibit an unusual seasonal pattern of

calcification maxima during a cooler season (spring) rather than during the warmest season (summer), which has been reported for many coral reefs worldwide (Crossland 1984; Hibino and van Woesik 2000; Kuffner et al. 2013). It also remains to be further determined whether reduced dissolved oxygen values and phosphate depletion contribute to the decrease of calcification capacities in corals during the summer.

Combining this data with previous studies on coral calcification from other Red Sea regions suggest that the coral's thermal optima may be exceeded during the summer in the central and southern Red Sea, but not in the northern region. Accordingly, growth rates of various coral species (*Stylophora pistillata*, *Pocillopora damicornis*, and *Acropora granulosa*) from the northern Red Sea (Sinai) were highest during the summer periods (Kotb 2001; Mass et al. 2007). For the coral *Pocillopora verrucosa* an inversed seasonal pattern was demonstrated along the latitudinal gradient (Sawall et al. 2015), showing calcification maxima during the summer in the north, and during the winter in the south. This pattern is likely to be also true for other coral genera, such as *Porites* and *Acropora*, when extrapolating results from this dissertation.

The future persistence of coral reefs will strongly depend on the calcification rates of reef-building corals, but ocean warming represents a serious threat to reef calcifiers in the central Red Sea. Particularly, calcification rates in one coral species have already been decreasing over the past two decades (Cantin et al. 2010). The question remains whether the overall reef growth in the central Red Sea is also already impaired as compared to the historical reef growth potential. Data from this

dissertation show a wide span of reef production states in the central Red Sea, ranging from net-erosion in the nearshore areas to net-accretion in midshore and offshore reefs (Figure 19 C). A lack of data from this same region impedes a comparison of the present-day carbonate budgets with historical reef production states. Comparisons with the historical census-based estimates and reef core analyses from the northern Red Sea (Dullo et al. 1996b) lead the assumption that reef growth in the Red Sea has not decreased over the past decades. In order to confirm or reject this assumption further study of historical and present-day reef growth will be required. Since carbonate budgets are a powerful tool to track the trajectories of modern-day and future reef states, the dataset in this dissertation will be particularly valuable when evaluating the impact of most recent disturbances in central Red Sea reefs, such as the Third Global Bleaching Event 2015/16 that had set in after the collection of data for this dissertation.

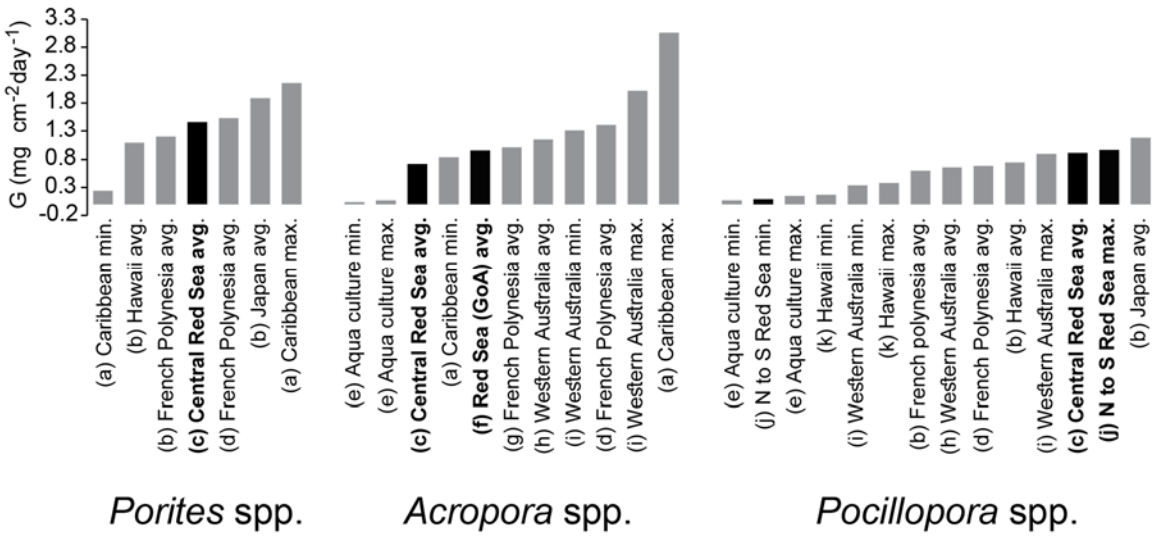

Figure 20 Global comparison of coral calcification rates [G] assessed with comparable methodologies (see Table 10). GoA = Gulf of Aqaba, N to S = north to south. References are marked with a – k; references and methods used: (a) (Goreau and Goreau 1959) $Ca^{45}Cl_2$-incubations, (b) (Comeau et al. 2014b) Buoyant weight, (c) (This dissertation) Buoyant weight, (d) (Comeau et al. 2013) Buoyant weight, (e) (Schoepf et al. 2013) Buoyant weight, (f) (Schneider and Erez 2006) Total alkalinity depletion method, (g) (Comeau et al. 2014a) Buoyant weight, (h) (Foster et al. 2014) Buoyant weight, (i) (Ross et al. 2015) Buoyant weight, (j) (Sawall et al. 2015) Total alkalinity depletion method, (k) (Clausen and Roth 1975b) $Ca^{45}Cl^2$-incubations. Figure from Ziegler, Roik et al. (in preparation) is based on data from chapter two of this dissertation.

This dissertation utilizes data concurrently collected from the abiotic and biotic realm to derive potential environmental drivers which are crucial for reef functioning in the central Red Sea coral reefs. Bacterial and algal assemblages of biofilms are remarkably dynamic along the cross-shelf gradient of reefs, but also between the four seasons. Temperature, salinity, dissolved oxygen, and chlorophyll-a are the driving forces for biofilm dynamics in the study area. Particularly, temperatures, salinity, and dissolved oxygen are forecasted to critically change with the progression of ocean warming (as discussed above). Taken together this predicts a restructuring of the bacterial and algal assemblages. Alarmingly, the reef-building community structure is very likely to be affected not only by the direct impact of ocean warming, but also

due to the bottom-up effect of bacterial and algal community changes (Heyward and Negri 1999; Jessen et al. 2012; Marhaver et al. 2013).

The herein presented data show that reef growth in the central Red Sea is positively influenced by the abundance of calcifiers, and strongly shaped by the abundances of parrotfish along the environmental gradient. Total alkalinity is the strongest predictor of reef growth in the study area. Notably, small differences in total alkalinity (~32 μmol Kg^{-1}) already explain more than 60 % of reef growth variability along the cross-shelf gradient. Considering that high variability of pH in the nearshore and the midshore lagoon habitats is associated with negative or neutral carbonate budgets, it is also suggested that large pH fluctuation can be a critical stressor for the carbonate accretion capacity in the reef habitats. A similar negative relationship of net-accretion rates with increased pH variability has been demonstrated in a recent study (Silbiger et al. 2014).

While ocean warming is already considered a strong driver for the central Red Sea coral reefs (Cantin et al. 2010), this dissertation sheds more light on carbonate chemistry and its role in reef growth. The results indicate that despite the beneficial carbonate chemistry levels, which may delay the arrival of critical pH and aragonite saturation thresholds in the progression of ocean acidification, even small changes within the non-critical ranges may cause transitions in reef growth processes.

This dissertation contributes to a more coherent understanding of coral reef functioning in general, but also specifically of coral reefs under challenging environmental conditions. Community composition dynamics, as well as carbonate

budgets, are useful tools to track the trajectories of coral reef conditions. These data provide a foundation for future Red Sea coral reef studies, and the dissertation is an important step towards the effort of quantifying the impact of environmental change on Red Sea coral reefs.

6.1. References

Andersson AF, Lindberg M, Jakobsson H, Bäckhed F, Nyrén P, Engstrand L (2008) Comparative Analysis of Human Gut Microbiota by Barcoded Pyrosequencing. PLoS ONE 3:e2836

Bates NR, Amat A, Andersson AJ (2010) Feedbacks and responses of coral calcification on the Bermuda reef system to seasonal changes in biological processes and ocean acidification. Biogeosciences 7:2509–2530

Bopp L, Resplandy L, Orr JC, Doney SC, Dunne JP, Gehlen M, Halloran P, Heinze C, Ilyina T, Séférian R, Tjiputra J, Vichi M (2013) Multiple stressors of ocean ecosystems in the 21st century: projections with CMIP5 models. Biogeosciences 10:6225–6245

Bouwmeester J, Baird AH, Chen CJ, Guest JR, Vicentuan KC, Berumen ML (2014) Multi-species spawning synchrony within scleractinian coral assemblages in the Red Sea. Coral Reefs 34:65–77

Cantin NE, Cohen AL, Karnauskas KB, Tarrant AM, McCorkle DC (2010) Ocean Warming Slows Coral Growth in the Central Red Sea. Science 329:322–325

Clausen CD, Roth AA (1975) Effect of temperature and temperature adaptation on calcification rate in the hermatypic coral *Pocillopora damicornis*. Mar Biol 33:93–100

Comeau S, Carpenter RC, Edmunds PJ (2014a) Effects of irradiance on the response of the coral *Acropora pulchra* and the calcifying alga *Hydrolithon reinboldii* to temperature elevation and ocean acidification. J Exp Mar Biol Ecol 453:28–35

Comeau S, Carpenter RC, Nojiri Y, Putnam HM, Sakai K, Edmunds PJ (2014b) Pacific-wide contrast highlights resistance of reef calcifiers to ocean acidification. Proc R Soc B Biol Sci 281:20141339–20141339

Comeau S, Edmunds PJ, Spindel NB, Carpenter RC (2013) The responses of eight coral reef calcifiers to increasing partial pressure of CO2 do not exhibit a tipping point. Limnol Oceanogr 58:388–398

Crossland CJ (1984) Seasonal variations in the rates of calcification and productivity in the coral *Acropora formosa* on a high-latitude reef. Mar Ecol Prog Ser 15:135–140

Drupp P, Carlo EHD, Mackenzie FT, Bienfang P, Sabine CL (2011) Nutrient Inputs, Phytoplankton Response, and CO2 Variations in a Semi-Enclosed Subtropical Embayment, Kaneohe Bay, Hawaii. Aquat Geochem 17:473–498

Dullo W-C, Reijmer J, Schuhmacher H, Eisenhauer A, Hassan M, Heiss G (1996) Holocene reef growth and recent carbonate production in the Red Sea. Global and Regional Controls of Biodenic Sedimentation. Gottinger Arb. Geol. Palaont., Gottingen, pp 13–17

Foster T, Short JA, Falter JL, Ross C, McCulloch MT (2014) Reduced calcification in Western Australian corals during anomalously high summer water temperatures. J Exp Mar Biol Ecol 461:133–143

Goreau TF, Goreau NI (1959) The Physiology Of Skeleton Formation In Corals. II. Calcium Deposition By Hermatypic Corals Under Various Conditions In The Reef. Biol Bull 117:239–250

Hentschel U, Piel J, Degnan SM, Taylor MW (2012) Genomic insights into the marine sponge microbiome. Nat Rev Microbiol 10:641–654

Heyward AJ, Negri AP (1999) Natural inducers for coral larval metamorphosis. Coral Reefs 18:273–279

Hibino K, van Woesik R (2000) Spatial differences and seasonal changes of net carbonate accumulation on some coral reefs of the Ryukyu Islands, Japan. J Exp Mar Biol Ecol 252:1–14

IPCC Working Group I (2013) IPCC, 2013: Climate Change 2013: The Physical Science Basis. Contribution of Working Group I to the Fifth Assessment Report of the Intergovernmental Panel on Climate Change. In: Stocker T., Quin D., Plattner G.-K., Tignor M., Allen S.K., Boschung J., Nauels A., Xia Y., Bex V., Midgley P.M. (eds) Cambridge University Press, United Kingdom and New York, NY, USA,

Jessen C, Roder C, Villa Lizcano J, Voolstra CR, Wild C (2012) Top-down and bottom-up effects on Red Sea coral reef algae. 12th International Coral Reef Symposium

Keeling RF, Körtzinger A, Gruber N (2010) Ocean Deoxygenation in a Warming World. Annu Rev Mar Sci 2:199–229

Kinsey D, Kinsey E (1967) Diurnal changes in oxygen content of the water over the coral reef platform at Heron I. Mar Freshw Res 18:23–34

Kleypas JA, Buddemeier RW, Archer D, Gattuso J-P, Langdon C, Opdyke BN (1999a) Geochemical Consequences of Increased Atmospheric Carbon Dioxide on Coral Reefs. Science 284:118–120

Kleypas JA, McManus JW, Menez LAB (1999b) Environmental Limits to Coral Reef Development: Where Do We Draw the Line? Am Zool 39:146–159

Klindworth A, Pruesse E, Schweer T, Peplies J, Quast C, Horn M, Glöckner FO (2012) Evaluation of general 16S ribosomal RNA gene PCR primers for classical and next-generation sequencing-based diversity studies. Nucleic Acids Res gks808

Kotb MM (2001) Growth rates of three reef-building coral species in the northern Red Sea, Egypt. Egypt J Aquat Biol Fish 5:165–185

Kuffner IB, Hickey TD, Morrison JM (2013) Calcification rates of the massive coral Siderastrea siderea and crustose coralline algae along the Florida Keys (USA) outer-reef tract. Coral Reefs 32:987–997

Lema KA, Willis BL, Bourne DG (2012) Corals Form Characteristic Associations with Symbiotic Nitrogen-Fixing Bacteria. Appl Environ Microbiol 78:3136–3144

Manzello DP, Kleypas JA, Budd DA, Eakin CM, Glynn PW, Langdon C (2008) Poorly cemented coral reefs of the eastern tropical Pacific: Possible insights into reef development in a high-CO2 world. Proc Natl Acad Sci 105:10450–10455

Marhaver KL, Vermeij MJA, Rohwer F, Sandin SA (2013) Janzen-Connell effects in a broadcast-spawning Caribbean coral: distance-dependent survival of larvae and settlers. Ecology 94:146–160

Mass T, Einbinder S, Brokovich E, Shashar N, Vago R, Erez J, Dubinsky Z (2007) Photoacclimation of *Stylophora pistillata* to light extremes: metabolism and calcification. Mar Ecol Prog Ser 334:93–102

Moitinho-Silva L, Bayer K, Cannistraci CV, Giles EC, Ryu T, Seridi L, Ravasi T, Hentschel U (2014) Specificity and transcriptional activity of microbiota associated with low and high microbial abundance sponges from the Red Sea. Mol Ecol 23:1348–1363

Muscatine L, Porter JW (1977) Reef Corals: Mutualistic Symbioses Adapted to Nutrient-Poor Environments. BioScience 27:454–460

Negri AP, Heyward AJ (2000) Inhibition of fertilization and larval metamorphosis of the coral *Acropora millepora* (Ehrenberg, 1834) by petroleum products. Mar Pollut Bull 41:420–427

Pari N, Peyrot-Clausade M, Le Champion-Alsumard T, Hutchings P, Chazottes V, Gobulic S, Le Champion J, Fontaine MF (1998) Bioerosion of experimental substrates on high islands and on atoll lagoons (French Polynesia) after two years of exposure. Mar Ecol Prog Ser 166:119–130

Perry CT, Murphy GN, Graham NAJ, Wilson SK, Januchowski-Hartley FA, East HK (2015) Remote coral reefs can sustain high growth potential and may match future sea-level trends. Sci Rep 5:18289

Perry CT, Murphy GN, Kench PS, Smithers SG, Edinger EN, Steneck RS, Mumby PJ (2013) Caribbean-wide decline in carbonate production threatens coral reef growth. Nat Commun 4:1402

Pörtner H-O (2010) Oxygen- and capacity-limitation of thermal tolerance: a matrix for integrating climate-related stressor effects in marine ecosystems. J Exp Biol 213:881–893

Raina J-B, Tapiolas D, Willis BL, Bourne DG (2009) Coral-Associated Bacteria and Their Role in the Biogeochemical Cycling of Sulfur. Appl Environ Microbiol 75:3492–3501

Rosenberg E, Koren O, Reshef L, Efrony R, Zilber-Rosenberg I (2007) The role of microorganisms in coral health, disease and evolution. Nat Rev Microbiol 5:355–362

Ross CL, Falter JL, Schoepf V, McCulloch MT (2015) Perennial growth of hermatypic corals at Rottnest Island, Western Australia (32°S). PeerJ 3:e781

Röthig T, Ochsenkühn MA, Roik A, van der Merwe R, Voolstra CR (2016) Long-term salinity tolerance is accompanied by major restructuring of the coral bacterial microbiome. Mol Ecol 25:1308–1323

Sawall Y, Al-Sofyani A, Hohn S, Banguera-Hinestroza E, Voolstra CR, Wahl M (2015) Extensive phenotypic plasticity of a Red Sea coral over a strong latitudinal temperature gradient suggests limited acclimatization potential to warming. Sci Rep 5:8940

Schaffelke B, Carleton J, Skuza M, Zagorskis I, Furnas MJ (2012) Water quality in the inshore Great Barrier Reef lagoon: Implications for long-term monitoring and management. Mar Pollut Bull 65:249–260

Schneider K, Erez J (2006) The effect of carbonate chemistry on calcification and photosynthesis in the hermatypic coral *Acropora eurystoma.* Limnol Oceanogr 51:1284–1293

Schoepf V, Grottoli AG, Warner ME, Cai W-J, Melman TF, Hoadley KD, Pettay DT, Hu X, Li Q, Xu H, Wang Y, Matsui Y, Baumann JH (2013) Coral Energy Reserves and Calcification in a High-CO2 World at Two Temperatures. PLoS ONE 8:e75049

Silbiger NJ, Guadayol O, Thomas FIM, Donahue MJ (2014) Reefs shift from net accretion to net erosion along a natural environmental gradient. Mar Ecol Prog Ser 515:33–44

Simister R, Taylor MW, Tsai P, Webster N (2012) Sponge-Microbe Associations Survive High Nutrients and Temperatures. PLOS ONE 7:e52220

Webster NS, Smith LD, Heyward AJ, Watts JEM, Webb RI, Blackall LL, Negri AP (2004) Metamorphosis of a Scleractinian Coral in Response to Microbial Biofilms. Appl Environ Microbiol 70:1213–1221

Wiedenmann J, D'Angelo C, Smith EG, Hunt AN, Legiret F-E, Postle AD, Achterberg EP (2013) Nutrient enrichment can increase the susceptibility of reef corals to bleaching. Nat Clim Change 3:160–164

Ziegler M, Roik A, Porter A, Zubier K, Mudarris MS, Ormond R, Voolstra CR (2016) Coral microbial community dynamics in response to anthropogenic impacts near a major city in the central Red Sea. Mar Pollut Bull 105:629–640

Ziegler M, Roik A, Röthig T, Wild C, Rädecker N, Bouwmeester J, Voolstra CR (in preparation) Physiology of scleractinian corals in the Red Sea. Corals of the World: The Red Sea. Springer